ZooKeys 980: 1–21 (2020)
doi: 10.3897/zookeys.980.52186
https://zookeys.pensoft.net

RESEARCH ARTICLE

A peer-reviewed open-access journal
ZooKeys
Launched to accelerate biodiversity research

Two new species of freshwater crabs of the genera *Eosamon* Yeo & Ng, 2007 and *Indochinamon* Yeo & Ng, 2007 (Crustacea, Brachyura, Potamidae) from southern Yunnan, China

Zewei Zhang[1*], Da Pan[1*], Xiyang Hao[1], Hongying Sun[1]

1 *Jiangsu Key Laboratory for Biodiversity and Biotechnology, College of Life Sciences, Nanjing Normal University, 1 Wenyuan Rd, Nanjing 210023, China*

Corresponding author: Hongying Sun (sunhongying@njnu.edu.cn)

Academic editor: K. Van Damme | Received 18 March 2020 | Accepted 14 September 2020 | Published 28 October 2020

http://zoobank.org/A72A4909-3C62-4176-9B29-CE9BA22A9923

Citation: Zhang Z, Pan D, Hao X, Sun H (2020) Two new species of freshwater crabs of the genera *Eosamon* Yeo & Ng, 2007 and *Indochinamon* Yeo & Ng, 2007 (Crustacea, Brachyura, Potamidae) from southern Yunnan, China. ZooKeys 980: 1–21. https://doi.org/10.3897/zookeys.980.52186

Abstract

Two new species of potamid crabs, *Eosamon daiae* **sp. nov.** and *Indochinamon malipoense* **sp. nov.** are described from the Sino-Burmese border, southwestern Yunnan and from the Sino-Vietnamese border, southeastern Yunnan, China. The two new species can be distinguished from their closest congeners by several characters, among which is the form of the first gonopod structures. Molecular analyses based on partial mitochondrial 16S rDNA sequences also support the systematic status of these new taxa.

Keywords

16S rDNA, *Eosamon daiae* sp. nov., *Indochinamon malipoense* sp. nov., new species, Potamidae, Potamiscinae, taxonomy

* Contributed equally as the first authors.

Introduction

China has the most freshwater crab species in the world and Yunnan is the epicenter of this diversity, with over 60 species in 17 genera (Dai 1999; Chu et al. 2018a, b; Naruse et al. 2018). Despite this, the biodiversity of freshwater crabs in this region appears to be still underestimated, especially in the remote areas (Chu et al. 2018b). In this paper we describe two new species belonging to two genera, *Eosamon* Yeo & Ng, 2007, and *Indochinamon* Yeo & Ng, 2007, from the Sino-Burmese and Sino-Vietnamese border areas in Yunnan Province, China. *Eosamon* and *Indochinamon* are widely distributed in the Indochina Peninsula (Yeo and Ng 2007). Including the two new species described in the present study, *Eosamon* and *Indochinamon* respectively contain 12 and 40 species (Yeo and Ng 2007; Yeo 2010; Naruse et al. 2011, 2018; Van et al. 2016; Ng and Mar 2018).

Material and methods

Specimens were collected from southwestern and southeastern Yunnan (Fig. 1), preserved in 95% ethanol and identified via a stereo dissection microscope (Nikon SMZ645). Materials examined are deposited in the Jiangsu Key Laboratory for Biodiversity and Biotechnology, College of Life Sciences, Nanjing Normal University (NNU), Nanjing, China. Carapace width and length were measured in millimeters. The terminology used here follows Guinot et al. (2013). The following abbreviations are used: G1 for male first gonopod, G2 for male second gonopod, a.s.l. for above sea level.

Molecular data. Genomic DNA was extracted from gill tissue using the the Trelief™ Animal Genomic DNA kit (Tsingke). 16S rDNA sequence was selected for amplification with polymerase chain reaction (PCR) using the primers 1471 and 1472 (Crandall and Fitzpatrick 1996). Parameters for PCR were as follows: initial denaturation at 95 °C for 3 min, followed by 35 cycles of 15 sec at 95 °C, 15 sec at 48 °C, 45 sec at 72 °C, and a subsequent 7 min final extension step at 72 °C. Both ends of PCR products were then sequenced using an ABI 3730 automatic sequencer. Sequences were assembled using SEQMAN II 5.05. Sequences of different haplotypes have been deposited in the Genbank (accession numbers listed in Table 1). To confirm the systematic position of newly described taxa, a total of 64 sequences were used in phylogenetic analyses, including 56 downloaded sequences (Table 1).

Phylogenetic analyses. Sequences were aligned using MAFFT 7.310 (Katoh and Standley 2013) based on the G-INS-I method. Gapped positions were treated as missing data. Maximum likelihood (ML) analysis for the dataset was performed using IQ-TREE 1.6.12 (Nguyen et al. 2015). The best substitution model was determined by ModelFinder (Kalyaanamoorthy et al. 2017). Node reliability was obtained through 1000 ultrafast bootstrap replicates (Minh et al. 2013). For Bayesian inference (BI), the best-fitting model was determined by MrModeltest 2.4 (Nylander 2004), selected by the Akaike information criterion (AIC). The best model obtained was GTR+I+G. Bayesian inference was performed using MRBAYES 3.2.6 (Ronquist et al. 2012) with four chains for 20 million generations, with trees sampled every 5000 generations.

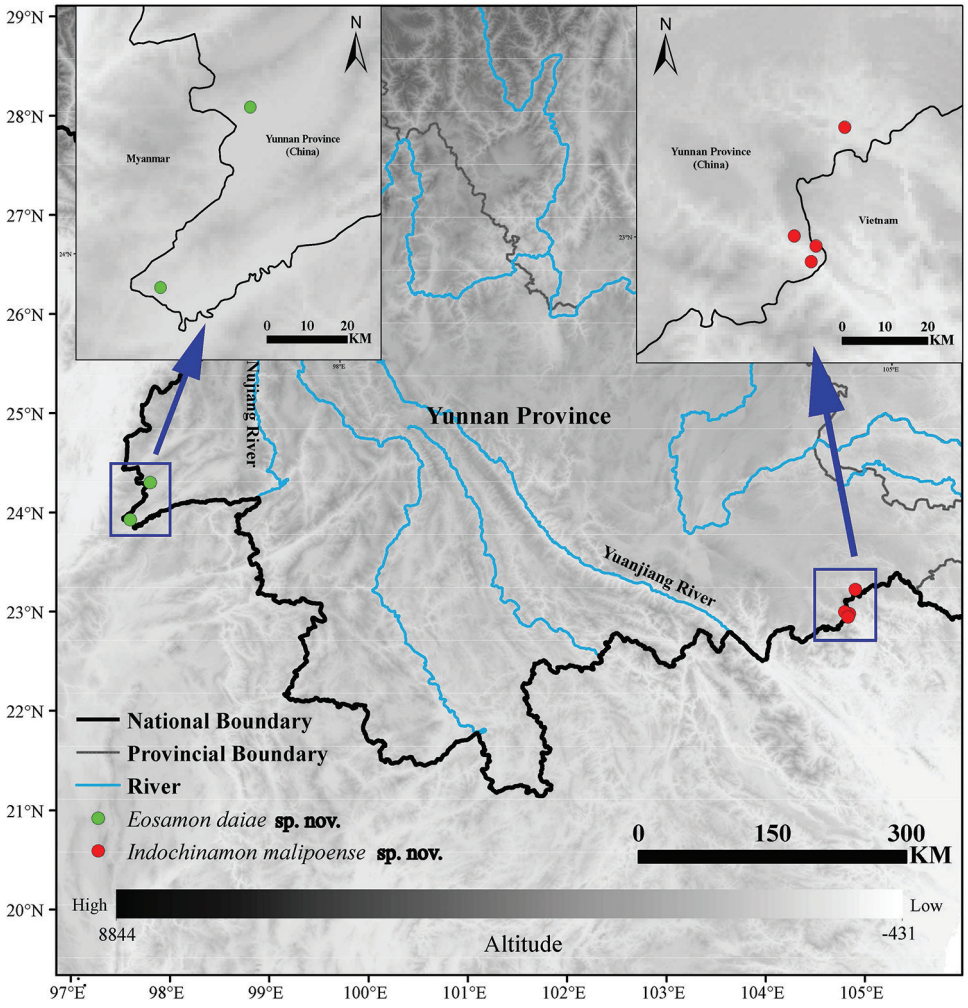

Figure 1. Locality of sampling sites for *Eosamon daiae* sp. nov. and *Indochinamon malipoense* sp. nov. in southwestern and southeastern Yunnan Province, China.

Table 1. 16S rDNA sequences sampled in this study.

Species	Accession No.	Voucher No.	Reference
Amamiku amamensis	AB428457	–	Shih et al. 2009
Aparapotamon grahami	AB428489	–	Shih et al. 2009
Apotamonautes hainanensis	AB428459	–	Shih et al. 2009
Arquatopotamon jizushanense	KY963596	–	Chu et al. 2017
Artopotamon latopeos	MH045061	–	Chu et al. 2018a
Beccumon jarujini	AB428479	–	Shih et al. 2009
Candidiopotamon rathbunae	AB208598	–	Shih et al. 2006
Chinapotamon glabrum	AB428451	–	Shih et al. 2009
Demanietta renongensis	AB428475	–	Shih et al. 2009
Diyutamon cereum	LC198519	–	Huang et al. 2016
Eosamon boonyaratae	AB428487	–	Shih et al. 2009
Eosamon daiae sp. nov.	MT887282	NNU 190508	This study

Species	Accession No.	Voucher No.	Reference
Eosamon daiae sp. nov.	MT887283	NNU 190509	This study
	MT887280	NNU 190405	This study
	MT887281	NNU 190406	This study
Eosamon lushuiense	MT887284	NNU LSWG1503	This study
Eosamon smithianum	AB428486	–	Shih et al. 2009
Eosamon tengchongense	MT887285	NNU TCML02	This study
Eosamon yotdomense	AB428485	–	Shih et al. 2009
Esanpotamon namsom	AB428463	–	Shih et al. 2009
Flabellamon sp.	AB428472	–	Shih et al. 2009
Geothelphusa albogilva	AB127366	–	Shih et al. 2004
Geothelphusa fulva	AB428456	–	Shih et al. 2009
Geothelphusa olea	AB428455	–	Shih et al. 2009
Hainanpotamon fuchengense	AB428461	–	Shih et al. 2009
Himalayapotamon atkinsonianum	AB428510	–	Shih et al. 2009
Huananpotamon angulatum	AB428454	–	Shih et al. 2009
Indochinamon malipoense sp. nov.	MT887278	NNU 180601	This study
	MT887279	NNU 180602	This study
Indochinamon ou	AB428481	–	Shih et al. 2009
Indochinamon tannanti	AB428482	–	Shih et al. 2009
Johora johorensis	AB290620	–	Yeo et al. 2007
Johora murphyi	AB290621	–	Yeo et al. 2007
Kanpotamon duangkhaei	AB428471	–	Shih et al. 2009
Kukrimon cucphuongensis	AB428483	–	Shih et al. 2009
Megacephalomon kittikooni	AB428462	–	Shih et al. 2009
Mindoron balssi	AB428464	–	Shih et al. 2009
Minpotamon nasicum	AB428450	–	Shih et al. 2009
Minutomon shanweiense	LC176065	–	Huang et al. 2016
Nanhaipotamon formosanum	AB212867	–	Shih et al. 2005
Nanhaipotamon nanriense	AB212868	–	Shih et al. 2005
Neotiwaripotamon jianfengense	AB428460	–	Shih et al. 2009
Ovitamon artifrons	AB428466	–	Shih et al. 2009
Parapotamon spinescens	AB428467	–	Shih et al. 2009
Pararanguna semilunata	AB428490	–	Shih et al. 2009
Paratelphusula gibbosa	AB428512	–	Shih et al. 2009
Potamiscus loshingense	AB428488	–	Shih et al. 2009
Potamiscus yiwuensis	AB428476	–	Shih et al. 2009
Potamiscus yunnanense	AB290629	–	Yeo et al. 2007
Potamon fluviatile	AB428514	–	Shih et al. 2009
Pudaengon sakonnakorn	AB428484	–	Shih et al. 2009
Pupamon nayung	AB428477	–	Shih et al. 2009
Ryukyum yaeyamense	AB428458	–	Shih et al. 2009
Semicirculara lincangense	MH045059	–	Chu et al. 2018a
Shanphusa curtobates	AB428478	–	Shih et al. 2009
Sinolapotamon anacoluthon	AB428453	–	Shih et al. 2009
Socotrapotamon nojidense	AB428493	–	Shih et al. 2009
Tenuilapotamon latilum	AB428468	–	Shih et al. 2009
Tenuipotamon huaningense	AB428491	–	Shih et al. 2009
Thaiphusa sp.	AB428474	–	Shih et al. 2009
Tomaculamon pygmaeus	AB428473	–	Shih et al. 2009
Trichopotamon daliense	AB428492	–	Shih et al. 2009
Yarepotamon gracilipa	AB428452	–	Shih et al. 2009
Yuebeipotamon calciatile	LC176064	–	Huang et al. 2016

The first 25% of MCMC chains were discarded as burn-in. The sampled parameters and convergence of four MCMC chains were investigated using TRACER 1.6 (Rambaut et al. 2014). The effective sampling sizes for all parameters were more than 200. Bootstrap support (BS) and Bayesian posterior probability (BPP) were used to assess statistical support.

Results

Taxonomy

Family Potamidae Ortmann, 1896
Subfamily Potamiscinae Bott, 1970
Genus *Eosamon* Yeo & Ng, 2007

***Eosamon daiae* Zhang & Sun, sp. nov.**
http://zoobank.org/3753C63F-4E88-4650-AC9D-D21A2A8880B7
Figs 2–6

Material examined. *Holotype*: China • 1 male, 26.6 × 22.2 mm, NNU 190503; Yunnan Province, Dehong Prefecture, Longchuan County, Longba Town, Bangyang Village; 24°18'15"N, 97°47'56"E; 998 m a.s.l.; 5 May 2019; leg. Xiyang Hao & Zewei Zhang. ***Paratypes*:** China • 1 female, 20.1 × 16.5 mm, NNU 190505; same data as holotype • 1 male, 24.8 × 20.4 mm, NNU 190504; same data as holotype. Other material: China • 3 males, 20.9 × 17.5 mm, NNU 190401, 23.0 × 19.3 mm, NNU 190402, 21.5 × 17.8 mm, NNU 190403; same data as holotype. CHINA • 1 female, 19.7 × 16.5 mm, NNU 190407; Yunnan Province, Ruili City, Nongdao Town, Dengga Village; 23°55'51"N, 97°47'56"E; 887 m a.s.l.; 4 May 2019, leg. Xiyang Hao & Zewei Zhang.

Comparative material. *Eosamon tumidum* (Wood-Mason, 1871): China • 1 male, 23.2 × 18.7 mm, IZCAS CB11382; Yunnan Province, Sipaishan; 1964; *Eosamon tengchongense* (Dai & Chen, 1985): China • 1 male, 37.9 × 30.1 mm, NNU 193261; Yunnan Province, Lianghe County; 9 May 2019; leg. Xiyang Hao & Zewei Zhang; *Eosamon lushuiense* (Dai & Chen, 1985): China • 1 male, 23.7 × 19.9 mm, NNU 162821; Yunnan Province, Lushui City; 4 May 2016; leg. Kelin Chu, Pengfei Wang & Hongying Sun.

Diagnosis. Carapace slightly broader than long, dorsal surface strongly convex, densely pitted (Fig. 2A). Third maxilliped exopod reaching proximal 1/3 of merus length, with long flagellum (Fig. 3A). Male pleon triangular, lateral margin almost straight (Fig. 2C), G1 subterminal segment broad, terminal segment relatively short, clearly sinuous, inferior margin of terminal segment straighter than superior margin, tip of terminal segment gradually tapering to a sharp tip (Fig. 3F), subterminal segment about 3.3 times as long as terminal segment (Fig. 3B, C). G1 strongly curved outwards, not reaching pleonal locking mechanism *in situ* (Fig. 3E). Female pleon ovate (Fig. 4A), vulvae on suture between thoracic sternites 5/6, ovate, opening inner upwards, vulvar cover margin slightly arched (Fig. 4B).

Description. Carapace about 1.2 times broader than long (N = 6), subquadrate, dorsal surface strongly convex transversely and longitudinally, punctate, smooth, regions distinctly defined (Fig. 2A); anterolateral region lined with granules; posterolateral margin with rugae (Fig. 2A); cervical groove and H-shaped groove between gastric and cardiac regions deep, distinct (Fig. 2A). Epigastric region distinct, separated by

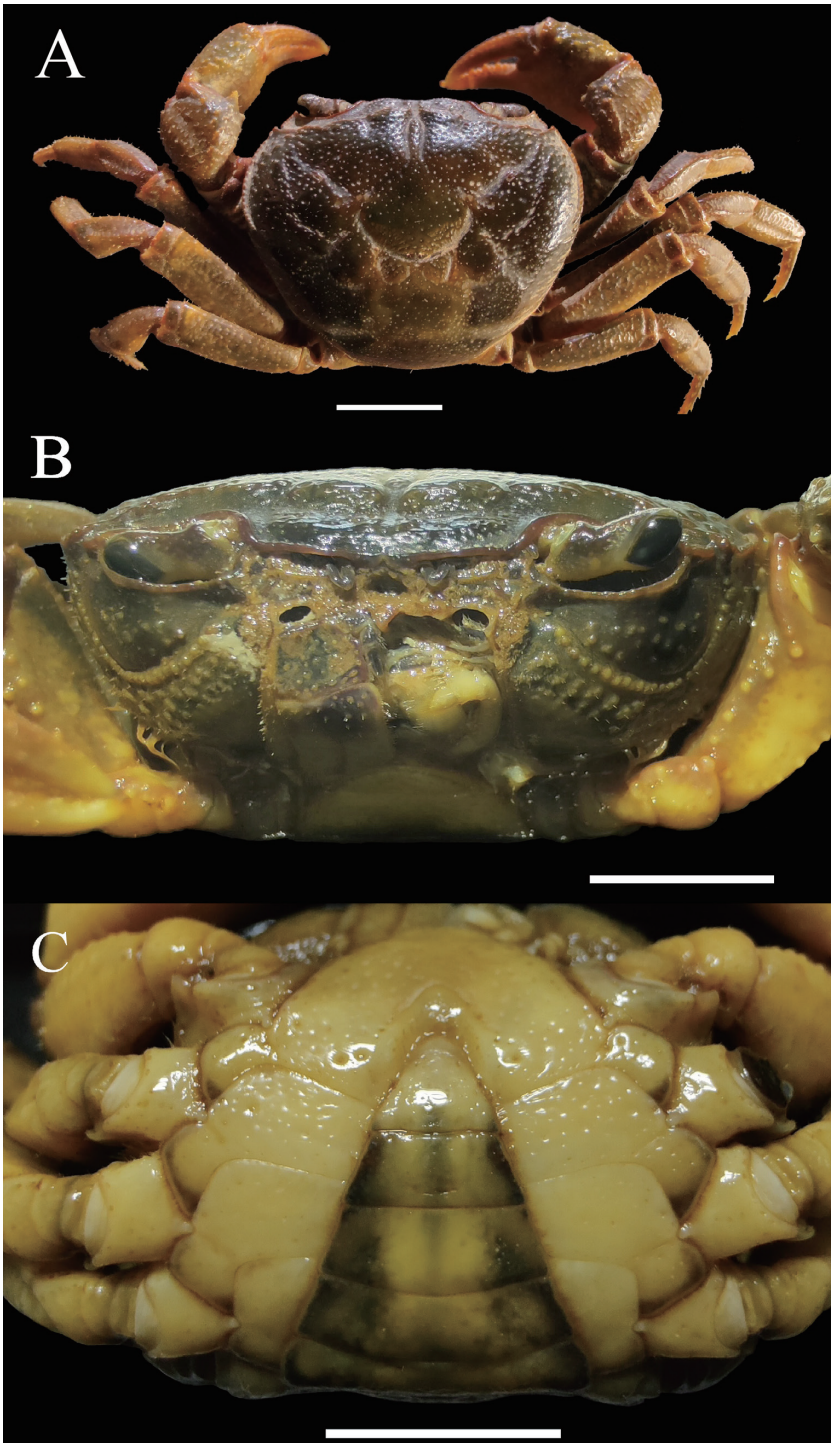

Figure 2. *Eosamon daiae* sp. nov. holotype, male, 26.6 × 22.2 mm, NNU 190503 **A** dorsal view **B** frontal view of cephalothorax **C** ventral view showing anterior thoracic sternum and pleon. Scale bars: 1.0 cm.

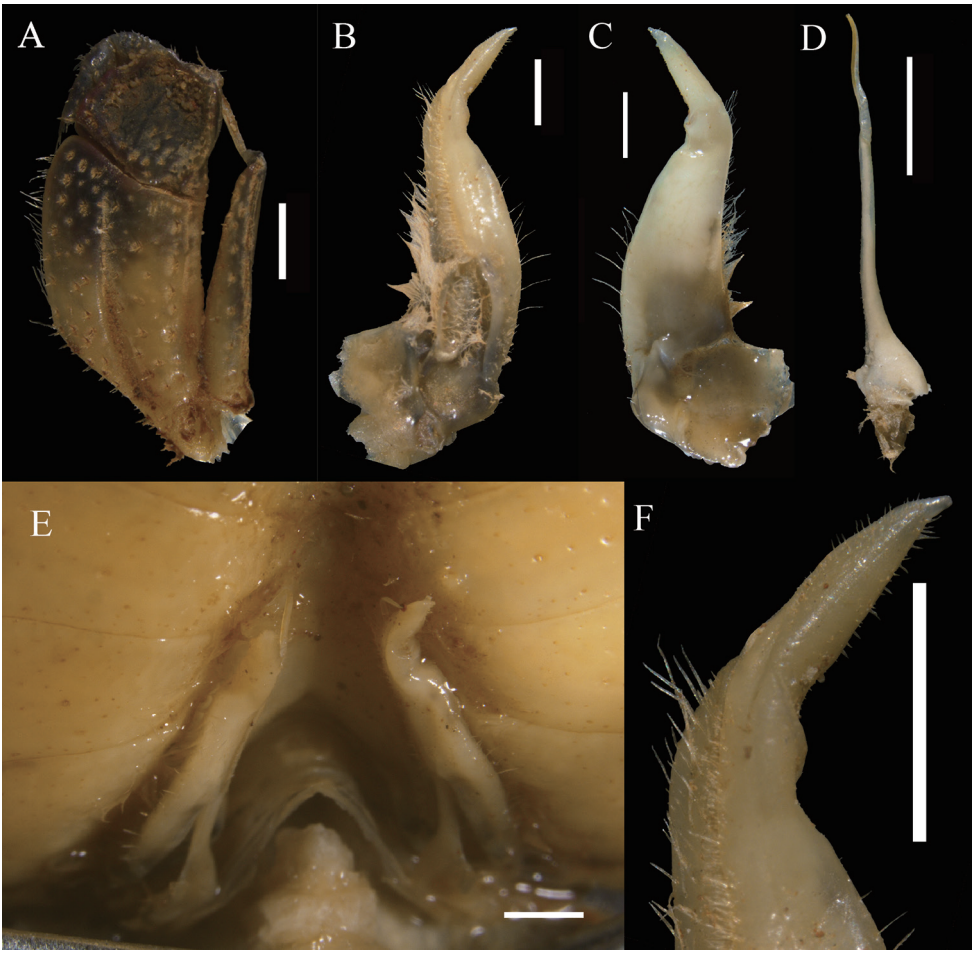

Figure 3. *Eosamon daiae* sp. nov. holotype, male, 26.6 × 22.2 mm, NNU 190503 **A** left third maxilliped **B** left G1 (ventral view) **C** left G1 (dorsal view) **D** left G2 **E** sterno-abdominal cavity with G1 *in situ* **F** G1 terminal segment (ventral view). Scale bars: 1.0 mm.

narrow groove (Fig. 2A). Postfrontal lobe slightly convex, separated medially by Y-shaped groove extending to frontal region (Fig. 2A). Front deflexed downwards, postorbital region distinctly concave (Fig. 2A, B). Dorsal orbital margin ridged, external orbital angle triangular, epibranchial tooth pointed, clearly demarcated from external orbital tooth by gap; supraorbital and infraorbital margins cristate (Fig. 2A, B). Branchial regions relatively flat, smooth with dense dots (Fig. 2A). Pterygostomial regions smooth with several granules; epistome lateral margins sinuous; median lobe triangular (Fig. 2B).

Third maxilliped merus about 1.2 times as broad as long, trapezoidal, with median depression; ischium about 1.2 times as long as broad, rectangular, with distinct median sulcus; exopod reaching proximal 1/3 of merus length with flagellum (Fig. 3A).

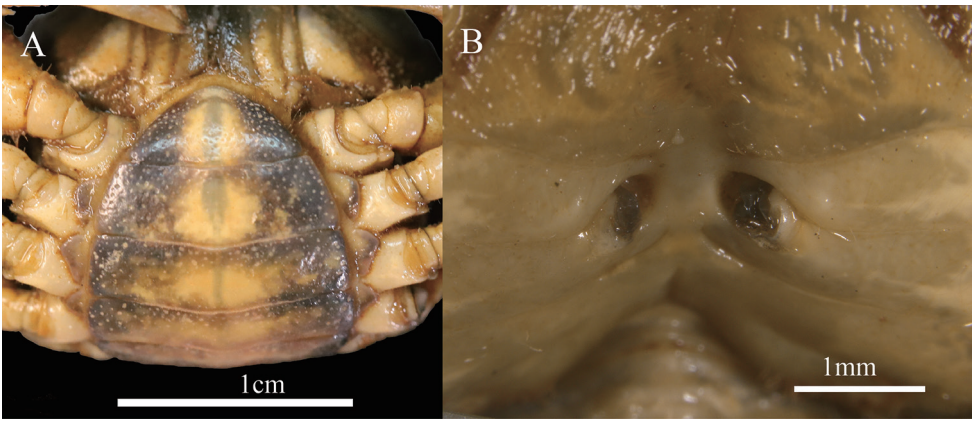

Figure 4. *Eosamon daiae* sp. nov. paratype, female, 20.1 × 16.5 mm, NNU 190505 **A** abdomen **B** vulvae. Scale bars: 1.0 cm (**A**); 1.0 mm (**B**).

Chelipeds slightly unequal; merus trigonal in cross section, margins crenulated (Fig. 2A); carpus with sharp spine on inner-distal angle, with spinule at base and striae (Fig. 2A); manus of major chela with convex granules, about 1.5 times as long as high (Fig. 2A); dactylus bent inwards (Fig. 2A), gap narrow when fingers closed, cutting edge lined with irregular sized teeth (Fig. 2A).

Ambulatory legs relatively stout, dactylus slender with spine-like setae (Fig. 2A); second ambulatory leg merus about 1.3 times as long as dactylus; last leg with propodus about 1.7 times as long as broad, slightly shorter than dactylus (Fig. 2A).

Male thoracic sternum generally smooth and pitted; sternites 3, 4 fused without median suture (Fig. 2C). Female thoracic sternum wider, sutures the same as male.

Male pleon triangular, third somite widest; sixth somite about 2.2 times broader than long; telson triangular, with about 1.3 times as broad as long; the lateral margin of pleon almost straight (Fig. 2C); sterno-pleonal cavity reaching anteriorly to level of mid-length of cheliped coxae bases, broad, deep, median longitudinal groove between sternites 7, 8 long (Fig. 3E). Female pleon ovate, surface pitted; sixth somite about 2.8 times as broad as long; telson semicircular, terminal gently protuberant, about 2.3 times as broad as long (Fig. 4A).

G1 stout, tip of terminal segment not reaching pleonal locking mechanism *in situ* (Fig. 3E); subterminal segment stout, about 3.3 times as long as terminal segment (Fig. 3B, C); G1 terminal segment cone-shape, bent outwards, inferior margin of terminal segment straighter than superior margin, tip of G1 terminal segment gradually tapering to sharp tip (Fig. 3F). G2 slightly longer than G1, basal segment about 2.1 times as long as distal segment (Fig. 3D). Female vulvae on suture between thoracic sternites 5/6, ovate, opening inwards towards the median of the cavity, vulvar cover slightly arched (Fig. 4B).

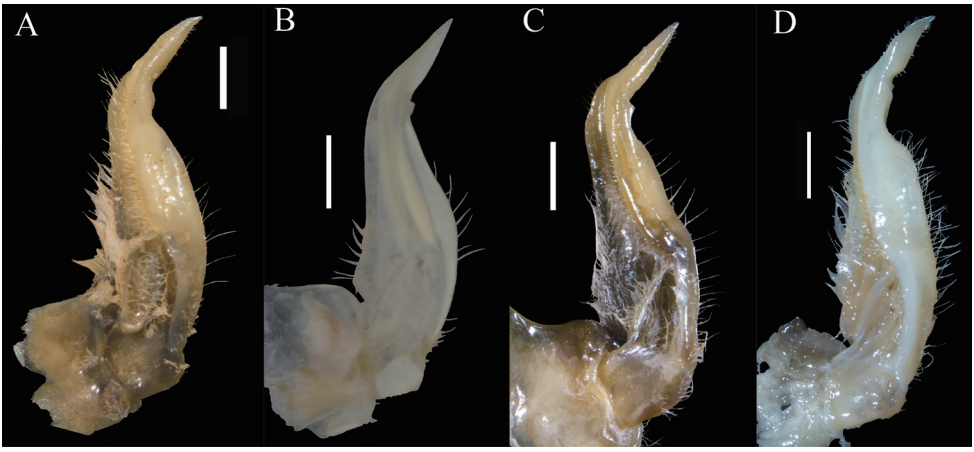

Figure 5. The ventral view of left G1 **A** *Eosamon daiae* sp. nov. holotype, male, 26.6 × 22.2 mm, NNU 190503 **B** *Eosamon tumidum*, male, 23.2 × 18.7 mm, IZCAS CB11382 **C** *Eosamon lushuiense*, male, 23.7 × 19.9 mm, NNU 162821 **D** *Eosamon tengchongense*, male, 37.9 × 30.1 mm, NNU 193261. Scale bars: 1.0 mm.

Figure 6. Habitat of *Eosamon daiae* sp. nov., the moist mud burrows at the type locality, Tianbao Town, Yunnan Province, China.

Live coloration. Carapace is usually dark brown, while chelipeds and ambulatory legs are usually light brown in life.

Etymology. The species is named after the late Prof. Aiyun Dai, who made a huge contribution to freshwater crab studies in China during her lifetime.

Remarks. *Eosamon daiae* sp. nov. can be distinguished from other *Eosamon* species by the combination of male abdomen with straight lateral margins, relatively broad G1 subterminal segment, conical and straight G1 terminal segment, the superior margin of G1 terminal segment curved and the inferior margin of G1 terminal segment comparatively straight.

Eosamon daiae sp. nov. is morphologically and geographically closest to *E. tumidum* (Wood-Mason, 1871), *E. tengchongense* (Dai & Chen, 1985) and *E. lushuiense* (Dai & Chen, 1985). These species are characterized by a male abdomen with straight lateral margins and superficially similar G1 structure (Fig. 5). But *Eosamon daiae* sp. nov. can be distinguished by the fact that the superior margin of G1 terminal segment is curved and the inferior margin is comparatively straight (Fig. 3F, 5A) (versus superior margin comparatively straight and inferior margin slightly curved in both *E. tumidum* and *E. lushuiense*, Fig. 5B, C; outer and inner margins all comparatively curved in *E. tengchongense*, Fig. 5D); the distal part of G1 subterminal segment slightly sunken (Fig. 5A) (versus barely sunken in *E. tumidum*, Fig. 5B, prominently sunken in *E. tengchongense*, Fig. 5D). Other characters as shown in Table 2.

Distribution and habitat. *Eosamon daiae* sp. nov. was found in Bangyang Village (24°18'15"N, 97°47'56"E, 998 m a.s.l.), Longba Town, Longchuan County and Dengga Village (23°55'51"N, 97°47'56"E, 887 m a.s.l.), Nongdao Town, Ruili City, Dehong Prefecture in the frontier of Yunnan, China (Fig. 1). They reside in moist mud burrows on the ridge of field and under low bushes (Fig. 6).

The new species was found not distant from localities with *E. tengchongense*. *Indochinamon* dominates the areas surrounding the new species, with *I. edwardsi*, *I. andersonianum*, *I. boshanense* and *I. gengmaense* having been recorded.

Table 2. Morphological differences for *Eosamon daiae* sp. nov., *Eosamon tumidum*, *Eosamon lushuiense* and *Eosamon tengchongense*.

Character	*E. daiae* sp. nov.	*E. tumidum* (cf. Dai 1999: pl. 174 fig. 91)	*E. lushuiense* (cf. Dai 1999: pl. 175 fig. 92)	*E. tengchongense* (cf. Dai 1999: pl. 177 fig. 93)
Carapace	Strongly convex (Fig. 2A, B)	Slightly convex	Slightly convex	Slightly convex
Margins of G1 terminal segment	superior margin Curved, inferior margin comparatively straight (Fig. 5A)	superior margin comparatively straight, inferior margin slightly curved (Fig. 5B)	superior margin comparatively straight, inferior margin slightly curved (Fig. 5C)	superior margin and inferior margin, comparatively curved (Fig. 5D)
Distal part of G1 subterminal segment	slightly sunken (Fig. 5A)	barely sunken (Fig. 5B)	slightly sunken (Fig. 5C)	obviously sunken (Fig. 5D)
Ratio of G1 subterminal segment to terminal segment	3–3.3	3.2	2.9	3.1

Genus *Indochinamon* Yeo & Ng, 2007

***Indochinamon malipoense* Zhang & Sun sp. nov.**
http://zoobank.org/6B741968-8048-454C-8040-50D3BC581A5F
Figs 7–10

Material examined. *Holotype*: China • 1 male, 53.0 × 42.7 mm, NNU 180505; Yunnan Province, Wenshan Prefecture, Malipo County, Tianbao Town, Bajiaoping Village; 22°58'53"N, 104°50'27"E; 1075 m a.s.l.; 5 April 2018; leg. Zhan Zhang, Zewei Zhang & Hongying Sun. ***Paratypes*:** China • 1 female, 48.0 × 38.2 mm, NNU 180603; Yunnan Province, Wenshan Prefecture, Malipo County, Babu Town; 23°13'29"N, 104°54'04"E; 550 m a.s.l.; 6 April 2018, leg. Zhan Zhang, Zewei Zhang & Hongying Sun • 2 males, 63.2 × 49.0 mm, NNU 180501, 60.5 × 48.0 mm, NNU 180506, same data as holotype.

Comparative material. *Indochinamon changpoense* Dai, 1995: China • 1 male, 44.1 × 35.6 mm, NNU 161701; Yunnan Province, Jinping County Changpotou; 17 May 2016; leg. Kelin Chu, Pengfei Wang & Hongying Sun; *Indochinamon tannanti* Rathbun, 1904: China • 1 male, 43.3 × 34.9 mm, NNU 180801; Yunnan Province, Hekou County; 8 April 2018; leg. Zhan Zhang, Zewei Zhang & Hongying Sun.

Diagnosis. Carapace broader than long, dorsal surface glabrous, gently convex; regions indistinctly defined; anterolateral margin lined with obvious granules (Fig. 7A). Third maxilliped exopod with flagellum (Fig. 8A). Male pleon triangular, lateral margin of sixth somite distinctly convex; telson triangular, tip rounded (Fig. 7C); G1 terminal segment distinctly curved, subterminal segment about 3.2 times as long as terminal segment (Fig. 8B, C); G1 strongly curved outwards, not reaching pleonal locking mechanism *in situ* (Fig. 8E). Female pleon ovate (Fig. 9A), vulvae on thoracic sternite 6, subrotund, opening inner, ventrolateral margin arched distinctly (Fig. 9B).

Description. Carapace about 1.2 – 1.3 times broader than long ($N = 4$), subtrapezoidal, dorsal surface gently convex, glabrous; anterolateral region lined with granules, border with spinose granulation (Fig. 7A); cervical groove shallow, inconspicuous; H-shaped groove between gastric and cardiac regions shallow but distinct (Fig. 7A). Front slightly deflexed, with anterior border emarginated medially (Fig.7A, B); postfrontal lobe distinctly convex, separated medially by Y-shaped groove; postorbital cristae obviously convex, separated from postfrontal lobe by distinct groove (Fig. 7A); postorbital region distinctly concave (Fig. 7A, B). Posterolateral margin comparatively smooth with few rugae; branchial regions relatively flat, smooth (Fig. 7A). External orbital angle acutely triangular; epibranchial tooth with sharp protuberance, separated from external orbital angle by distinct cleft (Fig. 7A). supraorbital, infraorbital margins cristate; pterygostomial regions comparatively smooth with several granules (Fig. 7B). Epistome superior margin cristate, inferior margin slightly curved with median triangle (Fig. 7B).

Ischium of third maxilliped elongate rectangular, about 1.3 times longer than broad, with distinct, longitudinal median sulcus; merus trapezoidal, about 1.1 times

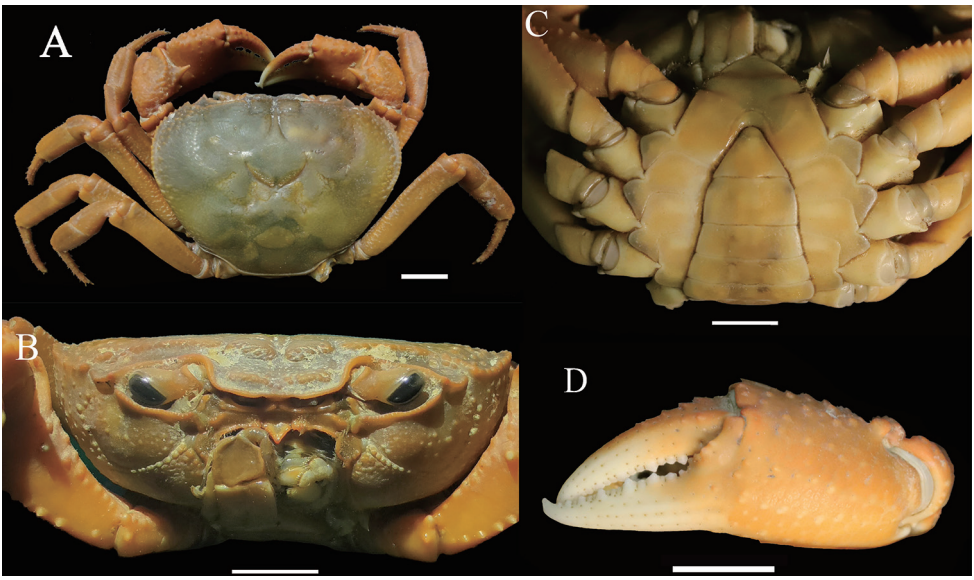

Figure 7. *Indochinamon malipoense* sp. nov. holotype, male, 53.0 × 42.7 mm, NNU 180505 **A** dorsal view **B** frontal view of cephalothorax **C** ventral view showing anterior thoracic sternum and pleon **D** outer surfaces of left major chela. Scale bars: 1.0 cm.

broader than long; exopod reaching beyond base of merus slightly, with short flagellum, about half the width of the merus (Fig. 8A).

Chelipeds unequal (Fig. 7A); merus margins crenulated (Fig. 7C); carpus with sharp spine at inner-distal angle, spinules and granules at base (Fig. 7A); outer surface of manus with convex granules, about 1.3 times as long as high; immovable, movable fingers curved inwards, with irregular teeth; gape narrow when fingers closed (Fig. 7D).

Ambulatory legs relatively slender, dactylus slender, with spine-like setae (Fig. 7A); second ambulatory leg merus about 1.8 times as long as dactylus; last leg with propodus about 2.7 times as long as broad, slightly shorter than dactylus (Fig. 7A).

Thoracic sternum glabrous, sternites 1, 2 completely fused to form triangular structure; suture between sternites 2, 3 distinct (Fig. 7C); suture between sternites 3, 4 shallow (Fig. 7C); sterno-pleonal cavity reaching anteriorly to level of mid-length of cheliped coxae bases, median longitudinal groove between sternites 7, 8 long (Fig. 8E). Male pleon triangular, third somite widest; sixth somite width 2.0 times length; telson triangular, width 1.4 times length, tip of telson round (Fig. 7C). Female pleon ovate, smooth, pitted; sixth somite about 2.9 times as broad as long, telson semicircular, about 2.2 times as broad as long (Fig. 9A).

G1 stout, bent; tip of terminal segment not reaching pleonal locking mechanism *in situ* (Fig. 8E); subterminal segment stout, about 3.2 times as long as terminal segment (Fig. 8B, C); terminal segment slender, unciform, clearly curved outwards, inferior and superior margins curved (Fig. 8E, F); base of G1 terminal segment slightly inflated, distal part tapered (Fig. 8F); G2 distinctly longer than G1, subterminal segment about 1.2

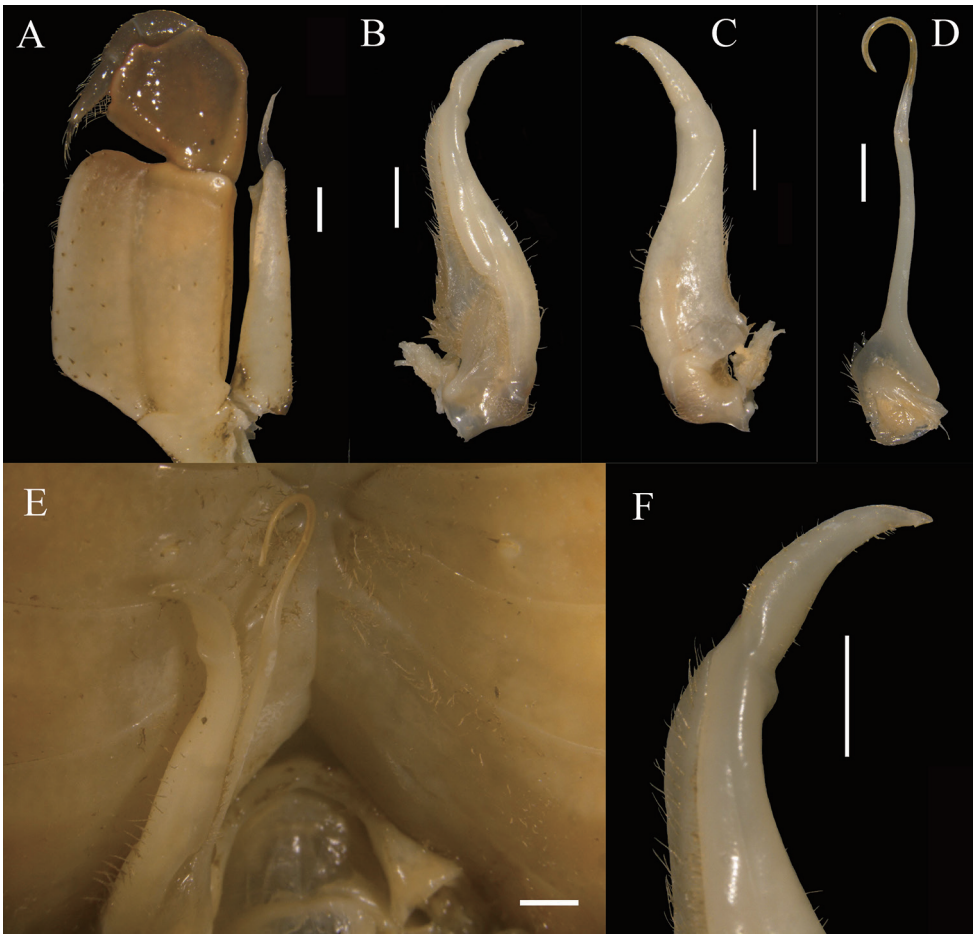

Figure 8. *Indochinamon malipoense* sp. nov. holotype, male, 53.0 × 42.7 mm, NNU 180505 **A** left third maxilliped **B** left G1 (ventral view) **C** left G1 (dorsal view) **D** left G2 **E** sterno-pleonal cavity with right G1 *in situ* **F** left G1 terminal segment (ventral view). Scale bars: 1.0 mm.

times as long as terminal segment (Fig. 8D). Female vulvae on thoracic sternite 6, ovate, opening inwards towards median of cavity, vulvar cover margin slightly arched (Fig. 9B).

Live coloration. The crabs usually have two colors: brownish-red (Fig. 11A) and yellowish-cyan (Fig. 11B). From the type locality, Tianbao Town, both brownish-red and yellowish-cyan crabs have been found, while from Babu Town, only yellowish-cyan crabs have been found. Morphologically, there is no distinct difference between individuals with different colors. Similar color variation also can be seen in another potamid crab, *Geothelphusa pingtung* Tan & Liu, 1998 (Shy et al. 2019).

Etymology. This species is named after the type locality, Malipo County, Yunnan Province, China.

Remarks. Based on the morphology of G1, Ng and Mar (2018) separated *Indochinamon* into several groups. The G1 terminal segment of *I. malipoense* sp. nov. is similar

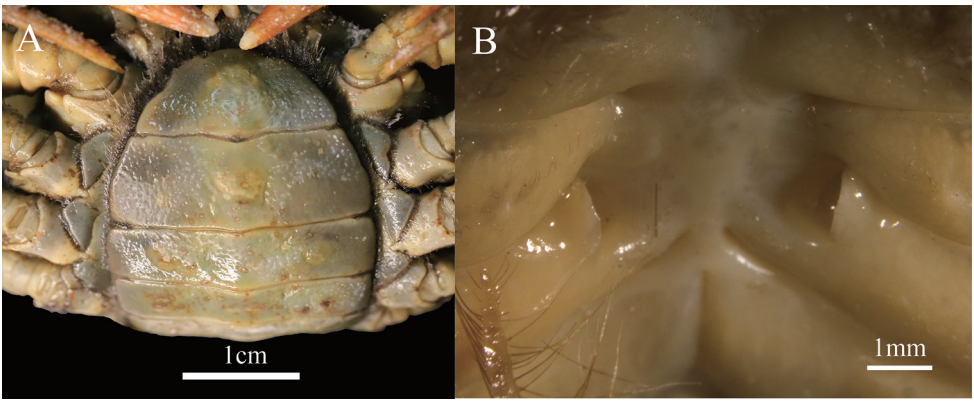

Figure 9. *Indochinamon malipoense* sp. nov. paratype, female, 48.0 × 38.2 mm, NNU 180603 **A** abdomen **B** vulvae.

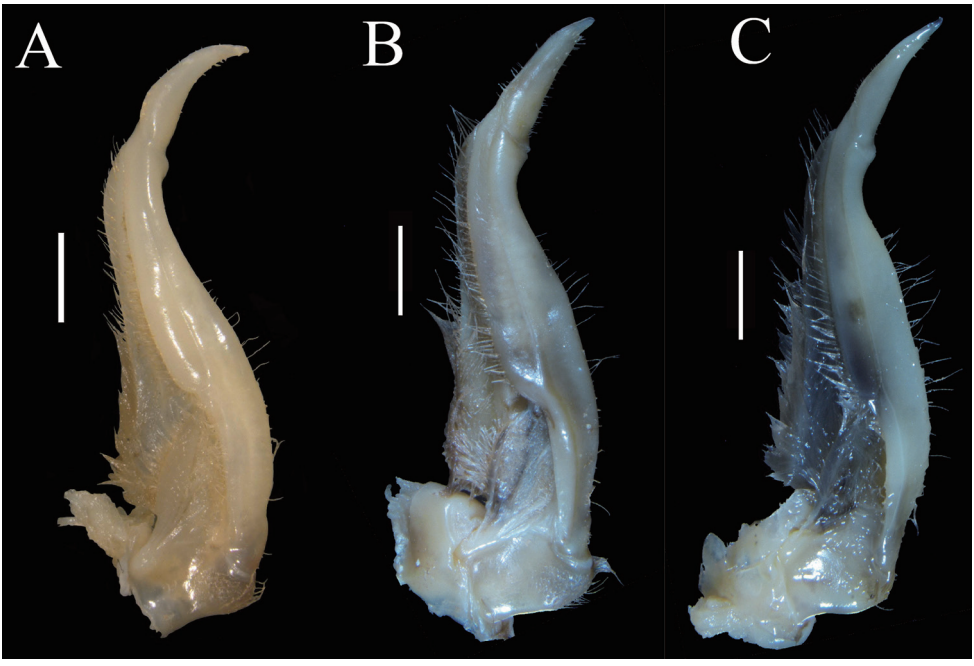

Figure 10. The ventral view of left G1 **A** *Indochinamon malipoense* sp. nov. holotype, male, 53.0 × 42.7 mm, NNU 180505 **B** *Indochinamon tannanti* male, 43.3 × 34.9 mm, NNU 180801 **C** *Indochinamon changpoense* male, 44.1 × 35.6 mm, NNU 161701. Scale bars: 1.0 mm.

to a large group including the type species, *I. villosum* (Yeo & Ng, 1998). Within this group, *I. malipoense* sp. nov. closely resembles *I. ahkense* Naruse, Chia & Zhou, 2018, *I. bavi* Naruse, Nguyen & Yeo, 2011, *I. changpoense* (Dai, 1995), *I. daweishanense* (Dai, 1995), *I. kimboiense* Naruse, Nguyen & Yeo, 2011, *I. orleanis* (Rathbun,

Figure 11. Color in life of *Indochinamon malipoense* sp. nov. **A** brownish-red male **B** yellowish-cyan male. Photographs by Hongying Sun, 5 April 2018, Tianbao Town, Yunnan Province, China.

Table 3. Morphological differences for *Indochinamon malipoense* sp. nov., *Indochinamon tannanti* and *Indochinamon changpoense*.

Character	***I. malipoense* sp. nov.**	***I. tannanti* (cf. Dai 1999: pl. 161 fig. 83)**	***I. changpoense* (cf. Dai 1999: pl. 164 fig. 85)**
carapace	gently convex, regions indistinctly defined (Fig. 7A)	flat, regions distinctly defined	gently convex, regions distinctly defined
G1 terminal segment	obviously curved, unciform (Fig. 10A)	slightly curved, conical, with short, conspicious setae,tip tapering (Fig. 10B)	slightly curved, conical, with few very short setae, dorsal lobe of pleopod opening visible (Fig. 10C)
base of G1 terminal segment	slightly inflated (Fig. 10A)	nearly straight (Fig. 10B)	nearly straight (Fig. 10C)
Ratio of G1 subterminal segment to terminal segment	2.8–3.2	2.7	2.9

1904), *I. ou* (Yeo & Ng, 1998), *I. parpidum* Naruse, Chia & Zhou, 2018, *I. tannanti* (Rathbun, 1904) and *I. yunlongense* (Dai, 1995), as their G1s are gently bent and G1 terminal segments are relatively slender and elongate (cf. Yeo and Ng 1998; Dai 1999; Naruse et al. 2011, 2018; Ng and Mar 2018). But *I. malipoense* sp. nov. can be distinguished from other species by the obviously curved G1 terminal segment.

All *Indochinamon* species have a well-developed flagellum on the exopod of the third maxilliped. The length of the flagellum varies among species. In some species, the flagellum does not exceed the width of the merus, e.g., *I. tannanti*, *I. changpoense*, *I. gengmaense* (Dai, 1995), *I. guttus* (Yeo & Ng, 1998), *I. hispidum* (Wood-Mason, 1871), *I. jinpingense*, *I. mieni* (Dang, 1967) and *I. yunlongense*. In *I. malipoense* sp. nov., the flagellum is about half the width of the merus, which is shorter than that in other species.

The G1 of *I. malipoense* sp. nov. is very similar to *I. tannanti*, *I. changpoense*, *I. ahkense*, and *I. daweishanense*. They are also geographically close. But *I. malipoense* sp. nov. can be distinguished from the similar *I. tannanti* and *I. changpoense* by several characters (Table 3), notably, the carapace regions are indistinctly defined (Fig. 7A)

(versus distinctly defined in *I. tannanti* and *I. changpoense* (Dai 1999)), the G1 terminal segment is obviously curved, unciform (Fig. 10A) (versus slightly curved, conical in both *I. tannanti* and *I. changpoense*, Fig. 10B, C)), the base of the G1 terminal segment is slightly inflated (Fig. 8F) (versus nearly straight in both *I. tannanti* and *I. changpoense*, Fig. 10B, C). The G1 structure of *I. malipoense* sp. nov. is also similar to *I. ahkense* (Naruse et al. 2018: fig. 4) and *I. daweishanense* (Dai 1999: fig. 87) by relatively slender terminal segment. However, the G1 terminal segment is more curved in *I. malipoense* sp. nov. and stronger bent outward in *I. daweishanense*. The carapace of *I. malipoense* sp. nov. is superficially similar to *I. ahkense* by smooth and shallow grooves of the dorsal surface. In *I. ahkense*, the carapace is subquadrate (versus subtrapezoidal in *I. malipoense* sp. nov.) and flatter (versus slightly convex in *I. malipoense* sp. nov.).

In *I. khinpyae*, the carapace and G1 show considerable variations (Ng and Mar 2018). In smaller individuals, the carapace is less sculptured and the G1 terminal segment is shorter and straighter (Ng and Mar 2018). In *I. malipoense* sp. nov., the morphology of the carapace is relatively stable while the ratio of G1 subterminal segment to terminal segment varies in sampled individuals.

Distribution and habitat. *Indochinamon malipoense* sp. nov. was collected from Tianbao Town (22°58'53"N, 104°50'27"E, 1075 m a.s.l.; 22°56'58"N, 104°49'48"E, 223 m a.s.l.; 23°00'07"N, 104°47'42"E, 979 m a.s.l.) and Babu Town (23°13'29"N, 104°54'04"E, 550 m a.s.l.) located in the frontier between China and Vietnam, Malipo County, Wenshan Prefecture in Yunnan, China. They were found under rocks in mountain streams with altitudes of 200–1100 m.

Indochinamon ahkense, *I. changpoense*, *I. daweishanense*, *I. jinpingense*, *I. tannanti* and *Somanniathelphusa brevipodum* Tai, Song, He, Cao, Xu & Zhong, 1975, have been recorded near the distribution areas of *I. malipoense* sp. nov..

Molecular results

In the present phylogenetic analyses, 60 species from 48 genera were included (Table 1). Phylogenetic trees reconstructed using BI and ML resulted in similar topologies. The phylogenetic trees indicate that two new species were placed in the 'Indochina – SW China' clade (Shih et al. 2009) with strong support (Fig. 12). *Eosamon daiae* sp. nov. clusters with *E. tengchongense* and *E. lushuiense* and *Indochinamon malipoense* sp. nov. clusters with *I. tannanti* (Fig. 12).

Discussion

The two new species cluster with several congeneric taxa (but not all), which tentatively supports recognition of the two genera, *Eosamon* and *Indochinamon*, following the systematic revision of Yeo and Ng (2007). However, based on our molecular analyses, *Eosamon* and *Indochinamon* are not monophyletic (Fig. 12). *Eosamon boonyaratae*

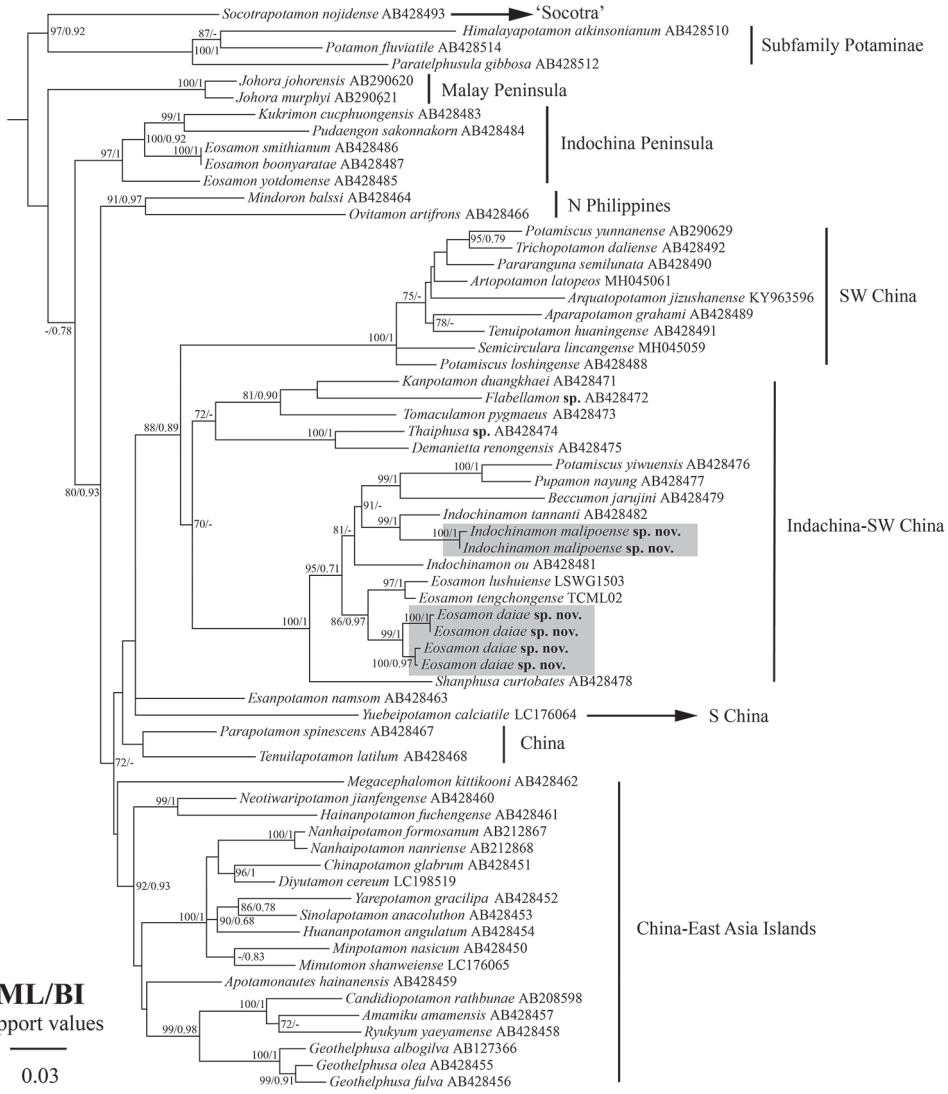

Figure 12. Phylogenetic tree reconstructed based on partial mitochondrial 16S rDNA sequences. The two new species are colored gray. Values at the nodes represent bootstrap (BS) values and posterior probability (BPP) values for ML and BI, respectively. Support values over 70/0.7 (BS/BPP) are provided.

(Naiyanetr, 1987), *E. smithianum* (Kemp, 1923) and *E. yotdomense* (Naiyanetr, 1984) were placed in the 'Indochina' clade instead of the 'Indochina – SW China' clade, suggesting a polyphyletic topological structure for the current composition of *Eosamon* sampled to date. Morphologically, some characters, e.g., carapace dorsally convex and male pleon with straight lateral margins, in *E. daiae* sp. nov., *E. tumidum*, *E. lushuiense* and *E. tengchongense*, distributed in China, also differ from the description of *Eosamon* that was proposed based on specimens of the species distributed in Thailand, Laos and

Vietnam (Yeo and Ng 2007). Several relatives, *Potamiscus yiwuensis* Dai & Cai, 1998, *Pupamon nayung* (Naiyanetr, 1993) and *Beccumon jarujini* (Ng & Naiyanetr, 1993), are nested within the *Indochinamon* clade suggesting that *Indochinamon* is paraphyletic (Fig. 12). Ng and Mar (2018) separated *Indochinamon* into several groups on the basis of their G1 structures. Although only few *Indochinamon* species were included, our molecular results indicate that their classification is still problematic. *Indochinamon tannanti* (Rathbun, 1904) is genetically closer to *Beccumon* Yeo & Ng, 2007, and *Pupamon* Yeo & Ng, 2007, rather than *I. ou* (Yeo & Ng, 1998). Due to the lack of taxa and sampling of molecular markers, we could not delve deeper into these questions in the present study. Further studies are needed to clarify the systematic treatments of *Eosamon* and *Indochinamon*.

Eosamon daiae sp. nov. and *Indochinamon malipoense* sp. nov. are not threatened by human activity. *Eosamon daiae* sp. nov. is distributed in the vicinity of the Tongbiguan Nature Reserve and *Indochinamon malipoense* sp. nov. is distributed in the vicinity of the Laoshan Nature Reserve. In these areas, large-scale developments are strictly regulated.

Yunnan is a global biodiversity hotspot (Myers et al. 2000), and also an important center for global biodiversity and endemism of primary freshwater crabs (Cumberlidge et al. 2011). Generations of scientists have done plenty of species discovery of freshwater crabs in this area (reviewed by Dai 1999; Chu et al. 2018b). However, investigations of freshwater crabs on the Sino-Burmese border, Sino-Vietnamese border and Sino-Lao border have rarely been carried out, because of the proximity of the 'Golden Triangle'. With constant efforts by the governments, conducting field surveys in these areas became possible. Many species have been newly described (e.g., Yu et al. 2019; Zhao et al. 2019; Lin and Li 2020; Zhang et al. 2020). In addition, some old type localities of freshwater crabs from Myanmar, e.g., *Indochinamon andersonianum* (Wood-Mason, 1871), *I. edwardsii* (Wood-Mason, 1871) and *I. hispidum* (Wood-Mason, 1871), are within Yunnan Province, China nowadays due to changes of national boundaries over one hundred years ago (Ng and Mar 2018). To fully understand the biodiversity of freshwater crabs in Yunnan, further investigations are expected in the poorly sampled frontier zones of China.

Acknowledgements

We thank subject editor Dr Kay Van Damme and reviewer Dr Peter K. L. Ng for their constructive criticisms, which greatly improved the manuscript. We also thank Dr Jun Chen and Mr Kaibayier Meng (National Zoological Museum of China, Institute of Zoology, Chinese Academy of Sciences) for permission of comparison of the type specimen with congeners deposited in IZCAS; We thank Zhan Zhang (College of Life Sciences, Nanjing Normal University) for assistance with collecting specimens; Yangqi Lv (College of Life Sciences, Nanjing Normal University) for help with lab work and molecular analyses; Boyang Shi (College of Life Sciences, Nanjing Normal University) for valuable comments on manuscript.

This work was supported by the National Natural Science Foundation of China (No. 31772427) and Ocean Park Conservation Foundation, Hong Kong (No. OT02.1920) to SHY. This work was also supported by Biodiversity Survey Observation and Assessment Program (2019–2023) of the Ministry of Ecology and Environment of China.

References

Chu KL, Zhou LJ, Sun HY (2017) A new genus and new species of freshwater crab (Decapoda: Brachyura: Potamidae Ortmann, 1896) from Yunnan Province, China. Zootaxa 4286(2): 241–253. hhttps://doi.org/10.11646/zootaxa.4286.2.7

Chu KL, Wang PF, Sun HY (2018a) A new genus and species of primary freshwater crab and a new species of *Artopotamon* Dai & Chen, 1985 (Crustacea, Brachyura, Potamidae) from western Yunnan, China. Zootaxa 4422(1): 115–131. https://doi.org/10.11646/zootaxa.4422.1.7

Chu KL, Ma XP, Zhang ZW, Wang PF, Lv LN, Zhao Q, Sun HY (2018b) A checklist for the classification and distribution of China's freshwater Crabs. Biodiversity Science 26(3): 274–282. [in Chinese with English summary]https://doi.org/10.17520/biods.2018062

Crandall KA, Fitzpatrick JF (1996) Crayfish molecular systematics: using a combination of procedures to estimate phylogeny. Systematic Biology 45(1): 1–26. https://doi.org/10.1093/sysbio/45.1.1

Cumberlidge N, Ng PKL, Yeo DCJ, Naruse T, Meyer KS, Esser LJ (2011) Diversity, endemism and conservation of the freshwater crabs of china (Brachyura: Potamidae and Gecarcinucidae). Integrative Zoology 6(1): 45–55. https://doi.org/10.1111/j.1749-4877.2010.00228.x

Dai AY (1999) Fauna Sinica. Arthropoda: Crustacea: Malacostraca: Decapoda: Parathelphusidae, Potamidae. Science Press, Beijing. [in Chinese with English summary]

Guinot D, Tavares M, Castro P (2013) Significance of the sexual openings and supplementary structures on the phylogeny of brachyuran crabs (Crustacea, Decapoda, Brachyura), with new nomina for higher-ranked podotreme taxa. Zootaxa 3665(1): 1–414. https://doi.org/10.11646/zootaxa.3665.1.1

Huang C, Shih HT, Mao SY (2016) *Yuebeipotamon calciatile*, a new genus and new species of freshwater crab (Crustacea: Decapoda: Brachyura: Potamidae) from southern China. ZooKeys 615: 61–72. https://doi.org/10.3897/zookeys.615.9964

Kalyaanamoorthy S, Minh BQ, Wong TK, von Haeseler A, Jermiin LS (2017) ModelFinder: fast model selection for accurate phylogenetic estimates. Nature methods 14(6): 587–589. https://doi.org/10.1038/nmeth.4285

Katoh K, Standley DM (2013) MAFFT multiple sequence alignment software version 7: improvements in performance and usability. Molecular Biology and Evolution 30(4): 772–780. https://doi.org/10.1093/molbev/mst010

Lin Y, Li S (2020) Two new genera and eight new species of jumping spiders (Araneae, Salticidae) from Xishuangbanna, Yunnan, China. ZooKeys 952: 95–128. https://doi.org/10.3897/zookeys.952.51849

Minh BQ, Nguyen MAT, von Haeseler A (2013) Ultrafast approximation for phylogenetic bootstrap. Molecular biology and evolution 30(5): 1188–1195. https://doi.org/10.1093/molbev/mst024

Myers N, Mittermeier RA, Mittermeier CG, Fonseca GAB, Kent J (2000) Biodiversity hotspots for conservation priorities. Nature 403: 853–858. https://doi.org/10.1093/sysbio/syp006

Naruse T, Nguyen XQ, Yeo DCJ (2011) Three new species of *Indochinamon* Yeo & Ng, 2007 (Crustacea: Brachyura: Potamoidea: Potamidae) from Vietnam, with a redescription of *Ranguna* (*Ranguna*) *kimboiensis* Dang, 1975. Zootaxa 2732(1): 33–48. https://doi.org/10.11646/zootaxa.2732.1.3

Naruse T, Chia JE, Zhou XM (2018) Biodiversity surveys reveal eight new species of freshwater crabs (Decapoda: Brachyura: Potamidae) from Yunnan Province, China. PeerJ 6: e5497. https://doi.org/10.7717/peerj.5497

Ng PKL, Mar W (2018) On a new species of freshwater crab, *Indochinamon khinpyae*, from northern Myanmar (Crustacea, Brachyura, Potamidae). ZooKeys (811): 1–47. https://doi.org/10.3897/zookeys.811.29187

Nguyen LT, Schmidt HA, von Haeseler A, Minh BQ (2015) IQ-TREE: a fast and effective stochastic algorithm for estimating maximum-likelihood phylogenies. Molecular biology and evolution 32(1): 268–274. https://doi.org/10.1093/molbev/msu300

Nylander JAA (2004) MrModeltest v2. Program distributed by the author.

Rambaut A, Suchard MA, Xie D, Drummond AJ (2014) Tracer v1.6. http://beast.bio.ed.ac.uk/Tracer

Ronquist F, Teslenko M, van der Mark P, Ayres DL, Darling A, Höhna S, Larget B, Liu L, Suchard MA, Huelsenbeck JP (2012) MrBayes 3.2: efficient Bayesian phylogenetic inference and model choice across a large model space. Systematic Biology 61: 539–542. https://doi.org/10.1093/sysbio/sys029

Shih H-T, Ng PKL (2011) Diversity and biogeography of freshwater crabs (Crustacea: Brachyura: Potamidae, Gecarcinucidae) from East Asia. Systematics and Biodiversity 9(1): 1–16. https://doi.org/10.1080/14772000.2011.554457

Shih H-T, Yeo DCJ, Ng PKL (2009) The collision of the Indian Plate with Asia: molecular evidence for its impact on the phylogeny of freshwater crabs (Brachyura: Potamidae). Journal of Biogeography 36: 703–719. https://doi.org/10.1111/j.1365-2699.2008.02024.x

Shih H-T, Hung HC, Schubart CD, Chen CA, Chang HW (2006) Intraspecific genetic diversity of the endemic freshwater crab *Candidiopotamon rathbunae* (Decapoda, Brachyura, Potamidae) reflects five million years of the geological history of Taiwan. Journal of Biogeography 33(6): 980–989. https://doi.org/10.1111/j.1365-2699.2006.01472.x

Shy J-Y, Shih H-T, Ng PKL (2019) Crustacean Fauna of Taiwan: Brachyuran Crabs. Volume 3 – Freshwater crabs – Potamidae, Gecarcinucidae. National Penghu University of Science and Technology, Taiwan.

Van TD, Nguyen TC, Le HA (2016) A new species of the genus *Indochinamon* Yeo & Ng, 2007 (Crustacea: Brachyura: Potamoidea: Potamidae) from northern Vietnam. Raffles Bulletin of Zoology 64.

Yeo DCJ (2010) A new species of *Eosamon* from southern Vietnam (Brachyura, Potamidae), with notes on *E. brousmichei* (Rathbun, 1904). Studies on Malacostraca: Lipke Bijdeley Holthuis Memorial Volume. Brill, 747–754. https://doi.org/10.1163/9789047427759_056

Yeo DCJ, Ng PKL (1998) Freshwater crabs of the *Potamon tannanti* species group (Crustacea: Decapoda: Brachyura: Potamidae) from northern Indochina. Raffles Bulletin of Zoology 46(2): 627–650.

Yeo DCJ, Ng PKL (2007) On the genus "*Potamon*" and allies in Indochina (Crustacea: Decapoda: Brachyura: Potamidae). Raffles Bulletin of Zoology 16(2): 273–308.

Yeo DCJ, Shih H-T, Meier R, Ng PKL (2007) Phylogeny and biogeography of the freshwater crab genus *Johora* (Crustacea: Brachyura: Potamidae) from the Malay Peninsula, and the origins of its insular fauna. Zoologica Scripta 36(3): 255–269. https://doi.org/10.1111/j.1463-6409.2007.00276.x

Yu G, Wu Z, Yang J (2019) A new species of the *Amolops monticola* group (Anura: Ranidae) from southwestern Yunnan, China. Zootaxa 4577(3): 548–560. https://doi.org/10.11646/zootaxa.4577.3.8

Zhang XS, Guo JJ, Yi TC, Jin DC (2020) Two new species of the genus *Onchodellus* (Acari: Pachylaelapidae) from China. Zootaxa 4801(3): 450–460. https://doi.org/10.11646/zootaxa.4577.3.8

Zhao X, Yao Z, Song Y, Li S (2019) Two new species of the spider genus *Belisana* Thorell (Araneae: Pholcidae) from Xishuangbanna, Yunnan, China. Zootaxa 4603(3): 559–567. https://doi.org/10.11646/zootaxa.4603.3.8

ZooKeys 980: 23–42 (2020)
doi: 10.3897/zookeys.980.54100
https://zookeys.pensoft.net

RESEARCH ARTICLE

A peer-reviewed open-access journal
ZooKeys
Launched to accelerate biodiversity research

The terrestrial microsnail genus *Aulacospira* Möllendorff, 1890 (Eupulmonata, Stylommatophora, Hypselostomatidae) in Thailand with key to Thai species

Pongrat Dumrongrojwattana[1], Kitti Tanmuangpak[2]

1 *Department of Biology, Faculty of Science, Burapha University, Bangsaen, Chonburi 20131 Thailand*
2 *Program of Biology, Department of Science, Faculty of Science and Technology, Loei Rajabhat University, Loei 42000 Thailand*

Corresponding author: Pongrat Dumrongrojwattana (pongrat@buu.ac.th)

Academic editor: M. Schilthuizen | Received 9 May 2020 | Accepted 9 September 2020 | Published 28 October 2020

http://zoobank.org/78EED563-089C-4804-A910-87DAF1B3D2EB

Citation: Dumrongrojwattana P, Tanmuangpak K (2020) The terrestrial microsnail genus *Aulacospira* Möllendorff, 1890 (Eupulmonata, Stylommatophora, Hypselostomatidae) in Thailand with key to Thai species. ZooKeys 980: 23–42. https://doi.org/10.3897/zookeys.980.54100

Abstract

Thai terrestrial microsnails in the genus *Aulacospira* Möllendorff, 1890 are revised based on the collection of the Zoological Research Collection, Burapha University, Chonburi Province, Thailand and recently collected material. Three new species are described: *Aulacospira nutadhirai* sp.nov. from Southern Thailand, and *Aulacospira tekavongae* **sp.nov.** and *Aulacospira vanwalleghemi* **sp. nov.** from Eastern Thailand. The radula and genital system are described, and a key to Thai species is presented.

Keywords

new species, taxonomy

Introduction

Microsnails in the genus *Aulacospira* Möllendorff, 1890 were first described by Möllendorff in 1890 from the Philippines where there are six species: *A. hololoma* (Möllendorff, 1887), *A. mucronata* (Möllendorff, 1887), *A. scalatella* (Möllendorff, 1888), *A. porrecta* Quadras & Möllendorff, 1894, *A. triptycha* Quadras & Möllendorff, 1895 and

A. rhombostoma Quadras & Möllendorff, 1896. Two species, *A. lampangensis* Panha & Burch, 2001 and *A. smaesarnensis* Panha & Burch, 2001 were described from Thailand by Panha and Burch (2001), but subsequent work by Panha et al. (2004), Dumrongrojwattana and Panha (2005, 2006), and Dumrongrojwattana (2008) increased the number of species to seven with the addition of *A. pluangtong* Panha & Burch, 2004 , *A. khaopratun* Dumrongrojwattana & Panha, 2005, *A. khaobote* Dumrongrojwattana & Panha, 2006, *A. depressa* Dumrongrojwattana & Panha, 2006, and *A. panhai* Dumrongrojwattana, 2008. Of the known Thailand species, only *A. lampangensis* is known from the north of the country and all other species are restricted to eastern Thailand (Panha and Burch 2005, Dumrongrojwattana and Panha 2006, Dumrongrojwattana, 2008) (Table 1). Most of previous taxonomic studies on *Aulacospira* were based only on shell morphology (Pilsbry 1916–1918; Panha et al. 2004; Panha and Burch 2005; Dumrongrojwattana and Panha 2005, 2006; Dumrongrojwattana 2008; Vermeulen et al. 2007; Páll-Gergely et al. 2019), and there is no information on the radula and genital system. We provide an overview of the Thai *Aulacospria* and describe three new species from eastern and southern Thailand based on the shell morphology, radula, and genital system. A key to Thai species is presented.

Materials and methods

Types and voucher specimens of previously described species were deposited in the reference collection of the Zoology Laboratory, Faculty of Science, Burapha University. The new species were collected from limestone hills in eastern Thailand. Collecting sites and their distribution shown in Figure 1. Shells were digitally photographed using a Cannon MP–E. Shell terminology (e.g., whorl number, apertural teeth, etc.) follows Panha and Burch (2005). Shell measurements (in mm) were taken by using a digital vernier caliper (Mitutoyo, Japan). Taxonomic identification of specimens was based mainly on Panha and Burch (2005), Dumrongrojwattana and Panha (2005, 2006), and Dumrongrojwattana (2008). Dichotomous key construction was based on shell morphology. The radula was exacted by boiling the dead snail in 1.0% NaOH for 1–2 minutes in a small test tube. The contents of the test tube were transfered into a small petri dish and radula removed under an Olympus SZ51 stereomicroscope. The radula was washed in three changes of distilled water, 3 minutes per rinse, and then dehydrated in an ethyl alcohol series of 10%, 30%, 50% and 70% v/v for 5 minutes in each concentration. The radula was then air-dried on a stub and scanned using an LEO 1450 VP scanning electron microscope at the Microscopic Center, Faculty of Science, Burapha University, Chonburi Province. Adult snails were also dissected to examine the genital system.

The following abbreviations are used in the text and figures: leg. = collected by, H = shell height, W = shell width, W/H = shell width/height ratio, ag = albumen gland, at = atrium, e = epiphallus, erc = epiphallic retractor caecum, fo = free oviduct,

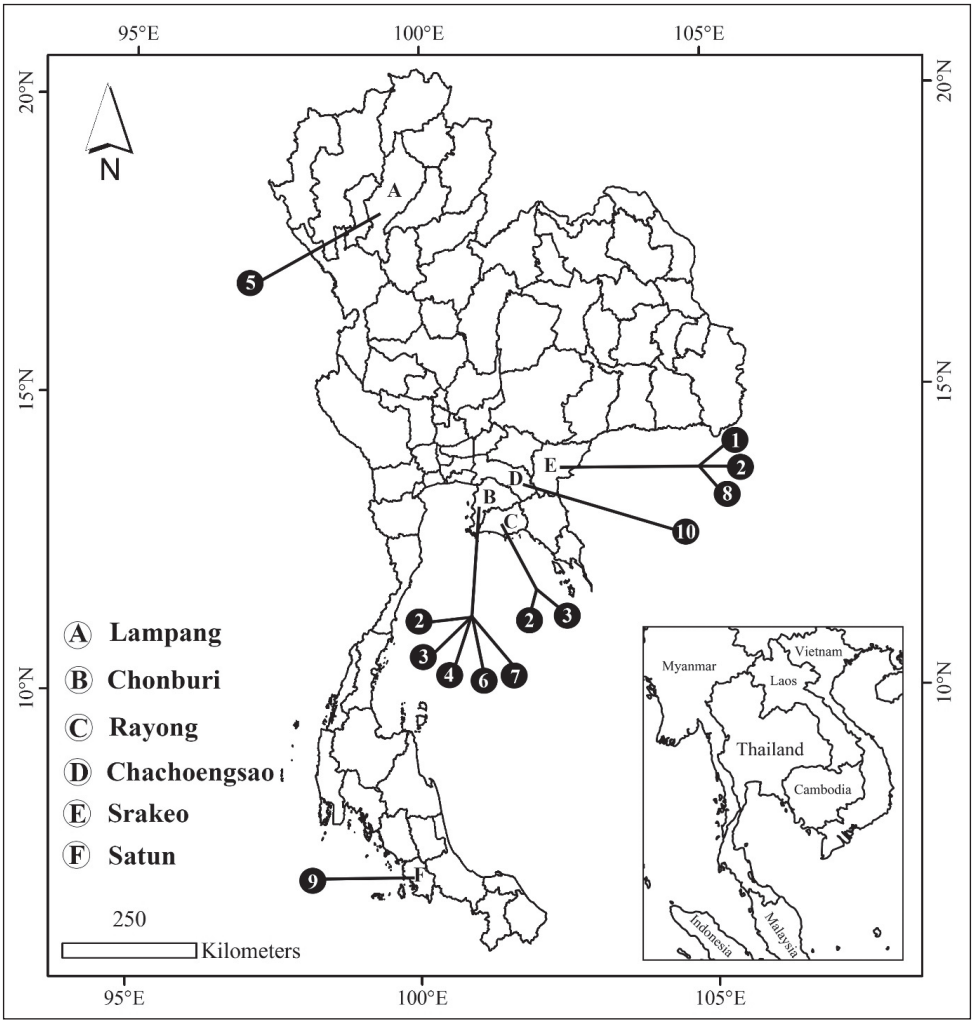

Figure 1. Distribution map of *Aulacospira* spp. in Thailand: **1** *A. depressa* **2** *A. khaopratun* **3** *A. panhai* **4** *A. khaobote* **5** *A. lampangensis* **6** *A. smaesarnensis* **7** *A. pluangtong* **8** *Aulacospira tekavongae* sp. nov. **9** *Aulacospira nudtadhirai* sp. nov. **10** *Aulacospira vanwalleghemi* sp. nov.

hd = hermaphroditic duct, p = penis, pro = prostate gland, gs = gametolytic sac, ut = uterus, v = vagina, vd = vas deferens.

Specimens were studied from the following collections:

MNHN Muséum national d'Histoire naturelle, Paris, France.
NHLRU Natural History Museum of Loei Rajabhat University, Loei, Thailand.
THNHM Thailand Natural History Museum, Pathum Thani, Thailand.
ZRCBUU Zoological Research Collection of Burapha University, Bangsaen, Thailand.

Taxonomy

Family Hypselostomatidae Zilch, 1959

Zilch 1959: 162, as Hypselostomatinae, subfamily of Chondrinidae.
Schileyko 1998: 136.
Bouchet et al. 2017: 43.

Genus *Aulacospira* Möllendorff, 1890

Aulacospira Möllendorff 1890: 224; Páll-Gergely et al. 2019.
Micropetasus Möllendorff 1890: 224, as section *Aulacospira*; type species: *Helix scalatella* Möllendorff, 1888.

Type species. *Helix scalatella* Möllendorff, 1888 by subsequent designation (Pilsbry 1895 in 1894–1895).

Diagnosis. Shell small (H = 1.5 mm, W = 2.9 mm), helicoid, depressed or triangular, wider than high. Color uniformly brown or purplish. Apex prominent; protoconch smooth or with dense mesh of granular reticulation. Teleoconch smoothish, but with uneven, oblique striatae. Spire slightly concave, sometimes scalariform. Body whorl keeled or rounded, often with a groove below suture. Shell umbilicate; umbilicus narrow to moderately narrow. Aperture oblique, rounded, with 0–5 apertural teeth; peristome thin, expanded.

Remarks. Páll-Gergely et al. (2019) suggested that Thai and Philippine *Aulacospira* may not be closely related due to their unusual distribution pattern and suggested that the similar shell shape of these snails may be due to convergence but more data are needed to support this hypothesis. However, we continue to use *Aulacospira* for Thai species following the description of this genus by Pilsbry (1916–1918).

Aulacospira depressa Dumrongrojwattana & Panha, 2006

Figures 2A, 3A

Aulacospira depressus Dumrongrojwattana and Panha 2006: 121–122, fig. 2.

Remarks. The specific epithet "*depressus*" must be corrected to "*depressa*" to agree in gender with *Aulacospira* (musculine).

Type locality. Thailand, Khao Chakan, an isolated limestone hill of Srakeo Province; 13°48'02"N, 102°12'49"E; ca 85 m a.s.l.

Types examined. ***Holotype.*** ZRCBUU 0076 (BuUZM-MS 0076) (Fig. 2A, B). ***Paratype.*** ZRCBUU 0077 (BuUZM-MS 0077).

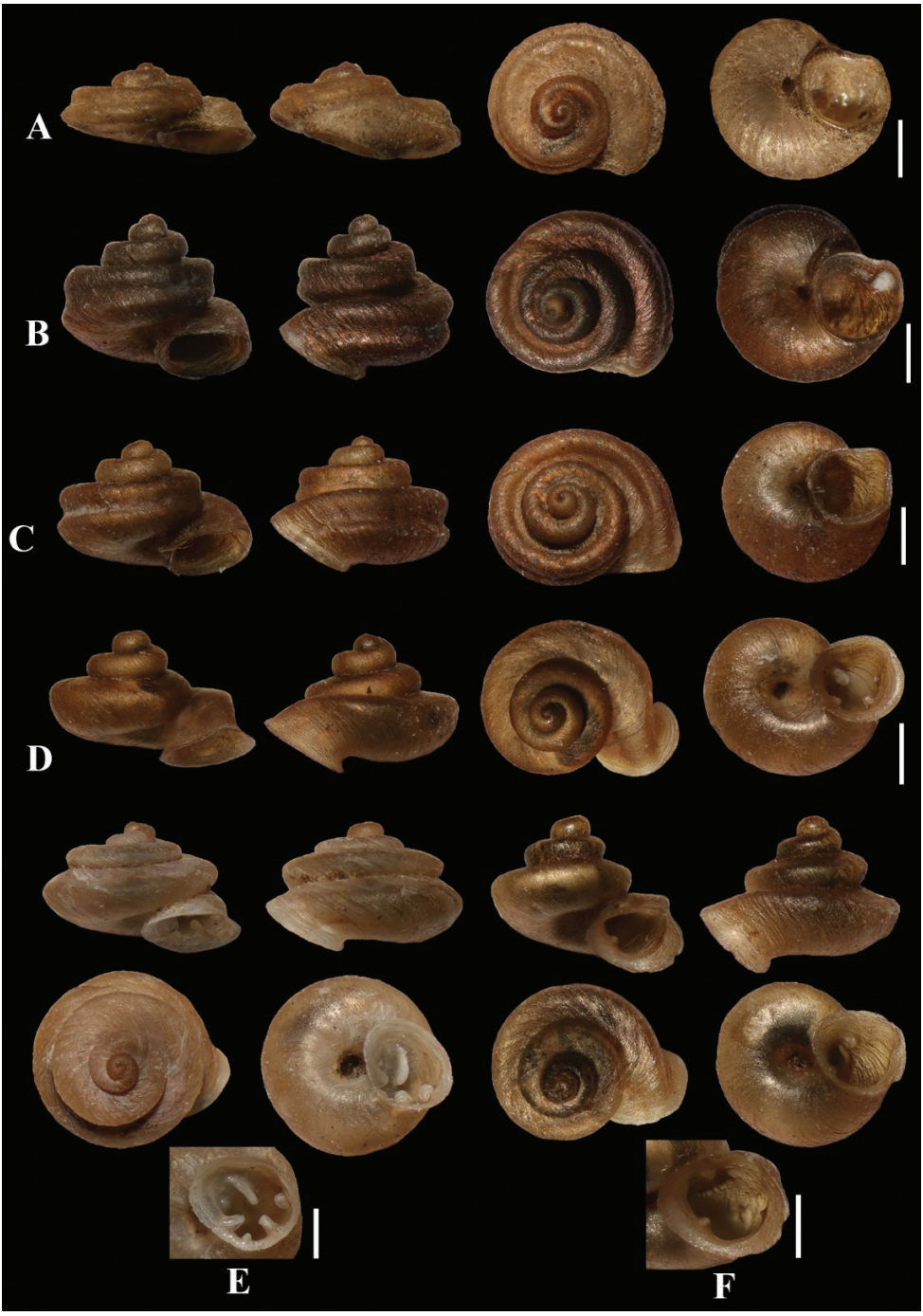

Figure 2. *Aulacospira* spp. **A** *A. depressa* (paratype, BuUZM-MS 0077) **B** *A. khaobote* (BuUZM-MS 0083) **C** *A. khaopratun* (paratype, BuUZM-MS 0070) **D** *A. lampangensis* (ZRCBUU 0403) **E** *A. panhai* (paratype, ZRCBuU 0293) **F** *A. smaesarnensis* (ZRCBUU 0370). Scale bars: 1 mm.

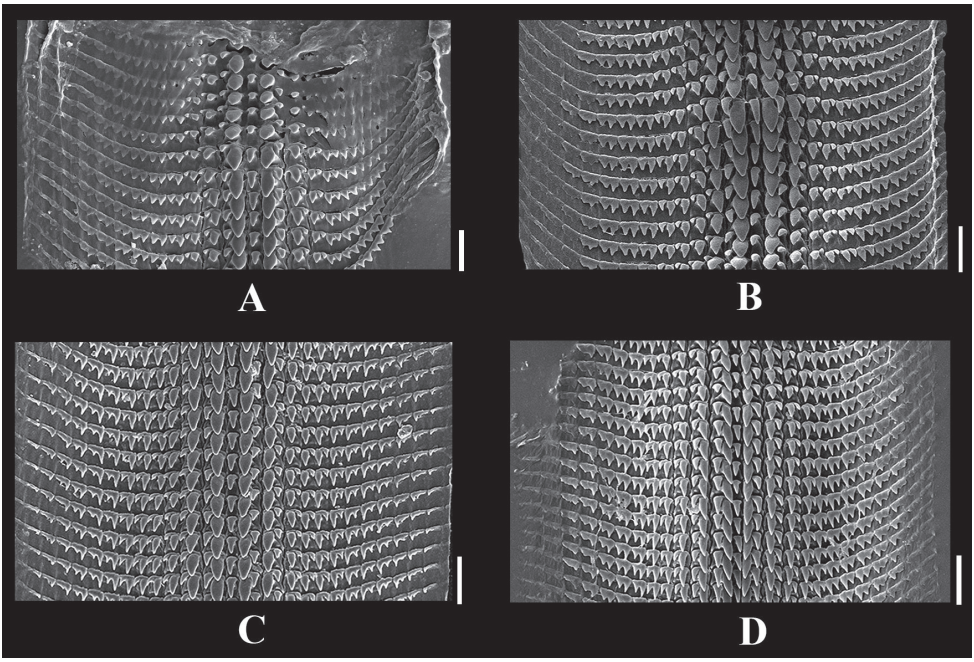

Figure 3. Radula of *Aulacospira* spp. **A** *A. depressa* **B** *A. khaopratun* **C** *A. panhai* **D** *A. smaesarnensis.* Scale bars: 20 μm.

Material examined. ZRCBUU 0078 (BuUZM-MS 0078) (3 shells); Thailand, Khao Chakan, an isolated limestone hill of Srakeo Province; 13°48'02"N,102°12'49"E; ca 85 m a.s.l.; 8.vi.2003; leg. Dumrongrojwattana P. ZRCBUU 0096 (BuUZM-MS 0096) (24 shells); 19.iv.2003; leg. Dumrongrojwattana, P. ZRCBUU 0352 (10 shells); Thailand, Khao Chakan, an isolated limestone hill of Srakeo Province; 13°48'02"N,102°12'49"E, ca 85 m a.s.l.; 18.i.2020; leg. Dumrongrojwattana, P.

Measurements. H = 0.97–1.14 mm, W = 2.51–3.15 mm.

Diagnosis. Shell minute, very depressed; spire very low; brownish. Protoconch smooth; teleoconch smooth; body whorl large, with a prominent groove which forms two carinae; tuba very short; peristome expanded; aperture lacking teeth (Fig. 2A).

Radula. Central tooth small, unicuspid, triangular. Laterals irregularly bicuspid and consisting of a large internal cusp near and adjacent to a smaller, shorter outer cusp. Four laterals on each side of central tooth; first tooth largest, other teeth sequentially smaller. Marginals also irregularly, unequally bicuspid, with internal cusp larger than outer cusp. Marginal teeth 7 or 8 on each side of central tooth (Fig. 3A).

***Radula formula*.** 7–8:4:1:4:7–8.

Genital system. Unknown.

Distribution. This species is known only from the type locality (Fig. 1).

Aulacospira khaobote **Dumrongrojwattana & Panha, 2006**
Figure 2B

Aulacospria khaobote Dumrongrojwattana and Panha 2006: 122–123, fig. 3.

Type locality. Thailand, Wat Tam Khao Bote, an isolated limestone hill of Rayong Province; 13°09'19"N,101°38'05"E.

Types examined. ***Holotype.*** ZRCBUU 0083 (BuUZM-MS 0083) (Fig. 2G). ***Paratype.*** ZRCBUU 0084 (BuUZM-MS 0084).

Measurements. H = 1.59–1.89 mm, W = 1.91–2.38 mm.

Diagnosis. Shell minute, triangular; spire high; brownish. Protoconch smooth; teleoconch smooth; body whorl with broad sulcus; tuba very short; peristome not expanded; aperture lacking teeth.

Radula. Unknown.

Genital system. Unknown.

Distribution. This species is known only from the type locality (Fig. 1).

Aulacospira khaopratun **Dumrongrojwattana & Panha, 2005**
Figures 2C, 3B

Aulacospria khaopratun Dumrongrojwattana and Panha 2005: 15–16, fig. 2.

Type locality. Thailand, Khaopratun, an isolated limestone hill of Rayong Province; 13°07'18"N,101°36'03"E.

Types examined. ***Holotype.*** ZRCBUU 0072 (BuUZM-MS 0072) (Fig. 2C, D). ***Paratype.*** ZRCBUU 0073 (BuUZM-MS 0073).

Material examined. ZRCBUU 0298 (10 shells); Thailand, Khao Cha-ang Hayod, an isolated limestone hill of Chonburi Province; 13°09'40.6"N,101°35'51.4"E; 23.iii.2008; leg. Dumrongrojwattana, P. ZRCBUU 0350 (15 shells); Thailand, Subthaworn Temple, a place located in an isolated limestone hill of Srakeo Province; 13°24'19.5"N,102°16'29.8"E; 19.vi 2010; leg. Inmadon, R. ZRCBUU 0440 (12 shells); Thailand, Phet Pananikom Temple, a place located in an isolated limestone hill of Srakeo Province; 13°29'17.5"N,102°04'48.6"E; 12.vii. 2015; leg. Inmadon, R. ZRCBUU 0490 (12 shells); Phet Pananikom Temple, a place located in an isolated limestone hill of Srakeo Province; 13°29'17.5"N,102°04'48.6"E; 23.vi. 2016; leg. Inmadon, R.

Measurements. H = 1.61–1.80 mm, W = 1.81–2.3 mm.

Diagnosis. Shell minute, depressed; spire moderately high; brownish. Protoconch smooth; teleoconch smooth; body whorl large, with two prominent spiral carinae; tuba short; peristome expanded; aperture lacking teeth.

Radula. As in *A. depressa* (Fig. 3B).

Genital system. Unknown

Distribution. Chonburi, Rayong, and Srakeo provinces, eastern Thailand (Fig. 1).

Aulacospira lampangensis Panha & Burch, 2002

Figure 2D

Aulacospira lampangensis Panha and Burch 2002: 70, fig. 3.

Type locality. Thailand, Ban Thasee, an isolated limestone hill of Lampang Province; 18°25'18.8"N,99°45'11.6"E.

Material examined. ZRCBUU 0403 (2 shells); Thailand, Ban Thasee, an isolated limestone hill of Lampang Province; 18°25'18.8"N, 99°45'11.6"E; 3.vi. 2012; leg. Meesukko, C.

Measurements. H = 1.6–1.8 mm, W = 2.0–2.3 mm.

Diagnosis. Shell minute, depressed, with rounded whorls; spire moderately high; brownish. Protoconch smooth; teleoconch smooth; body whorl large, with two prominent spiral carinae; tuba projecting downward; peristome expanded; aperture with five teeth, columellar, parietal lamellae, upper and lower palatal plicae, and basal plica (Fig. 2D).

Radula. Unknown.

Reproductive anatomy. Unknown.

Distribution. This species appears limited to the type locality (Fig. 1).

Aulacospira panhai Dumrongrojwattana, 2008

Figures 2E, 3C

Aulacospira panhai Dumrongrojwattana 2008: 57–59, fig. 1.

Type locality. Thailand, Khaopratun, an isolated limestone hill of Rayong Province; 13°07'19"N, 101°36'03"E.

Types examined. ***Holotype.*** ZRCBUU 0220. ***Paratype.*** ZRCBUU 0293.

Material examined. ZRCBUU 0353 (3 shells); Thailand, Khao Cha-ang Hayod, an isolated limestone hill of Chonburi Province; 13°09'40.6"N, 101°35'51.4"E; 31.i.2013; leg. Dumrongrojwattana, P. ZRCBUU 0393 (5 shells); Thailand, Khao Cha-ang Hayod, an isolated limestone hill of Chonburi Province; 13°09'40.6"N, 101°35'51.4"E; 23.vi.2014; leg. Dumrongrojwattana, P. ZRCBUU 0394 (2 shells); Thailand, Khaopratun, an isolated limestone hill of Rayong Province; 13°07'19"N, 101°36'03"E; 31.i.2013; leg. Dumrongrojwattana, P. ZRCBUU 0495 (2 shells); Thailand, Khao Cha-ang Hayod, an isolated limestone hill of Chonburi Province; 13°09'40.6"N,101°35'51.4"E; 15. x. 2016, leg. Dumrongrojwattana, P.

Measurements. H = 2.47–2.83 mm, W = 1.45–1.70 mm.

Diagnosis. Shell minute, semi-depressed; spire distorted; brownish. Protoconch granulose; teleoconch smooth; the first two whorls slightly flatten; the last two whorls large and inflated; tuba short and downwardly directed; peristome expanded; aperture with six teeth, parietal and infraparietal lamellae, upper palatal and lower palatal and basal plicae, and columella lamellae (Fig. 2E).

Radula. As in *A. depressa* (Fig. 3C).
Reproductive anatomy. Unknown.
Distribution. Chonburi and Rayong provinces, eastern Thailand (Fig. 1).

Aulacospira smaesarnensis Panha & Burch, 2001

Figures 2F, 3D

Aulacospira smaesarnensis Panha and Burch 2001: 65, fig. 2.

Type locality. Thailand, Smaesarn Village, a fishery village located in an isolated liestone hill of Chonburi Province; 12°34'06"N, 100°56'578"E.

Types examined. ZRCBUU 0370 (10 shells); Thailand, Smaesarn Village, a fishery village located in an isolated liestone hill of Chonburi Province; 12°34'06"N, 100°56'578"E; 12.v.2013; leg. Dumrongrojwattana, P. ZRCBUU 0425 (10 shells); Thailand, Smaesarn Village, a fishery village located in an isolated limestone hill of Chonburi Province; 12°34'06"N, 100°56'578"E; 20.iii.2015; leg. Dumrongrojwattana, P.

Measurements. H = 2.47–2.83 mm, W = 1.45–1.70 mm.

Diagnosis. Shell minute, helicoid, moderately elevated spire; brownish. Protoconch smooth; teleoconch rough; body whorl large, rounded peripherally; tuba projecting downward; peristome thickened and expanded; aperture with poorly developed barriers, parietal lamella palatal plica and columellar lamella (Fig. 2F).

Radula. As in *A. depressa* (Fig. 3D).
Reproductive anatomy. Unknown.
Distribution. This species appears limited to the type locality (Fig. 1).

Aulacospira pluangtong Panha & Burch, 2004

Figure 4A–D

Aulacospira pluangtong Panha and Burch 2004: 64, fig. 5.

Type locality. Thailand, Pluangtong Mountain, an isolated limestone hill of Chonburi Province; 13°11'50"N, 101°34'49"E.

Material examined. ZRCBUU 357 (3 shells); Thailand, Khao Mee Mountain, an isolated limestone hill of Chonburi Province; 13°09'02.7"N, 101°35'34.4"E; 15.x.2016; leg. Dumrongrojwattana, P.

Measurements. H = 1.75–1.82 mm, W = 1.82–1.93 mm.

Diagnosis. Shell minute; spire high; brownish. Protoconch smooth; teleoconch smoothish, with uneven growth striae. Final part of the last whorl free and projecting downward; peristome not expanded; aperture with four teeth, parietal and columnellar lamellae, and the upper and lower palatal plica.

Radula. As in *A. depressa* (Fig. 4B).

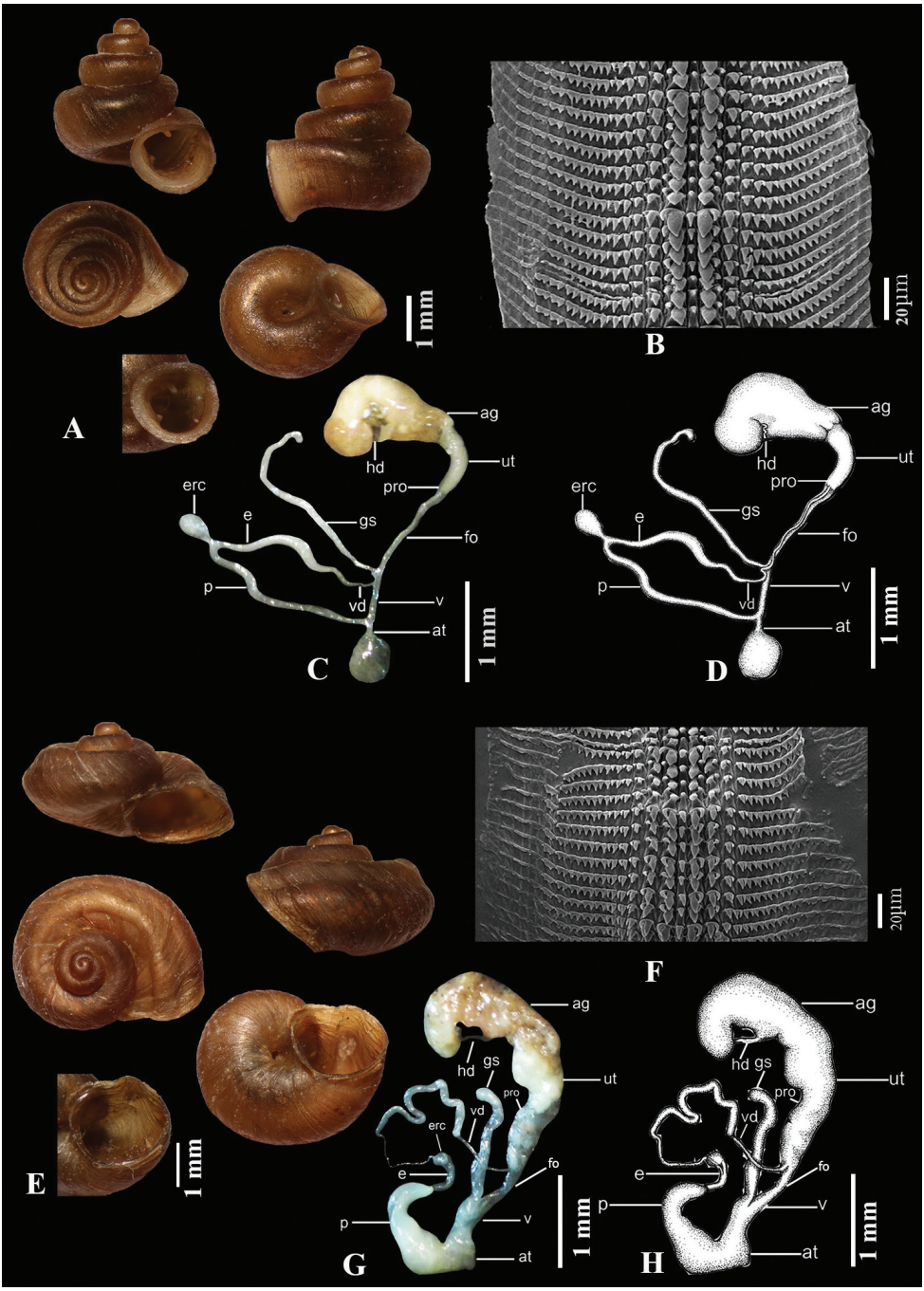

Figure 4. A–D *Aulacospira pluangtong* (ZRCBUU 357) **A** shell **B** radula **C, D** genital system **E–H** *Aulacospira nutadhirai* sp. nov. **E** holotype (ZRCBUU 0391) **F** radula **G, H** genital system.

Genital system. Atrium shorter than vagina. Penis longer than epiphallus, with anterior portion a slender tube. Epiphallus connected to distal end of penis. Epiphallus glossy white, longer than vas deferens, with its anterior portion slender and cylindrical, its central portion slender and more bulging than posterior portion. Epiphallic flagellum absent. Epiphallic retractor caecum rounded and bulbous, attached to posterior portion of epiphallus. Vas deferens very long, slender, entering epiphallus apically. Vagina and free oviduct cylindrical, with vagina shorter than free oviduct. Gametolytic sac very long and cylindrical, with anterior portion connecting vagina and free oviduct and posterior portion with curved knob. Uterus long and cylindrical, with very thin prostate gland adhering to it. Hermaphroditic duct loosely convolute. Albumen gland large and yellowish. Dart apparatus absent (Fig. 4C, D).

Distribution. This species is only known from the limestone hills in Botong District, Chonburi Province, eastern Thailand (Fig. 1).

***Aulacospira nutadhirai* sp. nov.**

http://zoobank.org/5FE507E0-15A0-4537-B3E3-429D95103C90

Figure 4E–H

Types examined. *Holotype*. ZRCBUU 0391; Thailand, Khao Thanan, an isolated limestone hill of Thung-wa District, Satun Province; 7°03'42.2"N, 99°41'32.9"E; 10.iv.2010; leg. Dumrongrojwattana, P. ***Paratypes*.** ZRCBUU 0392 (10 shells); 10.iv.2010; ZRCBUU 0420 (5 shells); THNHM-iv-18802 (2 shells); MNHN IM-2014-7121 (2 shells); NHLRU 0010 (2 shells); collected from location same as holotype, 27.iv.2015; leg. Dumrongrojwattana, P.

Measurments. Holotype H = 1.54 mm, W = 2.89 mm. Paratypes H = 1.47–2.50 mm, W = 2.61–3.07 mm.

Diagnosis. Shell minute, helicoid. Protoconch smooth; body whorl stout, with a short projecting downward tuba; peristome not expanded; aperture lacking teeth.

Aulacospira nutadhirai sp. nov. is very similar to the eastern Thai species, *A. khaopratun*, but differs in its lower spire and more greatly inflated last whorl. Compared to Philippines species, *Aulacospira nutadhirai* sp. nov. is similar to *A. porrecta* but differs in the shape of the shell and in having no keel on the body whorl.

Description. Shell minute, helicoid, brownish, with 4–4½ whorls. Body whorl stout. Last quarter of body whorl with a short tuba projecting downward. Protoconch, consisting of 1¼ whorls, with granulose wrinkles. Teleoconch smoothish, with uneven oblique growth striae. Suture deep. Shell narrowly umbilicate. Spire low; first two whorls rounded. Penultimate whorl and body whorl with two shallow spiral sulci that continuously to peristome. Peristome expanded; aperture round and lacking teeth (Fig. 4E).

Radula. As in *A. depressa* (Fig. 4F).

Genital system. Atrium shorter than vagina. Penis shorter than epiphallus, with anterior and central portion large, bulging and posterior portion curved. Epiphallus connected to distal end of penis. Epiphallus glossy white, longer than vas deferens, with anterior portion cylindrical, central and posterior portion cylindrical, and distal end curved. Epiphallic flagellum absent. Epiphallic retractor caecum rounded, connected to distal part of epiphallus. Vas deferens short, slender, entering epiphallus apically. Vagina and free oviduct cylindrical, with vagina large and shorter than free oviduct. Gametolytic sac long and cylindrical, with anterior portion connecting vagina and free oviduct, posterior portion swollen. Uterus long, large, with very thin prostate gland adhering to it. Hermaphroditic duct loosely convolute. Albumen gland large and yellowish. Dart apparatus absent (Fig. 4G, H).

Type locality. Thailand, Khao Thanan, an isolated limestone hill of Thungwa District, Satun Province; 7°03'42.2"N, 99°41'32.9"E.

Etymology. We name this species in honor of Mr Thammarat Nutathira or Kru Nok, a former staff member of Kampang Wittaya School, Thailand, who contributed to the study of the biodiversity and paleontology of the limestone in Satun Province.

Distribution. This species appears limited to the type locality (Fig. 1).

***Aulacospira tekavongae* sp. nov.**

http://zoobank.org/7572347F-FC91-4E19-BC65-748541761EE1

Figure 5A–D

Type material. ***Holotype*.** ZRCBUU 0610; Thailand, Khao Chakan, an isolated limestone hill of Srakeo Province; 240 m a.s.l.; 13°48'02"N, 102°12'49"E; 5.v.2019; leg. Kamtuptim, C. and Dumrongrojwattana, P. ***Paratypes*.** ZRCBUU 0611 (15 shells); ZRCBUU 0420 (10 shells); 19.v.2014; leg. Dumrongrojwattana, P. THNHM-Iv-18803 (5 shells); MNHN IM-2014-7122 (5 shells); 5.v.2019; location same as holotype; leg. Kamtuptim, C. and Dumrongrojwattana, P.

Measurments. Holotype H = 2.32 mm, W = 2.08 mm. Paratypes H = 1.94–2.35 mm, W = 1.95–2.21 mm.

Diagnosis. Shell minute, conical. Protoconch smooth, body whorl with a very short projecting downward tuba; peristome expanded; aperture lacking teeth.

Aulacospira tekavongae sp. nov. is very similar to *A. khaobote*, but the shell is a conical and with a high spire, while that of *A. khaobote* shell helicoid and with a low spire.

Description. Shell minute, conical, brownish, with 4–4½ whorls. Tuba very short, projecting downward. Protoconch consisting of 1 ¼ whorls, with granulose wrinkles. Teleoconch smoothish, sculptured with uneven, oblique growth striae. Suture deep. Shell narrowly umbilicate. Spire high; first two whorls rounded, penultimate and body whorl with two distinct spiral sulci continuously to peristome. Peristome expanded; aperture round and lacking teeth (Fig. 4A).

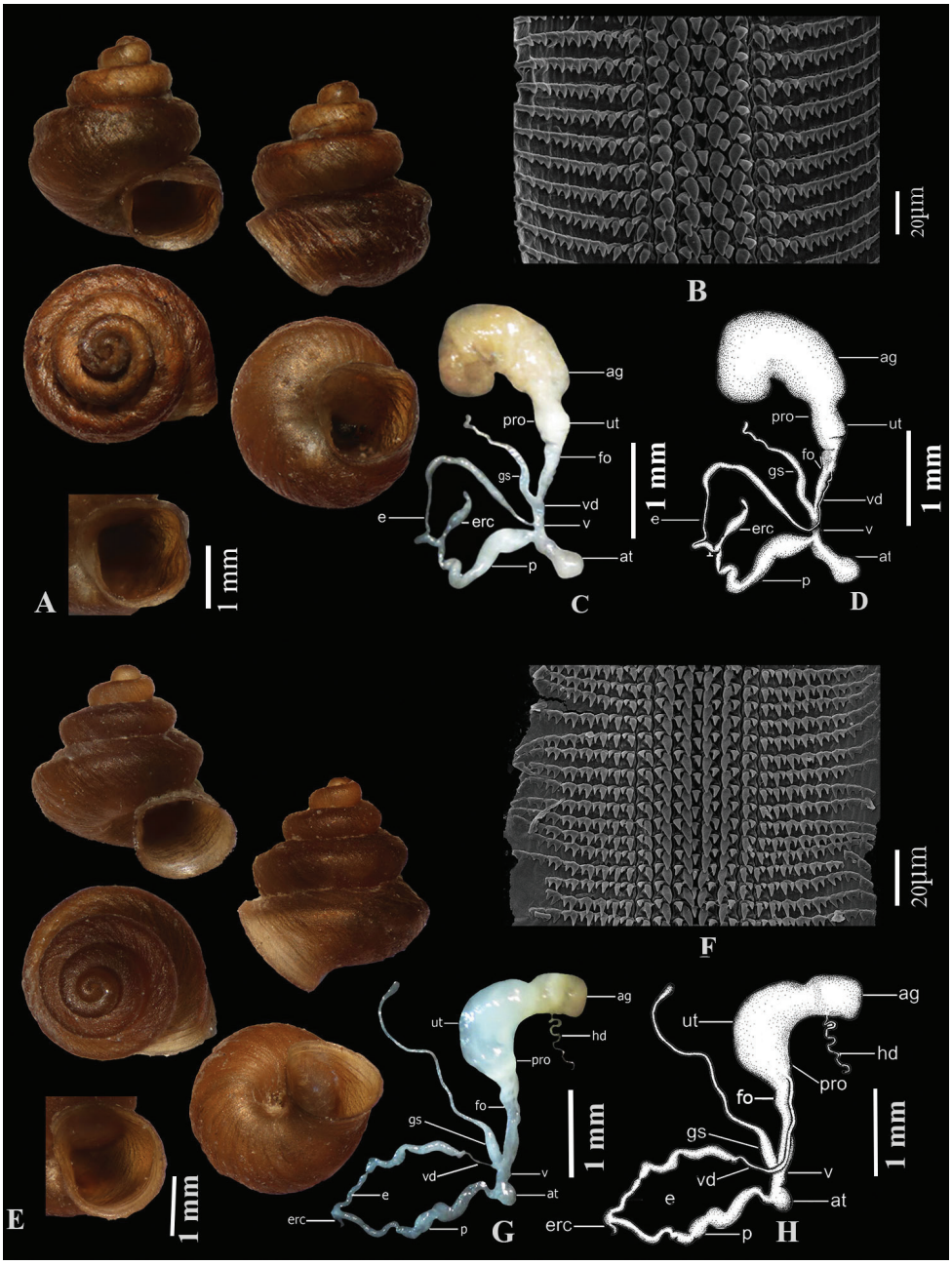

Figure 5. A–D *Aulacospira tekavongae* sp. nov. **A** holotype (ZRCBU 0610) **B** radula **C, D** genital system **E–H** *Aulacospira vanwalleghemi* sp. nov. **E** holotype (ZRCBUU 732) **F** radula **G, H** genital system.

Radula. As in *A. depressa* (Fig. 5B).

Genital system. Atrium longer than vagina. Penis shorter than epiphallus, with anterior portion a short tube and bulging. Epiphallus connected to distal end of penis. Epiphallus longer than vas deferens, with anterior portion slender and cylindrical, central portion slender and more bulging than anterior and posterior portion. Epiphallic flagellum absent. Epiphallic retractor caecum rather bulging, attached to posterior portion of epiphallus. Vas deferens long, slender, entering epiphallus apically. Vagina and free oviduct cylindrical, with vagina shorter than free oviduct. Gametolytic sac long and cylindrical, with anterior and central portion bulging, posterior portion slender and curved knob. Uterus long and large, with very thin prostate gland adhering to it. Hermaphroditic duct loosely convolute. Albumen gland large and yellowish. Dart apparatus absent (Fig. 5C, D).

Type locality. Thailand, Khao Chakan, an isolated limestone hill of Srakeo Province, eastern Thailand; 13°48'02"N, 102°12'49"E; ca 240 m a.s.l.

Etymology. We name this species in the hornor of Ms Rattanawadee Tekavong, a research collaborator, who has worked extensively on the eastern microsnail diversity.

Distribution. This species is known only from the type locality (Fig. 1).

***Aulacospira vanwalleghemi* sp. nov.**

http://zoobank.org/1683A4B8-98CB-40C0-A5BB-E720DAD400C8

Figure 5E–H

Types examined. *Holotype*. ZRCBUU 0732; Thailand, Wat Khao Tam Ratt, an isolated limestone hill of Ta Takeab District, Chacheongsao Province; ca 35 m a.s.l.; 13°23'30.4"N, 101°44'39.1"E; 19.i.2020; leg. Dumrongrojwattana, P. ***Paratype*.** ZRCBUU 0733 (8 shells); as in holotype.

Measurments (in mm). Holotype H = 3.17 mm, W = 3.28 mm. Paratypes H = 1.87–2.63 mm, W = 1.74–2.57 mm.

Diagnosis. Shell minute, conical. Protoconch smooth; body whorl peripherally with a very with a very short projecting downward tuba; peristome expanded; aperture round and lacking teeth.

The shell shape and periphery of the last whorl of *A. vanwalleghemi* sp. nov. is similar to *A. pluangtong*, but apertural teeth are absent. Apertural teeth are present in *A. pluangtong*.

Description. Shell minute, conical, brownish, with 4–4½ whorls. Tuba very short, projecting downward. Protoconch consists of 1¼ whorls, granulosely wrinkled. Teleoconch smoothish, sculptured with uneven, oblique growth striae. Suture deep. Shell narrowly umbilicate. Spire high, with peripherally of most whorls rounded; penultimate and body whorls with strong keel at periphery continuously to peristome. Peristome expanded; aperture obliquely oval and lacking teeth (Fig. 5E).

Radula. As in *A. depressa* (Fig. 5F)

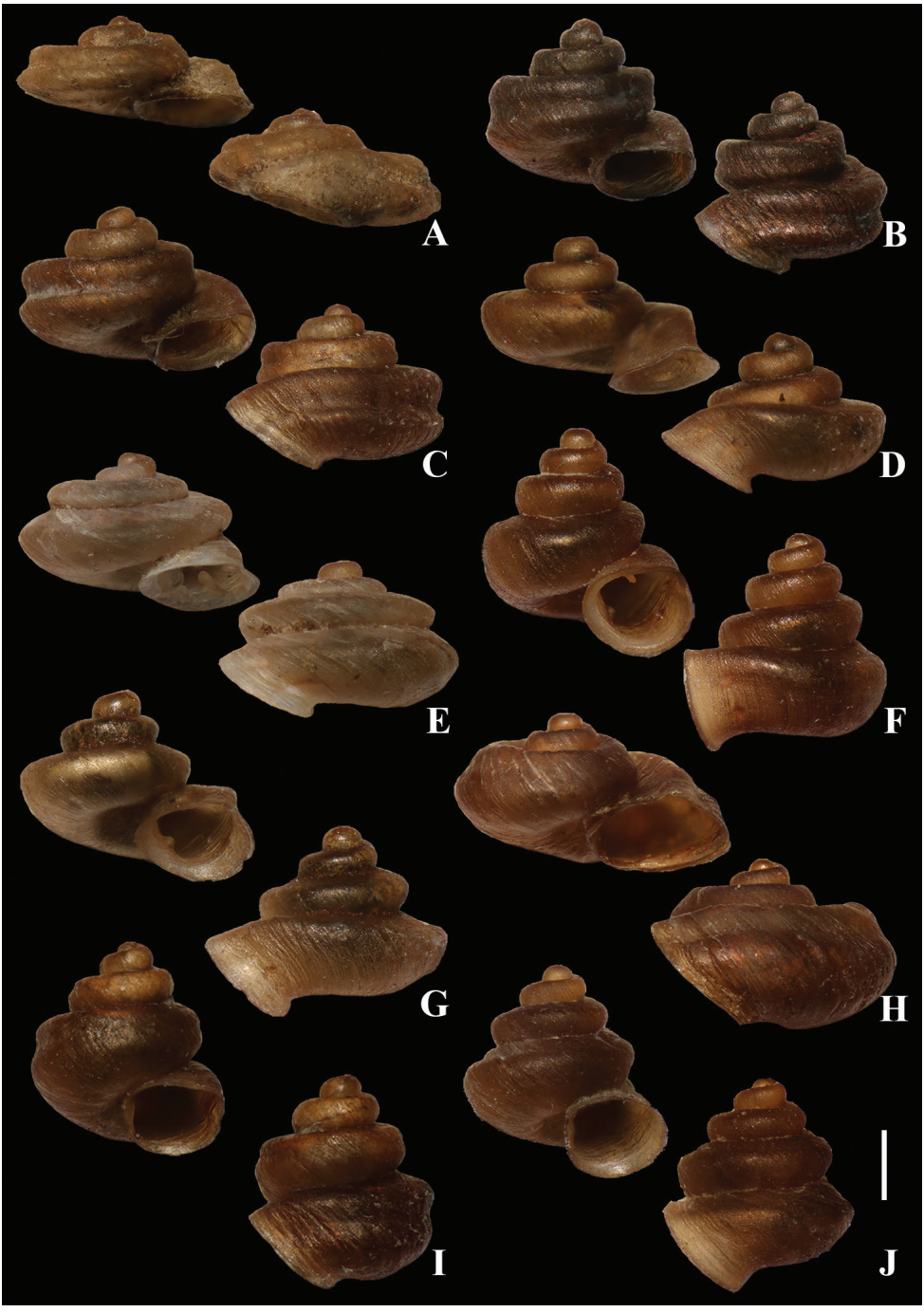

Figure 6. Synoptic view of *Aulacospira* Möllendorff, 1890 in Thailand **A** *A. depressa* **B** *A. khaobote* **C** *A. khaopratun* **D** *A. lampangensis* **E** *A. panhai*. **F** *A. pluangtong* **G** *A. smaesarnensis* **H** *Aulacospira nutadhirai* sp. nov. **I** *Aulacospira tekavongae* sp. nov. **J** *Aulacospira vanwalleghemi* sp. nov. Scale bars: 1 mm.

Genital system. Atrium shorter than vagina. Penis shorter than epiphallus, with anterior and central portion large, bulging and posterior portion curved. Epiphallus connected to distal end of penis. Epiphallus longer than vas deferens, with anterior portion with cylindrical, central and posterior portion cylindrical, distal end curved; white glossy. Epiphallic flagellum absent. Epiphallic retractor caecum rounded, connected to distal part of epiphallus. Vas deferens short, slender, entering epiphallus apically. Vagina and free oviduct cylindrical, with vagina large and shorter than free oviduct. Gametolytic sac a very long and slender, with anterior portion bulging, connects between vagina and free oviduct, posterior portion curved. Uterus long and large, with very thin prostate gland adhering to it. Hermaphroditic duct loosely convolute. Albumen gland large and yellowish. Dart apparatus absent (Fig. 5G, H).

Type locality. Thailand, Wat Khao Tam Ratt, an isolated limestone hill of Ta Takeab District, Chacheongsao Province; 13°23'30.4"N, 101°44'39.1"E; ca 35 m a.s.l.

Etymology. We name this species in honor of Mr René Vanwalleghem, a Belgian conchologist who inspired the senior author to pursue mollusc research.

Distribution. This species appears limited to the type locality (Fig. 1).

Key to species of *Aulacospira* in Thailand

This key is based on shell morphogy and is modified from Panha and Burch (2005).

1	Shell without spiral carinae; apertural teeth present.....**2**
–	Shell with or without spiral carinae; apertural teeth absent.....**5**
2	Shell depressed or conical-shaped; aperture with 3 or 4 barriers **3**
–	Shell globular; spire distorted; body whorl with peripheral angle; 6 apertural teeth present .....***Aulacospira panhai*** (Fig. 6E)
3	Spire depressed or high; apertureed with 4 barriers **4**
–	Spire moderately high; aperture with 3 barriers: parietal lamella, lower palatal plica and columella lamella ..... ***A. smaesarnensis*** (Fig. 6G)
4	Spire depressed; body whorl shouldered; aperture with 4 barriers: parietal lamella, upper and lower palatal plica and columella lamella..... ..... ***A. lampangensis*** (Fig. 6D)
–	Spire high; body whorl obtusely angular; aperture with 4 barriers, parietal lamella, upper and lower palatal plica and columella lamella..... .....***A. pluangtong*** (Fig. 6F)
5	Shell conical-shaped, spire high body whorl with or without spiral groove..... **6**
–	Shell depressed, body whorl with spiral groove.....**7**
6	Body whorl peripherally keeled.....***A. vanwalleghemi*** (Fig. 6J)
–	Body whorl with spiral groove .....***A. tekavongae*** (Fig. 6I)
7	Spire high or moderately high; body whorl with deep spiral groove **8**
–	Spire low, body whorl with deep or shallow spiral groove.....**9**

8 Spire moderately high, W/H = ca 1.71 ..... ***A. khaopratun*** (Fig. 6C)
– Spire high, W/H = ca 1.21 ..... ***A. khaobote*** (Fig. 6B)
9 Shell very flattened; body whorl with deep spiral groove; shell .... ***A. depressa*** (Fig. 6A)
– Shell stout; body whorl with shallow spiral groove ..... ***A. nutadhira*** (Fig. 6H)

Discussion

All species recorded here can be categorized into two groups based on shell morphology: 1) apertural teeth present and no conspicuous groove on the body whorl, and 2) the apertural teeth absent and with a conspicuous groove on the body whorl. The group with apertural teeth and without a conspicuous groove on the body whorl is composed of *A. lampangensis*, *A. panhai*, *A. pluangtong*, and *A. smaesarnensis*, while the other group without apertural teeth and with a conspicuous groove on the body whorl comprises *A. depressa*, *A. khaobote*, *A. khaopratun*, *A. nutadhirai* sp. nov., and *A. tekavongae* sp. nov. *Aulacospira vanwalleghemi* sp. nov. cannot be classified into either of these groups because both the apertural barrier and conspicuous groove are absent. The shell shape of *A. panhai* is distinctively different from other Thai species; its streptaxoid shell shape resembles the genus *Pseudostreptaxis* Mölendorff, 1890 and especially *P. azpeitiae* (Hidago, 1890) from the Philippines, which was described only by shell morphology (Möllendorff 1890; Páll-Gergely et al. 2019). We place *A. panhai* in *Aulacospira*, but more data, including anatomical and molecular, are needed to clarify its taxonomic placement.

The radulae of all examined species are tongue-shaped and with about 23–25 teeth per row. The radula formula is 7–8:4:1:4:7–8; there is a unicuspid central, larger bicuspid laterals, and a small, unequal bicuspid marginal. Compared with the microsnail genus *Pupoides* L. Pfeiffer, 1854 (Pupillidae Turton, 1831) there are 32 radula teeth per row, with the centrals trifid, laterals bifid, and marginal multicuspid. (Branson 1961) but in this study, the number of teeth per row in *Aulacospira* is fewer and shape of the teeth differs.

In this study, four species of the genus *Aulacospira* are described, based on characters of shells and genital systems. *Aulacospira pluangtong* was found to differ from other newly named species of the genus by its penis, vas deferens, and gametolytic sac. The penis of *A. pluangtong* is longer than the epiphallus and the vas deferens is a very long compared with the other new species.

Eastern Thailand and especially Chonburi and Rayong provinces seem to be a diversity hot spot for this genus and all species show high endemism (Fig. 1; Table 1). Páll-Gergely et al. (2019) remarked on the unusual geographic distribution of *Aulacospira* split between the Philippines and Thailand. Further studies, including over a broader geographical area and molecular analyses, are needed to explain the biogeography of this genus.

Table 1. Species list, diagnostic characteristics and geographic distribution of *Aulacospira* species in Thailand.

Species	Diagnostic characteristics					Geographic distribution	References
	Shell morphology	No. of apertural teeth	W/H ratio	Radula formula	Genital system		
With apertural teeth							
Aulacospira lampangensis	Shell moderately high, whorl shouldered	4	1.44	–	–	Type locality only	1, 4
Aulacospira panhai	Shell semi-depressed, body whorl acutely angular	6	0.61	7–8:4:1:4:7–8	–	Chonburi and Rayong provinces	6, 8
Aulacospira pluangtong	Shell high, body whorl obtusely angular	4	1.06	7–8:4:1:4:7–8	Penis longer than epiphallus; vas deferens very long, slender; gametolytic sac very long, cylindrical.	Limestone hills in Bothong District, Chonburi Province	2, 4, 7
Aulacospira smaesarnensis	Shell high, body whorl acutely angular	3	1.15	7–8:4:1:4:7–8	–	Type locality only	1, 4, 7
Without apertural teeth							
Aulacospira depressa	Shell flattened, spire very low	none	2.60	7–8:4:1:4:7–8	–	Type locality only	5, 9
Aulacospira khaobote	Spire high, body whorl with deep spiral groove	none	1.21	–	–	Type locality only	5, 8, 9
Aulacospira khaopratun	Shell moderately high, body whorl with two spiral carinae	none	1.71	7–8:4:1:4:7–8	–	Chonburi, Rayong, and Srakeo provinces	3, 4, 9
Aulacospira tekavongae sp. nov.	Shell high, body whorl with deep spiral groove	none	0.98	7–8:4:1:4:7–8	Penis shorter than epiphallus; vas deferens long, slender; gametolytic sac long, cylindrical, with anterior and central portion bulging.	Type locality only	Present study
Aulacospira nutadhirai sp. nov.	Spire low, body whorl inflation with shallow spiral groove	none	1.61	7–8:4:1:4:7–8	Penis shorter than epiphallus; vas deferens short, slender; gametolytic sac long, cylindrical.	Type locality only	Present study
Aulacospria vanwalleghemi sp. nov.	Spire high, body whorl strongly keel at periphery	none	1.04	7–8:4:1:4:7–8	Penis shorter than epiphallus; vas deferens short, slender; gametolytic sac very long, slender.	Type locality only	Present study

*References: 1 = Panha and Burch 2001; 2 = Panha et al. 2004; 3 = Dumrongrojwattana and Panha 2005; 4 = Panha and Burch 2005; 5 = Dumrongrojwattana and Panha 2006; 6 = Dumrongrojwattana 2008; 7 = Boon-ngam et al. 2008; 8 = Chidchua and Dumrongorjwattana 2010; 9 = Inmadon et al. 2011.

Acknowledgements

This work was supported by Research Grant of Burapha University through National Research Council of Thailand (grant no. 136/2561). We thank Ms Koraon Wongkamhaeng for kindly checking the English, as well as Ms Sararat Tanamai and Ms Chanakarn Kamtuptim for their generous help in shell photography and image processing. Thanks also due to the anonymous reviewers and the editor for their kindly suggestion for improving this manuscript.

References

Boon-ngam P, Dumrongrojwattana P, Matchacheep S (2008) The diversity of land snail fauna in Chonburi Province, Eastern Thailand. Kasetsart Journal (Natural Science) 42: 256–263.

Bouchet P, Rocroi J-P, Hausdorf B, Kaim A, Kano Y, Nützel A, Parkhaev P, Schrödl M, Strong EE (2017) Revised classification, nomenclator and typification of gastropod and monoplacophoran families. Malacologia 61(1–2): 1–526. https://doi.org/10.4002/040.061.0201

Branson BA (1961) The Recent Gastropoda of Oklahoma, III. Terrestrial species: Pupillidae, Carychiidae, Strobilopsidae and Oligyridae. Proceedings of the Oklahoma Academy of Science 40: 45–69.

Chidchua W, Dumrongorjwattana P (2010) Taxonomy of land snails in Klaeng District, Rayong Province and Kaenghangmaew District Chanthaburi Province, eastern Thailand (Gastropoda: Prosobranchia, Pulmonata). In: The Proceedings of 48th Kasetsart University Annual Conference, Subject Science, 3–5 March 2010. Bangkok, 161–170.

Dumrongrojwattana P (2008) A new species of *Aulacospira* (Pulmonata: Stylommatophora: Pupillidae) from Eastern Thailand. The Natural History Journal of Chulalongkorn University 8(1): 57–59.

Dumrongrojwattana P, Panha S (2005) A new species of *Aulacospira* from Thailand (Pulmonata: Stylommatophora: Pupillidae). The Natural History Journal of Chulalongkorn University 5: 15–16.

Dumrongrojwattana P, Panha S (2006) Two new species of *Aulacospira* from eastern Thailand (Pulmonata: Stylommatophora: Pupillidae). The Natural History Journal of Chulalongkorn University 6: 121–124.

Inmadon R, Tanamai S, Dumrongrojwattana P (2011) Species and habitats of mollusks in Srakeo Province. In: The Proceedings of 49th Kasetsart University Annual Conference, Subject Science, 1–4 February 2011. Bangkok, Thailand, 562–572.

Möllendorff OF von (1890) Die landschnecken-fauna der Insel Cebu. Bericht über die Senckenbergische Naturforschende Gesellschaft, Frankfurt am Main 1890: 189–292. https://doi.org/10.5962/bhl.title.13047

Páll-Gergely B, Schilthuizen M, Örstan A, Auffenberg K (2019) A review of *Aulacospira* Möllendorff, 1890 and *Pseudostreptaxis* Möllendorff, 1890 in the Philippines (Gastropoda, Pupilloidea, Hypselostomatidae). ZooKeys 842: 67–83. https://doi.org/10.3897/zookeys.842.33052

Panha S, Burch JB (2001) The pupillid genus *Aulacospira* in Thailand (Pulmonata: Stylommatophora). Walkerana 12: 65–76.

Panha S, Burch JB (2005) An introduction to the microsnails of Thailand. Malacological Review 37/38: 1–155.

Panha S, Tongkerd P, Sutcharit C, Burch JB (2004) New pupillid species from Thailand (Pulmonata: Pupillidae). The Natural History Journal of Chulalongkorn University 4: 57–82.

Pilsbry HA (1894–1895) Manual of Conchology, ser.2, vol. 9. (Helicidae, vol. 7). Guide to the study of Helices. Conchological Department, Academy of Natural Sciences Philadelphia, Philadelphia, 366 + 126 pp.

Pilsbry HA (1916–1918) Pulmonata, Pupillidae (Gastrocoptinae). Manual of Conchology, Second series: Pulmonata 24: i–xii, 1–380, pls 1–49.

Schileyko AA (1998) Treatise on Recent terrestrial pulmonate molluscs. Part 2. Gastrocoptidae, Hypselostomatidae, Vertiginidae, Truncatellinidae, Pachnodidae, Enidae, Sagdidae. Ruthenica, Supplement 2: 129–262.

Vermeulen JJ, Phung LC, Truong QT (2007) New species of terrestrial molluscs (Caenogas tropoda, Pupinidae & Pulmonata, Vertiginidae) of the Hon Chong–Ha Tien limestone hills, Southern Vietnam. Basteria 71: 81–92.

ZooKeys 980: 43–55 (2020)
doi: 10.3897/zookeys.980.47295
https://zookeys.pensoft.net

RESEARCH ARTICLE

A peer-reviewed open-access journal
ZooKeys
Launched to accelerate biodiversity research

An unusual new centipede subgenus *Lithobius* (*Sinuispineus*), with two new species from China (Lithobiomorpha, Lithobiidae)

Xiaodong Chang[1], Sujian Pei[1], Chunying Zhu[1], Huiqin Ma[1,2]

1 *Institute of Myriapodology, School of Life Sciences, Hengshui University, Hengshui, Hebei 053000, China*
2 *Hebei Key Laboratory of Wetland Ecology and Conservation, Hengshui, Hebei 053000, China*

Corresponding author: Huiqin Ma (mhq008@yahoo.com)

Academic editor: M. Zapparoli | Received 15 October 2019 | Accepted 22 September 2020 | Published 28 October 2020

http://zoobank.org/E3EB2FC3-3070-47DB-9C51-A65C793754F8

Citation: Chang X, Pei S, Zhu C, Ma H (2020) An unusual new centipede subgenus *Lithobius* (*Sinuispineus*), with two new species from China (Lithobiomorpha, Lithobiidae). ZooKeys 980: 43–55. https://doi.org/10.3897/zookeys.980.47295

Abstract

The present study describes a new Lithobiomorpha subgenus, *Lithobius* (*Sinuispineus*) **subgen. nov.**, and two new species, *L.* (*Sinuispineus*) *sinuispineus* **sp. nov.** and *L.* (*Sinuispineus*) *minuticornis* **sp. nov.** from China. The representatives of the new subgenus are characterized by a considerable sexual dimorphism of the ultimate leg pair 15, having the femur and tibia unusually enlarged in males, and the dorsal side of the femur with curved posterior spurs. These features distinguish *Lithobius* (*Sinuispineus*) **subgen. nov.** from all other subgenera of *Lithobius*. The diagnosis and the main morphological characters of the new subgenus and of the two new species are given for both male and female specimens.

Keywords

Chilopoda, *Lithobius* (*Sinuispineus*) *minuticornis* sp. nov., *Lithobius* (*Sinuispineus*) *sinuispineus* sp. nov., Myriapoda

Introduction

Located in the east of the Asian continent, on the western shore of the Pacific Ocean, the People's Republic of China has a land area of approximately 9.6 million square kilometres, and is the third largest country in the world (Zhang 2011).

Currently, the World Catalogue of Centipedes (Chilopoda) (Bonato et al. 2016) includes more than 1,200 valid species of Lithobiomorpha in nearly 130 extant genera and subgenera in only two families. However, the myriapod fauna of China is still poorly known, and very little attention has been paid to the study of Lithobiomorpha, which has only 85 species and subspecies (Pei et al. 2019; Qiao et al. 2019a, 2019b) currently known from the country. Knowledge of Chinese Lithobiomorpha is very fragmentary, and many species records and descriptions are widely scattered in the faunistic and taxonomic literature (Ma et al. 2014). A new subgenus and two new species have recently been discovered when examining material of Lithobiomorpha from Fujian and Henan provinces. The description of these new taxa is given below.

Materials and methods

Specimens were collected under leaf litter or stones and preserved in 75% ethanol. Illustrations and measurements were produced using a ZEISS SteREO Discovery.V20 microscope equipped with an Abbe drawing tube and an ocular micrometre and Axiocam 512 colour 12-megapixel microscope camera. The colour description is based on specimens fixed in 75% ethanol. The body length was measured from the anterior margin of the cephalic plate to the posterior end of the postpedal tergite. Type specimens and other material are deposited in the School of Life Sciences, Hengshui University, Hengshui, China (HUSLS). The terminology of the external anatomy follows Bonato et al. (2010). Measurements are shown in millimetres (mm). The following abbreviations are used in the text and the tables:

a = anterior;
C = coxa;
F = femur;
m = median;
P = prefemur;
p = posterior;
S, SS = sternite, sternites;
T, TT = tergite, tergites;
Ti = tibia;
Tr = trochanter.

Taxonomy

Class Chilopoda Latreille, 1817
Order Lithobiomorpha Pocock, 1895
Family Lithobiidae Newport, 1844
Genus *Lithobius* Leach, 1814

Subgenus *Sinuispineus* subgen. nov.
http://zoobank.org/35BCDB14-C94F-4E06-BAEC-1488605FCB4E

Type species. *Lithobius* (*Sinuispineus*) *sinuispineus* sp. nov.

Diagnosis. *Sinuispineus* subgen. nov. differs from the other subgenera of *Lithobius* in having curving posterior spurs on dorsal side of the femur of male leg 15; the

prefemur and femur and tibia of male leg 15 markedly incrassate; prefemur and femur and tibia of male legs 14 also thicker than legs 1–13. Antennae 20–25 articles, 9–13 ocelli in three irregular rows, posterior two ocelli comparatively large; Tömösváry's organ larger than the adjacent ocelli; prosternal teeth commonly 2+2, rarely 3+3; posterior angles of all tergites without triangular projections; coxal pore formula 3–6 in one row; tarsal articulation ill-defined on legs 1–13, well-defined on legs 14 and 15; female gonopods with 2+2 moderately small coniform spurs; male gonopods short and small.

Etymology. To emphasize the obviously curved posterior spurs on the dorsal side of the femur of the male leg 15.

Distribution. Fujian and Henan provinces, China.

Remarks. *Lithobius* (*Sinuispineus*) is identified as a member of Lithobiidae based on the following: forcipular pleurites not meeting ventrally, male gonopods not visible, 9–13 ocelli, antennomeres 20 or thereabouts, posterior angles of all tergites rounded, spiracle lacking on the first leg-bearing segment, spurs lacking on tibia, and at least some legs with regularly disposed distal spurs on various articles. *Lithobius* (*Sinuispineus*) is morphologically similar to *Lithobius* (*Monotarsobius*) Verhoeff, 1905 but can be readily distinguished by the following characters: posterior spurs on the dorsal side of the femur of legs 15 in males are curved in *Sinuispineus* in contrast to straight in *Monotarsobius*; tarsal articulation ill-defined on legs 1–13 versus very faint or indistinct in *Monotarsobius*; 9–13 ocelli versus ocelli generally few, 1+1-1+11, in *Monotarsobius*.

***Lithobius* (*Sinuispineus*) *sinuispineus* sp. nov.**

http://zoobank.org/43E532BB-A9DC-43CF-A352-9DADB204C9BD

Figs 1, 2A–L

Diagnosis. Antennae 20–25 articles; ocelli usually nine on each side, in three irregular rows; posterior two ocelli comparatively large; Tömösváry's organ larger than adjacent ocelli. Commonly 2+2 coxosternal teeth; porodonts lying posterolateral to lateral-most tooth. Coxal pore formula 3–5 in one row. Tarsal articulation ill-defined on legs 1–13, well-defined on legs 14 and 15. Female gonopods with 2+2 moderately small, coniform spurs; male gonopods short and small. Legs 15 are considerably modified in males: posterior spurs on dorsal side of femur of male legs 15 curving backward near base.

Material examined. ***Holotype***: ♂ (LS01-1) (Fig. 1A); body 11.56 mm long; cephalic plate 1.09 mm long, 1.24 mm wide. South East China, Huanggangshan, Wuyishan National Nature Reserve, Wuyishan County, Nanping City, Fujian Province, 27°52.025'S, 117°51.030'E, 544 m, 15 August 2010, leg. F. Zhang, H. Ma. ***Paratypes***: 1♀, 1♂ (LS01-1), same locality and date as holotype.

Other material examined. 2 ♂♂ (LS01-2), South East China**,** Yulinting, Wuyishan National Nature Reserve, Wuyishan County, Nanping City, Fujian Province, 27°40.917'S, 117°56.030'E, 462 m, 8 August 2010, leg. F. Zhang, H. Ma.

Description. Body 11.6–15.2 mm long; cephalic plate 1.1–1.3 mm long, 1.2–1.4 mm wide.

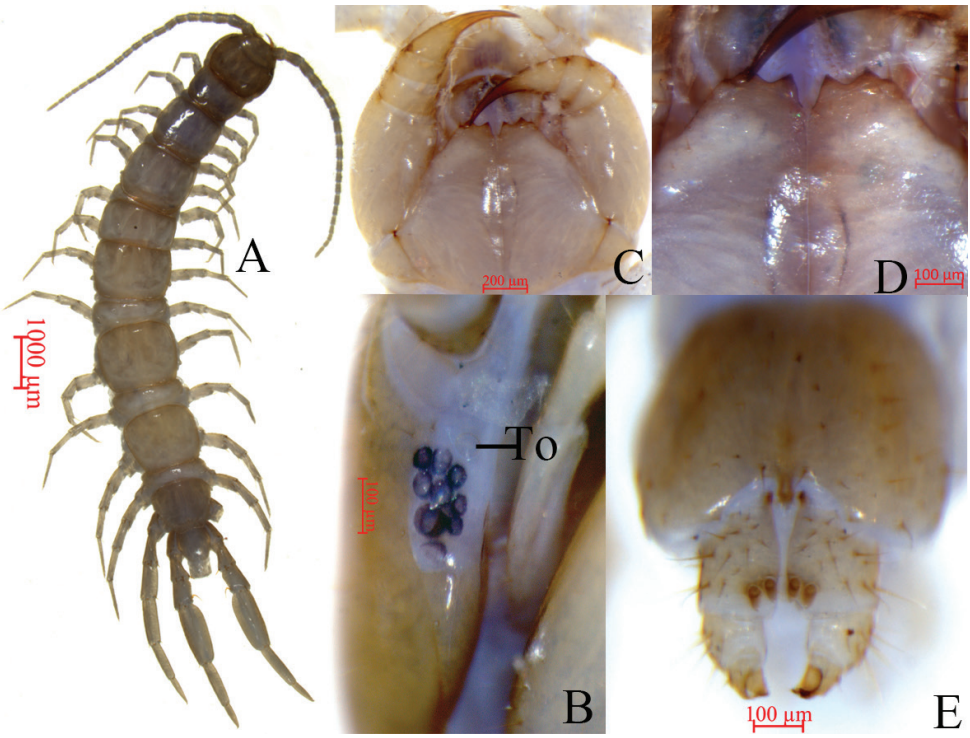

Figure 1. *Lithobius* (*Sinuispineus*) *sinuispineus* sp. nov. (holotype **A–D**, paratype female **E**) **A** habitus, dorsal view **B** ocelli and Tömösváry's organ (To), lateral view **C** cephalic plate, ventral view **D** forcipular coxosternite, ventral view **E** posterior segments and gonopods of female, ventral view.

***Colour*:** antennae pale brown to pale greyish yellow from base to end; tergites pale brown, pleural region pale lavender, and sternites pale greyish yellow; basal parts of forcipules, forcipular coxosternite, and SS14 and 15 darker; coxa, trochanter, prefemur, femur, and tibia of all legs pale lavender; tarsus 1 pale brown; tarsus 2 pale yellow-brown in all legs.

***Antennae*:** 25 articles in female, 20 articles in male (Fig. 1A). Length of first antennal article approximately equal to width of base; length of remaining articles longer than wide. Second article thicker and longer than other articles: from second article, each article gradually shortened, and distalmost articles still considerably longer than wide, 3.8–4.3 times as long as wide. Abundant setae on antennal surface, less so on basal articles; density of setae to approximately fourth article gradually increasing, then more or less constant.

Cephalic plate smooth, convex, slightly wider than long; tiny setae emerging from pores scattered very sparsely over the whole surface; frontal marginal ridge with shallow anterior median furrow; short to long setae scattered along the marginal ridge of the cephalic plate; lateral marginal ridge discontinuous, posterior margin continuous, wider than lateral marginal ridge (Fig. 1A).

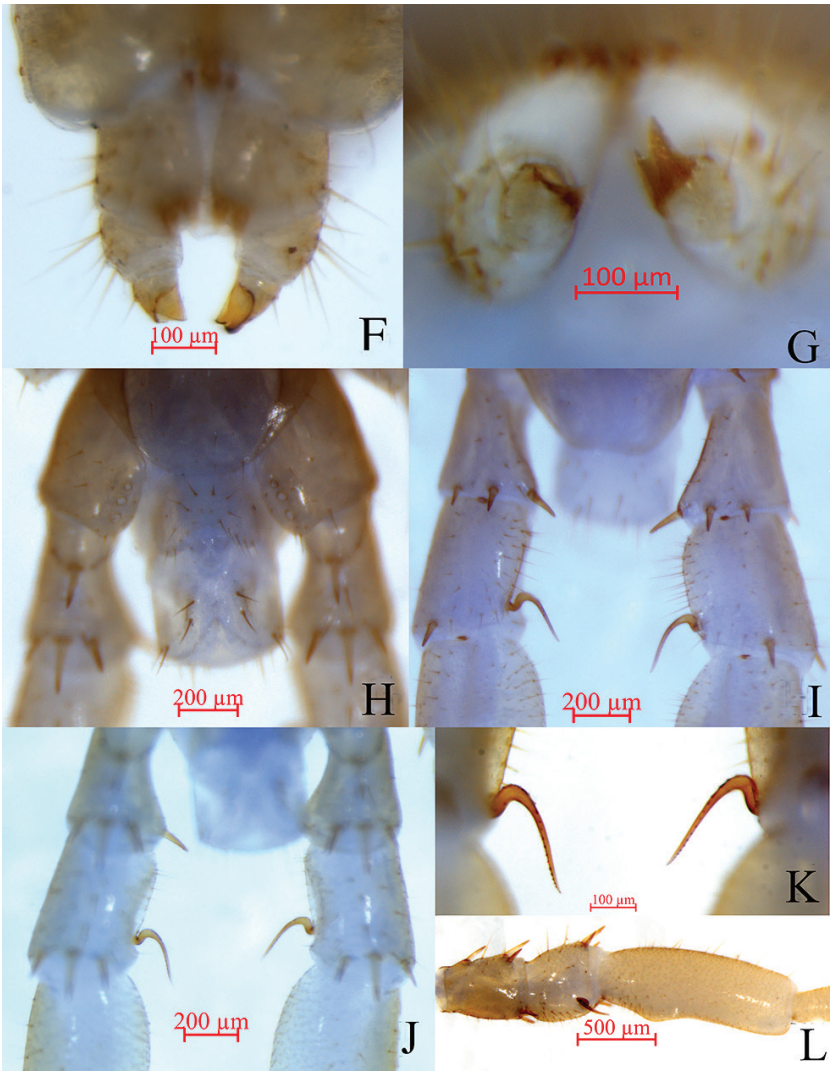

Figure 2. *Lithobius* (*Sinuispineus*) *sinuispineus* sp. nov. (paratype female **F, G**; holotype **H–L**) **F** claw of female gonopod, ventral view **G** claw of female gonopod, dorsal view **H** posterior segments and gonopods in male, ventral view **I** posterior spurs of the femur of legs 15, dorsal view **J** posterior spurs of the femur of legs 15, ventral view **K** posterior spurs of the femur of legs 15, ventral view, showing minor teeth **L** tibia of legs 15 raised inward.

Nine, oval to rounded ocelli on each side, from small to large, arranged in three irregular rows; posterior two ocelli comparatively large. Ventral ocelli slightly smaller than the dorsal, domed, translucent, and usually darkly pigmented (Fig. 1B).

Tömösváry's organ (Fig. 1B-To) near ocelli, at anterolateral margin of cephalic plate; moderately larger than adjoining ocelli; surrounding sclerotised area not obvious.

Table 1. Leg plectrotaxy of *Lithobius* (*Sinuispineus*) *sinuispineus* sp. nov. (female). Letters in brackets indicate variable spines.

Legs	Ventral					Dorsal				
	C	Tr	P	F	Ti	C	Tr	P	F	Ti
1			p	am	am			mp	ap	a
2			mp	am	am			mp	ap	(a)p
3–9			mp	amp	am			mp	ap	ap
10			mp	amp	am			(a)mp	ap	ap
11			mp	amp	am			amp	ap	ap
12			(a)mp	amp	am			amp	ap	ap
13		m	amp	amp	am		a	amp	ap	ap
14		m	amp	amp	am		a	amp	ap	p
15		m	amp	amp	a		a	amp	ap	

Coxosternite subtrapezoidal (Fig. 1C); anterior margin narrow; lateral margins slightly longer than medial margins. Median diastema moderately deep, narrowly V-shaped; anterior margin with 2+2 acute triangular teeth. Porodonts thicker, lying posteriolaterally to lateral-most tooth (Fig. 1C). Long, scattered setae on ventral side of coxosternite; longer setae near dental margin.

All tergites smooth, without wrinkles, tiny setae emerging from pores scattered sparsely over entire surface; near margin with few long setae. T1 narrower posterolaterally than antero-laterally, generally trapezoidal; T1 and T3 narrower than cephalic plate; T3 wider than T1; T8 widest. Lateral marginal ridges of all tergites continuous. Posterior margin of TT1 and 6 straight; TT 3, 5, 8, 10, 12, 14 slightly concave. Posterior angles of tergites rounded, without triangular projections. Miniscule setae scattered sparsely over the surface; one thick and long setae on both anterior angles of each tergite.

Posterior side of sternites narrower than anterior, generally trapezoidal, smooth. Setae emerging from sparsely scattered pores on the surface and lateral margin, very few long setae scattered sparsely among them. One comparatively long thick seta on both anterior angles of each sternite; more setae on surface of anterior and middle parts than posterior part of each sternite.

Legs relative robust; tarsi fused on legs 1–13; well-defined on legs 14–15. All legs with fairly long, curved claws. Legs 1–12 with anterior and posterior accessory spurs; anterior accessory spurs moderately long and slender, forming a moderately small angle with claw; posterior accessory spurs slightly more robust, forming a comparatively large angle with claw; legs 13 with anterior accessory spurs; legs 14 and 15 lacking accessory spurs. Short to long setae sparsely scattered over surface of coxa, trochanter, prefemur, femur, and tibia of all legs; more setae on tarsal surface; setae on dorsal surface of tarsus slightly shorter than ventral surface. Legs 14 and 15 in female thicker than anterior pairs; legs 15 in male considerably thicker and stronger than anterior pairs. Leg plectrotaxy presented in Tables 1 and 2.

Coxal pores 3–5 in a row, round or slightly oval, size of pores varies greatly from 19.3 μm to 48.7 μm; coxal pore field set in a relatively deep groove; coxal pore-field fringe with prominence; prominence with 4–8 moderately long setae sparsely scattered over the surface.

Table 2. Leg plectrotaxy of *Lithobius* (*Sinuispineus*) *sinuispineus* sp. nov. (male). Letters in brackets indicate variable spines.

Legs	Ventral					Dorsal				
	C	Tr	P	F	Ti	C	Tr	P	F	Ti
1			p	am	am			mp	ap	a
2			p	am (p)	am			mp	ap	ap
3–6			mp	amp	am			mp	ap	ap
7–11			mp	amp	am			amp	ap	ap
12			(a)mp	amp	am			amp	ap	ap
13		m	amp	amp	am		a	amp	ap	ap
14		m	amp	amp	am		a	amp	ap	p
15		m	amp	amp	a		a	amp	ap	p

Female. S15 anterior margin broader than posterior, generally trapezoidal, postero-medially slightly convex. Short to long setae sparsely scattered on S15 surface. Surface of lateral sternal margin of genital segment well chitinised, posterior margin of genital sternite deeply concave between condyles of gonopods, except for a small, median, tongue-shaped bulge. Relatively long setae scattered over ventral surface of genital segment, slightly more setae near S15. Gonopods: first article fairly broad, bearing 13 short to moderately long setae, arranged in three irregular rows; with 2+2 small coniform spurs; inner spur slightly smaller than the outer (Fig. 1E); second article ventrally with five or seven long setae, arranged in two irregular rows; third article ventrallywith two long setae, with a bidentate apical claw (Fig. 2F, G).

Male. S15 posterior margin narrower than anterior, postero-medially straight; sparsely covered with long setae, more than the anterior; sternite of genital segment slightly smaller than in female, usually weaker sclerotised; posterior margin deeply concave between gonopods, without medial bulge. Long setae scattered on ventral surface of genital segment; fewer setae near S15, fringed with 16–18 longer setae along posterior margin. Gonopods short, appearing as small finger-like bulges, with two long setae, apically slightly sclerotised (Fig. 2H). Legs 15 prominently modified, very thick; prefemur and femur very short, of unusual thickness (Fig. 2H–L); posterior spines of dorsal end of femur curved backward toward base of tibial segment at approximately 60° angle (Fig. 2H–K); anterior tibia raised inwards medially (Fig. 2L).

Lithobius (*Sinuispineus*) *minuticornis* sp. nov.

http://zoobank.org/BBC887BC-B357-4815-B5A2-B46B1431147A
Figs 3, 4 A–K

Diagnosis. Antennae composed of 20–23 articles; ocelli 8–10 on each side, arranged in three irregular rows; posterior two ocelli comparatively large. Tömösváry's organ larger than adjacent ocelli. Commonly 2+2 coxosternal teeth; porodonts lying posterolateral to the lateral-most tooth. Coxal pore formula 3–6, usually 4443 or 5555. Female gonopods with 2+2 moderately small, coniform spurs; male gonopods short and small.

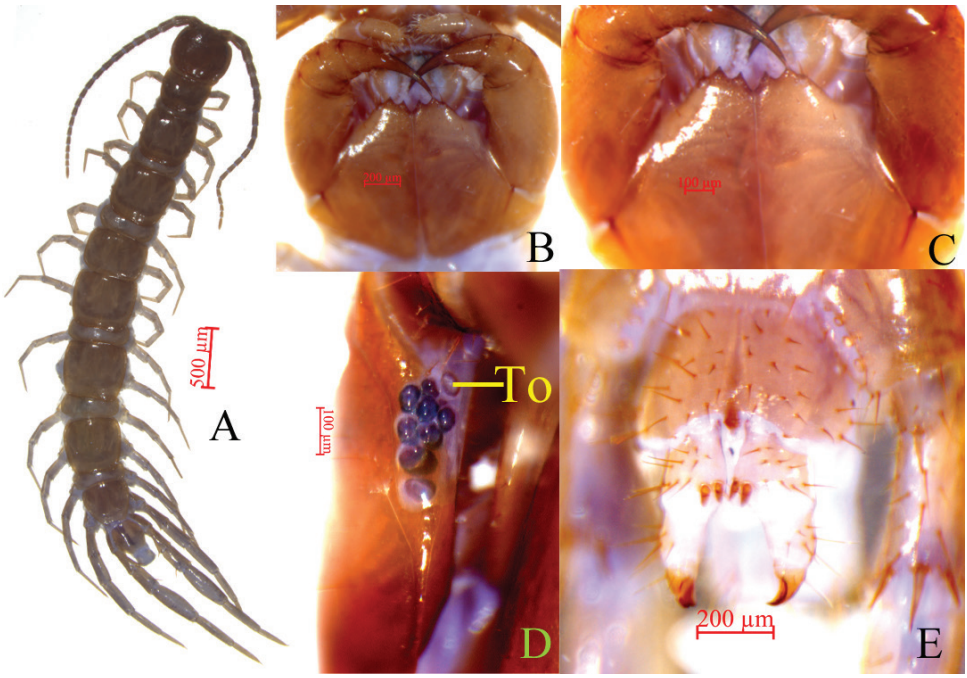

Figure 3. *Lithobius* (*Sinuispineus*) *minuticornis* sp. nov. (holotype **A–D**, paratype female **E**) **A** habitus, dorsal view **B** cephalic plate, ventral view **C** forcipular coxosternite, ventral view **D** ocelli and Tömösváry's organ (To), lateral view **E** posterior segments and gonopods of female, ventral view.

Legs 15 considerably modified; prefemur and femur markedly strong, slightly raised inwards, and posterior spurs on dorsal side of femur of male legs 15 curved backward at base of tibia at no more than 45° angle.

Etymology. The specific name refers to the small, backward-curved posterior spines on the dorsal end of the femur.

Material examined. ***Holotype***, ♂ (LS02-1) (Fig. 3A), 12.31 mm long, cephalic plate 1.31 mm long, 1.47 mm wide, Central China, Zhenlei Mountain Forest Park, Pingqiao County, Xinyang City, Henan Province, 32°04.445'S, 114°08.403'E, 256 m a.s.l. August 27, 2017, S. Pei, H. Ma leg. ***Paratypes***, 65 ♀♀, 50 ♂♂ (LS02-1), same date and locality as holotype.

Description. ***Body*** 10.8–16.7 mm long; ***cephalic plate*** 1.0–1.5 mm long, 1.1–1.5 mm wide.

Colour**:** antennae brown to pale yellow from basal to proximal; distal-most article yellow-brown; tergites brown; pleural region and sternites pale greyish yellow; basal and proximal parts of forcipules, forcipular coxosternite, and SS14 and 15 darker; coxa, trochanter, prefemur, femur, and tibia of all legs bluish; tarsus 1 yellow; tarsus 2 yellow-brown.

Antennae**:** 20–23 articles, commonly 20 articles (Fig. 3A). Except that length of first antennal article is approximately equal to width of base, length of remain-

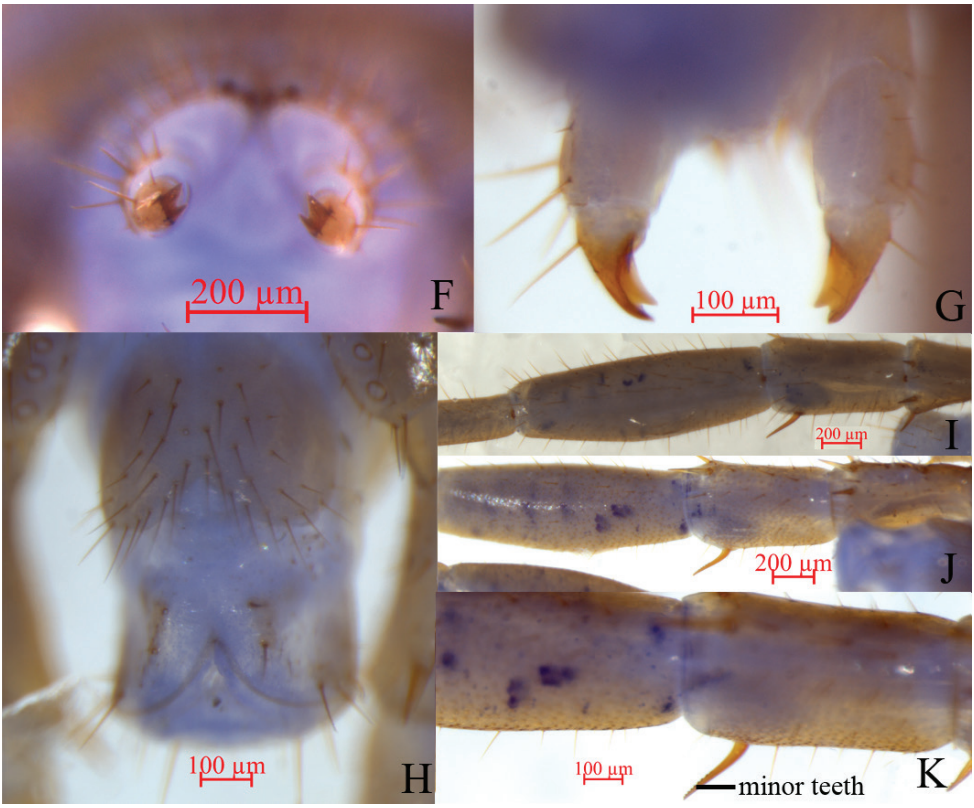

Figure 4. *Lithobius* (*Sinuispineus*) *minuticornis* sp. nov. (paratype female **F, G**; holotype **H–K**) **F** bidentate apical claw of female gonopod, dorsral view **G** bidentate apical claw of female gonopod, ventral view **H** posterior segments and gonopods in male, ventral view **I** femur and tarsus of legs 15, dorsral view **J** femur and tarsus of legs XV15, ventral view **K** posterior spurs of femur of legs 15, ventral view, showing minor teeth.

ing articles larger than width. Moreover, second article thicker and longer than other articles. Beginning with second article, each article gradually shortened; distal-most article considerably longer than width, 3.0–3.9 times longer as wide. Setae abundant on antennal surface; less so on basal articles; density of setae gradually increase to approximately fifth article, then more or less constant.

Cephalic plate smooth, convex, slightly longer than wide; tiny setae emerging from pores scattered very sparsely over the whole surface; frontal marginal ridge with shallow anterior median furrow; short to long setae scattered along marginal ridge of cephalic plate; lateral marginal ridge discontinuous, posterior margin continuous, wider than lateral marginal ridge; middle of the posterior edge straight.

Eight to ten (commonly nine) oval to rounded ocelli on each side, from small to large, in three irregular rows; posterior two ocelli comparatively large. Ventral ocelli slightly larger than dorsal ocelli, domed, translucent, and usually darkly pigmented (Fig. 3D).

Table 3. Leg plectrotaxy of *Lithobius* (*Sinuispineus*) *minuticornis* sp. nov. (female). Letters in brackets indicate variable spines.

Legs	Ventral					Dorsal				
	C	Tr	P	F	Ti	C	Tr	P	F	Ti
1			p	amp	am			mp	a(p)	a
2			p	amp	am			mp	ap	a
3			p	amp	am			mp	ap	ap
4–10			mp	amp	am			mp	ap	ap
11			(a)mp	amp	am			amp	ap	ap
12			amp	amp	am			amp	p	ap
13		m	amp	amp	am			amp	p	ap
14		m	amp	amp	(m)	a		amp	p	p
15		m	amp	am		a		amp	ap	

Tömösváry's organ (Fig. 3D-To) near the ocelli, at anterolateral margin of cephalic plate moderately larger than the adjoining ocelli, surrounding sclerotised area not obvious.

Coxosternite subtrapezoidal (Fig. 3B, C); anterior margin narrow; lateral margins slightly longer than medial margins; median diastema moderately deep, narrowly V-shaped; anterior margin with 2+2 slightly larger, acutely triangular teeth; porodonts thicker, with prominent basal protuberance, lying posterior-lateral to lateral-most tooth (Fig. 3B, C); long, scattered setae on ventral side of coxosternites; longer setae near dental margin.

All tergites smooth, without wrinkles; dorsum slightly convex; tiny setae emerging from sparsely scattered pores over entire surface; near margin bearing a few long setae; TT1 and 14 narrower postero-laterally than antero-laterally, generally trapezoidal; T1 narrower than cephalic plate; T3 approximately equal to cephalic plate; T10 widest. Lateral marginal ridges of all tergites continuous. Posterior margins of TT1, 3, 5, and 7 straight; TT8, 10, 12, and 14 slightly concave. Posterior angles of tergites rounded, without triangular projections. Miniscule setae sparsely scattered over surface.

Posterior side of sternites narrower than anterior, generally trapezoidal, smooth; SS6, 7, 8, 9, and 10 more wider, setae emerging from sparsely scattered pores on surface and lateral margin, with very few long setae sparsely scattered among of them; 2–4 comparatively thick, long setae on both of anterior angles of each sternite; one or two comparatively long, thick setae on both posterior angles of each sternite; more setae on surface of anterior and middle parts than posterior part of each sternite.

Legs relative robust; tarsi fused on legs 1–13; tarsi well-defined on legs 14–15; all legs with fairly long curved claws; legs 1–13 with anterior and posterior accessory spurs; anterior accessory spurs moderately long and slender, forming a moderately small angle with claw; posterior accessory spurs slightly more robust, forming a comparatively large angle with claw; legs 14 and 15 lacking accessory spurs. Short to long setae sparsely scattered over surface of coxa, trochanter, prefemur, femur, and tibia of all legs; more setae on tarsal surface; setae on dorsal tarsal surface slightly shorter than on ventral surface. Legs 14 and 15 in female thicker than anterior pairs; legs 15 in male considerably thicker and stronger than anterior pairs. In females, tarsus2 62.9%–78.8% length of tarsus 1 on legs 15; tarsus 2 5.1–6.5 times longer than its maximum

Table 4. Leg plectrotaxy of *Lithobius* (*Sinuispineus*) *minuticornis* sp. nov. (male). Letters in brackets indicate variable spines.

Legs	Ventral					Dorsal				
	C	Tr	P	F	Ti	C	Tr	P	F	Ti
1			(p)	am	am			mp	(a)p	a
2			mp	am	am			mp	ap	a
3			mp	am	am			mp	ap	ap
4–7			mp	am	am			mp	ap	ap
8–10			m	amp	am			mp	ap	ap
11			m	amp	am			amp	ap	ap
12			(a)mp	amp	am			amp	(a)p	ap
13		m	amp	amp	am			amp	p	ap
14		m	amp	amp	m	a		amp	p	
15		m	amp	am		a		amp	(a)p	

width. In males, tarsus 2 61.3%–70.1% length of tarsus 1 on legs 15; tarsus 2 is 3.5–4.7 times longer than its maximum width. Leg plectrotaxy as in Tables 3 and 4.

Coxal pores 3–6, in a row, round or slightly oval, greatly variable in size from 18.6 μm to 50.7 μm; coxal pore field set in a relatively deep groove; coxal pore-field fringe with prominence; prominence with 8–12 moderately long setae sparsely scattered over surface.

Female. S15 anterior margin broader than posterior, generally trapezoidal, both of anterior and posterior angles generally rounded, posteriomedially straight, short to long setae sparsely scattered on S15 surface. Sternite of genital segment longer than wide, with surface of its lateral sternal margin well chitinised and posterior margin deeply concave between condyles of gonopods, except for a small, median, approximately rhombic bulge. Relatively long setae scattered over ventral surface of genital segment and slightly more setae near S15. Gonopods: first article fairly broad, bearing 22–24 moderately long setae arranged in three irregular rows; with 2+2 small coniform spurs, inner spur slightly smaller than outer spurs (Fig. 3E); second article ventrally with 5–7 long setae, arranged in three irregular rows; third article ventrally with one long and one short setae and with a bidentate apical claw (Fig. 4F, G).

Male. S15 posterior margin narrower than anterior, with both posterior angles rounded; posterior-medially straight, sparsely covered with 31–33 long setae, more than on anterior; sternite of genital segment slightly smaller than in female, usually less sclerotised; posterior margin deeply concave between gonopods, without medial bulge. Long setae scattered on ventral surface of genital segment; fewer setae near S15; fringed with 8–16 longer setae along posterior margin. Gonopods short, appearing as small finger-like bulges, without setae, apically slightly sclerotised (Fig. 4H).

Legs 15 prominently developed, very thick; prefemur and femur very short (Fig. 4I–K), posterior spines of dorsal base of femur curved backwards toward base of tibial segment at no more than 45° angle; anterior tibia raised medially inwards. Distal-most anterior spines of dorsal of coxa bearing one or two small teeth; distal-most middle spines of ventral trochanter with a small tooth; posterior part of prefemur considerably larger than anterior part; distal-most part of anterior, middle, and pos-

terior spines of ventral prefemur with 2–4 small teeth; distal-most anterior, middle, and posterior spines of dorsal prefemur with 1–3 small teeth, with both left and right posterior spines arranged opposite each other; femur markedly thick, slightly raised inwards, with posterior spines of dorsal femur curving backwards towards base of tibial segment at no more than a 45° angle (Fig. 4I–K); distal-most anterior and middle spines of ventral femur with two or three small teeth.

Habitat. The specimens were collected in a *Larix* forest at approximately 200 m above sea level. Specimens were living in moderately moist places under roadside stones and litter on the forest floor.

Discussion

The two new species resemble each other in having the antennae with commonly 20 articles, 8–10 ocelli on each side arranged in three irregular rows, the posterior two ocelli comparatively large, the Tömösváry's organ larger than the adjoining ocelli, 2+2 prosternal teeth, a coxal pore formula of 3–5, and female gonopods with 2+2 coniform spurs. However, they can be distinguished easily by the following characters. T10 is the widest tergite in *S. minuticornis* instead of T8 in *S. sinuispineus*. The posterior spines of the dorsal base of femur curve backwards towards the base of tibial segment at an angle of no more than 45° in *S. minuticornis* in contrast to more than 45° in *S. sinuispineus*. The dorsal plectrotaxy of legs 13 in *S. minuticornis* is 0-0-3-1-2, compared to 1-0-3-2-2 in *S. sinuispineus*. Anterior spines are lacking on both the dorsal and the ventral sides of the tibia of legs 14 and 15 in *S. sinuispineus* vs. present in *S. minuticornis*. Legs 13 having posterior accessory spurs in *S. minuticornis* rather than lacking in *S. sinuispineus*.

Acknowledgements

This study was supported by the National Natural Science Foundation of China (NSFC grant no. 31572239) and the Key Discipline of Zoology of Hengshui University. We are grateful to Dr Gregory D. Edgecombe, London, UK, Dr Pavel Stoev, Sofia, Bulgaria, and Dr Marzio Zapparoli, Viterbo, Italy, for their hospitality and great help during our research. We thank Dr Rowland M. Shelley, North Carolina, USA, and Dr His-Te Shih, Taichung, China, for providing us with invaluable literature.

References

Bonato L, Chagas Jr A, Edgecombe GD, Lewis JGE, Minelli A, Pereira LA, Shelley RM, Stoev P, Zapparoli M (2016) ChiloBase 2.0 – A World Catalogue of Centipedes (Chilopoda). https://chilobase.biologia.unipd.it/ [Accessed on: 2020-10-6]

Bonato L, Edgecombe GD, Lewis JGE, Minelli A, Pereira LA, Shelley RM, Zapparoli M (2010) A common terminology for the external anatomy of centipedes (Chilopoda). ZooKeys 69: 17–51. https://doi.org/10.3897/zookeys.69.737

Ma H, Pei S, Hou X, Zhu T, Wu D, Gai Y (2014) An annotated checklist of Lithobiomorpha of China. Zootaxa 3847(3): 333–358. https://doi.org/10.11646/zootaxa.3847.3.2

Pei S, Liu H, Lu Y, Hou X, Ma H (2019) *Lithobius* (*Ezembius*) *ternidentatus* sp. n. (Lithobiomorpha, Lithobiidae), a new species from China. ZooKeys 829: 1–13. https://doi.org/10.3897/zookeys.829.30884

Qiao P, Ma H, Pei S, Zhang T, Su J (2019a) *Lithobius* (*Ezembius*) *polyommatus* sp. n. and *Lithobius* (*Ezembius*) *dulanensis* sp. n. (Lithobiomorpha: Lithobiidae), two new species from Qinghai-Tibet Plateau, China Biologia 74(5): 455–462. https://doi.org/10.2478/s11756-018-00173-z

Qiao P, Qin W, Ma H, Zhang T, Su J, Lin G (2019b) Two new species of lithobiid centipedes and the first record of *Lamyctes africanus* Porath (Chilopoda: Lithobiomorpha) in China. Journal of Natural History 53(15–16): 897–921. https://doi.org/10.1080/00222933.2019.1606355

Zhang R (2011) Zoogeography of China. Science Press, Beijing, 502 pp. [see P. 15]

ZooKeys 980: 57–77 (2020)
doi: 10.3897/zookeys.980.54805
https://zookeys.pensoft.net

RESEARCH ARTICLE

A peer-reviewed open-access journal
ZooKeys
Launched to accelerate biodiversity research

Mayfly response to different stress types in small and mid-sized lowland rivers

Marina Vilenica[1], Mladen Kerovec[2], Ivana Pozojević[2], Zlatko Mihaljević[2]

1 *University of Zagreb, Faculty of Teacher Education, Trg Matice Hrvatske 12, Petrinja, Croatia* **2** *University of Zagreb, Faculty of Science, Department of Biology, Rooseveltov Trg 6, Zagreb, Croatia*

Corresponding author: Marina Vilenica (marina.vilenica@gmail.com)

Academic editor: L. Pereira-da-Conceicoa | Received 27 May 2020 | Accepted 31 August 2020 | Published 28 October 2020

http://zoobank.org/50077C64-08AD-4E37-82F6-8C672A9235D4

Citation: Vilenica M, Kerovec M, Pozojević I, Mihaljević Z (2020) Mayfly response to different stress types in small and mid-sized lowland rivers. ZooKeys 980: 57–77. https://doi.org/10.3897/zookeys.980.54805

Abstract

Freshwater ecosystems are endangered worldwide by various human pressures, resulting in dramatic habitat and species loss. Many aquatic invertebrates respond to disturbances in their habitat, and mayflies are among the most sensitive ones. Therefore, we investigated mayfly response to anthropogenic disturbances at 46 study sites encompassing slightly to heavily modified small and mid-sized lowland streams and rivers. Mayfly nymphs were sampled between April and September 2016 using a benthos hand net. A total of 21 species was recorded, with *Cloeon dipterum* (Linnaeus, 1761) being the most frequently recorded one. Nevertheless, the taxa richness was rather low per site, i.e., between zero and nine. Assemblage structure had a high share of lower reaches and lentic (potamic and littoral) elements, and detritivores (gatherers/collectors and active filter feeders). This indicates that hydromorphological alterations lead to assemblage "potamisation" in small and mid-sized rivers. More mayfly species were related to higher oxygen concentration and lower water temperature, abundance of aquatic vegetation and total organic carbon. Additionally, the assemblage diversity and abundance were negatively associated with increasing intensive agriculture area at the catchment scale. This study confirms mayfly bio-indicative properties, i.e., their sensitivity to alterations of their habitat and pollution, but also provides new data related to mayfly response to the impacted environment. Those data can be used for management and protection activities of lowland rivers and their biota according to the requirements of the European Water Framework Directive.

Keywords

Environmental stress, Ephemeroptera, feeding guilds, longitudinal zonal associations, pollution

Introduction

Freshwater ecosystems represent an indispensable resource of water supplies for humans (Carpenter et al. 2011), but they also have a crucial role in biodiversity maintenance and conservation (Previšić et al. 2009; Ivković and Plant 2015). Therefore, it is essential they remain in good ecological status (Dudgeon et al. 2006; Vörösmarty et al. 2010). Nevertheless, the status of many aquatic systems is far from good worldwide (Carpenter et al. 2011). Various anthropogenic impacts represent major threats to aquatic biodiversity and make lotic habitats among the most endangered ones (Malmqvist and Rundle 2002; Hering et al. 2006; Stoddard et al. 2006). Human population growth, increased urbanisation and industrialisation have led to increased demands for land use for purposes of agriculture, forestry, irrigation activities and wetland drainage, resulting in alterations of habitat morphology, hydrological regime and causing degraded water quality, pollution and increased sediment erosion into lotic systems (Waters 1995; Dudgeon et al. 2006; Woodward et al. 2012). By altering their natural condition, such activities largely downgrade the habitat integrity, which results in reduced ecological function and biodiversity (Steffen et al. 2015), including native species loss (Carpenter et al. 2011). The habitat characteristics change dramatically: formation of macrophyte assemblages is disturbed (Jones et al. 2014; Turunen et al. 2017), habitat heterogeneity and availability for macroinvertebrates is reduced (Jones et al. 2012), while primary production (Louhi et al. 2017) and decomposition of organic matter (Lecerf and Richardson 2010) are highly altered.

As freshwater organisms live almost continuously in the aquatic environment, they clearly respond to all those environmental stresses (Morse et al. 2007; Vilenica et al. 2019; 2020). The aquatic assemblages can respond to alterations of their habitats with their structure differing from a reference state, i.e., they can show characteristics of "rhithralisation" (e.g., caused by channel straightening) or "potamisation" (e.g., caused by the impounding) (Jungwirth et al. 2000; Moog and Chovanec 2000; Kokavec et al. 2018; Vilenica et al. 2016; 2019), or there is a change in the trophic structure (Brasil et al. 2013). By observing the assemblages' structural alterations, we can conclude that the lotic system has been altered, which in the end indicates a certain level of ecological disturbance (Moog 2002; Vilenica et al. 2016). Mayflies are able to colonise all kinds of freshwater habitats but are found to be the most diverse in lotic ones. They are among particularly sensitive aquatic macroinvertebrates, mainly disappearing when faced even with small-scale disturbance in their habitat (Firmiano et al. 2017; Vilenica et al. 2019). Previous studies demonstrated that the majority of species can tolerate a rather narrow range of environmental factors, being highly sensitive to oxygen depletion, acidification, and various contaminants such as metals, ammonia, nitrogen, phosphorous (Moog et al. 1997; Vilenica et al. 2017, 2019). Therefore, the absence/presence of a particular species can tell us a lot about the quality of the environment it inhabits. Ecological assessments in different regions worldwide, as well as at habitats of various ecological status are necessary for effective conservation and management of freshwater habitats and their biota (Hughes et al. 1986; Stoddard et al. 2008). There-

fore, in order to obtain additional data on mayfly response to anthropogenic disturbances in their habitat, we investigated mayfly assemblages and their relationship with environmental factors at 46 slightly to heavily modified lotic habitats.

Materials and methods

Study area

The study encompassed 46 lotic slow-flowing study sites (Tables 1, 2, Fig. 1), including heavily modified streams and rivers (by, for instance, channelling and/or modification of the water flow or riverbed, removal of the riparian vegetation and pollution). The majority of the study sites are located in the vicinity of agricultural areas or cattle farms. Sampling was conducted between April and September 2016. Within the research, it was not possible to include a reference site. True reference sites are not available due to long-lasting and strong anthropogenic influence. The relatively high ratio of urban areas and even more agricultural ones are present in their catchment. The majority of the rivers have been channelled for agricultural land use purposes, or have limited lateral movement because of dykes protecting urban areas and settlements. During RFI (River Fauna Index) and assessment system development, the best available sites were chosen. The reference RFI and metrics value was calculated by adding 20% of the metric range to the high/good boundary. Study sites are part of the national monitoring program. From 25 m (small streams) to 50 m (mid-sized rivers) long sampling area was selected to cover the greatest possible diversity of microhabitats representative of the reach.

The study area is located in the Croatian part of the Pannonian lowland ecoregion (ER11) (Illies 1978). The area is characterised with temperate humid climate with warm summer (Cfb, Köppen classification) where the average temperature of the warmest month is below 22 °C (Šegota and Filipčić 2003). The average annual air temperature is around 12 °C and average annual rainfall is between 800 and 1100 mm (Zaninović et al. 2008).

Sampling protocol

Mayfly nymphs were collected together with other macroinvertebrates (AQEM protocol- AQEM expert consortium 2002). At each site, 20 subsamples were collected proportionally according to available microhabitat presence, using a benthos hand net (25 × 25 cm; mesh size = 500 μm) and pooled into one composite sample. The substrates were mainly composed of fine sediment (sand, silt, mud), lithal (stones, gravel), and aquatic vegetation (submerged and emergent). Samples were stored in 96% alcohol and analysed in the lab.

In the laboratory, subsampling was done to reduce the effort for sorting and identification. At least 1/6 of the sample was sorted until the minimum targeted number of 700 individuals was reached. The rest of the sample was also inspected searching for

Table 1. List of the 46 degraded lowland streams and rivers investigated in Croatia, with environmental parameters measured at the time of macroinvertebrate sampling. Codes of the study sites are as in Fig. 1. Legend: River size – S – small rivers (catchment area less than 100 km^2), M – medium-sized rivers (catchment area less than 1000 km^2). Channel width and water depth are expressed in meters. HYMO Group in SIMPER analysis – according to RFI EQR (1 – good and high; 2 – moderate; 3 – poor and bad). Tw – water temperature (°C), Oxy – dissolved oxygen content (mg/L), Con – conductivity (μS/cm), pH – pH, dominant substrates – lithal – stones, gravel; fine sediment – silt, mud, sand; phytal – aquatic vegetation.

Study site	River size	Width	Depth	HYMO Group	Coordinates (N/E)		Tw	Oxy	Con	pH	Dominant substrates
1	S	6.0	1.5	1	46.24	16.17	14	10.09	503	7.96	Lithal, fine sediment, phytal
2	S	3.0	0.8	1	46.17	17.15	19	3.64	718	7.54	Fine sediment, phytal
3	S	8.0	1.0	1	46.04	15.99	13	9.96	556	8.15	Fine sediment, phytal
4	M	18.0	2.0	3	45.83	15.82	16	9.02	605	8.16	Fine sediment, phytal
5	M	16.0	30.0	3	45.93	15.82	16	8.05	628	8.13	Lithal, fine sediment, phytal
6	M	8.0	1.0	3	46.03	15.91	19	8.77	710	8.05	Lithal, fine sediment
7	S	6.0	0.4	1	46.15	15.88	13	8.97	574	8.17	Lithal, fine sediment, phytal
8	S	5.0	0.5	2	45.86	16.33	16	8.20	796	8.50	Fine sediment, phytal
9	S	3.0	0.3	2	45.86	16.40	15	3.92	702	7.64	Fine sediment, phytal
10	S	5.0	0.4	2	45.98	15.94	17	10.20	484	8.15	Fine sediment
11	S	4.0	0.6	3	45.67	16.42	11	6.02	564	7.85	Fine sediment, phytal
12	S	3.0	0.4	1	46.05	16.07	13	10.25	545	8.47	Lithal, fine sediment
13	S	2.5	0.5	2	46.50	16.47	16	9.81	446	7.82	Fine sediment, phytal
14	S	1.5	0.3	1	46.40	16.45	14	7.81	316	7.60	Lithal, phytal
15	S	3.0	0.5	1	46.27	16.86	21	6.90	982	7.52	Fine sediment, phytal
16	S	1.5	0.3	1	46.12	17.03	25	9.20	885	9.20	Fine sediment, phytal
17	S	6.0	1.0	1	45.69	16.39	11	8.12	625	8.12	Fine sediment, phytal
18	S	2.0	0.5	1	46.48	16.51	14	9.55	332	7.58	Fine sediment, phytal
19	S	5.0	0.8	2	46.43	16.60	16	7.50	391	7.48	Fine sediment, phytal
20	S	4.0	1.0	2	46.37	16.69	16	9.89	735	8.19	Fine sediment, phytal
21	S	7.0	1.0	1	46.34	16.81	17	8.80	608	8.18	Fine sediment, phytal
22	M	4.0	0.8	3	45.82	16.28	14	8.41	592	8.22	Lithal (phytal sporadically)
23	M	10.0	0.8	3	45.81	16.41	12	10.70	616	8.48	Fine sediment, phytal
24	M	15.0	2.0	3	45.78	16.49	11	6.60	610	7.98	Lithal, fine sediment
25	M	10.0	1.0	3	45.63	16.56	12	5.75	581	8.02	Fine sediment, phytal
26	M	6.0	1.0	3	45.72	17.04	21	3.58	429	7.52	Fine sediment, phytal
27	M	12.0	1.2	3	45.83	16.64	25	5.05	396	7.70	Lithal, phytal
28	M	14.0	1.0	3	45.84	16.82	23	6.75	401	7.78	Fine sediment, phytal
29	M	9.0	0.6	3	46.16	15.61	16	8.29	553	8.16	Fine sediment
30	M	6.0	1.5	2	46.00	17.25	17	9.17	551	7.77	Fine sediment, phytal
31	M	5.0	1.5	3	46.04	15.85	21	8.85	713	7.97	Fine sediment, phytal
32	M	2.5	0.4	3	46.00	15.86	19	8.78	732	8.02	Fine sediment, phytal
33	M	10.0	1.5	3	46.12	17.03	20	7.87	588	7.62	Fine sediment, phytal
34	M	4.0	0.5	3	45.58	17.04	24	8.30	461	8.04	Fine sediment
35	S	5.0	0.5	1	45.59	17.19	22	6.52	539	7.65	Fine sediment, phytal
36	S	4.5	0.3	1	45.61	17.24	18	8.95	465	8.23	Lithal, fine sediment
37	S	1.5	0.2	1	45.88	16.39	22	8.93	207	8.15	Fine sediment
38	S	2.0	0.2	1	46.32	16.62	12	5.22	524	7.52	Fine sediment
39	S	1.5	1.0	1	46.52	16.43	16	8.29	629	7.77	Lithal, fine sediment, phytal
40	S	3.5	0.6	2	46.34	16.82	17	5.70	574	5.68	Phytal
41	S	2.0	0.4	2	46.01	16.45	25	1.53	619	7.85	Fine sediment, phytal
42	S	2.5	0.3	1	45.78	15.84	20	6.90	670	7.85	Fine sediment, phytal
43	S	2.5	0.3	2	45.60	16.99	20	4.52	601	7.75	Lithal, fine sediment
44	S	2.0	0.5	1	46.51	16.31	12	8.80	740	8.45	Lithal, fine sediment
45	S	3.0	0.7	2	46.45	16.59	14	3.50	541	7.36	Phytal
46	M	-	-	3	45.87	16.49	9	6.68	578	7.77	Fine sediment, phytal

Table 2. List of the 46 degraded lowland streams and rivers investigated in Croatia, with environmental parameters presented as mean value of 12 composite samples collected over a one-year period (January–December 2016) (including standard deviation, SD). Codes of the study sites are as in Fig. 1. Legend: NH_4^+ – ammonium (mgN/L), NO_3^- – nitrates (mgN/L), TN – total nitrogen (mgN/L), PO_4^{3-} – orthophosphates (mgP/L), TOC – total organic carbon (mg/L), BOD_5 – biological oxygen demand (mgO_2/L), COD_{Mn} – chemical oxygen demand (mgO_2/L).

Study site	NH_4^+ mean/SD	NO^{3-} mean/SD	TN mean/SD	PO_4^{3-} mean/SD	TOC mean/SD	BOD_5 mean/SD	COD_{Mn} mean/SD
1	0.373/0.199	1.090/0.282	1.940/0.454	0.062/0.030	4.037/0.531	2.308/0.915	3.942/1.033
2	0.014/0.008	0.100/0.077	0.466/0.115	0.016/0.016	5.235/2.197	2.531/2.294	4.463/2.286
3	0.224/0.142	1.033/0.235	1.788/0.332	0.094/0.053	3.429/0.952	2.192/0.960	3.567/1.120
4	0.178/0.237	1.284/0.438	1.928/0.473	0.050/0.035	3.671/1.026	1.767/1.314	3.733/1.700
5	0.316/0.268	1.227/0.323	2.073/0.449	0.065/0.037	3.671/1.002	2.150/1.218	3.933/1.522
6	0.437/0.221	1.392/0.294	2.443/0.496	<0.025	4.292/1.456	4.969/1.585	6.636/1.624
7	0.920/0.556	1.179/0.202	2.95/0.950	<0.025	4.917/1.575	6.663/1.021	8.878/2.742
8	0.460/0.533	0.948/0.793	1.772/1.328	0.333/0.137	6.297/1.451	3.153/1.441	8.469/1.714
9	3.240/3.931	1.110/0.977	6.379/6.053	1.952/2.799	9.971/4.071	3.028/1.937	10.308/2.030
10	0.061/0.036	1.038/0.424	1.517/0.799	<0.025	3.292/1.515	4.039/2.120	5.772/3.010
11	0.333/0.413	1.701/1.479	2.527/2.185	0.215/0.091	7.608/1.688	3.019/1.209	7.992/2.235
12	0.256/0.169	1.365/0.570	2.032/0.552	<0.025	2.233/0.463	3.395/0.460	4.822/1.926
13	0.279/0.112	2.600/0.553	3.775/0.758	0.046/0.058	1.874/0.569	1.525/0.652	1.898/0.894
14	1.599/1.792	2.304/1.205	5.025/2.419	0.340/0.269	5.582/1.108	2.683/0.878	4.694/2.138
15	0.158/0.188	0.540/0.286	1.080/0.130	0.058/0.057	4.561/1.100	1.880/1.132	5.070/1.630
16	0.513/1.238	1.416/0.853	2.880/1.608	0.141/0.141	5.922/4.891	1.650/1.297	5.147/4.094
17	0.306/0.264	1.852/1.071	2.370/1.135	0.310/1.148	7.352/1.694	3.240/1.087	8.449/2.717
18	0.018/0.005	3.918/0.865	5.250/1.091	0.010/0.008	2.095/0.777	1.033/0.473	2.085/1.088
19	0.064/0.103	1.317/2.013	1.694/3.011	0.020/0.022	1.333/4.571	1.317/0.709	1.338/0.543
20	0.276/0.781	6.541/1.196	8.192/1.483	0.080/0.207	<1.000/0.760	1.146/1.175	0.936/0.495
21	0.053/0.096	3.478/0.721	4.683/1.069	0.018/0.021	1.237/0.365	1.183/0.629	1.097/0.507
22	0.157/0.153	1.873/0.717	2.260/0.861	0.136/0.056	3.633/1.140	2.303/0.630	4.584/1.491
23	0.373/0.379	1.700/0.728	2.370/1.001	0.343/0.183	5.388/1.283	2.998/1.118	6.672/2.563
24	0.574/0.494	1.938/1.099	3.702/1.599	0.333/0.303	5.489/2.591	5.600/3.252	10.933/4.000
25	0.487/0.232	1.503/0.881	2.744/0.978	0.171/0.116	8.458/2.809	3.895/0.698	10.949/5.439
26	0.067/0.099	0.796/0.221	1.170/0.446	0.105/0.063	6.230/3.294	4.178/2.417	11.689/5.089
27	0.514/0.537	1.965/1.346	3.799/2.105	0.208/0.094	7.134/3.248	8.033/3.588	14.122/5.349
28	0.096/0.055	1.285/0.850	2.168/1.227	0.103/0.043	6.046/2.803	4.967/3.297	12.633/4.379
29	0.141/0.121	1.071/0.258	1.713/0.376	0.077/0.036	3.868/0.989	1.517/0.536	4.117/0.920
30	0.115/0.123	0.654/0.409	1.375/0.270	0.040/0.065	3.096/0.757	1.242/0.575	2.320/1.134
31	0.493/0.378	0.952/0.411	1.968/0.577	<0.025	3.761/0.987	4.683/1.356	6.483/1.925
32	0.198/0.156	1.031/0.429	1.733/0.457	<0.025	4.672/1.354	3.949/2.710	5.772/3.876
33	0.223/0.207	0.668/0.394	1.392/0.545	0.225/0.211	2.993/1.132	1.200/0.544	2.472/1.001
34	0.413/0.432	2.179/0.427	3.227/0.784	0.224/0.180	3.316/1.727	4.089/3.240	6.678/1.281
35	0.818/0.422	1.283/0.255	3.067/0.836	0.224/0.117	3.518/2.219	7.133/4.520	8.722/4.855
36	<0.015/0.000	1.070/0.157	1.000/0.439	0.035/0.022	2.184/1.759	4.963/11.023	4.850/3.754
37	0.211/0.262	3.127/1.100	3.615/1.260	6.545/3.751	7.596/1.717	2.734/1.460	8.558/1.782
38	1.919/0.962	0.967/0.804	3.758/1.141	0.131/0.149	2.023/0.977	3.058/1.561	1.443/0.795
39	0.537/1.151	1.251/0.699	2.567/1.315	0.092/0.187	3.866/1.503	2.208/1.308	3.451/1.431
40	4.093/3.559	0.554/0.432	5.033/3.206	0.248/0.308	4.695/1.898	4.042/1.254	3.568/2.977
41	5.007/9.111	1.484/0.903	9.567/10.991	1.569/0.850	9.585/4.024	6.225/1.299	15.489/7.189
42	1.240/1.059	2.915/1.127	5.168/1.728	0.387/0.124	4.146/0.727	4.626/1.106	5.897/1.183
43	3.495/2.977	3.880/5.995	14.023/10.061	1.488/1.851	8.142/4.419	22.856/27.457	18.933/8.407
44	0.320/0.520	0.931/0.568	1.858/0.678	0.069/0.063	3.651/0.975	1.500/0.729	3.224/1.660
45	0.103/0.190	5.545/1.319	7.258/1.939	0.025/0.031	2.120/0.298	0.729/0.378	1.807/0.802
46	1.220/1.098	1.996/0.912	3.970/2.179	0.322/0.154	5.082/1.524	4.366/1.171	6.112/1.952

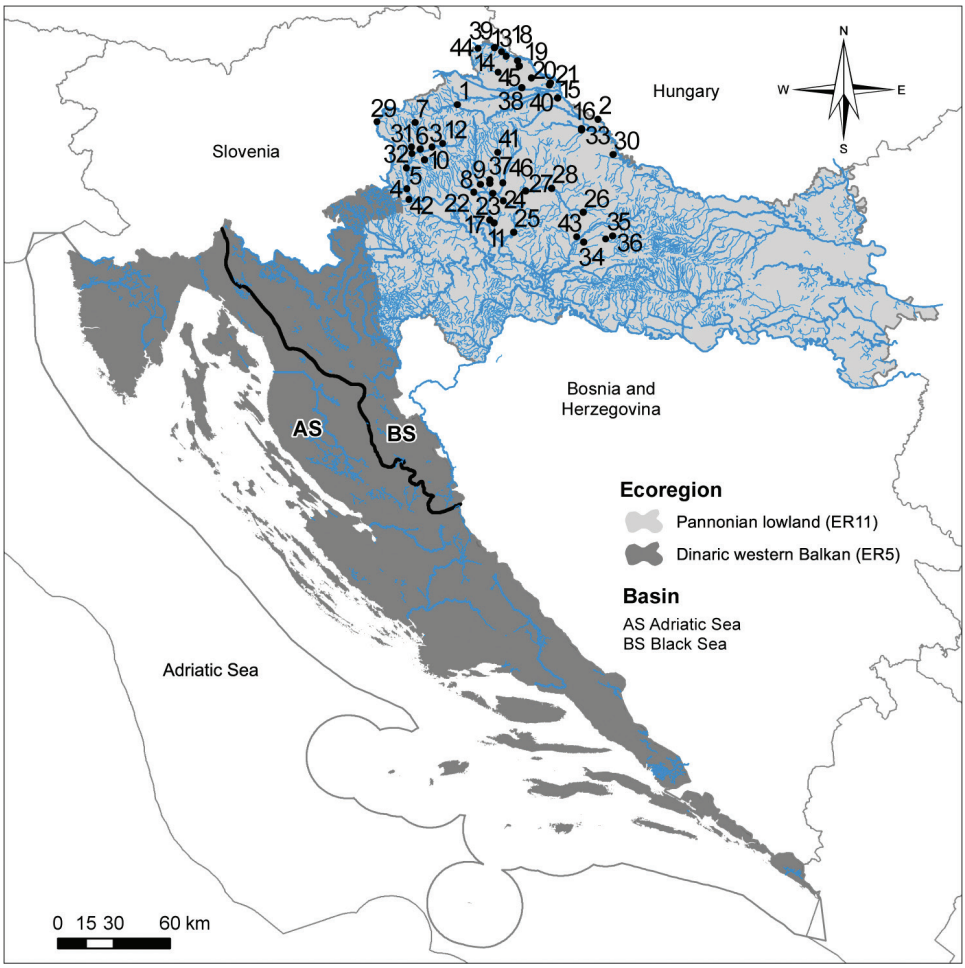

Figure 1. Map of the 46 study sites located in the Pannonian lowland ecoregion in Croatia. *Legend: Study sites: **1** Bednja, Stažnjevec village **2** Ždalica, Ždala village **3** Krapina, Bedekovčina village **4** Krapina, Zaprešić town **5** Krapina, Kupljenovo village **6** Krapinica, Zabok town **7** Krapinica, Krapina town **8** Rajna, between Vrbovec town and Lonjica village **9** Zlenin, Vrbovec village **10** Vukšinac, Stubice village **11** Deanovac lateral canal, near Ivanić Grad town **12** Reka, Lovrečan village **13** Brodec, Peklenica village **14** Lateral canal Mihovljan, Čakovec town **15** Poloj, between Legrad and Đelekovec villages **16** Zdelja, Molve village **17** Lonja, near Ivanić Grad town **18** Jalšovnica, Ferketinec village **19** Bošćak, Domašinec village **20** Bistrec, Rakovnica I **21** Bistrec, Rakovnica II **22** Zelina, Božjakovina village **23** Connecting canal Zelina-Lonja-Glogovnica-Česma, Poljanski lug village **24** Glogovnica, before mouth to Česma **25** Česma, Obedišće village **26** Česma, Pavlovac village **27** Česma, Sišćani village **28** Česma, Narta village **29** Sutla, Luke Poljanske village **30** Rogostrug, Podravske Sesvete village **31** Kosteljina, Jalšje village **32** Horvatska, Veliko Trgovišće village **33** Bistra Koprivnička, Molve village **34** Toplica, Sokolovac village **35** Toplica, downstream from Daruvar town **36** Toplica, upstream from Daruvar town **37** Luka, Vrbovec town **38** Sewage collector, Prelog town **39** Gornji potok, between Selnica and Praporčan villages **40** Kotoribski kanal, Kotoriba village **41** Črnec, Gornji Dubovec vilage **42** Gostiraj, Ježdovec village **43** Tomašica, Tomašica village **44** Jalšovec, between Bukovje and Štrigova villages **45** Murščak, between Domašinec and Stara Straža villages **46** Glogovnica, Koritna village.

macroinvertebrates which are not part of subsample analysed. Mayflies were identified to the lowest possible taxonomical level (very juvenile and/or damaged individuals were identified only to the genus or family level) using Müller-Liebenau (1969), Malzacher (1984) and Bauernfeind and Humpesch (2001). All voucher specimens are deposited at the Department of Biology, Faculty of Science, University of Zagreb, Croatia.

Environmental factors

At each study site, the following environmental parameters were measured at the time of macroinvertebrate sampling: water temperature, dissolved oxygen concentration (using the oximeter WTW Oxi 330/SET), conductivity (with the conductivity meter WTW LF 330), pH (using the pH-meter WTW ph 330), mean channel width and maximum water depth (using a hand meter on approximately 100 meter long reach of specific site) (Table 1). The remaining environmental parameters are presented as the mean value of 12 composite samples collected over a one-year period (January – December 2016) (Table 2). Water chemistry analyses were carried out according to standard methods (APHA 1992). Land use variables were defined from the share of land use categories at the catchment scale, extracted from Corine Land Cover (CLC) data (CLC Hrvatska 2013) using ArcGIS version 10.2.1 (Esri Corp., Redlands, CA, USA). A relative measure of hydromorphological (HYMO) alternation was given by calculating the River fauna index (RFI) using macroinvertebrate species sensitivity scores. A version of the RFI adapted for Croatian rivers and streams following Urbanič (2014) gives a score of HYMO alternation based on the response of macroinvertebrate assemblages. The scores are then normalised with regard to reference states in the form of the WFD (Water framework directive) recommended EQRs (ecological quality ratios) and range from 0 (the worst HYMO conditions) to 1 (reflecting reference states). The HYMO evaluation of rivers has been performed by European Standards EN 14614 and EN 15843. Type specific RFI was used as a relative measure of HYMO alternation because HYMO evaluations for all of the investigated rivers are not available.

Data analysis

Mayfly assemblages from sites classified as high and good by the RFI EQR (EQR > 0.6) represented Group 1, from sites classified as moderate (0.4 < EQR <0.6) represented Group 2 and from sites classified as poor and bad (EQR < 0.4) represented Group 3 in the analysis of similarity percentages (SIMPER) of the (Bray-Curtis) similarity (Clarke 1993) between mayfly assemblages. This was done in order to determine how mayfly assemblages differ among sites of different degrees in HYMO alternation in terms of species composition and abundance contribution.

The composition of mayfly assemblages in terms of the trophic structure and longitudinal zonal associations of species at each study site was analysed using the classification given by Buffagni et al. (2009; 2020), while the methodology was described in Vilenica et al. (2018). Study sites without mayfly records, and sites with one taxon

where we could not identify the specimens to the species level (i.e., sites 17 and 18) were excluded from the analysis.

In order to ordinate mayfly occurrence with respect to environmental variables, the Canonical Correspondence Analysis (CCA) was used. The analysis was performed using data for 21 taxa (rare species were downweighed) and 14 environmental variables. The Monte Carlo permutation test with 499 permutations was used to test the statistical significance of the relationship between all taxa and all variables.

Mayfly taxa abundances were correlated against agricultural land cover data, using the Spearman coefficient, in order to determine if and to what extent does this type of land cover in the catchment area influence specific taxa occurrence. Mayfly species richness, abundance and local diversity (Shannon index) were plotted against the ratio of intensive agriculture in the catchment in order to determine the "general" mayfly response in relation to increased agricultural pressures.

The Bray-Curtis similarity index, Shannon diversity index and SIMPER analyses were conducted in Primer 6 (Clarke and Gorley 2006). The CCA analysis was performed using CANOCO 5.00 (ter Braak and Šmilauer 2012). Mayfly/intensive agriculture graphs were plotted, and regression equations were calculated and tested for significance using Statistica 13.0 (TIBCO Software Inc. 2017). The species data were log-transformed prior to analyses. All figures were processed with Adobe Illustrator CS6.

Results

Mayfly assemblages

A total of 21 species (27 taxa) was recorded of which the most widespread was *Cloeon dipterum* (Linnaeus, 1761), recorded at 18 study sites, while *Serratella ignita* (Poda, 1761) was the most abundant (Table 3). Nine species were recorded at only one study site, with *Heptagenia flava* Rostock, 1878, *Alainites muticus* (Linnaeus, 1758), and *Oligoneuriella rhenana* (Imhoff, 1852) being the rarest ones (Table 3). The highest number of taxa was recorded at study sites 22 and 36 (nine), while no mayfly was recorded at sites 35, 37, 38, 41, 43, 45 (Table 3).

The SIMPER group similarity analysis (Table 4) showed that all groups of sites were dominated by juvenile instars of *Baetis* sp. and had significant abundances of *Cloeon dipterum* present at most sites. *Baetis fuscatus* (Linnaeus, 1761) and *Baetis buceratus* Eaton, 1870 were associated with sites of both ends of the HYMO gradient (Group 1 and Group 3). Furthermore, *Baetis vernus* Curtis, 1834 individuals were associated with sites that had a lower degree of HYMO degradation (Group 1 and Group 2). Juvenile instars of *Caenis* sp. were usually associated with more degraded sites (Group 3), whereas *Serratella ignita* and *Caenis luctuosa* (Burmeister, 1839) were associated only with sites of good and high ecological status following the RFI.

Generally, a high share of lower reaches and lentic elements (potamic and littoral elements) was recorded: it was dominant (> 50 %) at 13 study sites, eight sites had an

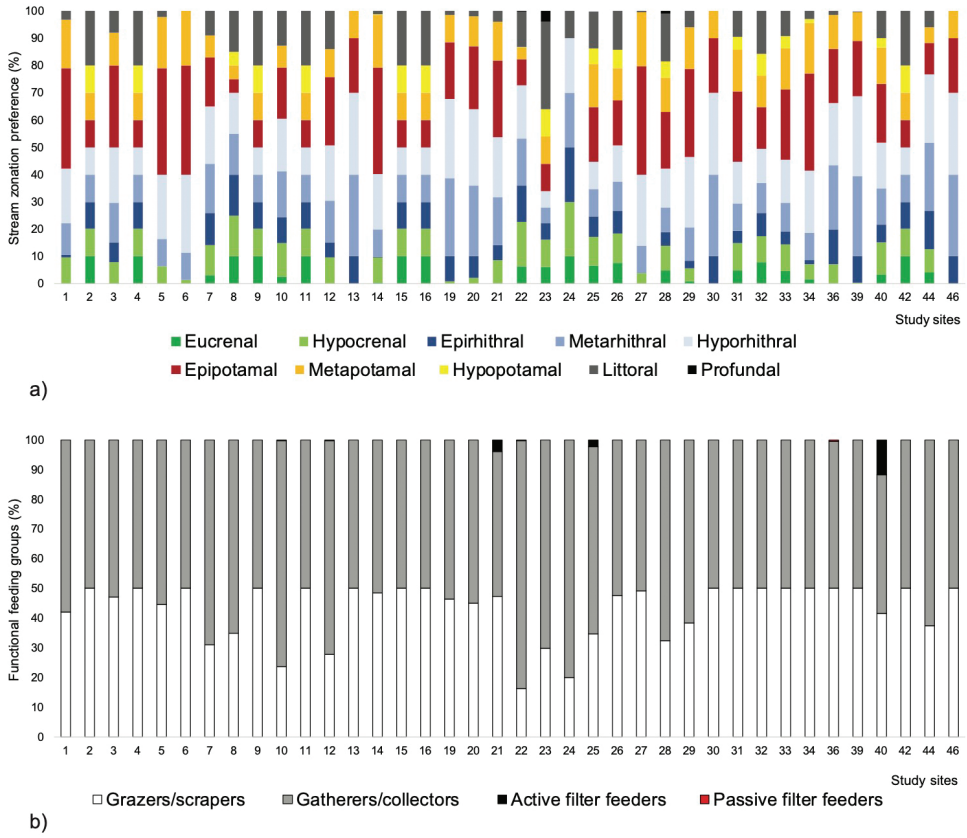

Figure 2. a Longitudinal zonal associations and **b** trophic structure of mayfly assemblages at the 46 degraded lowland streams and rivers investigated in Croatia. Study site codes are presented in Fig. 1.

equal share of lower reaches/lentic and upper reaches elements (crenal and rhithral) (50:50 %), while16 study sites were dominated by upper reaches elements (> 50 %) (Fig. 2a). We also recorded a high share of detritivores (gatherers/collectors and active filter feeders): they were dominant at 21 study sites and equally represented as grazers/scrapers at the rest of the sites (Fig 2b).

Mayflies and environmental variables

The results of the ordination of species and environmental data of the CCA are presented on the F1 × F2 ordination plot (Fig. 3). The eigenvalues for the first two CCA axes were 0.40 and 0.25 and explained 50.9 % of the species-environment relations. The Monte Carlo permutation test showed that the species-environment ordination was significant (first axis: F-ratio = 4.23, p = 0.002; overall: trace = 1.28, F = 1.54, p = 0.006) indicating that mayfly assemblages were significantly related to the tested set of environmental variables. Axis 1 was related to total organic carbon (R = 0.49)

Table 3. Mayfly taxa recorded (individuals/m^2) at the 46 degraded lowland streams and rivers investigated in Croatia. Codes of the study sites are as in Fig. 1.

Taxa codes	1	2	3	4	5	6	7	8	9	10	11	12	13	14	15	16	17	18	19	20	21	22
a	0	16	0	0	0	0	0	0	0	0	0	0	0	0	0	0	0	0	0	0	0	0
b	0	0	0	0	0	0	0	0	0	0	0	0	0	0	0	0	0	0	0	0	0	0
c	0	12	0	0	368	292	0	0	0	16	0	16	432	976	0	0	88	16	2224	330	906	16
d	120	0	48	0	120	36	0	0	0	0	0	0	0	1008	0	0	0	0	0	2	316	0
e	0	0	720	0	80	252	16	0	0	0	0	112	0	80	0	0	0	0	0	0	0	0
f	0	0	0	0	0	0	0	0	0	0	0	0	0	0	0	0	0	0	0	0	0	0
g	0	0	16	0	0	0	0	0	0	0	0	16	0	0	0	0	0	0	0	0	0	0
h	0	0	0	0	0	0	16	0	0	0	0	0	128	0	0	0	0	0	104	16	142	0
i	0	0	0	0	0	0	0	0	0	0	0	0	0	0	0	0	0	0	0	0	18	80
j	0	48	0	148	0	0	0	32	64	0	128	0	0	32	4	960	0	0	0	0	0	0
k	0	0	0	72	288	0	0	0	0	0	0	0	0	0	0	0	0	0	0	0	0	64
l	0	0	0	0	0	0	0	0	0	0	0	0	0	0	0	0	0	0	0	0	0	16
m	24	0	144	0	24	0	32	0	0	144	0	1424	0	32	0	0	0	0	8	2	6	208
n	0	0	0	0	0	0	0	0	0	0	0	0	0	0	0	0	0	0	0	0	0	0
o	0	0	1984	0	0	0	48	0	0	144	0	1664	0	0	0	0	0	0	0	0	214	48
p	0	0	0	0	0	0	0	0	0	0	0	16	0	0	0	0	0	0	0	0	40	0
r	0	0	0	0	0	0	0	0	0	0	0	0	0	0	0	0	0	0	0	0	0	0
s	0	0	48	0	0	0	48	32	0	112	0	0	0	0	0	0	0	0	0	0	0	640
t	0	0	0	0	0	0	0	0	0	0	0	0	0	0	0	0	0	0	0	0	0	0
u	0	0	0	0	0	0	0	0	0	0	0	0	0	0	0	0	0	0	0	0	0	0
v	0	0	0	0	0	0	0	0	0	0	0	0	0	0	0	0	0	0	0	0	0	16
z	0	0	0	0	0	0	0	0	0	0	0	0	0	0	0	0	0	0	0	0	0	0
w	0	0	0	0	0	0	0	0	0	16	0	0	0	0	0	0	0	0	0	0	0	0
x	8	0	0	0	0	0	0	0	0	0	0	0	0	0	0	0	0	0	0	0	0	0
y	0	0	0	0	0	0	0	0	0	0	0	0	0	0	0	0	0	0	0	0	0	0
xx	0	0	0	0	0	0	0	0	0	16	0	0	0	0	0	0	0	0	0	0	0	16
xy	0	0	0	0	0	0	0	0	0	0	0	0	0	0	0	0	0	0	0	0	0	0

*Legend: a – juvenile/damaged Baetidae, b – *Alainites muticus* (Linnaeus, 1758), c – juvenile/damaged *Baetis* sp., d – *Baetis buceratus* Eaton, 1870, e – *Baetis fuscatus* (Linnaeus, 1761), f – *Baetis lutheri* Müller-Liebenau, 1967, g – *Baetis rhodani* (Pictet, 1843), h – *Baetis vernus* Curtis, 1834, i – *Centroptilum luteolum* Müller, 1776, j – *Cloeon dipterum* (Linnaeus, 1760), k – juvenile *Caenis* sp., l – *Caenis horaria* – (Linnaeus, 1758), m – *Caenis luctuosa* (Burmeister, 1839), n – *Caenis robusta* Eaton, 1884, o – *Serratella ignita* (Poda, 1761), p – *Ephemera danica* Müller, 1764, r – juvenile/damaged Leptophlebiidae, s – *Habrophlebia fusca* (Curtis, 1834), t – juvenile/damaged *Paraleptophlebia* sp., u – juvenile/damaged Heptageniidae, v – *Electrogena ujhelyii* (Sowa, 1981), z – juvenile *Ecdyonurus* sp., w – *Ecdyonurus* cf. *macani* Thomas & Sowa, 1970, x – *Ecdyonurus torrentis* Kimmins, 1942, y – *Heptagenia flava* Rostock, 1878, xx – *Potamanthus luteus* (Linnaeus, 1767), xy – *Oligoneuriella rhenana* (Imhoff, 1852).

and dissolved oxygen (R = -0.46), and axis 2 to aquatic vegetation (R = -0.37) and water temperature (R = -0.36), indicating that these were the most important parameters in explaining patterns of mayfly assemblages (Fig. 3).

Mayfly species richness, abundance and consequently also local diversity, were found to significantly decrease with increased ratios of intensive agriculture areas in the catchment area (Fig. 4).

Abundances of *Alainites muticus* (R = -0.303; p=0.041), *Baetis lutheri* Müller-Liebenau, 1967 (R = -0.303; p = 0.041), *Baetis rhodani* (Pictet, 1843) (R = -0.318; p = 0.031), *Oligoneuriella rhenana* (R = -0.303; p = 0.041) and juvenile instars of *Ecdyonurus* sp. (R = -0.303; p = 0.041) were found to significantly decrease with increased ratios of intensive agriculture area in the catchment area. Only taxa with statistically significant correlations are presented.

Table 3. Continued.

Taxa codes	23	24	25	26	27	28	29	30	31	32	33	34	35	36	37	38	39	40	41	42	43	44	45	46
a	0	0	0	0	0	0	0	0	0	0	0	0	0	0	0	0	0	0	0	80	0	0	0	0
b	0	0	0	0	0	0	0	0	0	0	0	0	0	2	0	0	0	0	0	0	0	0	0	0
c	0	8	0	438	68	158	64	276	108	544	1376	22	0	364	0	0	336	52	0	0	0	0	0	8
d	0	0	0	16	168	17	0	0	172	96	408	12	0	0	0	0	0	8	0	0	0	0	0	0
e	0	0	0	0	292	1	328	0	0	0	0	12	0	98	0	0	16	0	0	0	0	0	0	0
f	0	0	0	0	0	0	0	0	0	0	0	0	0	4	0	0	0	0	0	0	0	0	0	0
g	0	0	0	0	0	0	0	0	0	0	0	0	0	206	0	0	0	0	0	0	0	0	0	0
h	0	0	0	0	0	0	0	80	0	32	24	0	0	0	0	0	832	0	0	0	0	224	0	8
i	0	0	16	0	0	0	0	0	0	0	0	0	0	6	0	0	0	0	0	0	0	0	0	0
j	24	0	160	44	0	59	0	0	154	480	360	4	0	0	0	0	0	8	0	128	0	0	0	0
k	0	0	0	0	0	68	0	0	2	0	0	0	0	0	0	0	0	4	0	0	0	0	0	0
l	16	0	0	0	0	0	0	0	0	0	0	0	0	0	0	0	0	0	0	0	0	0	0	0
m	0	0	0	0	8	32	104	0	0	0	0	0	0	0	0	0	0	0	0	0	0	0	0	0
n	0	0	0	0	0	10	0	0	0	0	0	0	0	0	0	0	0	0	0	0	0	0	0	0
o	0	0	0	0	0	0	80	0	0	0	0	0	0	36	0	0	24	4	0	0	0	0	0	0
p	0	0	0	0	0	0	0	0	0	0	0	0	0	0	0	0	0	4	0	0	0	0	0	0
r	0	0	48	0	0	0	0	0	0	0	0	0	0	0	0	0	0	0	0	0	0	0	0	0
s	0	8	16	5	0	0	40	0	0	0	0	0	0	0	0	0	0	0	0	0	0	160	0	0
t	0	0	16	0	0	0	0	0	0	0	0	0	0	0	0	0	0	0	0	0	0	0	0	0
u	0	0	0	0	0	0	4	0	0	0	0	0	0	0	0	0	0	0	0	0	0	0	0	0
v	0	0	0	0	0	0	0	0	0	0	0	0	0	0	0	0	0	0	0	0	0	0	0	0
z	0	0	0	0	0	0	0	0	0	0	0	0	0	46	0	0	0	0	0	0	0	0	0	0
w	0	0	0	0	0	0	0	0	0	0	0	0	0	0	0	0	0	0	0	0	0	0	0	0
x	0	0	0	0	0	0	0	0	0	0	0	0	0	0	0	0	0	0	0	0	0	0	0	0
y	0	0	0	0	0	1	0	0	0	0	0	0	0	0	0	0	0	0	0	0	0	0	0	0
xx	0	0	64	0	0	0	0	0	0	0	0	0	0	0	0	0	0	0	0	0	0	0	0	0
xy	0	0	0	0	0	0	0	0	0	0	0	0	0	2	0	0	0	0	0	0	0	0	0	0

*Legend: a – juvenile/damaged Baetidae, b – *Alainites muticus* (Linnaeus, 1758), c – juvenile/damaged *Baetis* sp., d – *Baetis buceratus* Eaton, 1870, e – *Baetis fuscatus* (Linnaeus, 1761), f – *Baetis lutheri* Müller-Liebenau, 1967, g – *Baetis rhodani* (Pictet, 1843), h – *Baetis vernus* Curtis, 1834, i – *Centroptilum luteolum* Müller, 1776, j – *Cloeon dipterum* (Linnaeus, 1760), k – juvenile *Caenis* sp., l – *Caenis horaria* – (Linnaeus, 1758), m – *Caenis luctuosa* (Burmeister, 1839), n – *Caenis robusta* Eaton, 1884, o – *Serratella ignita* (Poda, 1761), p – *Ephemera danica* Müller, 1764, r – juvenile/damaged Leptophlebiidae, s – *Habrophlebia fusca* (Curtis, 1834), t – juvenile/damaged *Paraleptophlebia* sp., u – juvenile/damaged Heptageniidae, v – *Electrogena ujhelyii* (Sowa, 1981), z – juvenile *Ecdyonurus* sp., w – *Ecdyonurus* cf. *macani* Thomas & Sowa, 1970, x – *Ecdyonurus torrentis* Kimmins, 1942, y – *Heptagenia flava* Rostock, 1878, xx – *Potamanthus luteus* (Linnaeus, 1767), xy – *Oligoneuriella rhenana* (Imhoff, 1852).

Discussion

Our results indicate that a relatively high number of mayfly species can be found in anthropogenically impacted freshwater habitats. Nevertheless, at a large part of the study sites (i.e., 72 %) taxa richness was low, i.e., between zero and four taxa, corroborating previous studies (Vilenica et al. 2016; 2019). Mayflies inhabit both lotic and lentic habitats, although upper and middle reaches of fast-flowing streams, and ecologically intact large rivers harbour the highest mayfly diversity (Bauernfeind and Soldán 2012; Vilenica et al. 2016; 2018). Therefore, such low species richness, not typical for a lotic habitat (Bauernfeind and Moog 2000; Zedková et al. 2014; Vilenica et al. 2018), could be a consequence of various disturbances present at those sites, such as channelling, eutrophication, pollution, and microhabitat homogeneity (Axelsson et al. 2011; Carvalho et al. 2013; Ligeiro et al. 2013). In many cases, we observed

Table 4. Results of the SIMPER analysis based on mayfly assemblages from sites of different hydromorphological (HYMO) alternation levels.

Species	Average abundance per site (ind/m^2)	Similarity contribution within group (%)
Group 1 good and high EQR based on RFI (EQR > 0.6)		
Average similarity: 18.68		
Baetis sp. juv.	2.54	33.12
Cloeon dipterum	1.38	16.42
Serratella ignita	2.07	12.01
Baetis fuscatus	1.73	10.82
Caenis luctuosa	1.63	10.32
Baetis vernus	1.33	6.58
Baetis buceratus	1.16	3.59
Group 2 moderate EQR based on RFI (0.4 < EQR < 0.6)		
Average similarity: 31.33		
Baetis sp. juv.	4.00	58.12
Baetis vernus	2.09	21.63
Cloeon dipterum	1.23	12.51
Group 3 poor and bad EQR based on RFI (EQR < 0.4)		
Average similarity: 31.54		
Baetis sp. juv.	3.51	39.10
Cloeon dipterum	2.63	28.10
Baetis buceratus	2.21	16.08
Baetis fuscatus	1.45	5.57
Caenis sp. juv.	1.14	3.27

shoreline erosion, as the emergent vegetation along the habitat edges, together with surrounding vegetation was mowed. This could have resulted in an increased input of sediments into the habitats, which could have influenced the habitat physico-chemical characteristics and hydrological cycle, resulting in reduced water quality and habitat heterogeneity (Mendes et al. 2017 and references herein). Consequently, these habitats showed to be less favourable for a high number of mayfly species. The majority of study sites were inhabited by widespread and generalist species (Popielarz and Neal 2007; Bauernfeind and Soldán 2012), yet sites with more microhabitat heterogeneity and higher water velocity, had also several microhabitat specialists, such as *Baetis lutheri* and *Ecdyonurus torrentis* for mesolithal, and *Centroptilum luteolum* as specialists for macrophytes (Buffagni et al. 2009; 2020).

The Zelina stream in Božjakovina (site 22) and Toplica River upstream from Daruvar town (site 36) showed somewhat higher species richness, yet their assemblages mainly consisted of species inhabiting a wide range of habitats, such as *Baetis rhodani*, *Centroptilum luteolum*, *Serratella ignita* and *Caenis luctuosa* (Buffagni et al. 2009; 2020; Bauernfeind and Soldán 2012). The most interesting finding was a record of *Oligoneuriella rhenana* at Toplica River, which is considered rare in Croatia (Vilenica et al. 2015; 2018). Although the species can tolerate some variations of environmental factors, its presence indicates that the ecological condition of Toplica River upstream from

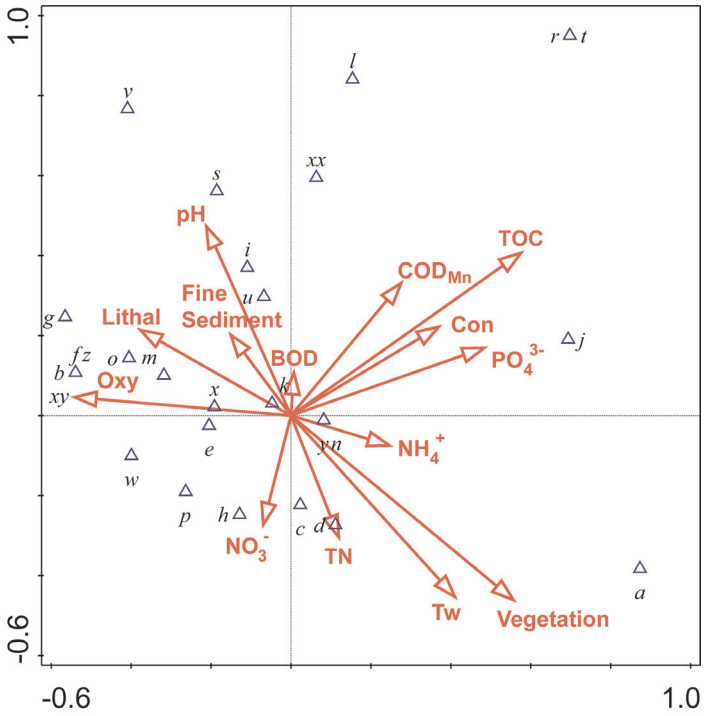

Figure 3. F1×F2 plane of the Canonical correspondence analysis (CCA) based on 21 mayfly taxa and 14 environmental variables. For the abbreviations of the taxa codes (blue triangle symbols) see Table 2. Legend: Environmental variables (red arrow symbols): Tw – water temperature (°C), Oxy – dissolved oxygen content (mg/L), Con – conductivity (µS/cm), pH – pH, NH_4^+ – ammonium (mgN/L), NO_3^- – nitrates (mgN/L), TN – total nitrogen (mgN/L), PO_4^{3-} – orthophosphates (mgP/L), TOC – total organic carbon (mg/L), BOD_5 – biological oxygen demand (mgO_2/L), COD_{Mn} – chemical oxygen demand (mgO_2/L), vegetation – aquatic vegetation/phytal, fine sediment – silt, mud and sand, lithal – stones and gravel.

Daruvar town is not as poor as at the majority of other sites (Găldean, 1999; Petrovici and Tudorancea 2000). Another interesting species was the rarest in our study, a riverine *Heptagenia flava*, uncommon in Croatian waters (Vilenica et al. 2015). Although the species was reported to have rather high ecological plasticity, usually it does not inhabit heavily polluted rivers (Vidinova and Rusev 1997). Therefore, the species record at Česma River in Narta (site 28) could be considered as an accidental finding, as shown by Vidinova and Rusev (1997). On the other hand, two eurytopic and euryvalent species (i.e., with wide tolerance towards the environmental conditions and habitat type), *Cloeon dipterum* and *Serratella ignita*, were recorded as the most common and the most numerous, respectively (Buffagni et al. 2009; 2020; Bauernfeind and Soldán 2012; Vilenica et al. 2019). Nevertheless, while discussing the total species richness at a particular site, we need to keep in mind that standardised sampling methods generally do not include sampling of underrepresented microhabitats, which could be important for some rare species (Haase et al. 2008). Therefore, in order to obtain a more complete

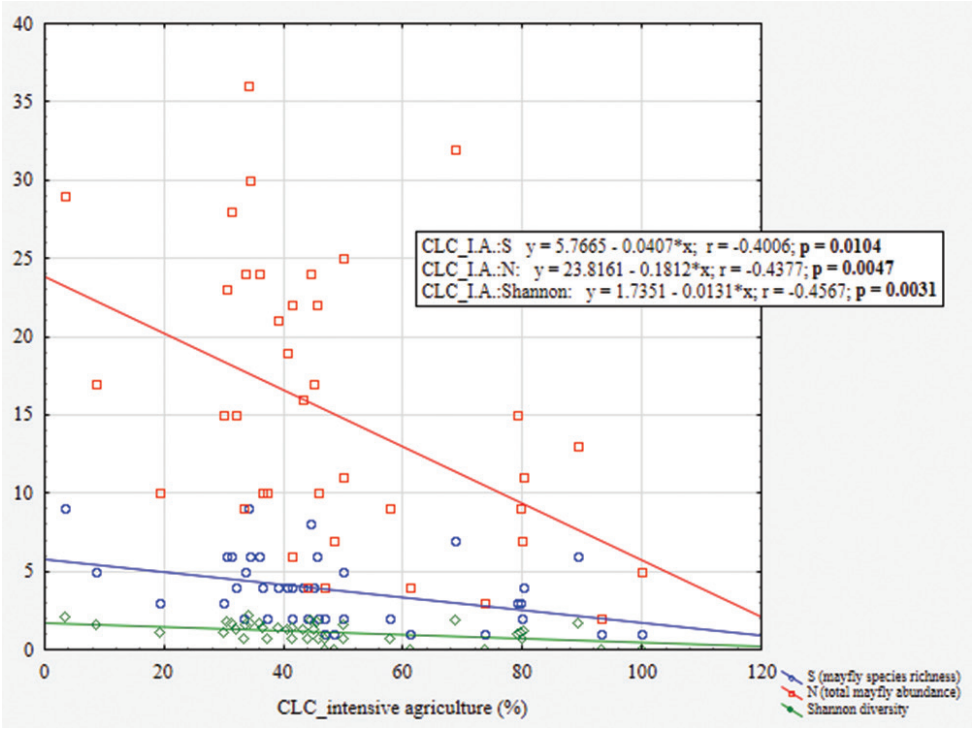

Figure 4. Scatterplot of mayfly species richness (S), abundance (N) and local diversity (Shannon index) against ratios of areas with intensive agriculture (CLC_I.A.) present in the catchment area of each study site.

species list, it might be beneficial to complement standardised quantitative sampling with a qualitative one.

Stream channelling is a widely used engineering practice designed for flood control and wetland draining, which affects the majority of hydrogeomorphological characteristics and processes at the channelled habitat. Due to these changes, the biota is also severely affected (Hupp 1992), i.e., the community structure and composition are changed and poorer (Waters 1995). Our results showed that mayfly assemblages have mainly consisted of taxa of potamic (lower reaches) and lentic preferences (e.g., *Baetis buceratus*, *Caenis horaria*) or wide range (e.g., *Cloeon dipterum*, *Centroptilum luteolum*, *Serratella ignita*) habitat type preferences (Buffagni et al. 2009; 2020; Bauernfeind and Soldán 2012). Moreover, *Baetis vernus*, *Caenis luctuosa* and *Serratella ignita*, species with relatively strong rhithral affinity (Biss et al. 2002) were predominantly associated with hydromorphologically less degraded sites, while species with more prominent potamic preference, such as *Baetis buceratus* and *Baetis fuscatus* (Schöll et al. 2005) were present at sites both with low and high degree of hydromorphological degradation. Some study sites showed a higher share of rhithral elements, yet that was mainly due to the dominance of eurytopic *Cloeon dipterum* (Buffagni et al. 2009; 2020). As

the majority of sites are characterised by low microhabitat diversity, a high level of sedimentation and nutrients, assemblages were dominated by detritivores (Buffagni et al. 2009, 2020).

Previous researches showed that mayflies are highly dependent on specific environmental cues, and many species rapidly disappear when faced with anthropogenic disturbances in their habitat (Bauernfeind and Moog 2000; Goulart and Callisto 2005; Stepanian et al. 2020). Our results corroborate previous studies that showed negative responses of mayflies to high water temperature (e.g., Chadwick and Feminella 2001; Alhejoj et al. 2014) and low oxygen concentrations (e.g., Nebeker 1972; Lock and Goethals 2011). Sites that were characterised by high water temperatures were also often accompanied by low oxygen content and dense aquatic vegetation. High levels of nutrients in the water support such dense growth of vegetation, leading to a decrease of oxygen level (Boeykens et al. 2017). Moreover, the decay of organic matter (especially aquatic vegetation), together with bacterial growth, animal/human metabolic activity and various synthetic sources (such as pesticides, fertilisers, pharmaceuticals, detergents) lead to elevated concentration of total organic carbon (TOC) in water (e.g., Volk et al. 2002). A part of the TOC can be explained by the increased shoreline erosion due to management and clearing of vegetation in the shoreland zone, which probably also negatively affected mayflies in this study. Riparian buffers, especially undisturbed vegetated riparian zones situated adjacent to river and streams, can greatly mitigate nutrients, sediment from surface and groundwater flow through the processes of deposition, absorption and denitrification (e.g., Peterjohn and Correll 1984). Finally, the strong negative association of mayfly assemblages with intensive agriculture in the catchment area corroborates results of previous studies that showed high mayfly sensitivity to agricultural pollution (Siegloch et al. 2014; Zedková et al. 2015). Here, as especially sensitive showed *Alainites muticus*, *Baetis lutheri* and *Oligoneuriella rhenana*, species with low and moderate tolerance to water pollution (mainly occurring in oligosaphrobic and beta-mesosaphrobic waters) (Bauernfeind et al. 2002; Mihaljević 2011). In addition, another species was distinguished as sensitive to such kind of pollution, *Baetis rhodani*. Those results could come as a surprise, as this eurytopic mayfly has a wide ecological tolerance, and generally contributes as a major part of the macroinvertebrate biomass in many European streams and rivers (Elliott et al. 1988). Nevertheless, as *Baetis rhodani* is a species complex (Williams et al. 2006), those results should be inspected in more details, using molecular analyses. Our results confirm that water pollution is one of the largest limitation factors for the majority of mayflies (Van Dijk et al. 2013; Zedková et al. 2015).

Conclusions

This study contributes to our knowledge of mayfly relationship with environmental conditions in heavily modified and anthropogenic habitats. Various anthropogenic pressures resulted in changes in mayfly assemblage composition and structure, whereas

species richness decreased. For instance, the assemblages consisted mainly of a relatively low number of widespread generalists and species characteristic for lower reaches and lentic habitats. This indicates that hydromorphological alterations could have resulted in assemblage's "potamisation". Moreover, highly polluted sites, with high temperatures and low oxygen content, were inhabited almost exclusively with the euryvalent *Cloeon dipterum*, or were completely unsuitable for any mayfly species, confirming the high sensitivity of mayflies to disturbances in their habitats. Our results can enable planning of management and conservation activities of lowland rivers and their biota according to the requirements of the European Water Framework Directive.

Acknowledgements

We would like to thank our colleagues from University of Zagreb (Faculty of Science, Department of Biology, Division of Zoology) for their indispensable assistance during the field investigations and for help with sorting the collected material. Miran Katar is thanked for helping us with the artwork. We thank Maja Kerovec for assisting with GIS analysis and Croatian Waters for providing hydromorphological, land use and water physico-chemical data. Finally, the reviewers are thanked for their useful comments and suggestions.

References

Alhejoj I, Salameh E, Bandel K (2014) Mayflies (Order Ephemeroptera): an effective indicator of water bodies conditions in Jordan. Environmental Science and Pollution Research 2(10): 361–370. https://doi.org/10.12983/ijsres-2014-p0361-0370

American Public Health Association (APHA) (1992) Standard Methods for the Examination of Water and Wastewater, 18th ed. Washington, DC, 13 pp.

AQEM consortium (2002) Manual for the application of the AQEM method. A comprehensive method to assess European streams using benthic macroinvertebrates, developed for the purpose of the Water Framework Directive. Version 1.0, February 2002, 166 pp.

Axelsson EP, Hajalten J, Leroy CJ, Whitham TG, Julkunen-Tiitto R, Wennstrom A (2011) Leaf litter from insect-resistant transgenic trees causes changes in aquatic insect community composition. Journal of Applied Ecology 48: 1472–1479. https://doi.org/10.1111/j.1365-2664.2011.02046.x

Bauernfeind E, Moog O (2000) Mayflies (Insecta: Ephemeroptera) and the assessment of ecological integrity: a methodological approach. Hydrobiologia 422: 71–83. https://doi.org/10.1023/A:1017090504518

Bauernfeind E, Humpesch UH (2001) Die Eintagsfliegen Zentraleuropas–Bestimmung und Ökologie. Verlag NMW, Vienna, 250 pp. [Book in German].

Bauernfeind E, Moog O, Weichselbaumer P (2002) Ephemeroptera. In: Moog O (Ed.) Fauna Aquatica Austriaca, Lieferung 2002. Wasserwirtschaftskataster, Bundesministerium für Land- und Forstwirtschaft, Umwelt und Wasserwirtschaft, Wien, 17 pp.

Bauernfeind E, Soldán T (2012) The mayflies of Europe (Ephemeroptera). Apollo Books, Ollerup, 781 pp.

Boeykens SP, Piol MN, Samudio Legal L, Saralegui AB, Vázquez C (2017) Eutrophication decrease: phosphate adsorption processes in presence of nitrates Journal of Environmental Management 203: 888–895. https://doi.org/10.1016/j.jenvman.2017.05.026

Buffagni A, Cazzola M, López-Rodríguez MJ, Alba-Tercedor J, Armanini DG (2009) Distribution and ecological preferences of European freshwater organisms. 3. Ephemeroptera. Pensoft Publishers, Sofia-Moscow, 254 pp.

Buffagni A, Armanini DG, Cazzola M, Alba-Tercedor J, López-Rodríguez MJ, Murphy J, Sandin L, Schmidt-Kloiber A (2020) Dataset "Ephemeroptera", ver. 7.0. www.freshwaterecology.info [22 April 2020]

Biss R, Kübler P, Pinter I, Braukmann U (2002) Leitbildbezogenes biozönotisches Bewertungsverfahren für Fließgewässer (aquatischer Bereich) in der Bundesrepublik Deutschland. Ein erster Beitrag zur integrierten ökologischen Fließgewässerbewertung. Umweltbundesamt. – Final report on CD-ROM. UBA Texts 62/02, Berlin.

Brasil LS, Shimano Y, Batista JD, Cabette HSR (2013) Effects of environmental factors on community structure of Leptophlebiidae (Insecta: Ephemeroptera) in Cerrado streams, Brazil. Iheringia, Série Zoologia 103: 260–265. https://doi.org/10.1590/S0073-47212013000300008

Carpenter SJ, Stanley EH, Vander Zanden MJ (2011) State of the World's Freshwater Ecosystems: Physical, Chemical, and Biological Changes. Annual Review of Environment and Resources 36: 75–99. https://doi.org/10.1146/annurev-environ-021810-094524

Carvalho FG, Silva-Pinto N, Oliveira-Junior JMB, Juen L (2013) Effects of marginal vegetation removal on Odonata communities. Acta Limnologica Brasiliensia 25: 10–18. https://doi.org/10.1590/S2179-975X2013005000013

Chadwick MA, Feminella JW (2001) Influence of salinity and temperature on the growth and production of a freshwater mayfly in the Lower Mobile River, Alabama. Limnology and Oceanography 46: 532–542. https://doi.org/10.4319/lo.2001.46.3.0532

Clarke KR (1993) Non-parametric multivariate analyses of changes in community structure. Australian Journal of Ecology 18: 117–143. https://doi.org/10.1111/j.1442-9993.1993.tb00438.x

Clarke KR, Gorley RN (2006) PRIMER V6: user manual/tutorial. Primer-E, Plymouth, 192 pp.

CLC Hrvatska, CORINE Land Cover Hrvatska (2013) Hrvatska agencija za okoliš i prirodu.

Dudgeon D, Arthington AH, Gessner MO, Kawabata Z-I, Knowler DJ, Lévêque C, Naiman RJ, Prieur-Richard A-H, Soto D, Stiassny MLJ, Sullivan CA (2006) Freshwater biodiversity: importance, threats, status and conservation challenges. Biological Reviews of the Cambridge Philosophical Society (London) 81: 163–182. https://doi.org/10.1017/S1464793105006950

Firmiano KR, Ligeiro R, Macedo DR, Juen L, Hughes RM, Callisto M (2017) Mayfly bioindicator thresholds for several anthropogenic disturbances in neotropical savanna streams. Ecological Indicators 74: 276–284. https://doi.org/10.1016/j.ecolind.2016.11.033

Găldean N (1999) Some considerations about the reophilic elements of the bentic fauna (ord. Ephemeroptera, Plecoptera and Trichoptera) of the Upper Tisza Region. In: Hamar J, Sárkány-Kiss A (Eds) The Upper Tisa Valley. Tiscia monograph series, Szeged, 413–425.

Goulart M, Callisto M (2005) Mayfly diversity in the Brazilian tropical headwaters of Serra do Cipó. The Brazilian Archives of Biology and Technology 48: 983–996. https://doi.org/10.1590/S1516-89132005000800015

Elliott JM, Humpesch UH, Macan T (1988) Larvae of the British Ephemeroptera: a key with ecological notes. Freshwater Biological Association Scientific Publication No. 49, Cumbria, England, 145 pp.

Haase P, Pauls SU, Engelhardt HM, Sundermann A (2008) Effects of sampling microhabitats with low coverage within the STAR/AQEM macroinvertebrate sampling protocol on stream assessment. Limnologica 38: 14–22. https://doi.org/10.1016/j.limno.2007.06.002

Hering D, Johnson RK, Kramm S, Schmutz S, Szoszkiewicz K, Verhonschot PFM (2006) Assessment of European streams with diatoms, macrophytes, macroinvertebrates and fish: a comparative metric-based analysis of organism response to stress. Freshwater Biology 51: 1757–1785. https://doi.org/10.1111/j.1365-2427.2006.01610.x

Hughes RM, Larsen DP, Omemik JM (1986) Regional reference sites: a method for assessing stream pollution. Environmental Management 10: 629–635. https://doi.org/10.1007/BF01866767

Hupp CR (1992) Riparian vegetation recovery patterns following stream channelization: a geomorphic perspective. Ecology 73: 1209–1226. https://doi.org/10.2307/1940670

Illies J (1978) Limnofauna Europaea. Gustav Fischer Verlag, Stuttgart and New York, 532 pp.

Ivković M, Plant A (2015) Aquatic insects in the Dinarides: identifying hotspots of endemism and species richness shaped by geological and hydrological history using Empididae (Diptera). Insect Conservation and Diversity 8: 302-312. https://doi.org/10.1111/icad.12113

Jones JI, Murphy JF, Collins AL, Sear DA, Naden PS, Armitage PD (2012) The impact of fine sediment on macroinvertebrates. River research and applications 28: 1055–1071. https://doi.org/10.1002/rra.1516

Jones JI, Duerdoth CP, Collins AL, Naden PS, Sear DA (2014) Interactions between diatoms and fine sediment. Hydrological processes 28: 1226–1237. https://doi.org/10.1002/hyp.9671

Lecerf A, Richardson JS (2010) Litter decomposition can detect effects of high and moderate levels of forest disturbance on stream condition. Forest Ecology and Management 259: 2433–2443. https://doi.org/10.1016/j.foreco.2010.03.022

Ligeiro R, Hughes RM, Kaufmann PR, Macedo DR, Firmiano KR, Ferreira WR, Oliveira D, Melo AS, Callisto M (2013) Defining quantitative stream disturbance gradients and the additive role of habitat variation to explain macroinvertebrate taxa richness. Ecological Indicators 25: 45–57. https://doi.org/10.1016/j.ecolind.2012.09.004

Lock K, Goethals PLM (2011) Distribution and ecology of the mayflies (Ephemeroptera) of 513 Flanders (Belgium). Annales de Limnologie International Journal of Limnology 47: 159–165. https://doi.org/10.1051/limn/2011011

Louhi P, Richardson JS, Muotka T (2017) Sediment addition reduces the importance of predation on ecosystem functions in experimental stream channels. Canadian Journal of Fisheries and Aquatic Sciences 74: 32–40. https://doi.org/10.1139/cjfas-2015-0530

Malmqvist B, Rundle S (2002) Threats to the running water ecosystems of the world. Environmental conservation 29: 134–153. https://doi.org/10.1017/S0376892902000097

Malzacher P (1984) Die europäischen Arten der Gattung Caenis Stephens (Insecta: Ephemeroptera). The European species of the genus Caenis Stephens (Insecta: Ephemeroptera). Stuttgarter Beiträge zur Naturkunde, Serie A (Biologie) 373, 48 pp.

Mendes TP, Luiza-Andrade A, Cabette HSR, Juen L (2017) How does environmental variation affect the distribution of dragonfly larvae (Odonata) in the Amazon-Cerrado transition zone in Central Brazil? Neotropical entomology 47: 37–45. https://doi.org/10.1007/s13744-017-0506-2

Mihaljević Z (2011) Revizija hrvatskog indikatorskog sustava (Revision of Croatian indicator system). In: Mihaljević Z (Ed.) Testiranje bioloških metoda ocjene ekološkog stanja (Okvirna direktiva o vodama, 2000/60/EC) u reprezentativnim slivovima panonske i dinaridske ekoregije (Testing of biological methods for ecological status assessment (Water Framework Directive 2000/60/EC) in representative river basins of the Pannonian and Dinaric ecoregions). Studija, Prirodoslovno-matematički fakultet Sveučilišta u Zagrebu, 253 pp. [In Croatian]

Moog O, Bauernfeind E, Weichselbaumer P (1997) The use of Ephemeroptera as saprobic indicators in Austria. In: Landolt P, Sartori M (Eds)Ephemeroptera & Plecoptera: BiologyEcology-Systematics. MTL, Fribourg, Switzerland, 254–260.

Moog O (2002) Fauna Aquatica Austriaca, Edition 2002. Wassserwirtschaftskataster, Bundesministerium für Land- und Forstwirtschaft, Umwelt und Wasserwirtschaft, Vienna, 28 pp.

Morse JC, Bae YJ, Munkhjargal G, Sangpradub N, Tanida K, Vshivkova TS, Wang B, Yang L, Yule CM (2007) Freshwater biomonitoring with macroinvertebrates in East Asia. Frontiers in Ecology and the Environment 5: 33–42. https://doi.org/10.1890/1540-9295(2007)5[33:FBWMIE]2.0.CO;2

Müller-Liebenau I (1969) Revision der europäischen Arten der Gattung Baetis Leach, 1815. (Insecta, Ephemeroptera). Gewässer und Abwässer 49/49: 1–214.

Nebeker AV (1972) Effects of low oxygen concentrations on survival and emergence of aquatic insects. Transactions of the American Fisheries Society 4: 675–679. https://doi.org/10.1577/1548-8659(1972)101%3C675:EOLOCO%3E2.0.CO;2

Peterjohn WT, Correll DL (1984) Nutrient dynamics in an agricultural watershed: observations on the role of a riparian forest. Ecology 65: 1466–1475. https://doi.org/10.2307/1939127

Petrovici M, Tudorancea C (2000) Structure and dynamics of mayflies' community (Insecta, Ephemeroptera) of Crişul Repede river and its tributaries. Studii şi Cercetări Ştiinţifice, Biologie, Bacău 5: 201–206.

Popielarz PA, Neal ZP (2007) The niche as a theoretical tool. Annual review of sociology 33: 65–84. https://doi.org/10.1146/annurev.soc.32.061604.123118

Previšić A, Walton C, Kučinić M, Mitrikeski PT, Kerovec M (2009) Pleistocene divergence of Dinaric Drusus endemics (Trichoptera, Limnephilidae) in multiple microrefugia within the Balkan Peninsula. Molecular ecology 18: 634–647. https://doi.org/10.1111/j.1365-294X.2008.04046.x

Schöll F, Haybach A, König B (2005) Das erweiterte Potamontypieverfahren zur ökologischen Bewertung von Bundeswasserstraßen (Fließgewässertypen 10 und 20: kies- und sandgeprägte Ströme, Qualitätskomponente Makrozoobenthos) nach Maßgabe der EU-Wasserrahmenrichtlinie. Hydrologie und Wasserwirtschaft 49(5): 234–247.

Siegloch AE, Suriano M, Spies M, Fonseca-Gessner A (2014) Effect of land use on mayfly assemblages' structure in Neotropical headwater streams. Anais Da Academia Brasileira De Ciencias 86, 1735–1747. https://doi.org/10.1590/0001-3765201420130516

Steffen W, Richardson K, Rockstrom J, Cornell SE, Fetzer I, Bennett EM, Biggs R, Carpenter SR, de Vries W, de Wit CA, Folke C, Gerten D, Heinke J, Mace GM, Persson LM, Ramanathan V, Reyers B, Sorlin S (2015) Planetary boundaries: guiding human development on a changing planet. Science 347: 1259855.

Stepanian PM, Entrekin SA, Wainwright CE, Mirkovic D, Tank JL, Kelly JF (2020) Declines in an abundant aquatic insect, the burrowing mayfly, across major North American waterways. Proceedings of the National Academy of Sciences of the United States of America 117(6): 2987–2992. https://doi.org/10.1073/pnas.1913598117

Stoddard JL, Herlihy AT, Peck DV, Hughes RM, Whittier TR, Tarquinio E (2008) A process for creating multimetric indices for large-scale aquatic surveys. Journal of the North American Benthological Society 27: 878–891. https://doi.org/10.1899/08-053.1

Stoddard JL, Larsen DP, Hawkins CP, Johnson RK, Norris RH (2006) Setting expectations for the ecological condition of streams: the concept of reference condition. Ecological Applications 16: 1267–1276. https://doi.org/10.1890/1051-0761(2006)016[1267:SEFTEC]2.0.CO;2

Šegota T, Filipčić A (2003) Köppenova podjela klima i hrvatsko nazivlje. Geoadria 8(1): 17–23. https://doi.org/10.15291/geoadria.93 [Article in Croatian]

ter Braak CJF, Šmilauer P (1998) Canoco for Windows: Software for Canonical Community Ordination (Version 4.02). Centre for Biometry Wageningen, CPRO-DLO, Wageningen.

TIBCO Software Inc. 2017. Statistica (data analysis software system), version 13. http://statistica.io

Turunen J, Aroviita J, Marttila H, Louhi P, Laamanen T, Tolkkinen M, Luhta P-L, Kløve B, Muotka T (2017) Differential responses by stream and riparian biodiversity to in-stream restoration of forestry-impacted streams. Journal of Applied Ecology 54: 1505–1514. https://doi.org/10.1111/1365-2664.12897

Urbanič G (2014) Hydromorphological degradation impact on benthic invertebrates in large rivers in Slovenia. Hydrobiologia 729: 191–207. https://doi.org/10.1007/s10750-012-1430-4

Van Dijk TC, Van Staalduinen MA, Van der Sluijs JP (2013) Macro-invertebrate decline in surface water polluted with imidacloprid. PLoS ONE 8(4): e61336. https://doi.org/10.1371/journal.pone.0062374

Vidinova Y, Russev B (1997) Distribution and ecology of the representatives of some Ephemeropteran families in Bulgaria. In: Landolt P, Sartori M (Eds) Ephemeroptera & Plecoptera: Biology Ecology -Systematics. MTL, Fribourg, 139–146.

Vilenica M, Gattolliat J-L, Mihaljević Z, Sartori M (2015) Croatian mayflies (Insecta, Ephemeroptera): species diversity and distribution patterns. ZooKeys 523: 99–127. https://doi.org/10.3897/zookeys.523.6100

Vilenica M, Previšić A, Ivković M, Popijač A, Vučković I, Kučinić M, Kerovec M, Gattolliat J-L, Sartori M, Mihaljević Z (2016) Mayfly (Insecta: Ephemeroptera) assemblages of a regulated perennial Mediterranean river system in the Western Balkans. Biologia 71(9): 1038–1048. https://doi.org/10.1515/biolog-2016-0121

Vilenica M, Mičetić Stanković V, Sartori M, Kučinić M, Mihaljević Z (2017) Environmental factors affecting mayfly assemblages in tufa-depositing habitats of the Dinaric Karst. Knowledge and Management of Aquatic Ecosystems 418(14): 1–12. https://doi.org/10.1051/kmae/2017005

Vilenica M, Ergović V, Mihaljević Z (2018) Mayfly (Ephemeroptera) assemblages of a Pannonian lowland mountain, with first records of the parasite *Symbiocladius rhithrogenae* (Zavrel, 1924) (Diptera: Chironomidae). Annales de Limnologie International Journal of Limnology 54(31): 1–10. https://doi.org/10.1051/limn/2018023

Vilenica M, Vučković N, Mihaljević Z (2019) Littoral mayfly assemblages in South-East European man-made lakes. Journal of Limnology 78(1): 1–13. https://doi.org/10.4081/jlimnol.2019.1853

Vilenica M, Pozojević I, Vučković N, Mihaljević Z (2020) How suitable are man-made water bodies as habitats for Odonata? Knowledge and Management of Aquatic Ecosystems 42(13): 1–10. https://doi.org/10.1051/kmae/2020008

Volk C, Wood L, Johnson B, Robinson J, Zhu HW, Kaplan L (2002) Monitoring dissolved organic carbon in surface and drinking waters. Journal of environmental monitoring 4: 43–47. https://doi.org/10.1039/b107768f

Vörösmarty CJ, McIntyre PB, Gessner MO, Dudgeon D, Prusevich A, Green P, Glidden S, Bunn SE, Sullivan CA, Liermann CR, Davies PM (2010) Global threats to human water security and river biodiversity. Nature 467: 555–561.

Waters TF (1995) Sediment in streams: sources, biological effects and control. American Fisheries Society symposium, Monograph 7: 1–251. https://doi.org/10.1038/nature09440

Williams HE, Ormerod SJ, Bruford MW (2006) Molecular systematics and phylogeography of the cryptic species complex *Baetis rhodani* (Ephemeroptera, Baetidae). Molecular Phylogenetics and Evolution 40: 370–382. https://doi.org/10.1016/j.ympev.2006.03.004

Woodward G, Gessner MO, Giller PS, Gulis V, Hladyz S, Lecerf A, Malmqvist B, McKie BG, Tiegs SD, Cariss H, Dobson M, Elosegi A, Ferreira V, Graca MAS, Fleituch T, Lacoursiere JO, Nistorescu M, Pozo J, Risnoveanu G, Schindler M, Vadineanu A, Vought LB-M, Chauvet E (2012) Continental-scale effects of nutrient pollution on stream ecosystem functioning. Science 336: 1438–1440. https://doi.org/10.1126/science.1219534

Zaninović K, Gajić-Čapka M, Perčec Tadić M, Vučetić M, Milković J, Bajić A, Cindrić K, Cvitan L, Katušin Z, Kaučić D, Likso T, Lončar E, Lončar Ž, Mihajlović D, Pandžić K, Patarčić M, Srnec L, Vučetić V (2008) Klimatski atlas Hrvatske / Climate atlas of Croatia 1961–1990., 1971–2000. Državni hidrometeorološki zavod, Zagreb, 200 pp. [In Croatian]

Zedková B, Rádková V, Bojková J, Soldán T, Zahrádková S (2015) Mayflies (Ephemeroptera) as indicators of environmental changes in the past five decades: a case study from the Morava and Odra River Basins (Czech Republic). Aquatic Conservation: Marine and Freshwater Ecosystems 25(5): 622–638. https://doi.org/10.1002/aqc.2529

ZooKeys 980: 79–91 (2020)
doi: 10.3897/zookeys.980.55865
https://zookeys.pensoft.net

RESEARCH ARTICLE

A peer-reviewed open-access journal
ZooKeys
Launched to accelerate biodiversity research

First record of a mermithid worm (Nematoda, Mermithidae) parasitizing a third instar nymph of *Triatoma sordida* (Stål, 1859) (Hemiptera, Reduviidae, Triatominae) from Mato Grosso, Brazil

Mirian Francisca Martins[1,2], Sinara Cristina de Moraes[1], Simone Chinicz Cohen[3], Melissa Querido Cárdenas[3], Cleber Galvão[4]

1 *Departamento de Vigilância em Saúde Ambiental, Secretaria de Estado de Saúde de Mato Grosso – SESMT. Amaro Leite, 474, Barra do Garças, MT, 78600–000, Brazil* **2** *Programa de Pós-Graduação em Biodiversidade e Saúde, Instituto Oswaldo Cruz, FIOCRUZ, Av. Brasil 4365, Rio de Janeiro, RJ, 21040–360, Brazil* **3** *Laboratório de Helmintos Parasitos de Peixes, Instituto Oswaldo Cruz, FIOCRUZ, Av. Brasil 4365, Pavilhão Cardoso Fontes, sala 45, Rio de Janeiro, RJ, 21040–360, Brazil* **4** *Laboratório Nacional e Internacional de Referência em Taxonomia de Triatomíneos, Instituto Oswaldo Cruz, FIOCRUZ, Av. Brasil 4365, Pavilhão Rocha Lima, sala 505, Rio de Janeiro, RJ, 21040–360, Brazil*

Corresponding author: Simone Chinicz Cohen (scohen@ioc.fiocruz.br)

Academic editor: David Fitch | Received 26 June 2020 | Accepted 30 July 2020 | Published 28 October 2020

http://zoobank.org/5435FEFD-4878-448C-AC63-F75FC5485231

Citation: Martins MF, de Moraes SC, Cohen, SC, Cárdenas MQ, Galvão C (2020) First record of a mermithid worm (Nematoda, Mermithidae) parasitizing a third instar nymph of *Triatoma sordida* (Stål, 1859) (Hemiptera, Reduviidae, Triatominae) from Mato Grosso, Brazil. ZooKeys 980: 79–91. https://doi.org/10.3897/zookeys.980.55865

Abstract

A juvenile specimen of a mermithid (Nematoda) was found parasitizing a third instar nymph of *Triatoma sordida* from Mato Grosso, Brazil. This is the first record of mermithid parasitism in a triatomine species. The Mermithidae represents a family of nematodes that are specialized insect parasites. Entomonematodes are one of the highly influential agents regulating the population dynamics of insects. This report introduces the opportunity to think about mermithids as a possible candidate for use as triatomine biological control.

Keywords

Mato Grosso, Brazil, Mermithidae, Nematoda, new host record, *Triatoma sordida*, Triatominae, parasite

Introduction

The insects of the subfamily Triatominae (Hemiptera, Reduviidae) are true bugs specialized in blood-sucking. All species are potential vectors of *Trypanosoma cruzi* (Chagas, 1909) (Trypanosomatida, Trypanosomatidae), the causative agent of Chagas disease in the Americas, where the disease remains an important public health problem. Although a few species of triatomines are also found in Asia and Oceania, in these regions the vector-borne transmission of *T. cruzi* does not occur as the parasite is absent. Galvão and Justi (2015) summarized the information available about ecology, niches, and associations with humans, and *T. cruzi* infection of all triatomine species.

Triatoma sordida (Stål, 1859) is a species endemic to Argentina, Bolivia, Brazil, Paraguay, and Uruguay (Galvão 2014). In Brazil, *T. sordida* is the most commonly collected triatomine species, predominantly in peridomiciliar environments (Obara et al. 2011; Rossi et al. 2015). *Triatoma sordida* presented the highest infection rate for *T. cruzi* in the state of Bahia, including the report of infected colonies in intradomiciary environments (Ribeiro-Jr. et al. 2019). According to Minuzzi-Souza et al. (2017), *T. sordida* plays a key role in maintaining the risk of transmission of *T. cruzi* to humans in the state of Góias and the Distrito Federal in Brazil. In the state of Bahia, Brazil, this species was associated with oral transmission of Chagas disease to humans (Dias et al. 2008).

Entomonematodes are one of the highly influential agents regulating the population dynamics of insect pests through association with their hosts in relationships ranging from fortuitous to parasitic. Many investigators have recognized these parasites as potential biological control agents (Poulin 2011). Results showed that entomonematodes are a safe and effective environmental alternative for controlling pests in crops of economic importance (Shapiro-Ilan et al. 2010; Duncan et al. 2013; Gumus et al. 2015), because of their capacity to retard development, induce female sterility, and cause death on host emergence (Kaiser 1991).

The mermithids represent a family of nematodes with more than fifty genera, specialized parasites of invertebrates, especially insects, parasitizing at least fifteen different orders (Nickle 1972; Poinar-Jr. 2015). The life cycle of mermithids includes five stages, as described in Poinar-Jr. (1983): egg, second stage juvenile (preparasitic infective juvenile), parasitic third stage juvenile, mature third stage postparasitic juvenile, two molts into adult (Kosulic and Masova 2019). The eggs of nematodes of terrestrial insects, containing juvenile forms, are deposited under leaves for ingestion as food. After ingestion, the eggs break, releasing juveniles that migrate to the insect hemolymph (Dolinski 2006). Another route involves the migration of the preparasitic larvae to the soil surface and climb grass or other vegetation to reach their hosts, when hatching occurs. They penetrate the body wall of recently hatched nymphs, entering in the body cavity. Within the host, the parasitic complete their growth and then emerge by forcing their way through the body wall to enter the soil (Christie 1936). Nematodes kill the host with their emergence to the soil where they molt into the adult stage to complete the cycle (Poinar-Jr. 1979). Emergence from its host by killing it, places them as parasitoids (Rusconi et al. 2017).

These parasitoids have parenteral intake of nutrition from the host tissues and hemolymph, which may strongly influence the physiological condition of the host,

from the first instars of parasite development (Nikdel et al. 2011), promoting severe competition for nutrients, resulting in atrophy of the thorax and abdomen, organ involvement, and changes in patterns of development of social insects and the general behavior of insects (Dolinski 2006). Parasitism by a mermithid is fatal to the host (Nickle 1972; Poinar-Jr. 1983; Nikdel et al. 2011).

Postparasitic juvenile and adult mermithids are most frequently collected. In this postparasitic free-living stage, the parasite does not feed anymore and only needs a suitable habitat to mature (Kosulic and Masova 2019).

Information about Mermithidae nematodes is scarce. In South America, there are a few studies about terrestrial mermithids in grasshoppers (Miralles and Camino 1983; Camino and Stock 1989; Camino and Lange 1997; Rusconi et al. 2017) and ants (Jouvenaz and Wojcik 1990; Poinar-Jr. et al. 2007) from Argentina. In Brazil, Rodrigues et al. (2005) reported an unidentified Mermithidae larva emerging from spiders from Brazil and Peru.

During entomological research for triatomine in the municipality of Araguaiana, Mato Grosso, Brazil, a single specimen of a mermithid nematode was collected from *T. sordida*. The purpose of the present paper is to report the first finding of a juvenile stage of a mermithid nematode parasitizing Triatominae from Brazil. To date, there are no records of endoparasitism by nematodes in triatomines in the world. A list of records of mermithids from hemipteran hosts is presented in Table 1.

Table 1. Worldwide mermithid host records for Hemiptera.

Host species	Genus	Locality	Reference
Acrosternum hilare (Say, 1832) *Euschistus servus* (Say, 1832)	*Hexamermis*	United States	Kamminga et al. (2012)
Aelia acuminata (Linnaeus, 1758)	Undetermined	Uzbekistan	Sultanov et al. (1990)
Aelia rostrata Boheman, 1852	*Hexamermis*	Turkey	Tarla et al. (2012)
	Mermis		Memişoğlu and Özer (1994)
Chinavia hilaris (Say, 1831)	*Hexamermis*	United States	Kamminga et al. (2012)
	Agamermis		Stubbins et al. (2016)
Coptosoma mucronatum Rubostov, 1977	*Pentatomermis*	Slovakia	Rubtsov (1977)
Euschistus servus (Say, 1832)	Undetermined	United States	Esquivel (2011)
	Agamermis		Stubbins et al. (2016)
Euschistus sp.	*Agamermis*	United States	Stubbins et al. (2016)
Eurygaster integriceps Puton, 1881	*Mermis*	Turkey	Dikyar (1981)
	Hexamermis		Memişoğlu and Özer (1994)
	Hexamermis	Turkey	Tarla et al. (2011)
Eurygaster maura (Linnaeus, 1758)	*Hexamermis*	Turkey	Tarla et al. (2015)
Elasmostethus interstinctus (Linnaeus, 1758)	*Pentatomermis*	Russia	Rubtsov (1969)
Halys dentatus (Fabricius, 1775)	*Hexamermis*	India	Yadav and Dhiman (2004)
Megacopta cribraria (Fabricius, 1778)	*Agamermis*	United States	Stubbins et al. (2016)
Nezara viridula (Linnaeus, 1758)	Undetermined	United States	Fuxa et al. (2000)
	Pentatomermis	India	Rubtsov (1977) Bhatnagar et al. (1985)
Euschistus spp.	*Agamermis*	United States	Stubbins et al. (2016)
Platynopus sp.	*Hexamermis*	India	Gokulpure (1970)
Piezodorus guildinii (Westwood, 1837)	Undetermined	United States	Kamminga et al. (2012)
	Hexamermis or *Mermis* *Hexamermis*	Uruguay United States	Riberiro and Castiglioni (2008) Kamminga et al. (2012)
Rhaphigaster nebulosa (Poda, 1761)	*Hexamermis*	Italy	Manachini and Landi (2003)
Sogatella furezfera (Horvath, 1899)	*Agamermis*	Asia	Choo and Kaya (1993)

Materials and methods

The municipality of Araguaiana is located in the northeast Mesoregion of Mato Grosso state, Brazil (15°43'47"S, 51°49'26"W), 270 m high, with 3,197 inhabitants spread over 6,429,386 km^2. The predominant biome is the Cerrado (IBGE 2012) and the main economic activity is livestock production (IMEA 2017).

The climate is characterized by two main seasons (dry winter and rainy summer), corresponding to type Aw according to the Köppen classification (Köppen 1948). The average annual humidity is 60% and the average annual temperature 24 °C, with a maximum of 40 °C and lowest minimum of 4 °C.

During the years 2017 to 2019, 28 rural localities of Araguaiana, Mato Grosso, Brazil, were monitored as part of entomological research for triatomine bugs. Insects were manually collected by the method of active search with the support of health surveillance agents from the "Secretaria Municipal de Saúde" of Araguaiana, inside the domicile environment from domiciliary units (DUs) with evidence of the presence of triatomines and/or reports of the presence of the bug by the resident and around artificial ecotopes in domicile environments. For the DUs with the presence of a triatomine the geographical coordinates were taken with a GPS Garmin.

In the entomological laboratory of the "Escritório Regional de Saúde de Barra do Garças" from the "Secretaria de Estado de Saúde de Mato Grosso" (ERSBG/SESMT), the insects were counted, separated according to developmental stage (nymphs, adults) and posterior classification of the evolutionary stage of the nymphs and sex of the adults. These latter were taxonomically identified using the taxonomic keys of Lent and Wygodzinsky (1979) and Galvão (2014).

For investigation of the natural infection of *T. cruzi* in these triatomine specimens, dissection of the last portion of the abdominal segment was performed, slowly removing the entire intestine in the direction of a microscope slide, with the aid of tweezers.

For the taxonomic identification, the specimen of nematode worm was placed in a 2 mm tube containing 70% ethanol and sent to the "Laboratório de Helmintos Parasitos de Peixes" of the Oswaldo Cruz Institute, FIOCRUZ. The nematode was clarified in phenol and mounted on temporary slides. Measurements were taken directly using an ocular micrometer and are given in millimeters. Light microscope pictures were taken using a Zeiss Axioscope 2 microscope equipped with a camera lucida and a Sony MPEG Movie EX DSC-S75 digital camera. The nematode was identified according to available literature (Nickle 1972; Choo and Kaya 1990; Kaiser 1991; Stubbins et al. 2016).

Results

During entomological research for triatomines in the municipality of Araguaiana, Mato Grosso, Brazil, 1,488 specimens of *T. sordida* were found, with 220 being caught in the locality "Fazenda Lago Azul", Mato Grosso, Brazil (Fig. 1).

Figure 1. Map of the distribution of *Triatoma sordida*, showing the studied locality "Fazenda Lago Azul" in Araguaiana, Mato Grosso, Brazil (15°43'47"S, 51°49'26"W).

During the standard procedure for the extraction of intestinal content of a nymph of a third stage *T. sordida* (15 mm deep), a long and slim parasite was observed emerging from the triatomine (Fig. 2).

The parasitized specimen of *T. sordida* was collected in December 2018, in a chicken coop on "Fazenda Lago Azul", Araguaiana, Mato Grosso, Brazil (15°33'43.9"S, 051°47'26.2"W, 294 m high). The triatomine nymph was found between wooden plates. One animal water dispenser was observed near the chicken coop (Fig. 3).

Examination of parasitic juveniles under the microscope revealed well-developed stichosomes, a diagnostic characteristic of the family Mermithidae. The absence of tail appendage and presence of a tail end ring provided robust evidence for identification of the genus *Agamermis*. The specimen was white in color and slightly transparent at the tapered rounded ends (Fig. 4). The mermithid was extremely long in respect to its triatomine host, 193 mm in length and a maximum of 0.45 mm wide.

Discussion

Although triatomines are obligatorily hematophagous in all phases of their development, feeding across a broad range of mammals and other vertebrate species, there are some species able to feed on invertebrates by kleptohematophagy, hemolym-

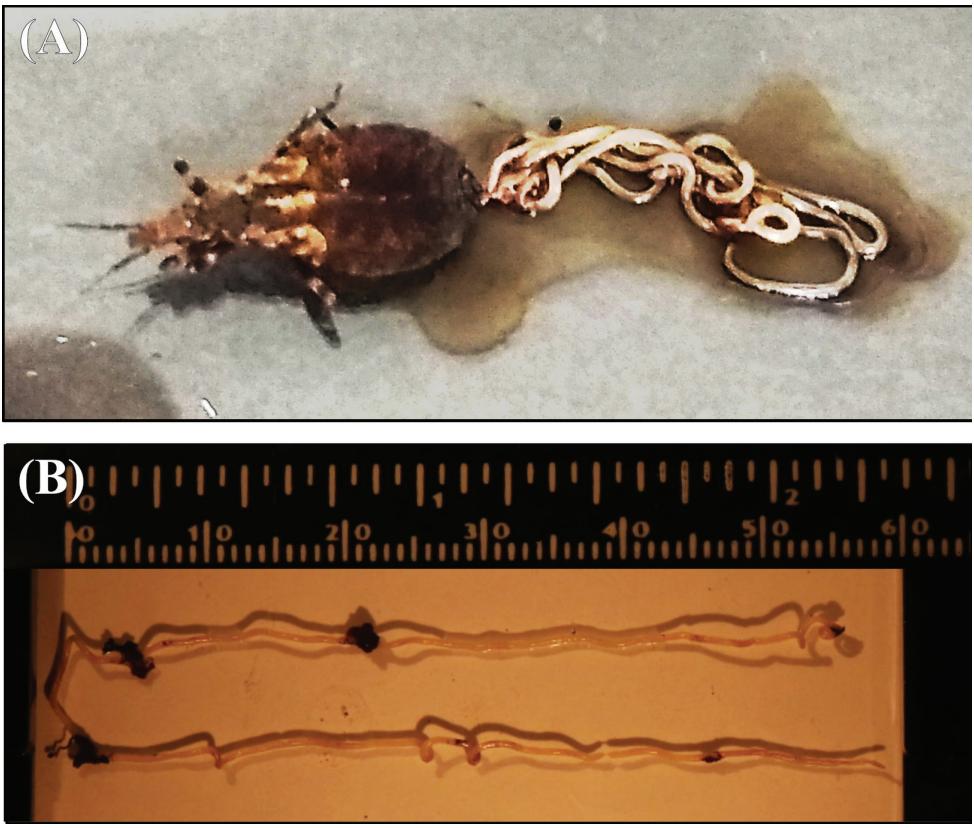

Figure 2. Mermithid: **A** specimen emerging from the posterior end of the third stage nymph of *Triatoma sordida* (Stål, 1859) collected in a chicken coop in Araguaiana, Mato Grosso, Brazil in December 2018 **B** specimen on microscope slide.

phagy, and coprophagy (Ruas-Neto et al. 2001; Sandoval et al. 2000, 2004, 2010; Otálora-Luna et al. 2015).

The chicken coop where the parasitized *T. sordida* nymph was collected showed the higher density of triatomines in artificial ecotopes in our entomological survey. It is noteworthy that December is a rainy season for this region, with record high rainfall and humidity for 2018. A high population density of triatomines can lead to increased local competition for food sources, leading insects to intense displacement in search of blood. Because they do not have wings, triatomine nymphs transit through the soil and an infective juvenile penetration from hatched eggs in the environment is supported (Christie 1936; Alves and Lopes 2008; Stubbins et al. 2016). Thus, it is likely that the juvenile form of this nematode present in the soil has penetrated in the nymph, explaining the presence of this mermithid parasitizing the *T. sordida*.

This study provides the first report worldwide of a mermithid nematode infecting the immature stages of the vector hemipteran, *T. sordida*. Terrestrial mermithids are a large group of obligate entomoparasitic nematodes that are considered important regu-

Figure 3. Chicken coop on "Fazenda Lago Azul", Araguaiana, Mato Grosso, Brazil where the nymph of *Triatoma sordida* was found.

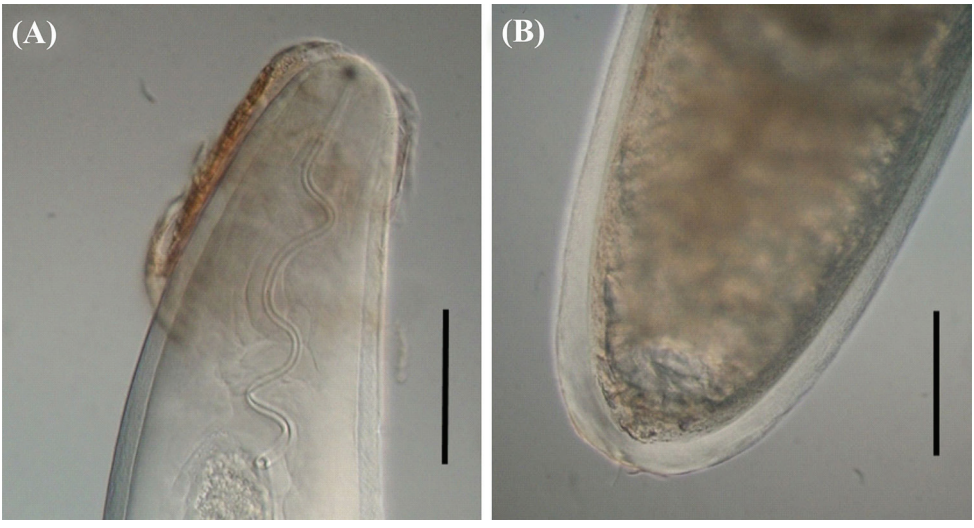

Figure 4. Mermithid nematode of *Triatoma sordida* observed by differential interference contrast (DIC). **A** Anterior portion **B** posterior portion showing the tail end ring. Scale bars: 60 mm (**A**); 150 mm (**B**).

lators for some insect populations, including hemipteran pests (Kaburaki and Imamura 1932; Choo and Kaya 1990), because of their capacity to retard development, induce female sterility, and cause death on host emergence (Kaiser 1991; Stubbins et

al. 2016). The majority of mermithid species constitute a significant regulatory influence on the population dynamics of plague insects (Rusconi et al. 2017).

Females can migrate from the soil onto the vegetation and lay eggs during periods of high moisture. These eggs are later consumed by the insects along with the vegetal material and hatch in the gut; the juveniles subsequently pass through the gut wall into the hemocoel and considerably increase in size inside the host. Nematodes kill the host with their emergence to the soil where they molt into the adult stage to complete the cycle (Poinar-Jr. 1979; Rusconi et al. 2017).

There is robust evidence that the nematode Mermithidae found parasitizing *T. sordida* belongs to the genus *Agamermis* Cobb, Steiner and Christie 1923. For accurate genus and species identification adult samples are required. The determination of mermithid species is difficult. One reason for this is that often only larval forms are obtainable, and another is that mermithids do not possess obvious morphological characteristics (Cobb et al. 1923). It is estimated that only one fifth of nematode species have so far been described (Storer and Usinger 1991).

Agamermis spp. have been reported infecting many insects species all over the world, including Pentatomidae and Plastaspidae (Hemiptera), in the brown plant hopper (BPH), *Nilaparvata lugens* (Stål), and the white backed plant hopper (WBPH), *Sogatella furcifera* (Horvath), which are considered serious pests of rice Acrididae (Orthoptera), as well as in crustaceans in the Isopoda *Armadillidium vulgare* (Cobb et al. 1923; Kaburaki and Imamura 1932; Christie 1936; Weaver and King 1954; Rubtsov 1969; Choo and Kaya 1990; Baker and Poinar-Jr. 1995; Choo et al. 1995; Igbinosa 1988; Zimmerman 2010; Stubbins et al. 2016; Rusconi et al. 2017).

The Mermithidae family nematodes have been studied as a biological control mechanism with promising results (Dhiman and Yadav 2004; Stubbins et al. 2016). The growing concern about the negative environmental effects of controlling vector insects makes the discovery of alternative control agents essential.

This report introduces the opportunity of considering Mermithid parasites as possible candidates for use as biological control against Triatomines. The capacity of these parasites as regulators of the population, a mechanism essential to control Chagas disease should be investigated. Studies on nematode parasites of other hemipteran species showed that these parasites could demonstrate potential for population suppression.

Acknowledgements

The research was supported by the Brazilian National Research Council (Conselho Nacional de Desenvolvimento Científico e Tecnológico - CNPq) and Fundação de Amparo à Pesquisa do Estado de Mato Grosso (FAPEMAT). We thank the Secretaria de Estado de Saúde de Mato Grosso for supporting the surveillance actions in health and the Secretaria Municipal de Saúde de Araguaiana for the support in field collections. To Nora B. Camino for help in identification of the specimen.

References

Alves SB, Lopes RB (2008) Controle microbiano de pragas na América Latina: avanços e desafios. Piracicaba: FEALQ, 414 pp. https://www.researchgate.net/publication/291352256

Baker GL, Poinar-Jr. GO (1995) *Agamermis catadecaudata* n. sp. (Nematoda: Mermithidae), a parasitoid of Orthoptera in southeastern Australia. Fundamental and applied Nematology 18: 139–148. http://horizon.documentation.ird.fr/exl-doc/pleins_textes/fan/42719.pdf

Bhatnagar VS, Pawar CS, Jadhav DR, Davies JC (1985) Mermithid nematodes as parasites of *Heliothis* spp. and other crop pests in Andhra Pradesh. Proceedings of the Indian Academy of Sciences Animal Sciences 94: 509–515. https://doi.org/10.1007/BF03186360

Camino NB, Lange CE (1997) Two new species of the genus *Amphimermis* Kaburaki and Imamura (Nematoda: Mermithidae) from argentine grasshoppers (Orthoptera: Acrididae). Fundamental and Applied Nematology 20: 239–242.

Camino NB, Stock SP (1989) Un nuevo nematodo parásito de lacrídido *Laplatacris dispar* Rhen, 1939, en Argentina. Revista Peruana de Entomología 32: 30–32.

Choo HY, Kaya HK (1990) Parasitism of brown planthopper and whitebacked planthopper by *Agamermis unka* in Korea. Journal of Nematology 22: 513–517.

Choo YK, Kaya HK (1993) Parasitism of brown planthopper by the mermithid nematode *Agamermis* in rice. In: Bedding R, Akhurst R, Kaya H (Eds) Nematodes and the biological control of insect pests. Melbourne CSIRO, 21–26.

Choo HY, Kaya HK, Kim HH (1995) Biological studies on *Agamermis unka* (Nematoda: Mermithidae), a parasite of the brown planthopper *Nilaparvata lugens.* Biocontrol Science and Technology 5: 209–224. https://doi.org/10.1080/09583159550039936

Christie JR (1936) Life history of *Agamermis decaudata*, a nematode parasite of grasshoppers and other insects. Journal of Agricultural Research 52: 161–198.

Cobb NA, Steiner G, Christie JR (1923) *Agamermis decaudata* Cobb, Steiner and Christie: a nema parasite of grasshoppers and other insects. Journal of Agricultural Research 23: 921–926.

Dias JCP, Bastos C, Araujo E, Mascarenhas AV, Netto EM, Grassi F (2008) Acute Chagas disease associated with oral transmission. Revista da Sociedade Brasileira de Medicina Tropical 41: 296–300. https://doi.org/10.1590/S0037-86822008000300014

Dhiman SC, Yadav YK (2004) Studies on parasitoids of *Halys dentatus* Fabr. (Heteroptera: Pentatomidae) and their bio-control efficacy. Annals of Plant Protection Sciences 12: 263–266.

Dikyar R (1981) Biology and control of *Aelia rostrata* in central Anatolia. EPPO Bulletin 11: 39–41. https://doi.org/10.1111/j.1365-2338.1981.tb01762.x

Dolinski C (2006) Uso de nematoides entomopatogênicos para o controle de pragas. In: Venzon M, Paula Jr TJ, Pallini A (Org.) Tecnologias Alternativas para o Controle Alternativo de Pragas e Doenças, Viçosa, 261–289. https://www.researchgate.net/publication/283360372

Duncan LW, Stuart RJ, El-Borai FE, Campos-Herrera R, Pathak E, Giurcan UM, Graham JH (2013) Modifying orchard planting sites conserves entomopathogenic nematodes, reduces weevil herbivory and increases citrus tree growth, survival and fruit yield. Biological Control 64: 26–36. https://doi.org/10.1016/j.biocontrol.2012.09.006

Esquivel JF (2011) *Euschistus servus* (Say) – A new host record for Mermithidae (Mermithida). Southwestern Entomologist 36: 207–211. https://doi.org/10.3958/059.036.0210

Fuxa JE, Fuxa JR, Richter AR, Weidner EH (2000) Prevalence of a trypanosomatid in the southern green stink bug, *Nezara viridula*. Journal of Eukaryotic Microbiology 47: 388–394. https://doi.org/10.1111/j.1550-7408.2000.tb00065.x

Galvão C (2014) Vetores da doença de Chagas no Brasil [online]. Sociedade Brasileira de Zoologia, Curitiba, 289 pp. Zoologia: guias e manuais de identificação. https://doi.org/10.7476/9788598203096 [Available from SciELO Books]

Galvão C, Justi S (2015) An overview on the ecology of Triatominae (Hemiptera: Reduviidae). Acta Tropica 151: 116–125. https://doi.org/10.1016/j.actatropica.2015.06.006

Gokulpure RS (1970) Some new hosts of a juvenile mermithid of the genus *Hexamermis* (Steiner). Indian Journal of Entomology 32: 387–389.

Gumus A, Karagoz M, Shapiro-Ilan D, Hazir S (2015) Novel approach to biocontrol: Release of live insect hosts pre-infected with entomopathogenic nematodes. Journal of Invertebrate Pathology 130: 56–60. https://doi.org/10.1016/j.jip.2015.07.002

Igbinosa IB (1988) Parasites of the immature stages of *Latoia viridissima* Holland (Lep, Limacodidae), a pest of palms in Nigeria. Journal of Applied Entomology 106: 527–530. https://doi.org/10.1111/j.1439-0418.1988.tb00628.x

IBGE [Instituto Brasileiro de Geografia e Estatística] (2012) http://www.ibge.gov.br/cidadesat/topwindow.htm?1 [Accessed on 26 May 2020]

IMEA [Instituto Matogrossense de Economia Agropecuária] (2017) Mapa das macrorregiões. https://docplayer.com.br/67975674-Mapa-das-macrorregioes-do-imea.html

Jouvenaz DP, Wojcik DP (1990) Parasitic nematode observed in the fireant, *Solenopsis richteri*, in Argentina Florida. Entomologist 73: 674–675. https://doi.org/10.2307/3495284

Kaburaki T, Imamura S (1932) Mermithid- worm parasitic in leaf-hoppers, with notes on its life history and habits. Proceedings of the Imperial Academy (Tokyo) 8: 139–141. https://doi.org/10.2183/pjab1912.8.139

Kaiser H (1991) Terrestrial and semiterrestrial Mermithidae In: Nickle WR (Ed.) Manual of agricultural nematology. Marcel Dekker, New York, 899–965.

Kamminga KL, Davis JA, Stock SP, Richter AR (2012) First report of a mermithid nematode infecting *Piezodorus guildinii* and *Acrosternum hilare* (Hemiptera: Pentatomidae) in the United States. Florida Entomologist 95: 214–217. https://doi.org/10.1653/024.095.0137

Köppen W (1948) Climatologia: conun estudio de los climas de latierra. Fondo de Cultura Economica, México, 478 pp.

Kosulic O, Masova S (2019) First Report on Mermithid Parasitism (Enoplea: Mermithidae) in a Southeast Asian Spider (Araneae: Araneidae). Helminthologia 56: 157–167. https://doi.org/10.2478/helm-2019-0012

Lent H, Wygodzinsky P (1979) Revision of the Triatominae (Hemiptera, Reduviidae) and their significance as vectors of Chagas' disease. Bulletin of the American Museaum of Natural History 163: 123–520.

Manachini B, Landi S (2003) New record of *Hexamermis* sp. (Nematoda: Mermithidae) parasiting (sic) *Rhaphigaster nebulosa* Poda (Hemiptera: Pentatomidae). Bollettino di Zoologia Agraria e di Bachicoltura 35: 91–94.

Memişoğlu H, Melan K, Özkan M, Kılıç AU (1994) Investigations on the crop losses the wheat caused by cereal bug (*Aelia rostrata* Boh.) in the region of central Anatolia. Bitki Koruma Bülteni 34: 111–121.

Minuzzi-Souza TTC, Nitz N, Cuba Cuba CA, Santalucia M, Knox MB, Hagström L, Furtado CB, Vital TE, Obara MT, Hecht MM, Gurgel-Gonçalves R (2017) Synanthropic triatomines as potential vectors of *Trypanosoma cruzi* in Central Brazil. Revista da Sociedade Brasileira de Medicina Tropical 50: 824–828. https://doi.org/10.1590/0037-8682-0199-2017

Miralles DA, Camino NB (1983) Una nueva especie de Mermithidae, *Amphimermis bonaerensis* sp. n. (Nematoda: Enoplida). Neotropica 29: 153–156.

Nickle WR (1972) A Contribution to our Knowledge of the Mermithidae (Nematoda). Journal of Nematology 4: 113–146.

Nikdel M, Kaiser H, Niknam G (2011) First record of *Hexamermis* cf *albicans* (Siebold, 1848) (Nematoda: Mermithidae) infecting Lepidopteran larvae from Iran. Nematology Medit 39: 81–83.

Obara MT, Otrera VCG, Gurgel-Gonçalves RG, Santos JP, Santalucia M, Rosa JA, Almeida OS, Barata JMS (2011) Monitoramento da suscetibilidade de populações de *Triatoma sordida* Stål, 1859 (Hemiptera: Reduviidae) ao inseticida deltametrina, na região Centro-Oeste do Brasil. Revista da Sociedade Brasileira de Medicina Tropical 44: 206–212. https://doi.org/10.1590/S0037-86822011005000004

Otálora-Luna F, Pérez-Sánchez AJ, Sandoval C, Aldana E (2015) Evolution of hematophagous habit in Triatominae (Heteroptera: Reduviidae). Revista Chilena de Historia Natural 88: 4. https://doi.org/10.1186/s40693-014-0032-0

Poinar-Jr. GO (1979) Nematodes for biological control of insects. CRC Press, Boca Raton, 274 pp.

Poinar-Jr. GO (1983) The natural history of Nematodes. Englewood Cliffs: Prentice Hall, 323 pp.

Poinar-Jr. GO (2015) Phylum Nemata. In Thorp and Covich's Freshwater Invertebrades. Ecology and General Biology, 273–302. https://doi.org/10.1016/B978-0-12-385026-3.00014-0

Poinar-Jr. GO, Porter SD, Tang S, Hyman BC (2007) *Allomermis solenopsi* n. sp. (Nematoda: Mermithidae) parasitising the fire ant *Solenopsis invicta* Buren. (Hymenoptera: Formicidae) in Argentina. Systematic Parasitology 68: 115–128. https://doi.org/10.1007/s11230-007-9102-x

Poulin R (2011) Evolutionary ecology of parasites. New York: Chapman & Hall, 325 pp. https://doi.org/10.1515/9781400840809

Ribeiro-Jr. G, Santos CGS dos, Lanza F, Reis J, Vaccarezza F, Diniz C, Miranda DLP, Araújo RF de, Cunha GM, Carvalho CMM de, Fonseca EOL, Santos RF dos, Sousa OMF de, Reis RB, Araújo WN de, Gurgel-Gonçalves R, Reis MG dos (2019) Wide distribution of *Trypanosoma cruzi*-infected triatomines in the State of Bahia, Brazil. Parasites Vectors 12: 604. https://doi.org/10.1186/s13071-019-3849-1

Riberiro A, Castiglioni E (2008) Characterization of populations of natural enemies of *Piezodorus guildinii* (Westwood) (Hemiptera: Pentatomidae). Agrociencia 12: 48–56.

Rodrigues T, Álvares ÉS, Machado ÉO, de Maria M (2005) New records of the family Mermithidae (Nematoda) as parasitoids of spiders (Arachnida: Araneae) in Brazil and Peru. Revista Ibérica de Aracnología 12: 119–120.

Rossi JC, Duarte EC, Gurgel-Gonçalves R (2015) Factors associated with the occurrence of *Triatoma sordida* (Hemiptera: Reduviidae) in rural localities of Central-West Brazil. Memórias do Instituto Oswaldo Cruz 110: 192–200. https://doi.org/10.1590/0074-02760140395

Ruas-Neto AL, Corseuil E, Cavalleri A (2001) Development of rupestrian triatomines (Hemiptera, Reduviidae, Triatominae) following hemolymphagy on blaberids (Blattodea, Blaberidae) in Rio Grande do Sul State, Brazil. Entomologia y Vectores 8: 205–216.

Rubtsov I.A (1969) New and little known species of nematodes from the Danube. Hydrobiologischeski Zhurnal 5: 49–59.

Rubtsov IA (1977) New genus and two new species of mermithids from bugs. Parazitologiia 11: 541–544.

Rusconi JM, Camino NB, Achinelly MF (2017) Nematodes (Mermithidae) parasitizing grasshoppers (Orthoptera: Acrididae) in the Pampean region, Argentina. Brazilian Journal of Biology 77: 12–15. https://doi.org/10.1590/1519-6984.06015

Sandoval CM, Duarte R, Gutíerrez R, Rocha DS, Angulo VM, Esteban L, Reyes M, Jurberg J, Galvão C (2004) Feeding sources and natural infection of *Belminus herreri* (Hemiptera, Reduviidae, Triatominae) from dwellings in Cesar, Colombia. Memórias do Instituto Oswaldo Cruz 99: 137–140. https://doi.org/10.1590/S0074-02762004000200004

Sandoval CM, Joya M, Gutiérrez M, Angulo VM (2000) Cleptohaemathophagia in *B. herreri*. Medical and Veterinary Entomology 14: 100–101. https://doi.org/10.1046/j.1365-2915.2000.00210.x

Sandoval CM, Nortiz N, Jaimes D, Lorosa E, Galvão C, Rodriguez O, Scorza JV, Gutierrez R (2010) Feeding behaviour of *Belminus ferroae* (Hemiptera: Reduviidae) a predaceous Triatominae colonizing rural houses in Norte de Santander, Colombia. Medical and Veterinary Entomology 24: 124–13. https://doi.org/10.1111/j.1365-2915.2010.00868.x

Shapiro-Ilan DI, Cottrell TE, Mizell RF, Horton DL, Behle RW, Dunlap CA (2010) Efficacy of *Steinernema carpocapsae* for control of the lesser peachtree borer, *Synanthedon pictipes*: Improved aboveground suppression with a novel gel application. Biological Control 54(1): 23–28. https://doi.org/10.1016/j.biocontrol.2009.11.009

Storer T, Usinger R (1991) Zoologia Geral. Companhia Editora Nacional, São Paulo, 816 pp.

Stubbins FL, Agudelo P, Reay-Jones FP, Greene JK (2016) *Agamermis* (Nematoda: Mermithidae) Infection in South Carolina Agricultural Pests. Journal of Nematology 48: 290. https://doi.org/10.21307/jofnem-2017-037

Sultanov MA, Artyukhovskii AK, Lysikova EA (1990) Hosts of mermithids – The most important pests of farm and forest plants in Uzbekistan In: Sonin MD, Kothekar VS (Eds) Helminths of insects. Oxonian Press, New Delhi, India, 186–191.

Tarla G, Tarla S, Islamoglu M (2015) First report of *Hexamermis* sp. (Nematoda: Mermithidae) parasitizing *Eurygaster maura* (Heteroptera: Scutelleridae) in an overwintering area. Florida Entomologist 98: 974–978. https://doi.org/10.1653/024.098.0328

Tarla G, Poinar-Jr. G, Tarla Ş (2011) *Hexamermis eurygasteri* sp. n. (Mermithidae: Nematoda) parasitizing the Sunn Pest, *Eurygaster integriceps* puton (Hemiptera: Scutelleridae) in Turkey. Systematic Parasitology 79: 195–200. https://doi.org/10.1007/s11230-011-9299-6

Tarla G, Tarla S, Islamoglu M, Kodan M (2012) Parasitism of the wheat stinkbug, *Aelia rostrata* Boh. (Heteroptera: Pentatomidae) with the entomopathogenic nematode, *Hexamermis* sp. (Nematoda: Mermithidae). Egyptian Journal of Biological Pest Control 22: 141–143.

Weaver CR, King DR (1954) Meadow spittlebug. Ohio Agricultural Experiment Station Research Bulletin, Ohio, 741 pp.

Zimmerman BL (2010) Aspectos da relação simbiótica entre as bactérias *Wolbachia* (Alphaproteobacteria, Rickettsiales) e os isópodos terrestres (Crustacea, Oniscidea). Dissertação apresentada ao Programa de Pós-Graduação em Biologia Animal, Instituto de Biociências, da Universidade Federal do Rio Grande do Sul. https://hdl.handle.net/10183/28424

ZooKeys 980: 93–117 (2020)
doi: 10.3897/zookeys.980.55979
https://zookeys.pensoft.net

RESEARCH ARTICLE

A peer-reviewed open-access journal
ZooKeys
Launched to accelerate biodiversity research

A DNA barcode library for ground beetles of Germany: the genus *Pterostichus* Bonelli, 1810 and allied taxa (Insecta, Coleoptera, Carabidae)

Michael J. Raupach[1], Karsten Hannig[2], Jérome Morinière[3], Lars Hendrich[4]

1 *Sektion Hemiptera, Bavarian State Collection of Zoology (SNSB – ZSM), Münchhausenstraße 21, 81247 München, Germany* **2** *Bismarckstraße 5, 45731 Waltrop, Germany* **3** *AIM – Advanced Identification Methods GmbH, Spinnereistraße 11, 04179 Leipzig* **4** *Sektion Insecta varia, Bavarian State Collection of Zoology (SNSB – ZSM), Münchhausenstraße 21, 81247 München, Germany*

Corresponding author: Michael J. Raupach (raupach@snsb.de)

Academic editor: B. Guéorguiev | Received 29 June 2020 | Accepted 4 September 2020 | Published 28 October 2020

http://zoobank.org/3F8D4154-F424-4E9F-B93F-CF77FEFB6404

Citation: Raupach MJ, Hannig K, Morinière J, Hendrich L (2020) A DNA barcode library for ground beetles of Germany: the genus *Pterostichus* Bonelli, 1810 and allied taxa (Insecta, Coleoptera, Carabidae). ZooKeys 980: 93–117. https://doi.org/10.3897/zookeys.980.55979

Abstract

Species of the ground beetle genus *Pterostichus* Bonelli, 1810 are some of the most common carabids in Europe. This publication provides a first comprehensive DNA barcode library for this genus and allied taxa including *Abax* Bonelli, 1810, *Molops* Bonelli, 1810, *Poecilus* Bonelli, 1810, and *Stomis* Clairville, 1806 for Germany and Central Europe in general. DNA barcodes were analyzed from 609 individuals that represent 51 species, including sequences from previous studies as well as more than 198 newly generated sequences. The results showed a 1:1 correspondence between BIN and traditionally recognized species for 44 species (86%), whereas two (4%) species were characterized by two BINs. Three BINs were found for one species (2%), while one BIN for two species was revealed for two species pairs (8%). Low interspecific distances with maximum pairwise K2P values below 2.2% were found for four species pairs. Haplotype sharing was found for two closely related species pairs: *Pterostichus adstrictus* Eschscholtz, 1823/*Pterostichus oblongopunctatus* (Fabricius, 1787) and *Pterostichus nigrita* Paykull, 1790/*Pterostichus rhaeticus* Heer, 1837. In contrast to this, high intraspecific sequence divergences with values above 2.2%

were shown for three species (*Molops piceus* (Panzer, 1793), *Pterostichus panzeri* (Panzer, 1805), *Pterostichus strenuus* (Panzer, 1793)). Summarizing the results, the present DNA barcode library does not only allow the identification of most of the analyzed species, but also provides valuable information for alpha-taxonomy as well as for ecological and evolutionary research. This library represents another step in building a comprehensive DNA barcode library of ground beetles as part of modern biodiversity research.

Keywords

Abax, Central Europe, cytochrome *c* oxidase subunit I, German Barcode of Life, mitochondrial DNA, molecular specimen identification, *Molops*, *Poecilus*, *Stomis*

Introduction

As part of the global International Barcode of Life initiative (IBoL; https://ibol.org), the German Barcode of Life initiative (GBoL; www.bolgermany.de) aims at capturing the genetic diversity of animals, fungi and plants of Germany using DNA barcodes in terms of modern biodiversity research (Hebert et al. 2003a, b). Despite the fact that various effects may limit the efficiency of a successful species identification, for example recent or ongoing hybridization events (e.g., Rougerie et al. 2012; Mutanen et al. 2016; Havemann et al. 2018), mitochondrial DNA-like sequences in the nucleus (numts) (e.g., Rogers and Griffiths-Jones 2012; Jordal and Kambestand 2014), or effects of *Wolbachia* infections (e.g., Smith et al. 2012; Klopfstein et al. 2016; Kolasa et al. 2018; Kajtoch et al. 2019), DNA barcoding has become the method of choice in terms of modern molecular species identification, including the identification of single specimens as well as metabarcoding of bulk samples (e.g., Casiraghi et al. 2010; Brandon-Mong et al. 2015). In recent years, various barcode libraries for numerous animal groups of Germany were established, including both marine and freshwater fish (Knebelsberger et al. 2014; Knebelsberger et al. 2015), amphibians and reptiles (Hawlitschek et al. 2016), echinoderms (Laakmann et al. 2017), molluscs (Gebhardt and Knebelsberger 2015; Barco et al. 2016), crustaceans (Raupach et al. 2015), spiders (Astrin et al. 2016), myriapods (Spelda et al. 2011), and numerous insect taxa, e.g., Coleoptera (Hendrich et al. 2015), Ephemeroptera, Plecoptera, Trichoptera (Morinière et al. 2017), Heteroptera (Raupach et al. 2014; Havemann et al. 2018), Hymenoptera (Schmidt et al. 2015; Schmidt et al. 2017; Schmid-Egger et al. 2019), Lepidoptera (Hausmann et al. 2011), Neuroptera (Morinière et al. 2014), and Orthoptera (Hawlitschek et al. 2017). Previous studies also laid the groundwork of a comprehensive DNA barcode library for the ground beetles (Coleoptera: Carabidae) of Germany (Raupach et al. 2010; Raupach et al. 2011; Hendrich et al. 2015; Raupach et al. 2016; Raupach et al. 2018; Raupach et al. 2019).

The Carabidae are a cosmopolitan family with an estimated number of probably more than 40,000 species world-wide (Lindroth 1986). The margined pronotum, large head, prominent mandibles, and striate elytra help to characterize this family

(Arnett and Thomas 2000). These features, however, vary considerably throughout this taxon. Ground beetles can be found in all habitats except deserts and polar regions. Most adults of this family present a somber appearance, that is, a uniformly dark color, although some species are bi- or tricolored dorsally, and can have striking patterns (e.g., *Callistus* Bonelli, 1810, *Omophron* Latreille, 1802 or *Panagaeus*, Latreille, 1804). Adult ground beetles range in size from 2 up to 70 mm (genus *Hyperion* Castelnau, 1834). Most carabids are predators of invertebrates and consume many pest species, and are therefore typically considered as beneficial organisms (e.g., Lövei 1996). Within the Carabidae, the genus *Pterostichus* Bonelli, 1810 is a very large and diverse taxon with a Holarctic distribution, also reaching the Oriental and Neotropical regions (Hůrka 1996). More than 1,000 species are known world-wide to date, with more than 200 species are recorded for Europe (Hůrka 1996; Luff 2007) and 36 documented in Germany, including some of the commonest carabids of Germany, e.g., *Pterostichus niger* (Schaller, 1783), *Pterostichus nigrita* (Paykull, 1790), or *Pterostichus strenuus* (Panzer, 1796) (Trautner et al. 2014). The genus is in the present concept, however, undoubtedly not monophyletic and has been subdivided into numerous subgenera or sometimes even genera in the past (e.g., Lindroth 1986; Hůrka 1996; Luff 2007). Unfortunately, a thorough and comprehensive revision is still missing. In order to accommodate this situation, the subgeneric arrangement used in this study follows the traditional arrangement (see Marggi 2006). In general, adults of the genus *Pterostichus* have a body length between 5 to 25 mm, with most species above average. They have normally a somewhat uniform appearance with a strongly sclerotized and stout pronotum, thick antennae, and rather long legs with pronounced tibiae (Lindroth 1986). The overwhelming majority of species are carnivorous, night-active black-colored insects; those with a metallic coloration are often diurnal (Lindroth 1986) (Fig. 1). Due to the fact that various species of this genus represent important and highly abundant elements of the carabid fauna of many habitats world-wide (e.g., Igondová and Majzlan 2015; Hong et al. 2017; Baranová et al. 2018), they have been intensively studied in the past, for example their general ecology (e.g., Rushton et al. 1990; Fournier and Loreau 2001; Allema et al. 2012; Brigić et al. 2014), feeding strategies (e.g., Symondson et al. 2000; Langan et al. 2001; Dinis et al. 2016), and zoogeography/phylogeography (e.g., Lagisz et al. 2010; Schmidt et al. 2012; Sasakawa et al. 2017).

In this study we present as part of the GBoL project a further step in generating a comprehensive DNA barcode library for the molecular identification of Central European ground beetle species, focusing on the genus *Pterostichus* and allied taxa. This barcode library included 36 species of *Pterostichus* as well as additional species of other genera belonging to the Pterostichini, including five species of the genus *Abax* Bonelli, 1810, three species of the genus *Molops* Bonelli, 1810, six species of the genus *Poecilus* Bonelli, 1810 and one species of the genus *Stomis* Clairville, 1806. In sum, 198 new barcodes were generated and a total number of 609 DNA barcodes examined in detail, including DNA barcodes of pinned museum specimens up to 39 years old.

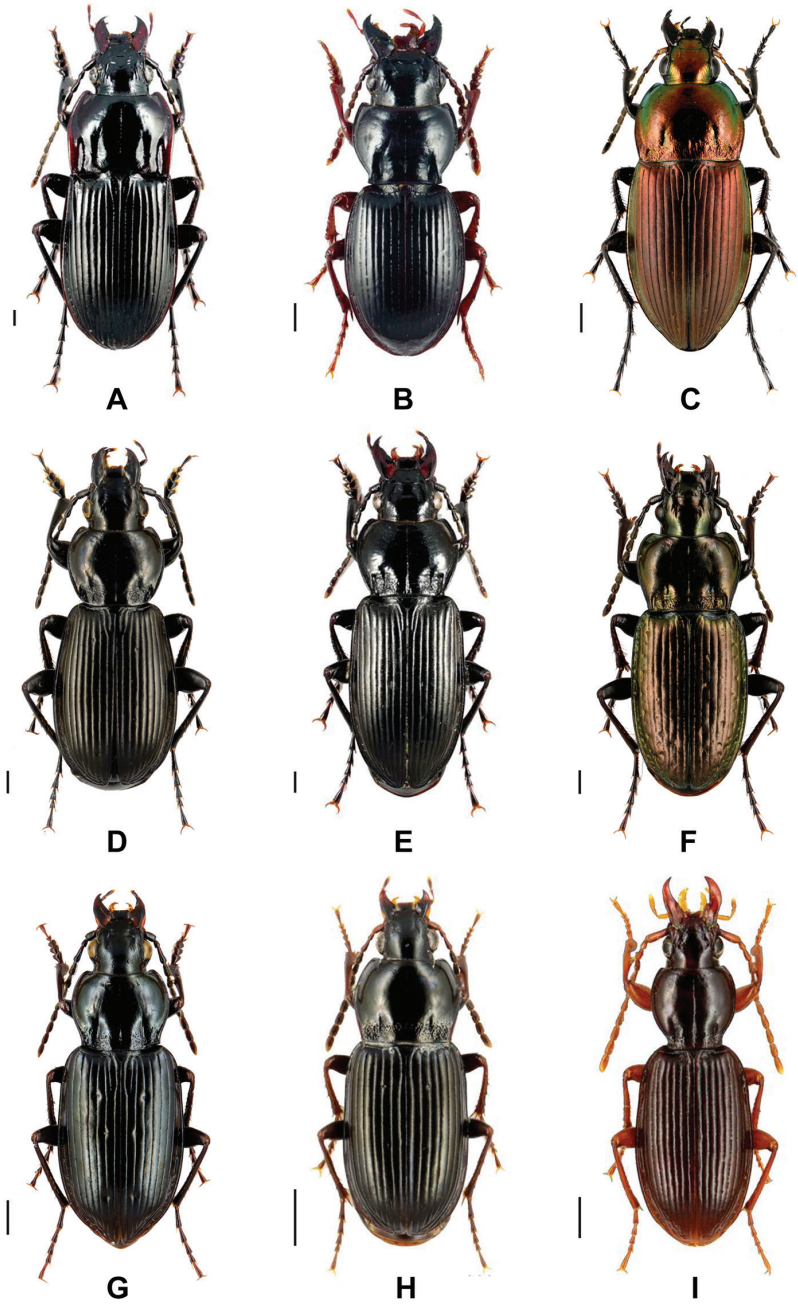

Figure 1. Representative images of analyzed beetle species **A** *Abax parallelepipedus* (Piller & Mitterbacher, 1783) **B** *Molops piceus* (Panzer, 1793) **C** *Poecilus versicolor* (Sturm, 1824) **D** *Pterostichus (Eosteropus) aethiops* (Panzer, 1796) **E** *Pterostichus (Omaseus) melanarius* (Illiger, 1798) **F** *Pterostichus (Oreophilus) multipunctatus* (Dejean, 1828) **G** *Pterostichus (Bothriopterus) quadrifoveolatus* Letzner, 1852 **H** *Pterostichus (Argutor) vernalis* Panzer, 1796 and **I** *Stomis pumicatus* (Panzer, 1795). Scale bars: 1 mm. All images were obtained from www.eurocarabidae.de.

Materials and methods

Sampling of specimens

Most studied ground beetles (n = 186, 93.9%) were collected between 2006 and 2018 using various sampling methods (i.e., hand collecting, pitfall traps). All beetles were stored in ethanol (96%). The analyzed specimens were identified using the identification key provided in Marggi (2006). It was also possible to generate DNA barcodes from pinned ground beetles of the carabid collection of the Bavarian State Collection of Zoology (n = 12, 6.1%), with an age between 22 and 39 years. In total, 198 new barcodes of 37 species were generated. Furthermore, we included 411 DNA barcodes from three previous studies (Raupach et al. 2010: 86 specimens, 16 species; Pentinsaari et al. 2014: 61 specimens, 15 species; Hendrich et al. 2015: 247 specimens, 37 species) and 17 sequences that were released without publication (7 species) in our analysis. Therefore, the complete dataset covered 609 DNA barcodes.

Most beetles were collected in Germany (n = 403, 66.2%), but for comparison various specimens were included from Austria (n = 82, 13.5%), Belgium (n = 16, 2.6%), Bulgaria (n = 1, 0.2%), Czech Republic (n = 4, 0.7%), Estonia (n = 2, 0.3%), Finland (n = 59, 9.7%), France (n = 16, 2.6%), Italy (n = 10, 1.6%), Romania (n = 2, 0.3%), Slovakia (n = 1, 0.2%), Slovenia (n = 10, 1.6%), and Switzerland (n = 3, 0.5%). The number of analyzed specimens per species ranged from one (6 species) to a maximum of 40 for *Poecilus versicolor* (Sturm, 1824).

DNA barcode amplification, sequencing, and data depository

All laboratory operations were carried out, following standardized protocols for the cytochrome *c* oxidase subunit I (COI) fragment amplification and sequencing (Ivanova et al. 2006, deWaard et al. 2008), at the Canadian Center for DNA Barcoding (CCDB), University of Guelph, the molecular labs of the Zoologisches Forschungsmuseum Alexander Koenig in Bonn, the German Centre of Marine Biodiversity Research, Senckenberg am Meer, in Wilhelmshaven, and the working group Systematics and Evolutionary Biology at the Carl von Ossietzky University Oldenburg, all in Germany. Photos from each studied beetle were taken before molecular work started. One or two legs of one body side were removed for the subsequent DNA extraction which was performed using the QIAmp Tissue Kit (Qiagen GmbH, Hilden, Germany) or NucleoSpin Tissue Kit (Macherey-Nagel, Düren, Germany), following the manufacturer`s extraction protocol. The PCR temperature profile for the barcode fragment (approx. 660 base pairs) using the primer pair LCO1480 and HCO2198 (Folmer et al. 1994) consisted of an initial denaturation at 94 °C (5 min), followed by 38 cycles at 94 °C (denaturation, 45 s), 48 °C (annealing, 45 s), 72 °C (extension, 80 s), and a final extension 72 °C (7 min). Purified PCR products were cycle-sequenced and sequenced in both directions at contract sequencing facilities (Macrogen, Seoul, Korea, or GATC, Konstanz, Germany),

using the same primers as used in PCR. Double stranded sequences were assembled and checked for mitochondrial pseudogenes (numts) analyzing the presence of stop codons, frameshifts as well as double peaks in chromatograms with Geneious Prime 2020.0.4 (https://www.geneious.com) (Biomatters, Auckland, New Zealand). For verification, BLAST searches (nBLAST, search set: others, program selection: megablast) were performed to confirm the identity of all new sequences as ground beetle barcodes based on already published sequences (high identity values, very low E-values).

Comprehensive voucher information, taxonomic classifications, photos, DNA barcode sequences, primer pairs used and trace files (including their quality) are publicly accessible through the public dataset "DS-BAPTE" (Dataset ID: dx.doi.org/10.5883/DS-BAPTE) on the Barcode of Life Data Systems (BOLD; www.boldsystems.org) (Ratnasingham and Hebert 2007). In addition, all new barcode data were deposited in GenBank (accession numbers: MN454529–MN454726).

DNA barcode analysis

The complete dataset was analyzed by using an established workflow as it was already performed in former studies (Raupach et al. 2016, Raupach et al. 2018). The analysis tools of the BOLD workbench were employed to calculate the nucleotide composition of the sequences and distributions of Kimura-2-parameter distances (K2P; Kimura 1980) within and between species (align sequences: BOLD aligner; ambiguous base/gap handling: pairwise deletion). All barcode sequences became subject of the Barcode Index Number (BIN) analysis system implemented in BOLD that clusters DNA barcodes in order to produce operational taxonomic units that typically closely correspond to species (Ratnasingham and Hebert 2013). A first threshold of 2.2% was applied for a rough differentiation between intraspecific and interspecific distances, followed by refinements through Markov clustering into the final BINs (Ratnasingham and Hebert 2013). These BIN assignments on BOLD are constantly updated as new sequences are added, splitting and/or merging individual BINs in the light of new data (Ratnasingham and Hebert 2013).

In addition, all sequences were aligned using MUSCLE (Edgar 2004) and analyzed using a neighbor-joining cluster analysis (NJ; Saitou and Nei 1987) based on K2P distances with MEGA 10.0.5 (Kumar et al. 2018). Non-parametric bootstrap support values were obtained by resampling and analyzing 1,000 replicates (Felsenstein 1985). It should be explicitly noted that this analysis is not intended to be phylogenetic. Instead of this, the shown topology represents a graphical visualization of DNA barcode distance divergences and species clustering. For species pairs with interspecific distances < 2.2%, maximum parsimony networks were constructed with TCS 1.21 based on default settings (Clement et al. 2000), implemented in the software package PopART v.1.7 (Leigh and Bryant 2015). Such networks allow the identification of possible haplotype sharing between species as a consequence of recent speciation or on-going hybridization processes.

Results

Overall, 609 DNA barcode sequences of 51 ground beetle species of the Pterostichini were analyzed. A full list of the analyzed species is presented in the supporting information (Suppl. material 1). For the genus *Pterostichus* we analyzed 31 species which represent 86% of all recorded species (n = 36) of this genus for Germany. Beside this, the given sampling covered four species of the genus *Abax* (recorded species for Germany: n = 4, therefore 100%), two species of the genus *Molops* (n = 2, 100%), six species of the genus *Poecilus* (n = 6, 100%), and the only known species for Germany of the genus *Stomis*. Seven additional analyzed species are actually not recorded from Germany but included for comparison: *Abax beckenhauptii* (Duftschmid, 1812) (n = 3), *Molops striolatus* (Fabricius, 1801) (n = 2), *Pterostichus adstrictus* Eschscholtz, 1823 (n = 5), *Pterostichus illigeri* (Panzer, 1803) (n = 3), *Pterostichus muehlfeldii* (Duftschmid, 1812) (n = 3), *Pterostichus schmidtii* (Chaudoir, 1838) (n = 3), and *Pterostichus ziegleri* (Duftschmid, 1812) (n = 8).

In total, fragment lengths of the analyzed DNA barcode fragments ranged from 420 to 658 base pairs. As it is typically known for arthropods, the DNA barcode region was characterized by a high AT-content: the mean sequence compositions were A = 29.7%, C = 15.1%, G = 16.2%, and T = 39%. Intraspecific K2P distances ranged from 0 to a maximum of 3.15% (*Molops piceus*), whereas interspecific distances within the analyzed species had values between 0 and 11.19%. Lowest interspecific distances were found for *Pterostichus adstrictus* Eschscholtz, 1823 and *Pterostichus oblongopunctatus* (Fabricius, 1787) (0%; BIN: ABY4764) as well as *Pterostichus nigrita* Paykull, 1790 and *Pterostichus rhaeticus* Heer, 1837 (0%; BIN: AAM9738). In total, unique BINs were revealed for 44 species (86%), two BINs for two species (4%), three BINs for one species (2%) and one BIN for two species for two species pairs (8%). Due to the fact that the numbers of unspecified nucleotides ("Ns") exceeds more than 1% of their total length, a distinct cluster of two sequences for *Pterostichus panzeri* (Panzer, 1803) received no BIN. The NJ analyses based on K2P distances revealed non-overlapping clusters with bootstrap support values > 95% for 40 species (78%) with more than one analyzed specimen (Fig. 2). A more detailed topology of all analyzed specimens is presented in the supporting information (Suppl. material 2).

Our statistical maximum parsimony analysis showed multiple sharing of haplotypes for *Pterostichus nigrita* (n = 29)/*Pterostichus rhaeticus* (n = 11) and *Pterostichus adstrictus* (n = 5)/*Pterostichus oblongopunctatus* (n = 26) (Fig. 3). For *Pterostichus nigrita* and *Pterostichus rhaeticus* a number of 13 different haplotypes was found (Fig. 3A) One dominant haplotype (h1) was shared by 22 specimens of *Pterostichus nigrita* and three specimens of *Pterostichus rhaeticus* (Fig. 3A). Most other haplotypes, however, were revealed only for one specimen (singletons; *Pterostichus nigrita*: h5-h13, *Pterostichus rhaeticus*: h4) and located at the tips of the network, separated from haplotype h1 or other core haplotypes (h2, h3, h10) by up to nine additional mutational steps. In case of *Pterostichus adstrictus* and *Pterostichus oblongopunctatus*, the analysis identified six haplotypes (Fig. 3B). The dominant haplotype h1 was

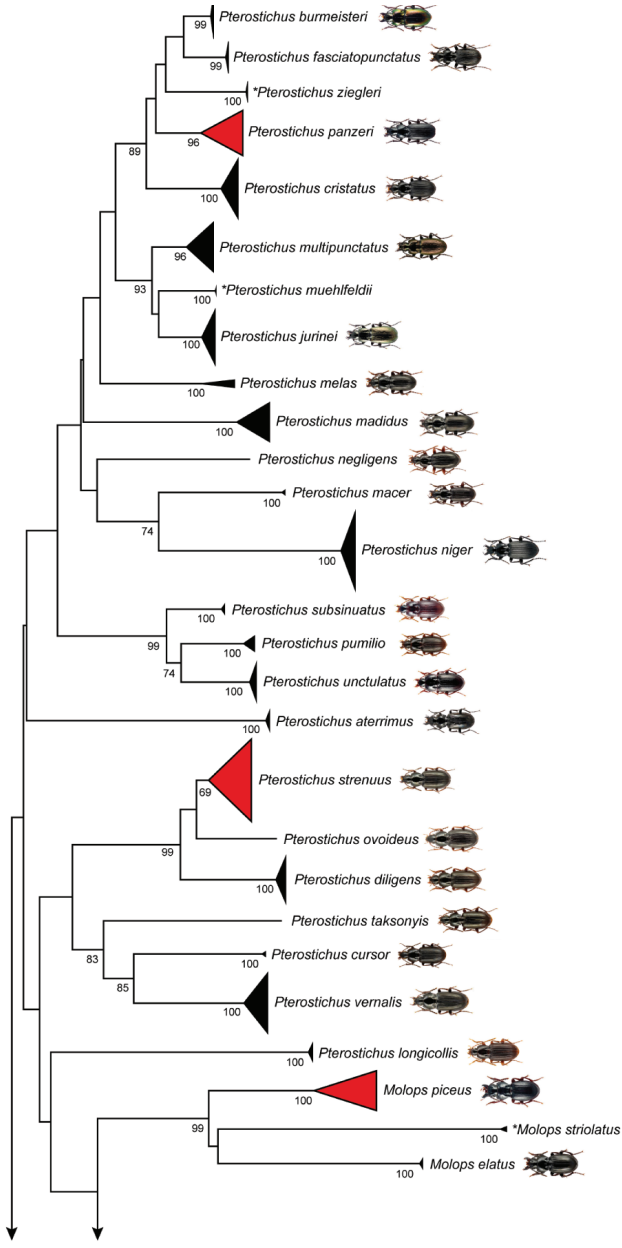

Figure 2. Neighbor-joining (NJ) topology of the analyzed ground beetle species based on Kimura 2-parameter distances. Triangles show the relative number of individual's sampled (height) and sequence divergence (width). Red triangles indicate species with intraspecific maximum pairwise distances > 2.2%, blue triangles species pairs with interspecific distances < 2.2%. Numbers next to nodes represent non-parametric bootstrap values > 90% (1,000 replicates). Images are provided for species recorded in Germany whereas asterisks indicate species not recorded in Germany. All beetle images were obtained from www.eurocarabidae.de except of *Poecilus sericeus* (photographer: Katja Neven, Lars Hendrich).

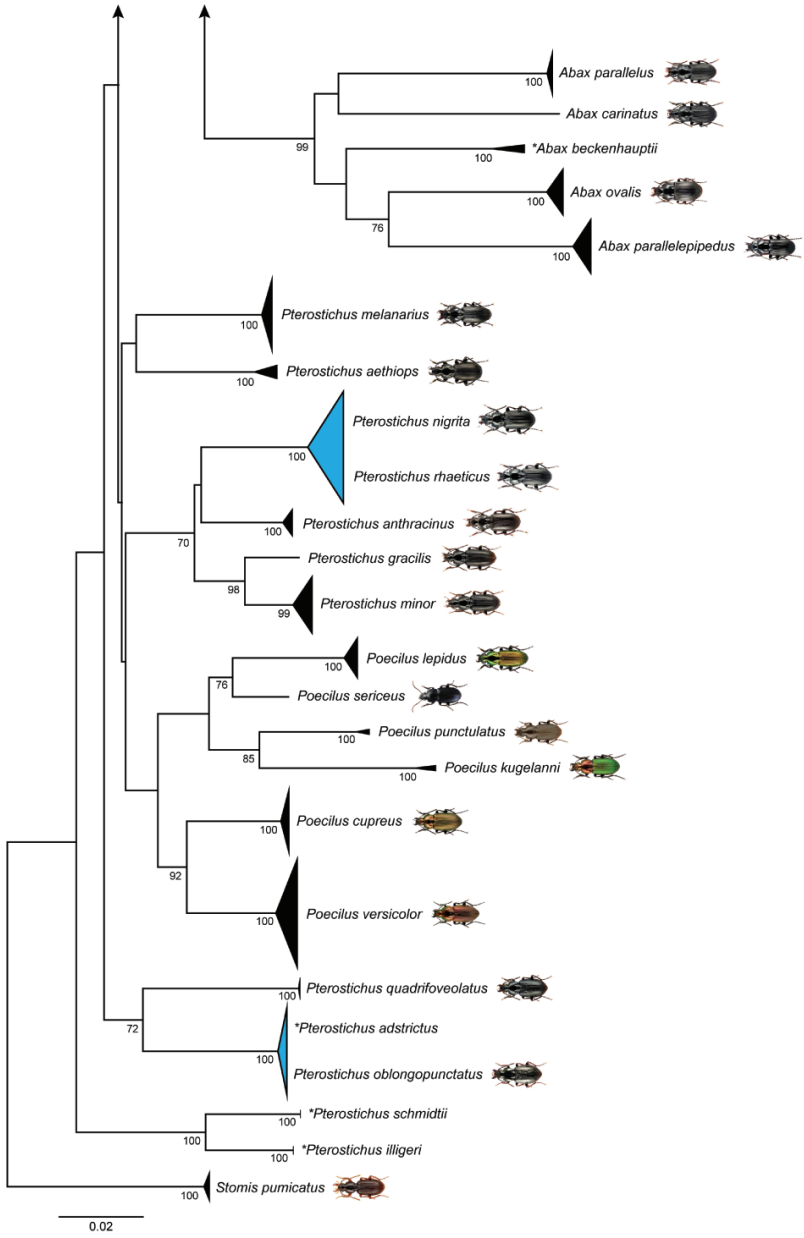

Figure 2. Continued.

shared by four specimens of *Pterostichus adstrictus* and 21 specimens of *Pterostichus oblongopunctatus*, representing the 81% of the analyzed specimens. All others were connected to this haplotype by a maximum of four mutational steps in a star-like pattern, generating a compact network.

Discussion

As a result of preservative, passionate and intensive work in the past centuries, carabid beetles have become one of the most prominent model groups of insects for biodiversity studies (Kotze et al. 2011). Generations of carabidologists clarified most aspects of their taxonomy and phylogeny, geographic distribution, habitat associations and ecological requirements, life history strategies and adaptations, in particular for those species found in Central Europe (Kotze et al. 2011). Due to the habitat specificity of various species, ground beetles are routinely used as biological indicators to assess land use changes among different ecosystems (Lövei and Sunderland 1996; Rainio and Niemelä 2003; Pearce and Venier 2004; Koivula 2011; Kotze et al. 2011).

The present study highlights the use of DNA barcodes for the identification of species of the five genera of Pterostichini found in Germany. Unique BINs were revealed for 44 species (86%) of the analyzed 51 taxa. This result coincides with high rates of successful species identification of previous barcoding studies in terms of carabid beetles (Raupach et al. 2010; Raupach et al. 2011; Pentinsaari et al. 2014; Hendrich et al. 2015; Raupach et al. 2018). Nevertheless, the data revealed some species pairs with low interspecific distances (< 2.2%) and shared haplotypes but also three species with intraspecific distances > 2.2%.

Species with low interspecific variability

Interspecific distances with values below 2.2% were found for four ground beetle species pairs. Whereas *Pterostichus burmeisteri* Heer, 1838 and *Pterostichus fasciatopunctatus* (Creutzer, 1799) as well as *Pterostichus ovoideus* (Sturm, 1824) and *Pterostichus strenuus* (Panzer 1796) were characterized by distinct lineages, haplotype sharing was revealed for two species pairs that will be discussed more in detail in the following.

The species complex *Pterostichus nigrita* Paykull, 1790/*Pterostichus rhaeticus* Heer, 1837

Pterostichus rhaeticus and *Pterostichus nigrita* of the subgenus *Pseudomaseus* Chaudoir, 1838 are commonly considered as closely related but distinct, sibling species (Koch and Thiele 1980; Koch 1984; Müller-Motzfeld and Hartmann 1985; Koch 1986; Angus et al. 2000). Both species have a Palearctic distribution and are found in Northern and Central Europe (e.g., Hůrka 1996; Marggi 2006; Trautner et al. 2014; Muilwijk et al. 2015), but have been also recorded on the Balkan recently (Brigić et al. 2014). They differ only in a few, subtle morphological features (Koch 1984, 1986; Angus et al. 2000, 2008; Brigić et al. 2014): Specimens of *Pterostichus rhaeticus* are typically smaller and narrower than those of *Pterostichus nigrita*, but in mixed populations, the differences in body size, length and width of the elytra were not observed and the overlap in sizes is considerable (Brigić et al. 2014). Furthermore, male specimens can be differen-

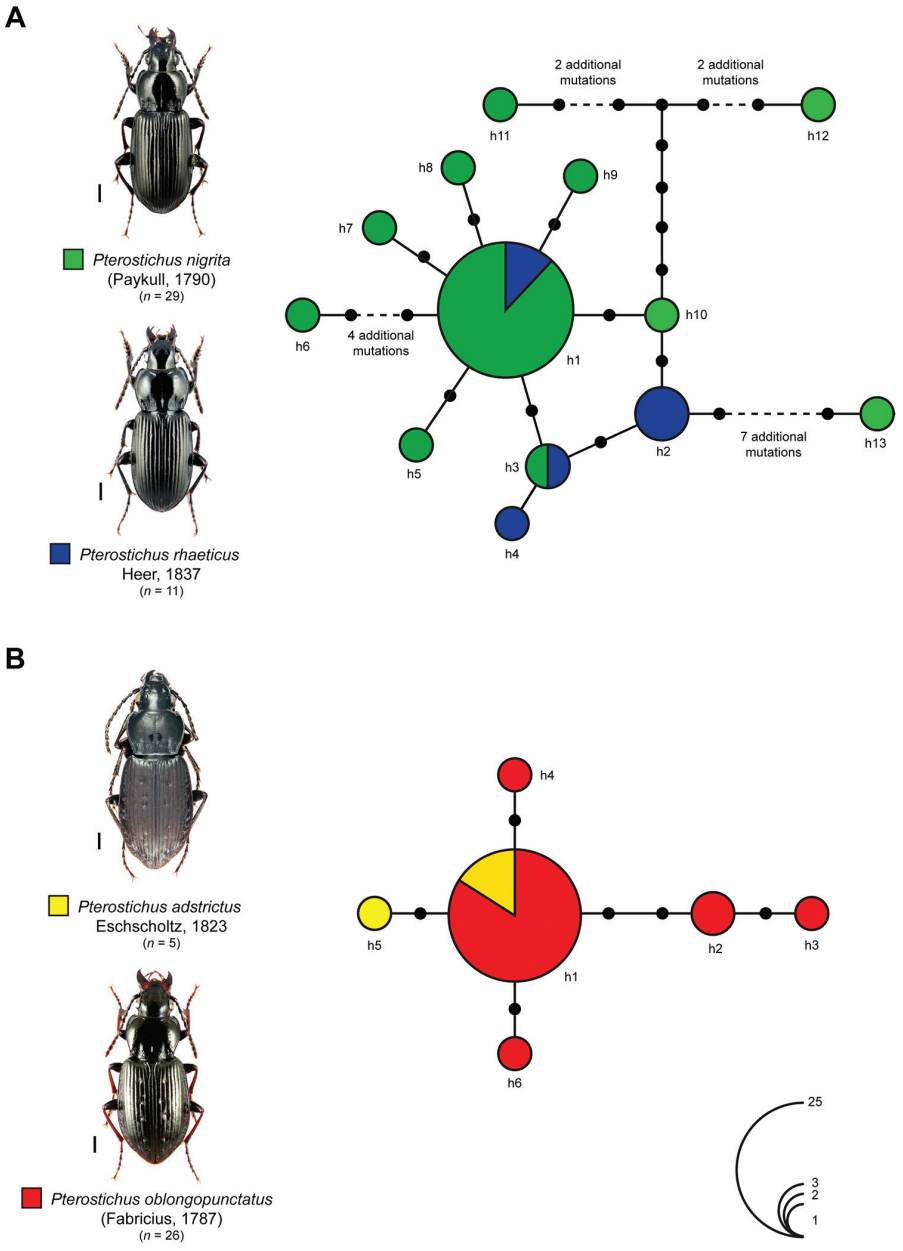

Figure 3. Maximum statistical parsimony networks of the sibling species pairs **A** *Pterostichus nigrita* Paykull, 1790 (green) and *Pterostichus rhaeticus* Heer, 1837 (blue) and **B** *Pterostichus adstrictus* Eschscholtz, 1823 (yellow) and *Pterostichus oblongopunctatus* (Fabricius, 1787) (red). Used parameters included default settings for connection steps, gaps were treated as fifth state. Each line represents a single mutational change whereas small black dots indicate missing haplotypes. The numbers of analyzed specimens (*n*) are listed, whereas the diameter of the circles is proportional to the number of haplotypes sampled (see given open circles with numbers). Scale bars 1 mm. Beetle images were obtained from www.eurocarabidae.de except *Pterostichus adstrictus* (photographer: Ditta Balke).

tiated by the shape of the right paramere, which is larger for *Pterostichus nigrita* and is also characterized by a shallow incision (e.g., Hůrka 1996; Marggi 2006). In contrast to this, a deeper incision is found at the right paramere of *Pterostichus rhaeticus*. Nevertheless, considerable variations and intermediate forms have been documented in mixed populations of some regions and may limit the use of this character (e.g., Luff 1990; Angus et al. 2000; Brigić et al. 2014; Kendall 2017). In the case of females, both species can be distinguished by the form of the coxostylus and the shape of sclerotized part of the 8th abdominal sternite (e.g., Koch 1986; Hůrka 1996; Angus et al. 2000). A previous study already showed that both species cannot be differentiated by the means of DNA barcodes based on shared haplotypes (Raupach et al. 2010). This result is supported by the analysis of additional data as part of this study (Fig. 3A). Various alternative hypothesis can explain these results. First, both species are distinct and do not hybridize, but lineage sorting has not been completed for the mitochondrial genome so far. Second, both species are not undergoing hybridization, but a relatively recent introgression event of the mitochondrial genome across the species boundary without concordant introgression of the nuclear genome took place. Third, extensive hybridization between both taxa is given, and these two forms might or might not be considered as different species. As consequence, additional fine scale ecological, morphological, morphometric as well as molecular data, in particular from the nuclear genome, have to be analyzed carefully to answer these questions in detail, with a focus on mixed populations from different localities.

The species complex *Pterostichus* adstrictus Eschscholtz, 1823/*Pterostichus oblongopunctatus* (Fabricius, 1787)

All DNA barcodes data of *Pterostichus adstrictus* (n = 5) and some sequences of *Pterostichus oblongopunctatus* (n = 3) were part of a previous study but not discussed in detail (Pentinsaari et al. 2014). Both species belong to the subgenus *Bothriopterus* Chaudoir, 1835 and are considered as closely related but distinct species (Lindroth 1986; Persohn 1996; Luff 2007). Whereas *Pterostichus adstrictus* is an inhabitant of the Northern coniferous regions (e.g., of Sweden, Norway, North America, or North Britain), *Pterostichus oblongopunctatus* represents a common and widely distributed Euro-Siberian species that is typically found in eurytopic woodlands (Lindroth 1986). Both species are morphological highly similar and their ranges overlap broadly in Scandinavia, but specimens of *Pterostichus adstrictus* can be differentiated from those of *Pterostichus oblongopunctatus* by unicolored, usually black legs, and the wider pronotal side border (Lindroth 1986; Persohn 1996; Luff 2007). The already hypothesized close relationship of both species is supported by haplotype sharing of DNA barcodes (see h1) (Fig. 3B). Similar to the previously discussed species pair it is unclear if both species represent closely but distinct and "valid" species or hybridization events – which have not been documented so far – still take place.

Species with high intraspecific variability

Intraspecific pairwise distances with values > 2.2% were found for three species. Whereas *Pterostichus strenuus* (Panzer, 1796) showed no conspicuous substructure for the analyzed COI sequences (see Suppl. material 2), three clearly distinct monophyletic cluster/lineages were revealed within *Pterostichus panzeri* (Panzer, 1803) (Fig. 4, Table 1) and *Molops piceus* (Panzer, 1793) (Fig. 5, Table 1), respectively, and will be discussed more in detail.

Ménage à trois: three distinct clusters within *Pterostichus panzeri* (Panzer, 1803)

The carabid *Pterostichus panzeri* is a subalpine/alpine brachypterous species associated with chalk and distributed in the Central European mountain regions (e.g., Horion 1941; Holdhaus 1954; Müller-Kroehling 2013; Trautner and Rietze 2017). Interestingly, all three clusters correlate with different geographic localities: cluster A included all specimens (n = 8) from Garmisch-Partenkirchen (Germany) (BIN: ACC4332), cluster B contained only specimens from Bihor Mountains (Romania, n = 2, no BIN), and cluster C included beetles sampled in Austria (Totes Gebirge, n = 7, BIN: ACD0986) (Fig. 4). K2P distances between all clusters ranged from 1.4 to 2.3% (Table 1). Due to the fact that *Pterostichus panzeri* is associated to a specific habitat, it is likely that the observed genetic variability represents a result of phylogeographic effects. As a consequence of recurrent glaciation events, populations could have become isolated and gene flow disrupted, resulting in specific local haplotypes. Similar results have been found for other ground beetle species in the past (e.g., Zhang et al. 2006; Homburg et al. 2013; Faille et al. 2015). The existence of cryptic species, however, cannot be fully excluded, but no morphological variations between different populations have been reported so far. Furthermore, it should be also noted that the loss of the ability to fly can lead to a relaxed purifying selection on genes that are involved in the oxygen metabolism including COI, leading to accelerated rates of divergence in the barcode region within insects (Mitterboeck and Adamowicz 2013). The molecular analysis of additional specimens from other regions, as well as linkage groups in the nuclear genome, combined with thoroughly morphological studies will help to interpret the given results more in detail.

Molops piceus austriacus Ganglbauer, 1889: not a subspecies but "real" species?

For *Molops piceus*, an oligophagous, brachypterous species that is found in forests, two subspecies are known*: Molops piceus piceus* Panzer 1793 and *Molops piceus austriacus* Ganglbauer, 1889. Whereas most analyzed beetles were specimens of the subspecies *Molops piceus piceus* (n = 14), only one specimen of *Molops piceus aus-*

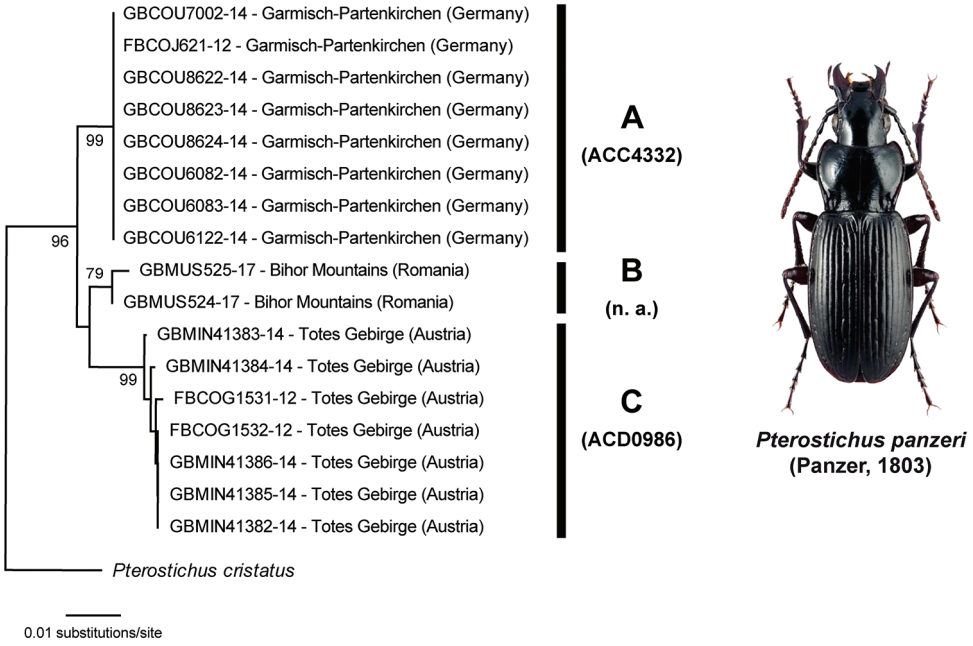

Figure 4. Subtree of the Neighbor-joining topology based on Kimura 2-parameter distances of all analyzed specimens of *Pterostichus panzeri* (Panzer, 1805) and nearest neighbor. Branches with specimen ID-number from BOLD, species names and sample localities. Numbers next to internal nodes are non-parametric bootstrap values (in %). Cluster (A-C) with BINs (if available) based on the barcode analysis from 11-05-2020. Beetle image was obtained from www.eurocarabidae.de.

Table 1. Intraspecific Kimura 2-distances for all distinct clusters of *Pterostichus panzeri* (Panzer, 1805).

	Cluster A (Germany) BIN: ACC4332	Cluster B (Romania) BIN: n. a.	Cluster C (Austria) BIN: ACD0986
Cluster A (Germany) BIN: ACC4332	0		
Cluster B (Romania) BIN: n. a.	0.014	0	
Cluster C (Austria) BIN: ACD0986	0.019 – 0.023	0.018 – 0.02	0 – 0.005

triacus was studied. Nevertheless, this beetle was clearly separated from all other specimens with high K2P distance values (BIN: ADO8343) (Fig. 5, Table 2). In the past, *Molops piceus austriacus* has been already considered as species (Marcuzzi 1956), but only the analysis of additional specimens, additional molecular markers (e.g., hypervariable elements of the nuclear rRNA genes (Raupach et al. 2010)) and careful morphological studies will help to clarify this taxonomic problem. Furthermore, all beetles of *Molops piceus piceus* from Germany (n = 12) (BIN: ADO0860) were separated from one animal collected in Carinthia (Austria) (BIN: ADO8319), highlighting the necessity of additional comprehensive morphological and molecular analysis for this species.

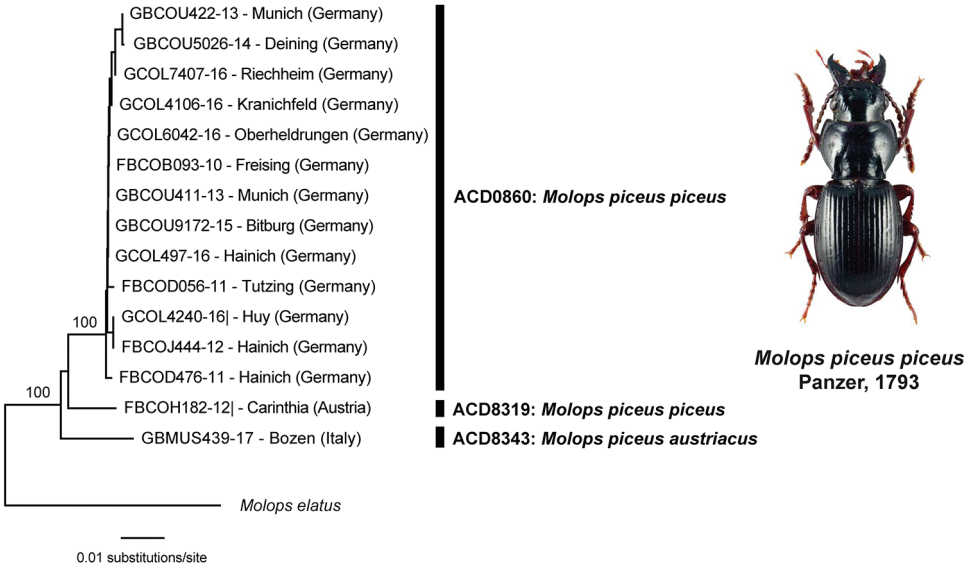

Figure 5. Subtree of the Neighbor-joining topology based on Kimura 2-parameter distances of all analyzed specimens of *Molops piceus* (Panzer, 1793) and nearest neighbor. Branches with specimen ID-number from BOLD, species names and sample localities. Numbers next to internal nodes are non-parametric bootstrap values (in %). Cluster (A-C) with BINs based on the barcode analysis from 11-05-2020. Beetle image was obtained from www.eurocarabidae.de.

Table 2. Intraspecific Kimura 2-distances for all distinct clusters of *Molops piceus* (Panzer, 1793).

	M. piceus piceus **(Germany) BIN: ADO0860**	***M. piceus piceus*** **(Austria) BIN: ADO8319**	***M. piceus austriacus*** **(Italy) BIN: ADO8343**
M. piceus piceus **(Germany) BIN: ADO0860**	0–0.003		
M. piceus piceus **(Austria) BIN: ADO8319**	0.019–0.028	0	
M. piceus austriacus **(Italy) BIN: ADO8343**	0.029–0.032	0.028	0

Conclusions

The build-up of comprehensive DNA barcode libraries represents a pivotal task for modern molecular biodiversity research and species surveys (e.g., Brandon-Mong et al. 2015, Curry et al. 2018). This is especially true for the hyperdiverse and numerous species of insects. Within the beetles, carabids are highly valuable bioindicators that are used routinely to characterize disturbances in various habitats such as forests, meadows, river banks, or fens for a long time. Our DNA barcode library clearly encourages the application of DNA barcodes as effective method for the molecular identification of species of *Pterostichus* and allied taxa even if a few species pairs cannot be resolved. The given data, however, also revealed distinct lineages that correlate with high distances within a few species, indicating significant phylogeographic patterns and/or even the possible existence of overlooked cryptic species.

Acknowledgments

We would like to thank Christina Blume, Claudia Etzbauer (both ZFMK, Bonn) and Jana Deppermann (DZMB, Wilhelmshaven) for their laboratory assistance. Furthermore, we are grateful to Frank Köhler (Bonn), Karl-Hinrich Kielhorn (Berlin), and Wolfgang Lorenz (Tutzing) for providing various specimens, and to Ortwin Bleich for giving permission to use his excellent photographs of ground beetles taken from www.eurocarabidae.de. We also thank David Maddison and one anonymous reviewer for their helpful comments. This publication was partially financed by German Federal Ministry for Education and Research (FKZ01LI1101A, FKZ01LI1101B, FKZ03F0664A), the Land Niedersachsen and the German Science Foundation (INST427/1-1), as well as by grants from the Bavarian State Government (Barcoding Fauna Bavarica) and the German Federal Ministry of Education and Research (GBOL1, GBOL2, GBOL3: 01LI1901B). We are grateful to the team of Paul Hebert in Guelph (Ontario, Canada) for their great support and help and in particularly to Sujeevan Ratnasingham for developing the BOLD database infrastructure and the BIN management tools. Sequencing work was partly supported by funding from the Government of Canada to Genome Canada through the Ontario Genomics Institute, whereas the Ontario Ministry of Research and Innovation and NSERC supported development of the BOLD informatics platform.

References

Allema AB, Rossing WAH, van der Werf W, Heusinkveld BG, Bukovinszky T, Steingröver E, van Lenteren JC (2012) Effect of light quality on movement of *Pterostichus melanarius* (Coleoptera: Carabidae). Journal of Applied Entomology 136: 793–800. https://doi.org/10.1111/j.1439-0418.2012.01728.x

Angus RB, Brown RE, Bryant LJ (2000) Chromosomes and identification of the sibling species *Pterostichus nigrita* (Paykull) and *P. rhaeticus* Heer (Coleoptera: Carabidae). Systematic Entomology 25: 325–337. https://doi.org/10.1046/j.1365-3113.2000.00108.x

Angus RB, Galián J, Wrase DW, Chaladze G (2008) The western Palaearctic species of the *Pterostichus nigrita* (Paykull) complex, with the description of a new species from Spain and a new subspecies of *P. nigrita* from Anatolia (Coleoptera, Carabidae). Nouvelle Revue d`Entomologie 25: 297–316.

Arnett RH, Thomas MC (2000) American Beetles, Volume 1: Archostemata, Myxophaga, Adephaga, Polyphaga: Staphyliniformia CRC Press, Boca Raton, 464 pp. https://doi.org/10.1201/9781482274325

Astrin JJ, Höfer H, Spelda J, Holstein J, Bayer S, Hendrich L, Huber BA, Kielhorn K-H, Krammer H-J, Lemke M, Monje JC, Morinière J, Rulik B, Petersen M, Janssen H, Muster C (2016) Towards a DNA barcode reference database for spiders and harvestmen of Germany. PLOS One 11: e0162624. https://doi.org/10.1371/journal.pone.0162624

Baranová B, Fazekašová D, Manko P, Jászay T (2018) Variations in Carabidae assemblages across the farmland habitats in relation to selected environmental variables including soil

properties. Journal of Central European Agriculture 19: 1–23. https://doi.org/10.5513/JCEA01/19.1.202

Barco A, Raupach MJ, Laakmann S, Neumann H, Knebelsberger T (2016) Identification of North Sea molluscs with DNA barcoding. Molecular Ecology Resources 16: 288–297. https://doi.org/10.1111/1755-0998.12440

Brigić A, Vujčić-Karlo S, Alegro A, Šegota V, Ternjej I (2014) Ecology, biology and conservation of *Pterostichus rhaeticus* Heer, 1837 (Coleoptera: Carabidae) at the edge of its distribution range, in the Western Balkans. Italian Journal of Zoology 81: 517–529. https://doi.org/10.1080/11250003.2014.947338

Brandon-Mong GJ, Gan HM, Sing KW, Lee PS, Lim PE, Wilson JJ (2015) DNA metabarcoding of insects and allies: an evaluation of primers and pipelines. Bulletin of Entomological Research 105: 717–727. https://doi.org/0.1017/S0007485315000681

Casiraghi M, Labra M, Ferri E, Galimberti A, De Mattia F (2010) DNA barcoding: a six-question tour to improve users` awareness about the method. Briefings in Bioinformatics 11: 440–453. https://doi.org/10.1093/bib/bbq003

Clement M, Posada D, Crandall KA (2000) TCS: a computer program to estimate gene genealogies. Molecular Ecology 9: 1657–1660. https://doi.org/10.1046/j.1365-294x.2000.01020.x

Curry CJ, Gibson JF, Shokralla S, Hajibabaei M, Baird DJ (2018) Identifying North American freshwater invertebrates using DNA barcodes: are existing COI sequence libraries fit for purpose? Freshwater Science 37: 178–189. https://doi.org/10.1086/696613

deWaard JR, Ivanova NV, Hajibabaei M, Hebert PDN (2008) Assembling DNA barcodes: analytical protocols. In: Martin C (Ed.) Methods in Molecular Biology: Environmental Genetics. Humana Press, Totowa, 275–293. https://doi.org/10.1007/978-1-59745-548-0_15

Dinis AM, Pereira JA, Benhadi-Marin J, Santos SAP (2016) Feeding preferences and functional responses of *Calathus granatensis* and *Pterostichus globosus* (Coleoptera: Carabidae) on pupae of *Bactrocera olea* (Diptera: Tephritidae). Bulletin of Entomological Research 106: 701–709. https://doi.org/10.1017/S0007485316000213

Edgar RC (2004) MUSCLE: a multiple sequence alignment method with reduced time and space complexity. BMC Bioinformatics 5: 113. https://doi.org/10.1186/1471-2105-5-113

Faille A, Tänzler R, Toussaint EFA (2015) On the way to speciation: shedding light on the Karstic phylogeography of the microendemic cave beetle *Aphaenops cerberus* in the Pyrenees. Journal of Heredity 106: 692–699. https://doi.org/10.1093/jhered/esv078

Felsenstein J (1985) Confidence limits on phylogenies: an approach using the bootstrap. Evolution 39: 783–791. https://doi.org/10.2307/2408678

Folmer O, Black M, Hoeh W, Lutz R, Vrijenhoek R (1994) DNA primers for amplification of mitochondrial cytochrome c oxidase subunit I from diverse metazoan invertebrates. Molecular Marine Biology and Biotechnology 3: 294–299.

Fournier E, Loreau M (2001) Activity and satiation state in *Pterostichus melanarius*: an experiment in different agricultural habitats. Ecological Entomology 26: 235–244. https://doi.org/10.1046/j.1365-2311.2001.00314.x

Gebhardt K, Knebelsberger T (2015) Identification of cephalopod species from the North and Baltic Seas using morphology, COI and 18S rDNA sequences. Helgoland Marine Research 69: 259–271. https://doi.org/10.1007/s10152-015-0434-7

Hausmann A, Haszprunar G, Hebert PDN (2011) DNA barcoding the geometrid fauna of Bavaria (Lepidoptera): successes, surprises, and questions. PLOS One 6: e17134. https://doi.org/10.1371/journal.pone.0017134

Havemann N, Gossner MM, Hendrich L, Morinière J, Niedringhaus R, Schäfer P, Raupach MJ (2018) From water striders to water bugs: The molecular diversity of aquatic Heteroptera (Gerromorpha, Nepomorpha) of Germany based on DNA barcodes. PeerJ 6: e4577. https://doi.org/10.7717/peerj.4577

Hawlitschek O, Morinière J, Dunz A, Franzen M, Rödder D, Glaw F, Haszprunar G (2016) Comprehensive DNA barcoding of the herpetofauna of Germany. Molecular Ecology Resources 16: 242–253. https://doi.org/10.1111/1755-0998.12416

Hawlitschek O, Morinière J, Lehmann GUC, Lehmann AW, Kropf M, Dunz A, Glaw F, Detchaeron M, Schmidt S, Hausmann A, Szucsich NU, Caetano-Wyler SA, Haszprunar G (2017) DNA barcoding of crickets, katydids and grasshoppers (Orthoptera) from Central Europe with focus on Austria, Germany and Switzerland. Molecular Ecology Resources 17: 1037–1053. https://doi.org/10.1111/1755-0998.12638

Hebert PDN, Cywinska A, Ball SL, deWaard JR (2003a) Biological identifications through DNA barcodes. Proceedings of the Royal Society of London Series B: Biological Sciences 270: 313–321. https://doi.org/10.1098/rspb.2002.2218

Hebert PDN, Ratnasingham S, deWaard JR (2003b) Barcoding animal life: cytochrome *c* oxidase subunit 1 divergences among closely related species. Proceedings of the Royal Society of London Series B: Biological Sciences 270: S96–S99. https://doi.org/10.1098/rsbl.2003.0025

Hendrich L, Morinière J, Haszprunar G, Hebert PDN, Hausmann A, Köhler F, Balke M (2015) A comprehensive DNA barcode database for Central European beetles with a focus on Germany: Adding more than 3,500 identified species to BOLD. Molecular Ecology Resources 15: 795–818. https://doi.org/10.1111/1755-0998.12354

Holdhaus K (1954) Die Spuren der Eiszeit in der Tierwelt Europas. Abhandlungen der Zoologisch-Botanischen Gesellschaft in Wien 28: 1–606. [In German]

Homburg K, Drees C, Gossner MM, Rakosy L, Vrezec A, Assmann T (2013) Multiple glacial refugia of the low-dispersal ground beetle *Carabus irregularis*: molecular data support predictions of species distribution models. PLOS One 8: e61185. https://doi.org/10.1371/journal.pone.0061185

Hong EJ, Kim Y, Jeong J-C, Kang S-H, Jung J-K, Suk S-W (2017) Community structure and distribution of ground beetles (Coleoptera: Carabidae) in Sobaeksan National Park, Korea. Journal of Ecology and Environment 41: 17 https://doi.org/10.1186/s41610-017-0036-1

Horion A (1941) Faunistik der Deutschen Käfer, Band 1, Adephaga. Goecke, Krefeld, 463 pp. [In German]

Hůrka K (1996) Carabidae of the Czech and Slovak Republics. Kabouek, Zlín, 565 pp.

Igondová E, Majzlan O (2015) Assemblages of ground beetles (Carabidae, Coleoptera) in peatland habitat, surrounding dry pine forests and meadows. Folia Oecologica 42: 21–28.

Ivanova NV, deWaard JR, Hebert PDN (2006) An inexpensive, automation-friendly protocol for recovering high-quality DNA. Molecular Ecology Notes 6: 998–1002. https://doi.org/10.1111/j.1471-8286.2006.01428.x

Jordal BH, Kambestand M (2014) DNA barcoding of bark and ambrosia beetles reveals excessive NUMTs and consistent east-west divergence across Palearctic forests. Molecular Ecology Resources 14: 7–17. https://doi.org/10.1111/1755-0998.12150

Kajtoch Ł, Kolasa M, Kubisz D, Gutowski JM, Ścibior R, Mazur MA, Holecová (2019) Using host species traits to understand the *Wolbachia* infection distribution across terrestrial beetles. Scientific Reports 9: 847. https://doi.org/10.1038/s41598-018-38155-5

Kendall P (2017) The problem of two closely related ground beetles (Coleoptera: Carabidae) from Thorne Moors: Habitats and Separation of *Pterostichus nigrita* (Payk.) and *P. rhaeticus* Heer. Thorne & Hatfield Moor Papers 10: 110–117.

Kimura M (1980) A simple method for estimating evolutionary rates of base substitutions through comparative studies of nucleotide sequences. Journal of Molecular Evolution 16: 111–120. https://doi.org/10.1007/BF01731581

Klopfstein S, Kropf C, Baur H (2016) *Wolbachia* endosymbionts distort DNA barcoding in the parasitoid wasp genus *Diplazon* (Hymenoptera: Ichneumonidae). Zoological Journal of the Linnean Society 177: 541–557. https://doi.org/10.1111/zoj.12380

Knebelsberger T, Landi M, Neumann H, Kloppmann M, Sell A, Campbell P, Laakmann S, Raupach MJ, Carvalho G, Costa FO (2014) A reliable DNA barcode reference library for the identification of the European shelf fish fauna. Molecular Ecology Resources 14: 1060–1071. https://doi.org/10.1111/1755-0998.12238

Knebelsberger T, Dunz AR, Neumann D, Geiger MF (2015) Molecular diversity of Germany`s freshwater fishes and lampreys assessed by DNA barcoding. Molecular Ecology Resources 15: 562–572. https://doi.org/10.1111/1755-0998.12322

Koch D (1984) *Pterostichus nigrita*, ein Komplex von Zwillingsarten. Entomologische Blätter 79: 141–151. [In German]

Koch D (1986) Morphological-physiological studies on "*Pterostichus nigrita*" (Col., Carab.), a complex of sibling species. In: den Boer PJ, Luff ML, Mossakowski D, Weber F (Eds) Carabid beetles, their evolution, natural history and classification. Gustav Fischer, Stuttgart/New York, 267–279.

Koch D, Thiele HU (1980) Zur ökologisch-physiologischen Differenzierung und Speziation der Laufkäfer-Art *Pterostichus nigrita* (Coleoptera: Carabidae). Entomologia Generalis 6: 135–150. [In German]

Koivula MJ (2011) Useful model organisms, indicators, or both? Ground beetles (Coleoptera, Carabidae) reflecting environmental conditions. ZooKeys 100: 287–317. https://doi.org/10.3897/zookeys.100.1533

Kolasa M, Kubisz D, Mazur MA, Ścibior R, Kajtoch Ł (2018) *Wolbachia* prevalence and diversity in selected riverine predatory beetles (Bembidiini and Paederini). Bulletin of Insectology 71: 193–200.

Kotze DJ, Brandmayr P, Casale A, Dauffy-Richard E, Dekoninck W, Koivula MJ, Lövei GL, Mossakowski D, Noordijk J, Paarmann W, Pizzolotto R, Saska P, Schwerk A, Serrano J, Szyszko J, Taboada A, Turin H, Venn S, Vermeulen R, Zetto T (2011) Forty years of carabid beetle research in Europe – from taxonomy, biology, ecology and population studies to bioindication, habitat assessment and conservation. In: Kotze DJ, Assmann T, Noordijk J, Turin

H, Vermeulen R (Eds) Carabid Beetles as Bioindicators: Biogeographical, Ecological and Environmental Studies. ZooKeys 100: 55–148. https://doi.org/10.3897/zookeys.100.1523

Kumar S, Stecher G, Li M, Knyaz C, Tamura K (2018) MEGA X: Molecular Evolutionary Genetics Analysis across computing platforms. Molecular Biology and Evolution 35: 1547–1549. https://doi.org/10.1093/molbev/msy096

Laakmann S, Boos K, Knebelsberger T, Raupach MJ, Neumann H (2017) Species identification of echinoderms from the North Sea by combining morphology and molecular data. Helgoland Marine Research 70: 18. https://doi.org/10.1186/s10152-016-0468-5

Lagisz M, Wolff K, Sanderson RA, Laskowski R (2010) Genetic population structure of the ground beetle, *Pterostichus oblongopunctatus*, inhabiting a fragmented and polluted landscape: Evidence for sex-biased dispersal. Journal of Insect Science 10: 105. https://doi.org/10.1673/031.010.10501

Langhan AM, Pilkington G, Wheater CP (2001) Feeding preferences of a predatory beetle (*Pterostichus madidus*) for slugs exposed to lethal and sub-lethal dosages of metaldehyde. Entomologia Experimentalis et Applicata 98: 245–248. https://doi.org/10.1046/j.1570-7458.2001.00780.x

Leigh JW, Bryant D (2015) POPART: Full-feature software for haplotype network construction. Methods in Ecology and Evolution 6: 1110–1116. https://doi.org/10.1111/2041-210X.12410

Lindroth CH (1986) The Carabidae (Coleoptera) of Fennoscandia and Denmark. Fauna Entomologica Scandinavica 15: 232–497.

Lövei GL, Sunderland KD (1996) Ecology and behavior of ground beetles (Coleoptera: Carabidae). Annual Review in Entomology 41: 231–256. https://doi.org/10.1146/annurev.en.41.010196.001311

Luff ML (1990) *Pterostichus rhaeticus* Heer (Col., Carabidae), a British species previously confused with *P. nigrita* (Paykull). Entomologist`s Monthly Magazine 126: 245–249.

Luff ML (2007) The Carabidae (ground beetles) of Britain and Ireland (2nd edition). Handbooks for the Identification of British Insects Vol. 4 Part 2. Field Studies Council, Shrewsbury, 247 pp.

Marcuzzi G (1956) Fauna delle Dolomiti. Memorie Classe die Scienza Mathematche e Naturali 31: 1–595. [In Italian]

Marggi W (2006) Bd. 2, Adephaga 1: Carabidae (Laufkäfer). In: Freude H, Harde KW, Lohse GA, Klausnitzer B (Eds) Die Käfer Mitteleuropas. Spektrum-Verlag, Heidelberg/Berlin, 521 pp. [In German]

Mitterboeck TF, Adamowicz SJ (2013) Flight loss linked to faster molecular evolution in insects. Proceedings of the Royal Society of London Series B – Biological Sciences 280: 20131128. https://dx.doi.org/1098/rspb.2013.1128

Morinière J, Hendrich L, Hausmann A, Hebert PDN, Haszprunar G, Gruppe A (2014) Barcoding Fauna Bavarica: 78% of the Neuropteroida fauna barcoded! PLOS One 9: e109719. https://doi.org/10.1371/journal.pone.0109719

Morinière J, Hendrich L, Balke M, Beermann AJ, König T, Hess M, Koch S, Müller R, Leese F, Hebert PDN, Hausmann A, Schubart CD, Haszprunar G (2017) A DNA barcode library for Germany`s mayflies, stoneflies and caddisflies (Ephemeroptera, Plecoptera and Tri-

choptera). Molecular Ecology Resources 17: 1293–1307. https://doi.org/10.1111/1755-0998.12683

Muilwijk J, Felix R, Dekoninck W, Bleich O (2015) De loopkevers van Nederland and België (Carabidae). Entomologische Tabellen 9: 1–215. [In Dutch]

Mutanen M, Kivelä SM, Vos RA, Doorenweerd C, Ratnasingham S, Hausmann A, Huemer P, Dincâ V, van Nieukerken EJ, Lopez-Vaamonde C, Vila R, Aarvik L, Decaëns T, Efetov KA, Hebert PDN, Johnsen A, Karsholt O, Pentinsaari M, Rougerie R, Segerer A, Tarmann G, Zahiri R Godfray HCJ (2016) Species-level para- and polyphyly in DNA barcode gene trees: Strong operational bias European Lepidoptera. Systematic Biology 65: 1024–1040. https://doi.org/10.1093/sysbio/syw044

Müller-Kröhling S (2013) Prioritäten für den Wald-Naturschutz – Die Schutzverantwortung Bayerns für die Artenvielfalt in Wäldern, am Beispiel der Laufkäfer (Coleoptera: Carabidae). Waldökologie, Landschaftsforschung und Naturschutz 13: 57–72. [In German]

Müller-Motzfeld G, Hartmann M (1985) Zur Trennung von *Pterostichus rhaeticus* HEER und *P. nigrita* PAYK. (Col., Carabidae). Entomologische Nachrichten und Berichte 29: 13–17. [In German]

Pearce JL, Venier LA (2004) The use of ground beetles (Coleoptera: Carabidae) and spiders (Araneae) as bioindicators of sustainable forest management. A review. Ecological Indicators 6: 780–793. https://doi.org/10.1016/j.ecolind.2005.03.005

Pentinsaari M, Hebert PDN, Mutanen M (2014) Barcoding beetles: a regional survey of 1872 species reveals high identification success and unusually deep interspecific divergences. PLOS One 9: e108651. https://doi.org/10.1371/journal.pone.0108651

Persohn M (1996) *Pterostichus adstrictus* Eschscholtz, 1823 – eine Ergänzung zur Kenntnis der mitteleuropäischen Laufkäfer-Fauna (Col., Carabidae). Entomologische Nachrichten und Berichte 40: 252. [In German]

Rainio J, Niemelä J (2003) Ground beetles (Coleoptera: Carabidae) as bioindicators. Biodiversity and Conservation 12: 487–506. https://doi.org/10.1023/A:1022412617568

Ratnasingham S, Hebert PDN (2007) BOLD: The Barcode of Life Data Systems. Molecular Ecology Notes 7: 355–364. https://doi.org/10.1111/j.1471-8286.2007.01678.x

Ratnasingham S, Hebert PDN (2013) A DNA-based registry for all animal species: the Barcode Index Number (BIN) system. PLOS One 8: e66213. https://doi.org/10.1371/journal.pone.0066213

Raupach MJ, Astrin JJ, Hannig K, Peters MK, Stoeckle MY, Wägele JW (2010) Molecular species identifications of Central European ground beetles (Coleoptera: Carabidae) using nuclear rDNA expansion segments and DNA barcodes. Frontiers in Zoology 7: 26. https://doi.org/10.1186/1742-9994-7-26

Raupach MJ, Hannig K, Wägele JW (2011) Identification of Central European ground beetles of the genus *Bembidion* (Coleoptera: Carabidae) using DNA barcodes: a case study of selected species. Angewandte Carabidologie 9: 63–72.

Raupach M, Hendrich L, Küchler SM, Deister F, Morinière J, Gossner MM (2014) Building-up of a DNA barcode library for true bugs (Insecta: Hemiptera: Heteroptera) of Germany reveals taxonomic uncertainties and surprises. PLOS One 9: e106940. https://doi.org/10.1371/journal.pone.0106940

Raupach MJ, Barco A, Steinke D, Beermann J, Laakmann S, Mohrbeck I, Neumann H, Kihara TC, Pointner K, Radulovici A, Segelken-Voigt A, Weese C, Knebelsberger T (2015) The application of DNA barcodes for the identification of marine crustaceans from the North Sea and adjacent regions. PLOS One 10: e0139421. https://doi.org/10.1371/journal.pone.0139421

Raupach MJ, Hannig K, Moriniére J, Hendrich L (2016) A DNA barcode library for ground beetles (Insecta: Coleoptera: Carabidae) of Germany: The genus *Bembidion* Latreille, 1802 and allied taxa. ZooKeys 592: 121–141. https://doi.org/10.3897/zookeys.592.8316

Raupach MJ, Hannig K, Moriniére J, Hendrich L (2018) A DNA barcode library for ground beetles of Germany: The genus *Amara* Bonelli, 1810 (Insecta: Coleoptera: Carabidae). ZooKeys 759: 57–80. https://doi.org/10.3897/zookeys.759.24129

Raupach MJ, Hannig K, Moriniére J, Hendrich L (2019) About *Notiophilus* Duméril, 1806 (Coleoptera, Carabidae): Species delineation and phylogeny using DNA barcodes. Deutsche Entomologische Zeitschrift 66: 63–73. https://doi.org/10.3897/dez.66.34711

Rogers HH, Griffiths-Jones S (2012) Mitochondrial pseudogenes in the nuclear genomes of *Drosophila*. PLOS One 7: e32593. https://doi.org/10.1371/journal.pone.0032593

Rougerie R, Haxaire J, Kitching IJ, Hebert PDN (2012) DNA barcodes and morphology reveal a hybrid hawkmoth in Tahiti (Lepidoptera: Sphingidae). Invertebrate Systematics 26: 445–450. https://doi.org/10.1071/IS12029

Rushton SP, Luff ML, Eyre MD (1990) Habitat characteristics of grassland *Pterostichus* species (Coleoptera, Carabidae). Ecological Entomology 16: 91–104. https://doi.org/10.1111/j.1365-2311.1991.tb00196.x

Sasakawa K, Kim J-L. Kim J-K, Kubota K (2017) Morphological phylogeny and biogeography of the *Pterostichus raptor* species group (Coleoptera: Carabidae) of ground beetles, endemic to the Korean Peninsula and adjacent islands. Journal of Asia-Pacific Entomology 20: 7–12. https://doi.org/10.1016/j.aspen.2016.11.001

Saitou N, Nei M (1987) The neighbor-joining method: a new method for reconstructing phylogenetic trees. Molecular Biology and Evolution 4: 406–425. https://doi.org/10.1093/oxfordjournals.molbev.a040454

Schmidt J, Opgenoorth L, Höll S, Bastrop R (2012) Into the Himalayan exile: The phylogeography of the ground beetle *Ethira* clade supports the Tibetan origin of forest-dwelling Himalayan species groups. PLOS One 7: e45482. https://doi.org/10.1371/journal.pone.0045482

Schmid-Egger C, Straka J, Ljubomirov T, Blagoev GA, Morinière J, Schmidt S (2019) DNA barcodes identify 99 per cent of apoid wasp species (Hymenoptera: Ampulicidae, Crabronidae, Sphecidae) from the Western Palearctic. Molecular Ecology Resources 19: 476–484. https://doi.org/10.1111/1755-0998.12963

Schmidt S, Schmid-Egger C, Morinière J, Haszprunar G, Hebert PDN (2015) DNA barcoding largely supports 250 years of classical taxonomy: identifications for Central European bees (Hymenoptera, Apoidea *partim*). Molecular Ecology Resources 15: 985–1000. https://doi.org/10.1111/1755-0998.12363

Schmidt S, Taeger A, Morinière J, Liston A, Blank SM, Kramp K, Kraus M, Schmidt O, Heibo E, Prous M, Nyman T, Malm T, Stahlhut J (2017) Identification of sawflies and horntails (Hymenoptera, "Symphyta") through DNA barcodes: successes and caveats. Molecular Ecology Resources 17: 670–685. https://doi.org/10.1111/1755-0998.12614

Smith MA, Bertrand C, Crosby K, Eveleigh ES, Fernandez-Triana J, Fisher BL, Gibbs J, Hajibabaei M, Hallwachs W, Hind K, Hrcek J, Huang D-W, Janda M, Janzen DH, Li Y, Miller SE, Packer L, Quicke D, Ratnasingham S, Rodriguez J, Rougerie R, Shaw MR, Sheffield C, Stahlhut JK, Steinke D, Whitfield J, Wood M, Zhou X (2012) *Wolbachia* and DNA barcoding insects: Patterns, potential, and problems. PLOS One 7: e36514. https://doi.org/10.1371/journal.pone.0036514

Spelda J, Reip HS, Oliveira-Biener U, Melzer RR (2011) Barcoding Fauna Bavarica: Myriapoda – a new contribution to DNA-based identifications of centipedes and millipedes. In: Mesibov R, Short M (Eds) Proceedings of the 15th International Congress of Myriapodology, 18–22 July 2011, Brisbane, Australia. ZooKeys 156: 123–139. https://doi.org/10.3897/zookeys.156.2176

Symondson WOC, Glen DM, Erickson ML, Lidell JE, Langdorn CJ (2000) Do earthworms help to sustain the slug predator *Pterostichus melanarius* (Coleoptera: Carabidae) within crops? Investigations using monoclonal antibodies. Molecular Ecology 9: 1279–1292. https://doi.org/10.1046/j.1365-294x.2000.01006.x

Trautner J, Fritze M-A, Hannig K, Kaiser M (2014) Distribution atlas of ground beetles in Germany. Books on Demand, Norderstedt, 348 pp.

Trautner J, Rietze J (2017) Tribus Pterostichini. In: Trautner J (Ed) Die Laufkäfer Baden-Württembergs. Band 1. Ulmer, Stuttgart, 416 pp. [In German]

Zhang A-B, Kubota K, Takami Y, Kim J-L, Kim J-K, Sota T (2006) Comparative phylogeography of three *Leptocarabus* ground beetle species in South Korea, based on the mitochondrial COI and nuclear 28S rRNA genes. Zoological Science 23: 745–754. https://doi.org/10.2108/zsj.23.745

Supplementary material 1

Barcode analysis using the BOLD workbench

Authors: Michael J. Raupach, Karsten Hannig, Jérome Morinière, Lars Hendrich

Data type: Data table

Explanation note: Molecular distances based on the Kimura 2-parameter model of the analyzed specimens of the analyzed species of the genera *Abax*, *Molops*, *Poecilus*, *Pterostichus*, and *Stomis*. Divergence values were calculated for all studied sequences, using the Nearest Neighbour Summary implemented in the Barcode Gap Analysis tool provided by the Barcode of Life Data System (BOLD). Align sequencing option: BOLD aligner (amino acid based HMM), ambiguous base/gap handling: pairwise deletion. ISD = intraspecific distance. BINs are based on the barcode analysis from 11-05-2020. Asterisks indicate species not recorded from Germany. Species with intraspecific maximum pairwise distances > 2.2% and species pairs with interspecific distances < 2.2% are marked in bold. As consequence that the numbers of unspecified nucleotides ("Ns") exceeds more than 1% of their total length, a distinct cluster with two sequences for *Pterostichus panzeri* (Panzer, 1803) received no BIN. Country codes (alpha-2 code): AT = Austria, BE = Belgium, BG = Bulgaria, CZ = Czech Republic, EE = Estonia, FI = Finland, FR = France, DE = Germany, IT = Italy, RO = Romania, SK = Slovakia, SL = Slovenia and CH = Switzerland.

Link: https://doi.org/10.3897/zookeys.980.55979.suppl1

Supplementary material 2

Neighbor-joining topology

Authors: Michael J. Raupach, Karsten Hannig, Jérome Morinière, Lars Hendrich

Data type: Neighbor-joining topology

Explanation note: Neighbor-joining topology of all analyzed carabid beetles based on Kimura 2-parameter distances. Specimens are classified using ID numbers from BOLD and species name. Numbers next to nodes represent non-parametric bootstrap values (1,000 replicates, in %). *Pterostichus crenatus* (Duftschmid, 1812) (see five specimens from Pentinsaari et al 2014) is a junior synonym of *Pterostichus vernalis* (Panzer, 1795). Furthermore, a specimen of *Pterostichus hagenbachii* (Sturm, 1824) (see Hendrich et al. 2015) was incorrectly determined. A careful re-inspection revealed this specimen as *Pterostichus cristatus* (Dufour, 1820).

Link: https://doi.org/10.3897/zookeys.980.55979.suppl2

ZooKeys 980: 119–140 (2020)
doi: 10.3897/zookeys.980.56807
https://zookeys.pensoft.net

RESEARCH ARTICLE

A peer-reviewed open-access journal
ZooKeys
Launched to accelerate biodiversity research

Jumping plant lice of the genus *Aphalara* (Hemiptera, Psylloidea, Aphalaridae) in the Neotropics

Daniel Burckhardt[1], Giulia Dalle Cort[2], Dalva Luiz de Queiroz[3]

1 *Naturhistorisches Museum, Augustinergasse 2, 4001 Basel, Switzerland* **2** *Universidade Federal do Paraná, CIFLOMA – Centro de Ciências Florestais e da Madeira, CEP 80210-170, Curitiba, PR, Brazil* **3** *Embrapa Florestas, Estrada da Ribeira, Km 111, CP. 319, CEP 83411-000, Colombo, PR, Brazil*

Corresponding author: Daniel Burckhardt (daniel.burckhardt@bs.ch)

Academic editor: I. Malenovský | Received 22 July 2020 | Accepted 17 September 2020 | Published 28 October 2020

http://zoobank.org/7EFBE806-533A-4C11-9810-262270E91835

Citation: Burckhardt D, Dalle Cort G, Queiroz DL (2020) Jumping plant lice of the genus *Aphalara* (Hemiptera, Psylloidea, Aphalaridae) in the Neotropics. ZooKeys 980: 119–140. https://doi.org/10.3897/zookeys.980.56807

Abstract

The Neotropical species of the predominantly north temperate genus *Aphalara* are reviewed. Four species are recorded here from this region, two of which are described as new. *Aphalara ritteri* **sp. nov.** occurs in southern Brazil (Paraná, Rio Grande do Sul, Santa Catarina) and represents the first and only species reported from South America. A second new species, *Aphalara ortegae* **sp. nov.**, is described from Mexico and Puerto Rico. Another two species, *Aphalara persicaria* Caldwell, 1937 and *A. simila* Caldwell, 1937, have been previously reported from Mexico and the USA, and one of them also from Cuba. The two new species are both associated with *Persicaria hydropiperoides* and *P. punctata* (Polygonaceae) on which the immatures induce leaf roll galls. The two new species are morphologically similar to *A. persicaria*, to which they are probably closely related. A key is provided for the adults and immatures of the Neotropical species of *Aphalara*.

Keywords

Brazil, leaf roll galls, Mexico, *Persicaria*, Polygonaceae, psyllids, Puerto Rico, Sternorrhyncha

Introduction

Jumping plant lice or psyllids (Hemiptera, Psylloidea) are generally very host specific sternorrhynchous insects developing on eudicots, Magnoliales and, exceptionally, also on monocots and conifers. The largest diversity is encountered in the tropics and south tem-

perate regions where the majority of species are associated with woody plants. However, there are some typical north temperate taxa which develop on herbaceous plants (Burckhardt 2005; Hodkinson 2009; Hollis 2004; Ouvrard et al. 2015). Examples are the two genera *Aphalara* Foerster, 1848 and *Craspedolepta* Enderlein, 1921 (both Aphalaridae) comprising, according to Ouvrard (2020), 46 and 158 species, respectively. Most species of the former develop on Polygonaceae and many of the latter on Compositae.

Burckhardt and Lauterer (1997) judged *Aphalara* "a taxonomically difficult genus as species are mostly defined by host plant ranges. Morphological differences between species tend to be few and subtle whereas intraspecific variability is pronounced." In the Palaearctic, the taxonomy of the genus evolved by piecemeal additions of species creating considerable taxonomic confusion. Ossiannilsson (1951, 1987, 1992), Ossiannilsson and Jansson (1981) and Burckhardt and Lauterer (1997) addressed and solved most of these problems so that today the Palaearctic fauna of *Aphalara* can be considered fairly well-known. The situation is quite different in North America from where Hodkinson (1988) reported 13 species, eight of which were described in a single paper by Caldwell (1937) and the other five each by a different author (Mally 1894; Patch 1912; Caldwell 1938b; Richards 1970; Hodkinson 1973). Caldwell's (1937) descriptions are not diagnostic as they lack information on taxonomically relevant characters, such as surface spinules on the forewing, details of the distal portion of the aedeagus, immatures or host plants. It is, therefore, currently difficult or impossible to identify Nearctic *Aphalara* species without major revisionary work of type material and new collections of large series of specimens, including immatures, with host information (Halbert and Burckhardt 2020).

In the Old World, three of the around 30 species are known exclusively from outside the Palaearctic realm, viz. *Aphalara ossiannilssoni* Mathur, 1975 from India, *A. siamensis* Burckhardt & Lauterer, 1997 from Thailand and *Aphalara taiwanensis* Burckhardt & Lauterer, 1997 from Taiwan (Ouvrard 2020). A fourth species, *A. fasciata* Kuwayama, 1908 also occurs in Taiwan, in addition to China, Japan, Korea and Far East Russia (Burckhardt and Lauterer 1997). The situation in the New World is comparable. *Aphalara persicaria* Caldwell, 1937 and *A. simila* Caldwell, 1937 were described from the USA and subsequently reported from Mexico, the former is also known from Cuba (Caldwell 1941,1944; Halbert and Burckhardt 2020). Each a single unidentified specimen was reported from Argentina (Tucuman) (Burckhardt 1987) and Panama (Canal Zone) (Brown and Hodkinson 1988). Burckhardt (1987) suspected that the Argentinian specimen may represent an introduction from North America.

During recent intensive field work in Brazil we collected, much to our surprise, an *Aphalara* species (Fig. 1) in several localities in the states of Paraná, Rio Grande do Sul and Santa Catarina, associated with the native *Persicaria hydropiperoides* (Michx.) Small (Fig. 2C–E) and *P. punctata* (Elliott) Small as well as with the introduced *P. maculosa* Gray (Polygonaceae). Another species we found in Mexico, also associated with *P. hydropiperoides* and *P. punctata*. Both species are new and are described below along with information on their host plants, habitats and distribution. We also discuss the other known species from the Neotropics, arbitrarily delimited in the north by the Mexico–USA border, and their phylogenetic and biogeographic relationships.

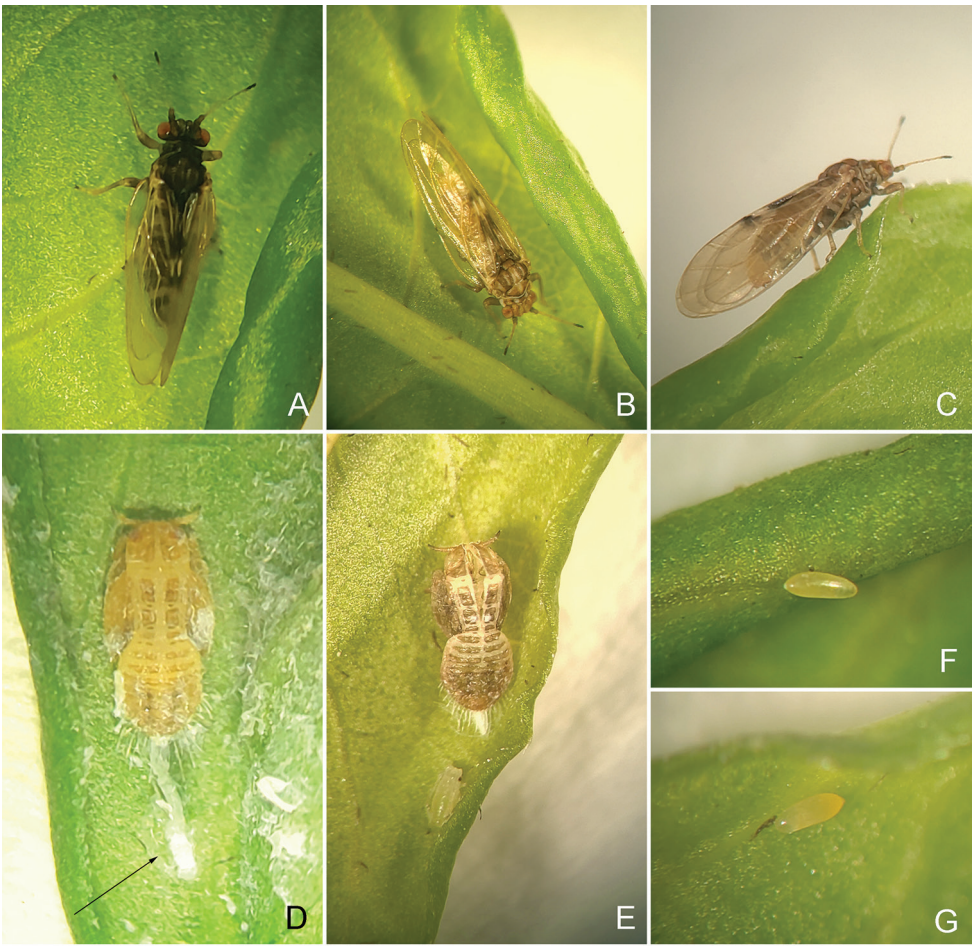

Figure 1. *Aphalara ritteri* sp. nov. **A** male **B** female **C** female on a gall **D** fifth instar immature with secretions (arrow) **E** skin in opened gall and aphid **F, G** egg on a gall.

Materials and methods

The material of the new species was collected by D. Burckhardt and D. L. de Queiroz in Brazil (Paraná–PR, Rio Grande do Sul–RS, Santa Catarina–SC) and Mexico (México–MEX, Michoacán–MIC, Tlaxcala–TLA). Material was examined or is cited from following institutions: Naturhistorisches Museum, Basel, Switzerland (**NHMB**); Coleção Entomológica Padre Jesus Santiago Moure, Centro Politécnico, Universidade Federal do Paraná, Curitiba, PR, Brazil (**UFPR**); United States National Museum collections, Beltsville, MD, USA (**USNM**). Plant vouchers were identified by M.L. Brotto and J.T.W. Motta (Museu Botânico Municipal, Curitiba, PR), as well as Laura Maria Ortega (Colegio de Postgraduados, Campus Montecillo, Texcoco, Estado de México, Mexico). They are deposited at the NHMB; Embrapa Florestas, Colombo, PR, Brazil; and Museu Botânico Municipal, Curitiba, PR, Brazil.

Figure 2. *Persicaria hydropiperoides* (Michx.) Small **A, C** plants with galls by *Aphalara ritteri* sp. nov. **B** examples of galled and ungalled leaves **D** plant with flowers **E** plant growing along pond **F** artificial habitat in Parque Tingui, Curitiba, PR, Brazil with clusters of *P. hydropiperoides* (arrow).

The morphological terminology follows mostly Brown and Hodkinson (1988), Ossiannilsson (1992), Burckhardt and Lauterer (1997) and Hollis (2004). The terminology of the structures on the head is detailed in Fig. 4. Plant names correspond with WFO (2020).

Taxonomy

***Aphalara ortegae* sp. nov.**
http://zoobank.org/05E38881-75A5-49A0-8A0E-27FE0C52981F
Figures 3A–D, 4A, C, 5A–D, I, J, 6A–D, 7A, B, I, 8A, D, G

Type locality. Mexico, Tlaxcala state, Nanacamilpa municipality, San Felipe Hidalgo; 19.4573/4678, –98.5615/567; 2800–2890 m a.s.l.

Type material. *Holotype*: Mexico • ♂; TLA, Nanacamilpa, San Felipe Hidalgo; 19.4573/4678, –98.5615/567; 2800–2890 m a.s.l.; 15 Aug. 2015; D. Burckhardt & D.L. Queiroz leg.; *Persicaria hydropiperoides*, #15-19(1); NMB-PSYLL0004615; NHMB, dry mounted. ***Paratypes*:** Mexico • 1 ♂; MEX, Lomas de Chapultepec; 19.4242, –99.2117; 2330 m a.s.l.; 25 Jul. 1939; A. Dampf leg.; USNM, dry mounted • 10 ♂, 18 ♀; MEX, Teotihuacán, San Franzisco Mazapa; 19.6847, –98.8428; 2300 m a.s.l.; 9 Aug. 2015; D. Burckhardt & D.L. Queiroz leg.; *Persicaria hydropiperoides*, #15-13(5); NMB-PSYLL0006656, NMB-PSYLL0006698, NMB-PSYLL0006699; NHMB, slide mounted and in 70% ethanol • 2 ♂; MIC, Morelia; 19.7029, –101.1964; 1920 m a.s.l.; Jun. 1965; N.L.H. Krauss leg.; USNM, dry mounted • 21 ♂, 27 ♀, 20 immatures, 9 skins; MIC, Salvador Escalante, Lago de Zirahuén; 19.4468, –101.7281; 2020 m a.s.l.; 20 Aug. 2015; D. Burckhardt & D.L. Queiroz leg.; *Persicaria punctata*, #15-30A(2); NMB-PSYLL0006653 to NMB-PSYLL0006655, NMB-PSYLL0006757, NMB-PSYLL0006758; NHMB, in 70% ethanol • 45 ♂, 54 ♀; same data as holotype; NMB-PSYLL0006657, NMB-PSYLL0006658, NMB-PSYLL0006741 to NMB-PSYLL0006756; NHMB, dry and slide mounted, in 70% ethanol. Puerto Rico • 1 ♂; San Juan, Trujillo; 18.3621, –66.0047; 50 m a.s.l.; 6 May 1934; 5447; in field; USNM, dry mounted.

Other material examined (not included in type series). Mexico • 1 ♀ severely damaged; MEX, Mixquic; 19.2255, –98.9628; 2240 m a.s.l.; 29 Apr. 1938; A. Dampf leg.; USNM, dry mounted.

Diagnosis. *Adults.* General body colour dark brown in males, medium brown in females. Forewing with brown clavus. Head with small anteorbital tubercles; anterior tubercles small, rounded; outer anterior margin weakly concave. Clypeus long, tubular, visible in dorsal view. Forewing 2.6–2.9× as long as wide; surface spinules moderately thick, in males leaving narrow or no spinule-free stripes along the veins, arranged in squares or rhombi or indistinct transverse rows, in females covering the whole mem-

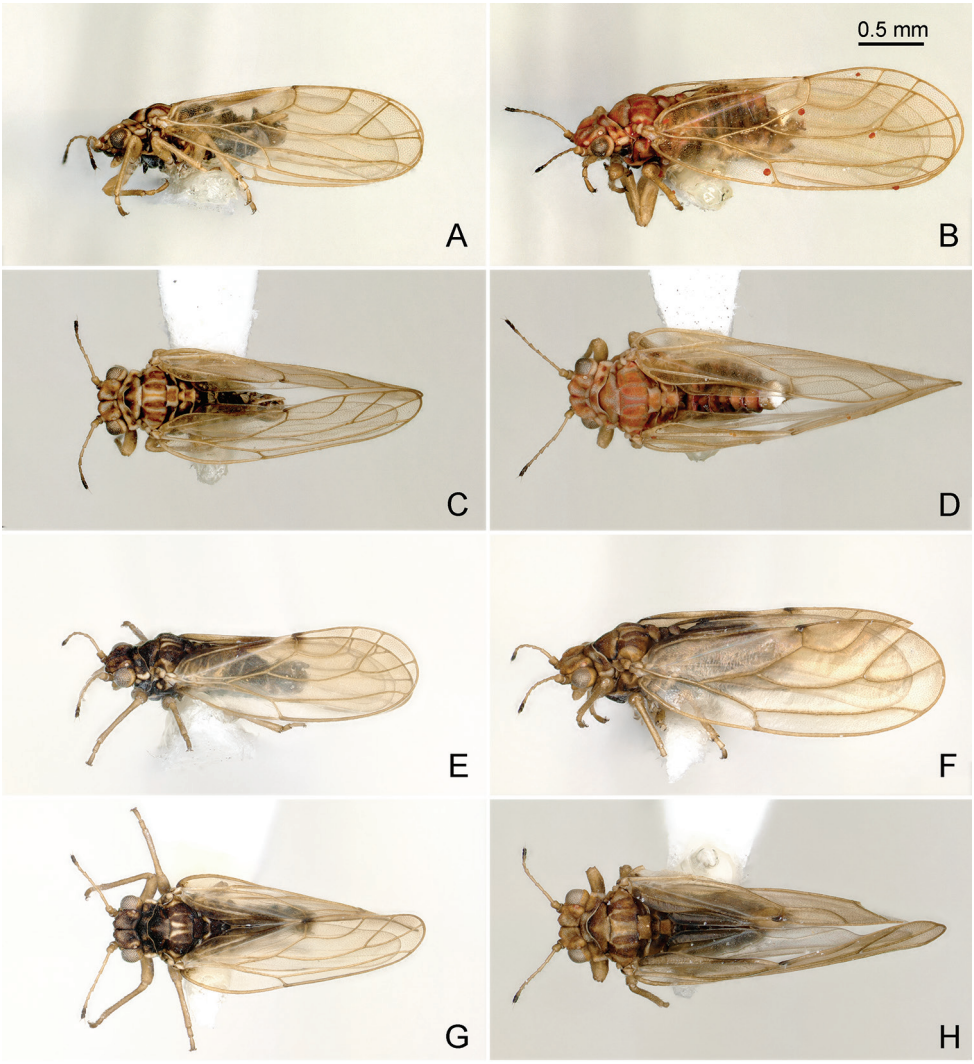

Figure 3. Habitus of *Aphalara* spp. **A–D** *Aphalara ortegae* sp. nov. **E–H** *Aphalara ritteri* sp. nov. **A, C, E, G** male **B, D, F, H** female **A, B, E, F** lateral view **C, D, G, H** dorsal view. Scale bar: 0.5 mm.

brane up to veins, arranged in irregular transverse rows. Paramere, in profile, lamellar with large, claw-like antero-subapical inner process, which is relatively deeply incised, postero-apical edge large, inner face with a few scattered setae. Distal portion of aedeagus with straight shaft and semi-circular apical inflation. Female proctiger strongly incised in the middle forming a slightly curved apical process; circumanal ring expanded into a large, apron-shaped, slightly angular area distally. Subgenital plate with apex almost straight, in ventral view. Valvula dorsalis only weakly curved dorsally. ***Fifth instar immatures.*** Body 1.5–1.6× as long as wide. Antenna 0.5× as long as forewing pad. Outer circumanal ring angular laterally, relatively strongly convex postero-laterally.

Description. ***Adults*** (Fig. 3A–D). Colour. General body colour dark brown in males, medium brown in females. Vertex dark straw-coloured with slightly oblique dark band on either half of vertex. Clypeus dirty yellowish. Antennal segments 1 and 2 light brown, 3–8 yellow becoming darker towards the apical segments, 8 and 9 dark brown. Pronotum with three large yellow areas on either half. Mesopraescutum with yellow posterior third; mesoscutum with three longitudinal yellow stripes on either side. Femora light brown, tibiae and tarsi yellow. Forewing transparent, membrane often yellow or with light brown stripes along the veins; clavus brown. Younger specimens lighter.

Structure. Head (Fig. 4A), in dorsal view, approximately as wide as pronotum, slightly narrower than mesoscutum. Vertex subtrapezoidal with indented foveal pits; anteorbital tubercles small; anterior tubercles small, rounded; outer anterior margin weakly concave; lacking macroscopic setae on vertex. Preocular sclerite small. Lateral tubercle on ventral head surface small, flattened, not indented basally (Fig. 4C). Clypeus tubular, apex visible from above, usually widest across apical third, narrower proximally and distally. Antenna 1.2–1.3× as long as head width, relative length of flagellar segments from base to apex as 1.0 : 0.6 : 0.6 : 0.6 : 0.5: 0.6: 0.4: 0.5; relative length of segment 10 and terminal setae as 1.0 : 0.6 : 0.9. Metatibia 0.7–0.8× as long as head width, with an open crown of 9 or 10 strongly sclerotised apical spurs. Forewing (Fig. 5A–D) oblong oval, 3.7–4.3× as long as head width, 2.6–2.9× as long as wide; cell cu_1 low, vein Cu_{1a} evenly curved. Surface spinules exhibiting sexual dimorphism, more spaced in males, denser in females; moderately thick, present in all cells; in males leaving narrow or no spinule-free stripes along the veins, arranged in squares or rhombi or indistinct transverse rows (Fig. 5I); in females covering the whole membrane up to veins, arranged in irregular transverse rows (Fig. 5J). Costal margin of hindwing with 1 or 2 setae proximal to costal break and 6–14 ungrouped setae distal to costal break.

Terminalia. Male proctiger 0.3× as long as head width, posterior lobes relatively short and wide, less than twice as long as proctiger. Paramere, in profile, lamellar with large, claw-like antero-subapical inner process, which is relatively deeply incised, postero-apical edge large, inner face with a few scattered setae (Fig. 6A, B). Distal portion of aedeagus with straight shaft and semicircular apical inflation which bears an antero-apical hook (Fig. 6C, D). Female terminalia (Fig. 7A) relatively short; proctiger 0.6–0.7× as long as head width, strongly incised in the middle forming a slightly curved apical process; circumanal ring expanded into a large, apron-shaped, slightly angular area distally (Fig. 7I). Subgenital plate 0.5–0.6× as long as proctiger, in profile, cuneate; apex almost straight, in ventral view (Fig. 8A). Valvula dorsalis only weakly curved dorsally (Fig. 7B).

Measurements (5 ♂, 5 ♀, in mm). Head width 0.54–0.60; antenna length 0.66–0.78; forewing length 2.00–2.52; male proctiger length 0.14–0.16; paramere length 0.16–0.18; length of distal portion of aedeagus 0.14–0.18; female proctiger length 0.36–0.44.

Fifth instar immatures (Fig. 8D, G). Colour. General body colour light greyish brown, membranes yellow, dorsally slightly darker than ventrally.

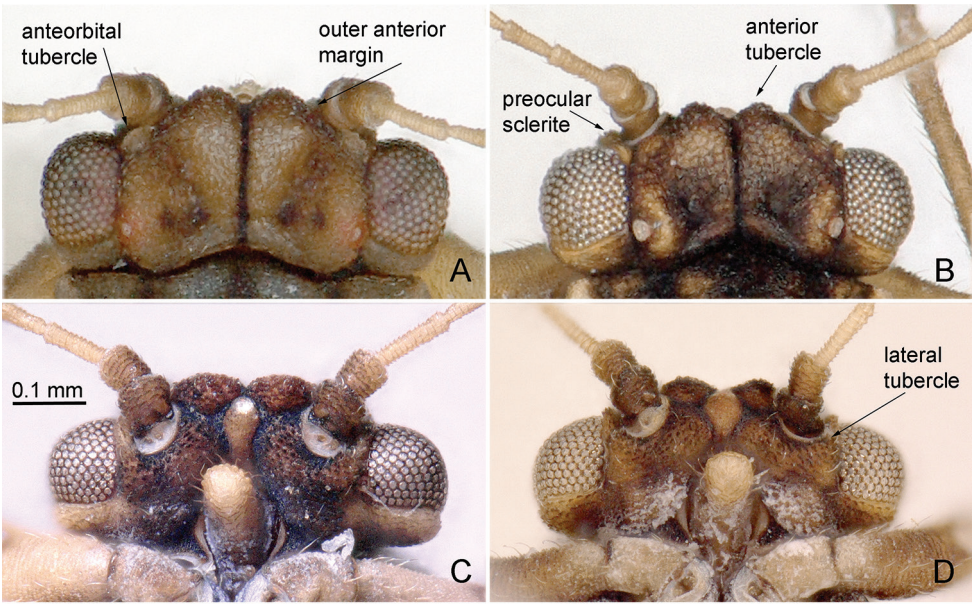

Figure 4. Head of *Aphalara* spp. **A, C** *Aphalara ortegae* sp. nov. **B, D** *Aphalara ritteri* sp. nov. **A, B** dorsal view **C, D** ventral view. Scale bar: 0.1 mm.

Structure. Body 1.5–1.6× as long as wide. Head, antennae and legs with slender lanceolate setae. Antenna 0.5× as long as forewing pad. Tarsal arolium slightly longer than claws, rounded, without unguitractor and pedicel. Forewing pads large with marginal lanceolate setae of irregular length; humeral lobe well developed. Caudal plate irregularly rounded posteriorly, dorsally with sparse microscopic setae, margin with lanceolate setae. Outer circumanal ring angular laterally, relatively strongly convex postero-laterally, consisting of two unequal rows of pores (Fig. 8G).

Measurements (2 immatures, in mm). Body length 1.94–2.04; antenna length 0.38; forewing pad length 0.82–0.84; caudal plate length 0.56–0.58.

Eggs. Colour unknown. Oblong oval; with short apical filament.

Etymology. Named after Professor Dr Laura Maria Ortega, Texcoco, Mexico, in recognition for her support and help during our field work in Mexico. A noun in the genitive case.

Distribution. Mexico (México, Mexico City, Michoacán, San Luis Potosí, Tlaxcala), Puerto Rico.

Host plants, biology and habitats. *Persicaria hydropiperoides* (Michx.) Small, *P. punctata* (Elliott) Small (Polygonaceae). Immatures induce leaf roll galls in which they develop. In Mexico, we collected the species in damp areas around a pond or near a river.

Affinities. *Aphalara ortegae* sp. nov. belongs to the *A. calthae* (Linnaeus, 1761) group, as defined by Burckhardt and Lauterer (1997), which is characterised by the apical inflation of the distal portion of the aedeagus which lacks a dorso-apical mem-

branous sack. It is morphologically similar, and probably closely related, to *A. curta* Caldwell, 1937, *A. persicaria* and *A. ritteri* sp. nov. in the caudally strongly expanded circumanal ring on the female proctiger and the absence of a brown transverse band on the forewing. *Aphalara ortegae* differs from these species in the surface spinules on the forewing which are denser, forming often transverse rows, and the caudal pore field on the female proctiger which is slightly narrowed distad to circumanal ring, large and relatively angular. The paramere of *A. ortegae* has a slightly smaller antero-apical claw than that of *A. curta*, and a larger postero-apical lobe than that of *A. persicaria* and *A. ritteri*. The immatures of *A. ortegae* and *A. ritteri* are almost identical but differ from those of *A. persicaria* in the angular outer circumanal ring (immatures of *A. curta* are unknown). See also identification keys.

Aphalara persicaria Caldwell, 1937

Figures 5K, L, 6I, J, 7C, D, J, 8E, H

Aphalara persicaria Caldwell, 1937: 565; Caldwell (1938a): 237; Hodkinson (1988): 1182; Burckhardt and Lauterer (1997): 305; Halbert and Burckhardt (2020).

Aphalara persicaria var. *cubana* Caldwell, 1937: 565; Hodkinson (1988): 1182; Burckhardt and Lauterer (1997): 305.

Material examined. Cuba • ♂ holotype, 1 ♂, 1 ♀ paratypes of *Aphalara persicaria* var. *cubana*; Havana; 23.1005, –82.3611; 40 m a.s.l.; Baker leg.; USNM, dry mounted. Mexico • 1 ♀; TLA, Nanacamilpa, San Felipe Hidalgo; 19.4573/4678, –98.5615/5671, 2800–2890 m a.s.l.; 15 Jul. 2015; D. Burckhardt & D.L. Queiroz leg.; *Persicaria hydropiperoides*; #15-19(1); NMB-PSYLL0004616; NHMB, dry mounted.

Diagnosis. ***Adults.*** General body colour orange to light brown. Forewing with brown apical part of clavus. Head with small anteorbital tubercles; anterior tubercles small, rounded; outer anterior margin strongly concave. Clypeus long, tubular, visible in dorsal view. Forewing 2.5–2.7× as long as wide; surface spinules fine, forming irregular squares or rhombi; in males often leaving narrow spinule-free stripes along veins (Fig. 5K), in females usually covering the entire wing membrane up to veins (Fig. 5L). Paramere, in lateral view, lamellar, straight, only weakly narrowed in the middle; dorsal margin sclerotised, straight or weakly curved; thumb-like process near antero-apical edge, short, narrow and weakly curved (Fig. 6I). Distal portion of aedeagus with straight shaft and inflated apical third that bears an antero-apical hook of variable length (Fig. 6J). Female proctiger, in lateral view, incised distal to circumanal ring (Fig. 7C), which is strongly expanded caudally (Fig. 7J). Dorsal margin of valvula dorsalis almost straight (Fig. 7D). ***Fifth instar immatures.*** Body (Fig. 8E) 1.6–1.7× as long as wide. Forewing pads narrow, humeral lobes broadly rounded; small lanceolate setae present along margin but not on dorsum. Caudal plate narrowly rounded; lanceolate setae present along margin, approximately as long as distance between them. Outer circumanal ring rounded laterally (Fig. 8H).

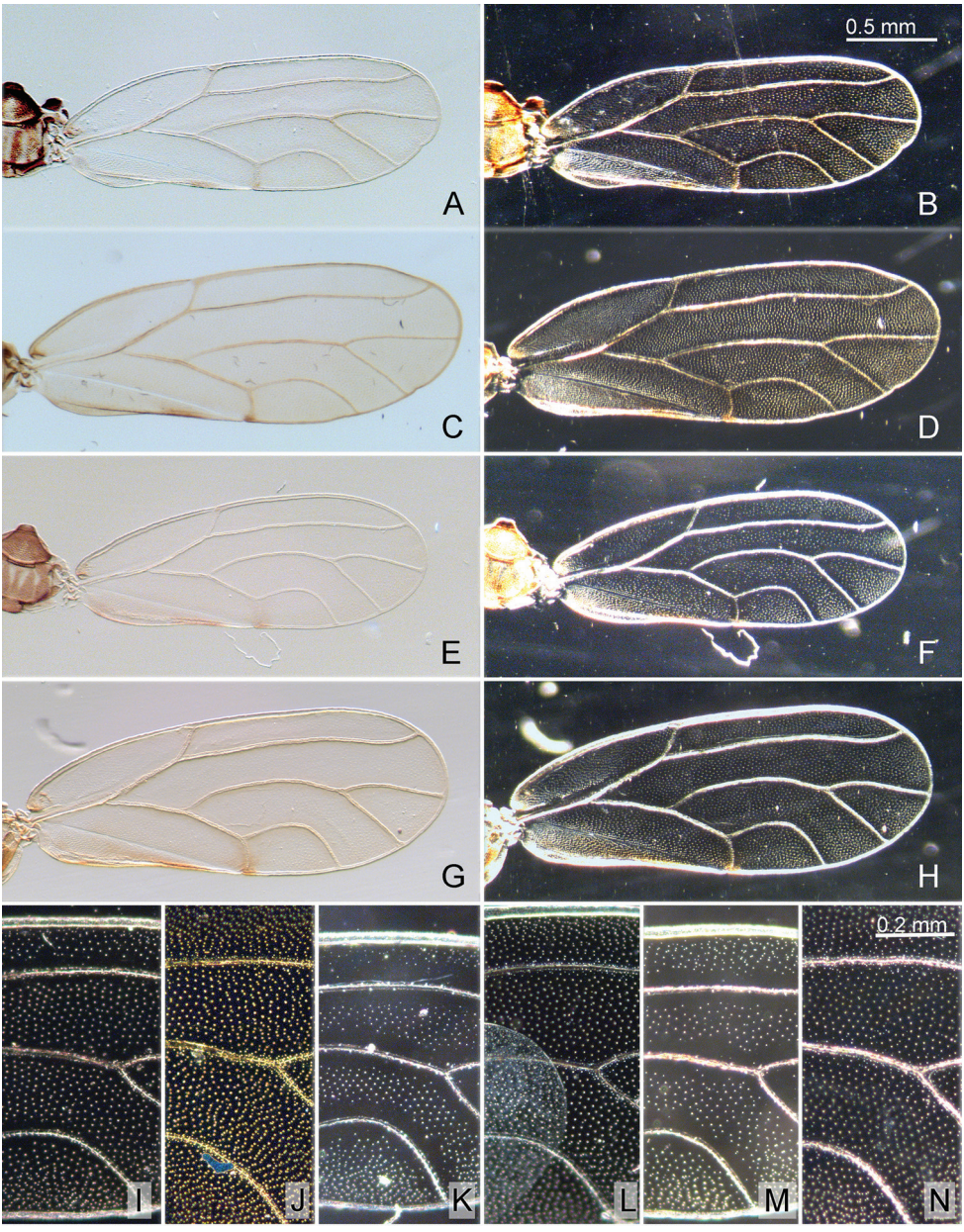

Figure 5. Forewing of *Aphalara* spp. **A–D, I, J** *Aphalara ortegae* sp. nov. **E–H, M, N** *Aphalara ritteri* sp. nov. **K, L** *Aphalara persicaria* Caldwell **A, B, E, F, I, K, M** male **C, D, G, H, J, L, N** female **A, C, E, G** venation **B, D, F, H** surface spinules **I–N** details of surface spinules. Scale bars: 0.5 mm (**A–H**); 0.2 mm (**I–N**).

Distribution. Recorded from Cuba, Mexico (Tlaxcala) and the USA (Florida, Maryland, Michigan, Ohio, Virginia) (Halbert and Burckhardt 2020).

Host plants, biology and habitats. *Persicaria glabra* (Willd.) M.Gómez, *P. lapathifolia* (L.) Delarbre, *P. maculosa* Gray, and *P. punctata* (Elliott) Small (Polygonaceae).

The single female from Mexico was collected on *P. hydropiperoides* (Michx.) Small, which is a probable host. We collected specimens in Mexico and the USA (Florida, Michigan, Virginia) in wet meadows near ponds or rivers.

***Aphalara ritteri* sp. nov.**
http://zoobank.org/65495D01-4F04-42C9-A23B-73E4FBD57ACF
Figures 1, 2A–C, 3E–H, 4B, D, 5E–H, M, N, 6E–H, 7E, F, K, 8B, C, F, I

Type locality. Brazil, Paraná state, Curitiba municipality, Tingui Park, –25.3887/3953, –49.3061/3062, 910–920 m a.s.l.

Type material. ***Holotype:*** Brazil • ♂; PR, Curitiba, Parque Tingui, –25.3887/3953, –49.3061/3062; 910–920 m a.s.l.; 31 Jan. 2016; D. Burckhardt & D.L. Queiroz leg.; *Persicaria hydropiperoides*, #189(12), planted park vegetation and remnants of *Araucaria* forest edge; UFPR, dry mounted. ***Paratypes*:** Brazil • 1 ♀; PR, Cerro Azul, BR-476, km 69; –25.0685, –49.0877; 1080 m a.s.l.; 18–19 Apr. 2013; D. Burckhardt & D.L. Queiroz leg.; #106(-), Atlantic forest; NMB-PSYLL0006671; NMHB, in 70% ethanol • 10 ♂, 5 ♀; PR, Curitiba, Parque Atuba; –25.3816, –49.2033; 890 m a.s.l.; 12 Feb. 2013; D. Burckhardt & D.L. Queiroz leg.; *Persicaria hydropiperoides*, #92(5), planted park vegetation, river bank and remnants of Atlantic forest; NMB-PSYLL0006666; NHMB, in 70% ethanol • 5 ♂, 4 ♀, 6 immatures; PR, Curitiba, Parque Barigui; –25.4269, –49.3134; 910 m a.s.l.; 4 Dec. 2012; D. Burckhardt & D.L. Queiroz leg.; *Persicaria hydropiperoides*, #85(11), planted park vegetation and edge of remnants of *Araucaria* forest; NMB-PSYLL0006667, NMB-PSYLL0006679, NMB-PSYLL0006680; NHMB, slide mounted, in 70% ethanol • 5 ♂, 1 ♀, 1 immature; PR, Curitiba, Parque São Lourenço; –25.3816, –49.2650; 930 m a.s.l.; 5 Dec. 2012; D. Burckhardt & D.L. Queiroz leg.; *Persicaria hydropiperoides*, #86(4), planted park vegetation; NMB-PSYLL0006668; NHMB, in 70% ethanol • 2 ♀; PR, Curitiba, Parque Tanguá; –25.3816, –49.2850; 930 m a.s.l.; 6 Feb. 2013; D. Burckhardt & D.L. Queiroz leg.; *Persicaria hydropiperoides*, #90(12), old mine redone as park with seminatural biotopes, mixed Atlantic and *Araucaria* forest; NMB-PSYLL0006670; NHMB, in 70% ethanol • 3 ♂, 1 ♀; PR, Curitiba, Parque Tingui; –25.3950, –49.3050; 870 m a.s.l.; 10 Dec. 2012; D. Burckhardt & D.L. Queiroz leg.; *Persicaria hydropiperoides*, #88(7), planted park vegetation and edge of remnants of *Araucaria* forest; NMB-PSYLL0006669; NHMB, in 70% ethanol • 17 ♂, 19 ♀; same data as holotype; NMB-PSYLL0004614, NMB-PSYLL0006661 to NMB-PSYLL0006665, NMB-PSYLL0006695, NMB-PSYLL0006696; NHMB, UFPR, dry and slide mounted, in 70% ethanol • 3 ♂, 1 ♀, 5 immatures, 5 skins; PR, Curitiba, Parque Tingui; –25.3950, –49.305; 870 m a.s.l.; 13 Jul. 2020; D.L. Queiroz leg.; *Persicaria hydropiperoides*; NHMB; in 70% ethanol • 11 ♂, 8 ♀, 2 immatures; PR, Tunas do Paraná, Parque Campinhos; –25.0376/0424, –49.0899/1003; 870 m a.s.l.; 8 May 2014; D. Burckhardt & D.L. Queiroz leg.; *Persicaria hydropiperoides*, #137(2), edges of transitional *Araucaria*/Atlantic forest, park; NMB-PSYLL0006673 to NMB-PSYLL0006678; NHMB, dry and slide mounted, 70% in ethanol • 7 ♂, 14

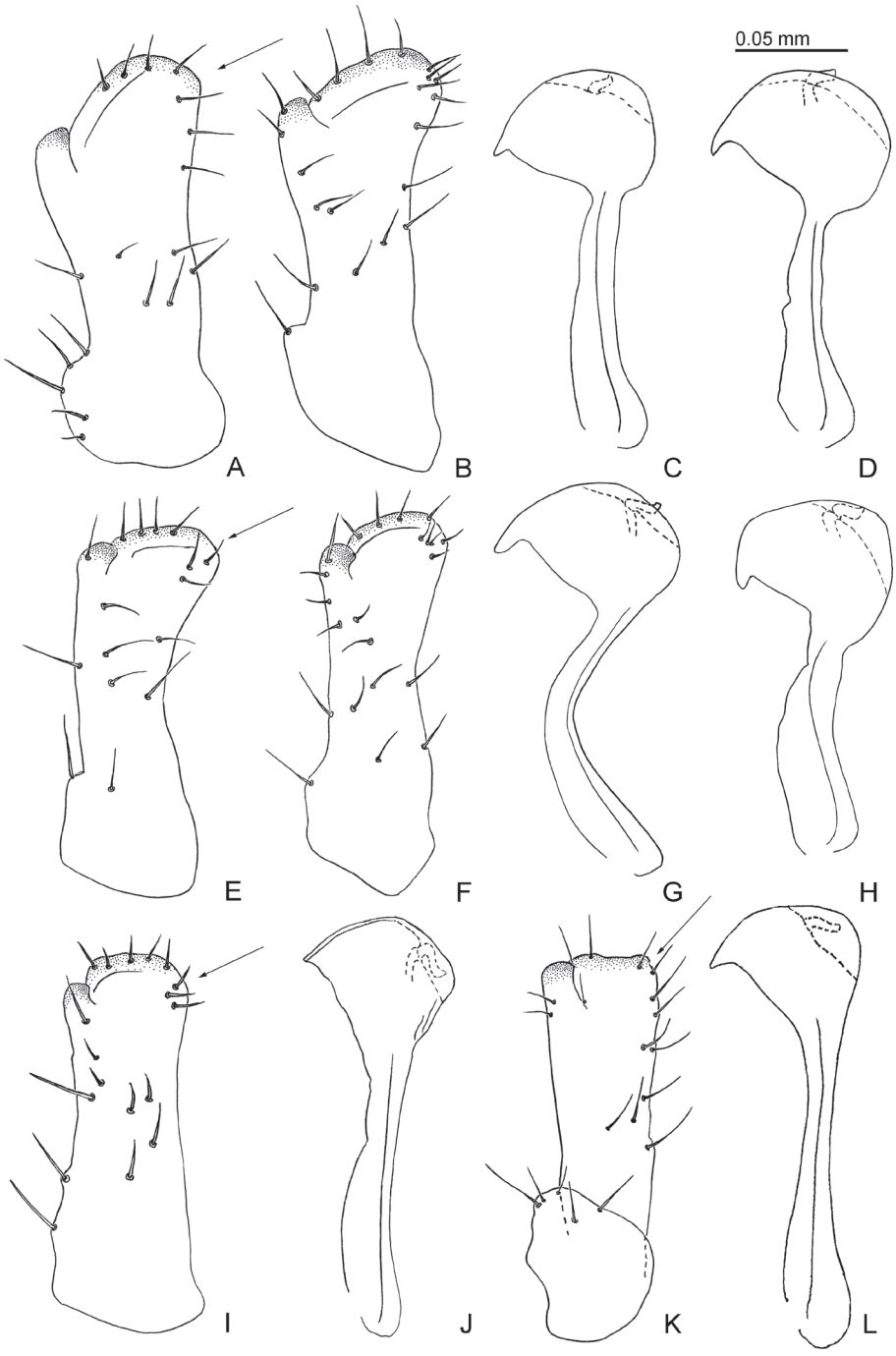

Figure 6. Male terminalia of *Aphalara* spp. **A–D** *Aphalara ortegae* sp. nov. **E–H** *Aphalara ritteri* sp. nov. **I, J** *Aphalara persicaria* Caldwell **K, L** *Aphalara simila* Caldwell **A, B, E, F, I, K** inner face of paramere, in profile; arrows point to apico-posterior lobe/angle **C, D, G, H, J, L** distal portion of aedeagus, in profile. Scale bar: 0.05 mm.

♀, 18 immatures, 1 skin; RS, Cambará do Sul, Parque Nacional de Aparados da Serra, Macieira; –28.1233, –50.1333; 980 m a.s.l.; 24–27 Jan. 2016; D. Burckhardt & D.L. Queiroz leg.; *Persicaria punctata*, #186(15), edge of *Araucaria* and Atlantic forests, *Baccharis* scrub, swamp; NMB-PSYLL0006688 to NMB-PSYLL0006691; NHMB, slide mounted, in 70% ethanol • 1 immature; RS, Passo Fundo, Área da Brigada Militar; –28.2396, –52.3403; 720 m a.s.l.; 26 Jun. 2013; D.L. Queiroz leg.; #515, degraded vegetation; NMB-PSYLL0006697; NHMB, slide mounted • 12 ♂, 14 ♀, 6 immatures, 30 skins; SC, Urubici, Parque Nacional de São Joaquim, 2–3 km from Vacas Gordas to Santa Barbara; –28.1317, –49.6533; 1280 m a.s.l.; 20 Jan. 2016; D. Burckhardt & D.L. Queiroz leg.; *Persicaria hydropiperoides*, #188(3), scrub along road, riverine vegetation; NMB-PSYLL0006682 to NMB-PSYLL0006687, NMB-PSYLL0006759, NMB-PSYLL0006672; NHMB, dry and slide mounted, in 70% ethanol.

Diagnosis. ***Adults*****.** General body colour dark brown to almost black in males, brown to dark brown in females. Forewing with clavus dark brown or almost black, contrasting from surroundings. Head with small anteorbital tubercles; anterior tubercles small, rounded; outer anterior margin weakly concave. Clypeus long, tubular, visible in dorsal view. Forewing 2.6–2.9× as long as wide; surface spinules relatively fine, in males leaving narrow or wide spinule-free stripes along the veins, arranged in squares or rhombi, in females leaving narrow or no spinule-free stripes along the veins, arranged in squares or rhombi. Paramere, in profile, lamellar with medium-sized, claw-like antero-subapical inner process, which is shallowly incised, postero-apical edge medium-sized. Distal portion of aedeagus with curved shaft. Female proctiger strongly incised in the middle forming a hardly curved apical process; circumanal ring expanded into a large, apron-shaped, transverse, laterally rounded area distally. Subgenital plate with apex slightly indented, in ventral view. Valvula dorsalis distinctly curved dorsally. ***Fifth instar immatures.*** Body 1.5–1.6× as long as wide. Antenna 0.4× as long as forewing pad. Outer circumanal ring angular laterally, relatively weakly convex postero-laterally.

Description. ***Adults*** (Figs 1A–C; 3E–H)**.** Colour. General body colour dark brown to almost black in males, brown to dark brown in females. Vertex ochreous with slightly oblique dark band on either half of vertex. Clypeus dirty yellowish. Antennal segments 1 and 2 brown, 3–8 yellow, strongly contrasting from dark brown segments 9 and 10. Pronotum with three ochreous dots on either half. Mesopraescutum with yellow posterior margin and a narrow lighter longitudinal stripe in posterior half; mesoscutum with three narrow longitudinal yellow stripes on either side. Femora brown, tibiae and tarsi yellow. Forewing transparent, membrane often yellow or fumate, veins light to dark brown; stripe along vein Cu_{1b} and clavus dark brown or almost black, contrasting from surroundings. Young specimens lighter, sometimes orange or light brown.

Structure. Head (Fig. 4B), in dorsal view, slightly wider than pronotum, slightly narrower than mesoscutum. Vertex subtrapezoidal with indented foveal pits; anteorbital tubercles small; anterior tubercles small, rounded; outer anterior margin weakly concave; lacking macroscopic setae on vertex. Preocular sclerite small. Lateral tubercle on ventral head surface small, flattened, indented basally (Fig. 4D). Clypeus tubular, apex visible from above, usually widest apically and slightly constricted subapically.

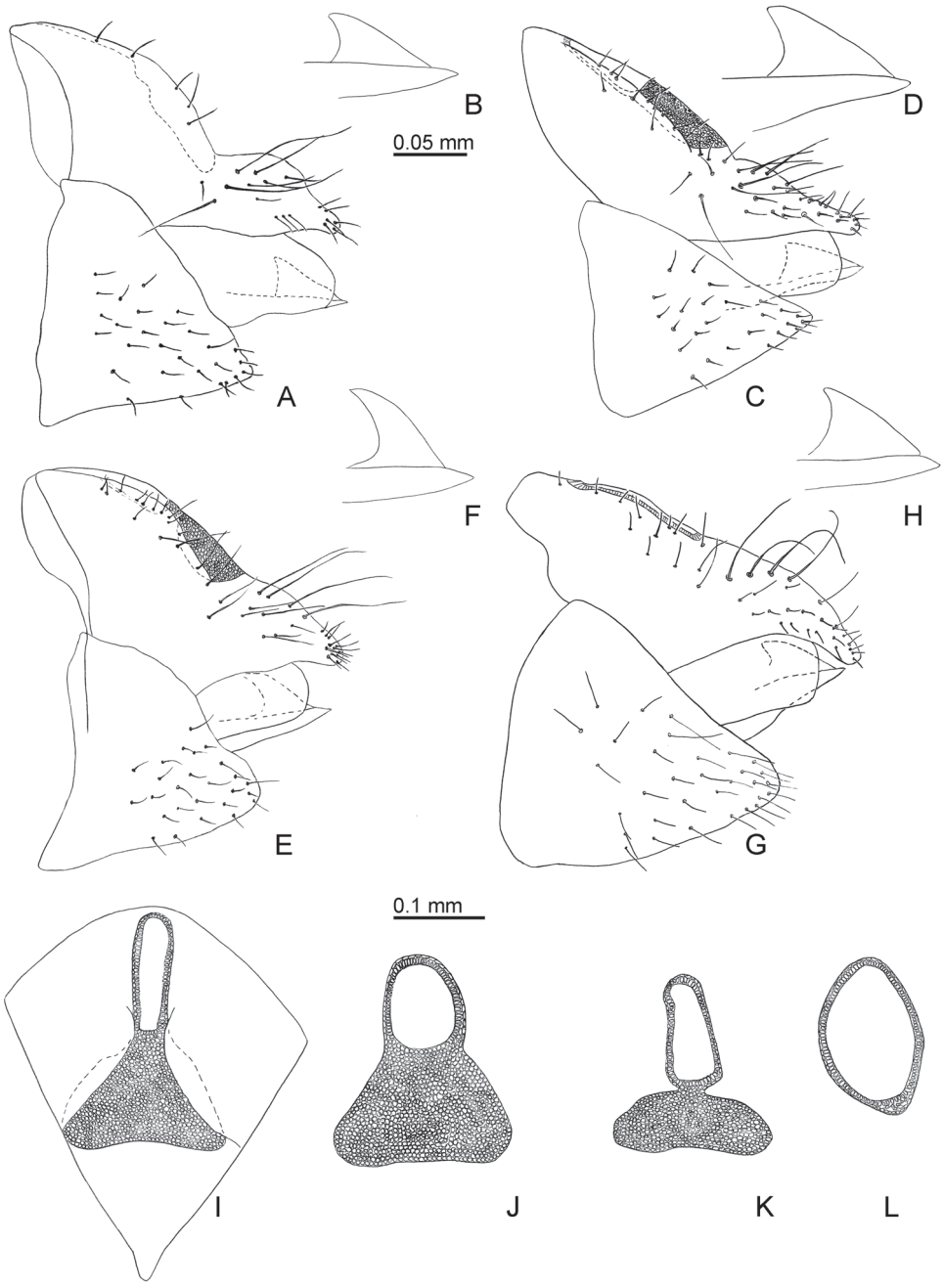

Figure 7. Female terminalia of *Aphalara* spp. **A, B, I** *Aphalara ortegae* sp. nov. **C, D, J** *Aphalara persicaria* Caldwell **E, F, K** *Aphalara ritteri* sp. nov. **G, H, L** *Aphalara simila* Caldwell **A, C, E, G** female terminalia, in profile **B, D, F, H** valvulae dorsales and ventrales, in profile **I–L** circumanal ring, dorsal view. Scale bars: 0.1 mm (**A, C, E, G, I–L**); 0.05 mm (**B, D, F, H**).

Antenna 1.2–1.5× as long as head width, relative length of flagellar segments from base to apex as 1.0 : 0.6 : 0.6 : 0.5 : 0.5 : 0.5 : 0.4 : 0.4; relative length of segment 10 and terminal setae as 1.0 : 0.9 : 1.0. Metatibia 0.7–0.8× as long as head width, with an open crown of 9–11 strongly sclerotised apical spurs. Forewing (Fig. 5E–H) oblong oval, 3.5–4.3× as long as head width, 2.6–2.9× as long as wide; cell cu_1 low, vein Cu_{1a} evenly curved. Surface spinules exhibiting sexual dimorphism, more spaced in males, denser in females; relatively fine, present in all cells; in males leaving narrow or wide spinule-free stripes along the veins, arranged in squares or rhombi (Fig. 5M); in females leaving narrow or no spinule-free stripes along the veins, arranged in squares or rhombi (Fig. 5N). Costal margin of hindwing with 1–3 setae proximal to costal break and 6–11 ungrouped or indistinctly grouped setae distal to costal break.

Terminalia. Male proctiger 0.3× as long as head width, posterior lobes relatively short and wide, less than twice as long proctiger. Paramere, in profile, lamellar with medium-sized, claw-like antero-subapical inner process, which is shallowly incised, postero-apical edge medium-sized, inner face with a few scattered setae (Fig. 6E, F). Distal portion of aedeagus with curved shaft, semi-circular apical inflation with a small hook directed antero-ventrad (Fig. 6G, H). Female terminalia (Fig. 7E) relatively short; proctiger 0.6–0.7× as long as head width, strongly incised in the middle forming a hardly curved apical process; circumanal ring expanded into a large, apron-shaped, transverse, laterally rounded area distally (Fig. 7K). Subgenital plate 0.6× as long as proctiger, in profile, cuneate; apex slightly indented, in ventral view (Fig. 8B). Valvula dorsalis distinctly curved dorsally (Fig. 7F).

Measurements (5 ♂, 5 ♀, in mm). Head width 0.50–0.58; antenna length 0.68–0.74; forewing length 1.82–2.40; male proctiger length 0.14–0.16; paramere length 0.16–0.18; length of distal portion of aedeagus 0.14–0.18; female proctiger length 0.36–0.44.

Fifth instars immature (Figs 1D, 8F)**.** Colour. General body colour, when alive, with yellowish to brown sclerites and yellow membranes; in ethanol straw-coloured to light brown, membranes yellow, dorsally slightly darker than ventrally.

Structure. Body 1.5–1.6× as long as wide. Head, antennae and legs with slender lanceolate setae. Antenna 0.4× as long as forewing pad. Tarsal arolium slightly longer than claws, rounded, without unguitractor and pedicel (Fig. 8C). Forewing pads large with marginal lanceolate setae of irregular length; humeral lobe well developed. Caudal plate irregularly rounded posteriorly, dorsally with sparse microscopic setae, margin with lanceolate setae. Outer circumanal ring angular laterally, relatively weakly convex postero-laterally, consisting of two unequal rows of pores (Fig. 8I).

Measurements (8 immatures, in mm). Body length 1.60–1.88; antenna length 0.30–0.36; forewing pad length 0.72–0.86; caudal plate length 0.48–0.58.

Eggs (Fig. 1F, G)**.** Yellow or light orange. Oblong oval, 2.5× as long as wide; with short apical filament.

Etymology. Named after Markus Ritter, Basel, Switzerland, in recognition of his support of the project on Brazilian psyllids as a president of the Pro Entomologia. A noun in the genitive case.

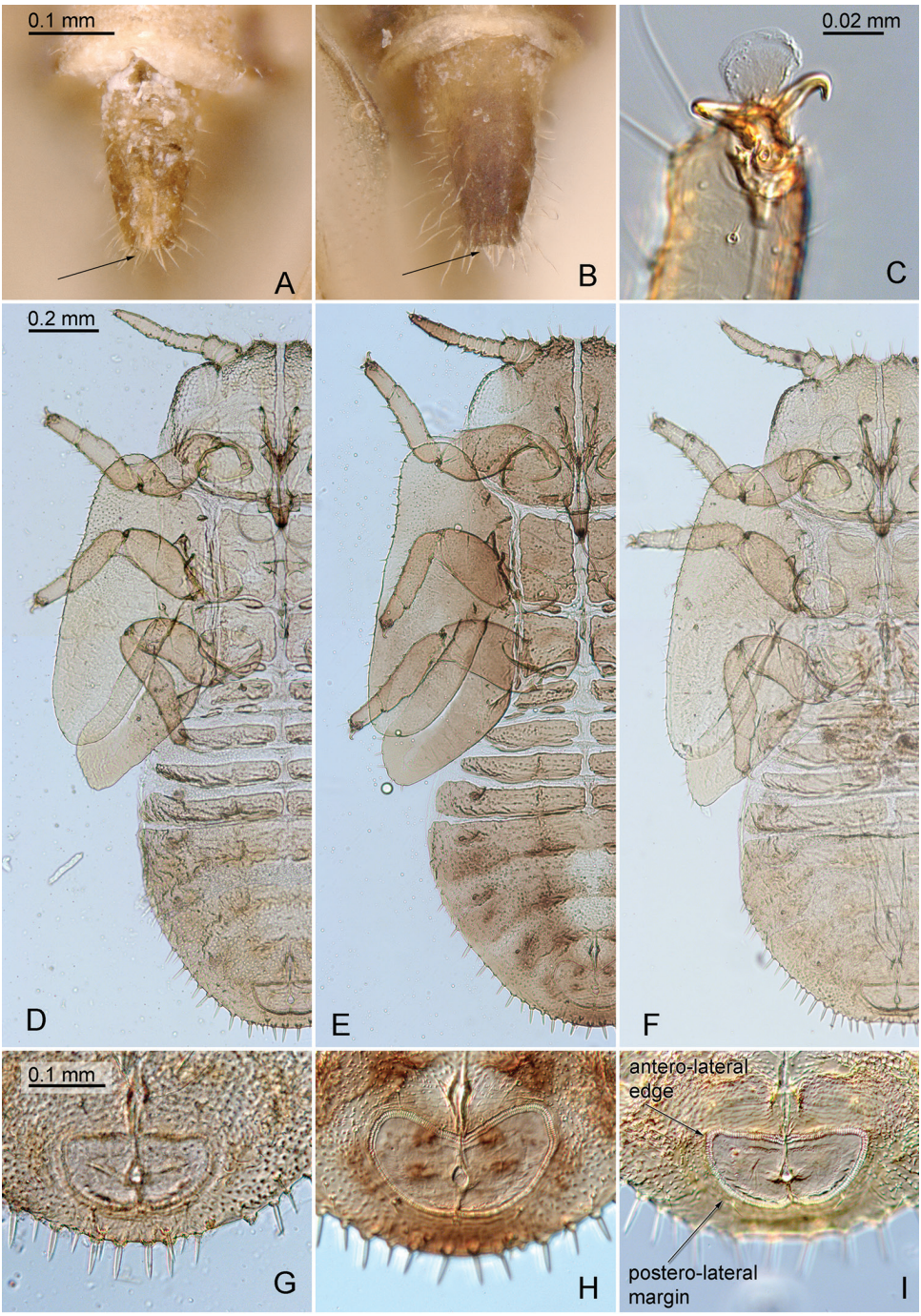

Figure 8. *Aphalara* spp. **A, D, G** *Aphalara ortegae* sp. nov. **B, C, F, I** *Aphalara ritteri* sp. nov. **E, H** *Aphalara persicaria* Caldwell **A, B** female subgenital plate, in ventral view; arrow points to apex **C** tarsus with arolium and claws of immature **D–F** fifth instar immature, left body side **G–I** circumanal ring of fifth instar immature; arrows point to antero-lateral edge and postero-lateral margin. Scale bars: 0.1 mm (**A, B**); 0.02 mm (**C**); 0.2 mm (**D–F**); 0.1 mm (**G–I**).

Distribution. Brazil (Paraná, Rio Grande do Sul, Santa Catarina).

Host plants, biology and habitats. *Persicaria hydropiperoides* (Michx.) Small, *P. maculosa* Gray, *P. punctata* (Elliott) Small (Polygonaceae). The immatures induce leaf roll galls in which they live, usually one immature per gall. The galls are uniformly green or rarely reddish (Fig. 2A–C). Sometimes aphids (Fig. 1E), soft scales and thrips are found in the galls which may be there accidentally or for the nutritionally favourable conditions the galls offer. Eggs are laid on the margin of the leaf rolls. Adults, often together with immatures, were collected from December to February and April to July. It is currently not possible to decide whether this reflects the presence of well-defined generations or an artefact of insufficient collection. Recorded in humid areas in parks, riverine vegetation and Atlantic forest.

Affinities. See under *Aphalara ortegae* sp. nov.

Aphalara similа Caldwell, 1937

Figures 6K, L, 7G, H, L

Aphalara similа Caldwell, 1937: 564; Caldwell (1941): 420; Caldwell (1944): 57; Hodkinson (1988): 1182; Burckhardt and Lauterer (1997): 305.

Material examined. Mexico • 1 ♀; MEX, Mexico City to Toluca road km 20; 19.2952, –99.4201; 2850 m a.s.l.; 24 Nov. 1938; J.S. Caldwell leg.; USNM, dry mounted • 1 ♀; MIC, Uruapan; 19.4128, –102.0475; 1620 m a.s.l.; 1 Oct. 1941; D.M. DeLong, C.C. Plummer & G. Good leg.; from roadside weeds; USNM, dry mounted • 1 ♂, 5 ♀; San Luis Potosí, Tamazunchale; 21.2578, –98.7869; 140 m a.s.l.; 29 Aug. 1939; D.M. & F.M. DeLong leg.; USNM, dry mounted.

Diagnosis. *Adults.* General body colour orange to light brown. Forewing with light or brown clavus. Head with small anteorbital tubercles; anterior tubercles small, rounded; outer anterior margin strongly concave. Clypeus long, tubular, visible in dorsal view. Forewing 2.4× as long as wide; surface spinules moderately thick, forming irregular squares or rhombi; in males often leaving narrow spinule-free stripes along veins, in females usually covering the entire wing membrane up to vein). Paramere, in lateral view, lamellar, straight, weakly widening to apex; dorsal margin sclerotised, straight, postero-apical edge angular; apex of thumb-like process level with antero-apical edge, long, broad (Fig. 6K). Distal portion of aedeagus with straight shaft and relatively evenly widening apical inflation (Fig. 6L). Female proctiger, in lateral view, not incised distal to circumanal ring (Fig. 7G), which is not expanded caudally (Fig. 7L). Dorsal margin of valvula dorsalis almost straight (Fig. 7H).

Fifth instar immature. Unknown.

Distribution. Mexico (Distrito Federal, Michoacán, Morelos, San Luis Potosí) (Caldwell 1941, 1944), USA (California, Colorado, Idaho, Oregon, Utah, Washington, Wyoming) (Caldwell 1937).

Host plants, biology and habitats. *Rumex* sp. (Polygonaceae) (Burckhardt and Lauterer 1997).

***Aphalara* spp.**

Comments. Burckhardt (1987) reported a single female from Argentina (Tucuman) suggesting that it may be introduced from North America. Whether this specimen belongs to *A. ritteri* sp. nov. cannot be checked as it appears to be lost (T. Vasarhelyi, pers. comm.).

Brown and Hodkinson (1988) recorded a female in poor condition from Panama (Canal Zone, Herbert Osborn Collection) (USNM, slide mounted) that they questionably referred to *A. curta*. As the specimen is in poor condition, its identity cannot be determined.

Keys to the Neotropical *Aphalara* species

Adults

1 Male **2**
– Female **5**
2 Paramere with distinctly expanded lobe postero-apically (Fig. 6A, B, E, F, arrow). Distal portion of aedeagus with abruptly widening apical dilatation (Fig. 6 C, D, G, H) **3**
– Paramere not expanded postero-apically (Fig. 6I, K, arrow). Distal portion of aedeagus with gradually widening apical dilatation (Fig. 6J, L) **4**
3 Paramere with relatively large antero-apical thumb-like process (Fig. 6A, B). Distal portion of aedeagus straight basally (Fig. 6C, D). Mexico ..... ***Aphalara ortegae* sp. nov.**
– Paramere with relatively small antero-apical thumb-like process (Fig. 6E, F). Distal portion of aedeagus curved basally (Fig. 6G, H). Brazil ..... ***Aphalara ritteri* sp. nov.**
4 Forewing relatively slender, 2.5–2.7× as long as wide. Paramere with postero-apical edge rounded (Fig. 6I, arrow)..... ***Aphalara persicaria* Caldwell**
– Forewing relatively broad, 2.4× as long as wide. Paramere with postero-apical edge angular (Fig. 6K, arrow)..... ***Aphalara simila* Caldwell**
5 Circumanal ring consisting mostly of two unequal rows of pores, hardly expanded caudally (Fig. 7L) ..... ***Aphalara simila* Caldwell**
– Circumanal ring strongly expanded caudally to form apron-shaped field (Fig. 7I–K)..... **6**
6 Surface spinules moderately thick, arranged in irregular transverse rows (Fig. 5D, J) ..... ***Aphalara ortegae* sp. nov.**
– Surface spinules fine, arranged in irregular squares or rhombi (Fig. 5H, L, N)...**7**
7 Pore field caudad of circumanal ring evenly widening to apex (Fig. 7J). Cuba, Mexico, USA ..... ***Aphalara persicaria* Caldwell**
– Pore field caudad of circumanal ring narrowed just adjacent to pore ring and then widening to a transverse ribbon shaped area (Fig. 7K). Brazil..... ***Aphalara ritteri* sp. nov.**

Key to immatures (immatures of *Aphalara simila* unknown)

1 Circumanal ring rounded antero-laterally (Fig. 8H). Cuba, Mexico, USA .... ***Aphalara persicaria*** **Caldwell**

– Circumanal ring angular antero-laterally (Fig. 8G, I, arrow). Brazil, Mexico ... **2**

2 Body longer than 1.9 mm. Antenna slightly longer; antenna/ forewing pad ratio = 0.5. Outer circumanal ring relatively strongly convex postero-laterally (Fig. 8G). Mexico ..... ***Aphalara ortegae*** **sp. nov.**

– Body shorter than 1.9 mm. Antenna slightly shorter; antenna/ forewing pad ratio = 0.4. Outer circumanal ring relatively weakly convex postero-laterally (Fig. 8I, arrow). Brazil..... ***Aphalara ritteri*** **sp. nov.**

Discussion and conclusions

Aphalara is an atypical psyllid genus with respect to distribution and host plant range as it is predominantly north temperate and associated with herbaceous plants, mostly Polygonaceae. Ouvrard (2020) lists 46 *Aphalara* species, five of which of unresolved taxonomic status or considered nomina dubia (*Aphalara crassinervis* Rudow, 1875; *A. hedini* Enderlein, 1933; *A. multipunctata* Kuwayama, 1908; *A. poligoni* (Shinji, 1938); and *A. tecta* Maskell, 1898). Among the remaining species (plus the two new added here), 15 occur in the New World and 28 in the Old World. Three Asian species (11% of the Old World species) are known only from outside the Palaearctic realm (*Aphalara ossiannilssoni*, *A. siamensis* and *A. taiwanensis*), the first two from a single locality in India (West Bengal) and northern Thailand, respectively, and the last from several localities in Taiwan (Mathur 1975; Burckhardt and Lauterer 1997). *Aphalara fasciata* occurs in both the Palaearctic and Oriental regions (Burckhardt and Lauterer 1997). Hence, 14% of the Old World species are found outside the Palaearctic region. A similar pattern is found in the New World where four of the 15 known species (27%) are found south of the Mexico–USA border though the number of species existing in the Nearctic is probably much higher. *Aphalara ortegae* sp. nov. is widely distributed and likely native in Mexico and Puerto Rico. *Aphalara ritteri* sp. nov. is widely distributed in Southern Brazil (PR, RS, SC) in suitable habitats and most probably native as it is associated with native hosts.

Of the 15 New World species, five are associated with *Rumex*, three with *Persicaria*, and one with *Polygonum* spp. (all Polygonaceae) as well as each one on the unrelated *Lysimachia ciliata* (Primulaceae) and *Sisymbrium canescens* (Brassicaceae); hosts of four species are unknown. In the Old World, seven species are associated with *Rumex*, four each with *Persicaria* and *Polygonum*, one with *Persicaria* and *Polygonum* and two with *Reynoutria* spp. (all Polygonaceae) as well as two species with the unrelated *Caltha* (Ranunculaceae) and one with *Stellaria* (Caryophyllaceae), in addition to six species with unknown hosts. Among the Polygonaceae feeders, 18 *Aphalara* species appear monophagous, seven oligophagous on plant species of the same genus and one oligophagous on several plant species of two genera (Burckhardt and Lauterer 1997; Ouvrard 2020). The

three closely related, *A. ortegae*, *A. persicaria* and *A. ritteri*, are oligophagous on *Persicaria* spp. sharing some host species, such as *P. hydropiperoides* and *P. punctata*.

The two odd specimens recorded from Argentina (Burckhardt 1987) and Panama (Brown and Hodkinson 1988) seem, in the light of the new records from Brazil and Mexico, less out of place and may represent the two species newly described here.

Aphalara ortegae sp. nov. and *A. ritteri* sp. nov. are morphologically similar to each other and to *A. persicaria* with many characters intergrading between species, emphasising the importance of sufficiently large series of material with adults and immatures together with host information for taxonomic work in this genus.

Acknowledgements

We are very grateful to D. Creel and C. O'Donnell (USNM) for the loan of material and for providing access to the psyllid collection. We are also much indebted to M.L. Brotto and J.T.W. Motta (Museu Botânico Municipal, Curitiba, PR, Brazil) as well as Laura Maria Ortega (Colegio de Postgraduados, Campus Montecillo, Texcoco, Estado de México, Mexico) for the identification of plant vouchers. We thank I. Malenovský and L. Štarhová Serbina (Masaryk University, Brno, Czech Republic) as well as an anonymous reviewer for their careful review of a previous manuscript draft.

We are grateful to Pro Entomologia, Basel, and its former president Markus Ritter, for financial support of the project "Biodiversidade de Psylloidea no Brasil" (DLQ and DB). Collecting and export permits were provided by IBAMA/SISBIO (permit numbers: 11832–Licença permanente para coleta de material zoológico; 37053–Autorização para atividades com finalidade científica: áreas fora de parques em PR, SC e RS; 41169–Autorização para atividades com finalidade científica: Parque Nacional de Jericoacoara CE, Parque Nacional do Pantanal Mato-grossense, Parque Nacional de São Joaquim SC, Parque Nacional da Chapada dos Veadeiros GO, Parque Nacional da Chapada dos Guimarães MT, Parque Nacional do Iguaçu PR, Floresta Nacional de Canela RS, Parque Nacional Aparados da Serra SC, Área de Proteção Ambiental de Ibirapuitã RS, Parque Nacional do Superagui; IAP (Autorização de pesquisa em unidades de conservação no Paraná, collecting permits numbers 493.1-13 and 029/18), DEBIO/SEMA (Autorização para pesquisa em unidades de conservação no Estado do Rio Grande do Sul, permit number DUC 640); Prefeitura de Curitiba (collections in Curitiba parks) and CNPq (Projeto "Biodiversidade de Psylloidea no Brasil", processo de Expedição Científica n° 002152/2012).

References

Brown RG, Hodkinson ID (1988) Taxonomy and Ecology of the Jumping Plant-lice of Panama (Homoptera: Psylloidea). Entomonograph 9. E.J. Brill, Scandinavian Science Press, Leiden–New York–København–Köln, 304 pp. https://doi.org/10.1163/156853988X00241

Burckhardt D (1987) Jumping plant lice (Homoptera: Psylloidea) of the temperate Neotropical region: Part 1. Psyllidae (subfamilies Aphalarinae, Rhinocolinae and Aphalaroidinae). Zoological Journal of the Linnean Society 89: 299–392. https://doi.org/10.1111/j.1096-3642.1987.tb01568.x

Burckhardt D (2005) Biology, ecology, and evolution of gall-inducing Psyllids (Hemiptera: Psylloidea). In: Raman A, Schaefer CW, Withers TM (Eds) Biology, Ecology, and Evolution of Gall-inducing Arthropods. Science Publishers, Enfield–Plymouth, 143–157.

Burckhardt D, Lauterer P (1997) Systematics and biology of the *Aphalara exilis* (Weber and Mohr) species assemblage (Hemiptera: Psyllidae). Entomologica Scandinavica 28: 271–305. https://doi.org/10.1163/187631297X00088

Caldwell JS (1937) Some North American relatives of *Aphalara calthae* Linnaeus. Annals of the Entomological Society of America 30: 563–571. https://doi.org/10.1093/aesa/30.4.563

Caldwell JS (1938a) The jumping plant-lice of Ohio (Homoptera: Chermidae). Ohio Biological Survey, Bulletin 34(6): 228–281.

Caldwell JS (1938b) Three new species of psyllids and the description of the allotype of *Livia opaqua* Cald. (Homoptera: Psyllidae). Annals of the Entomological Society of America 31: 442–444. https://doi.org/10.1093/aesa/31.4.442

Caldwell JS (1941) A preliminary survey of Mexican Psyllidae (Homoptera). The Ohio Journal of Science 41: 418–425.

Caldwell JS (1944) Notes on Mexican and Central American Psyllidae. The Ohio Journal of Science 44: 57–64.

Halbert SE, Burckhardt D (2020) The psyllids (Hemiptera: Psylloidea) of Florida: newly established and rarely collected taxa and checklist. Insecta Mundi 0788: 1–88.

Hodkinson ID (1973) A new species of *Aphalara* Först. (Homoptera: Psylloidea: Aphalaridae) from Alberta. The Canadian Entomologist 105: 1413–1415. https://doi.org/10.4039/Ent1051413-11

Hodkinson ID (1988) The Nearctic Psylloidea (Insecta: Homoptera): an annotated check list. Journal of Natural History 22: 1179–1243. https://doi.org/10.1080/00222938800770751

Hodkinson ID (2009) Life cycle variation and adaptation in jumping plant lice (Insecta: Hemiptera: Psylloidea): a global synthesis. Journal of Natural History 43: 65–179. https://doi.org/10.1080/00222930802354167

Hollis D (2004) Australian Psylloidea: Jumping Plantlice and Lerp Insects. Australian Biological Resources Study, Canberra, 216 pp.

Mally CW (1894) Psyllidae found at Ames. Proceedings of the Iowa Academy of Sciences 3: 152–171.

Mathur RN (1975) Psyllidae of the Indian Subcontinent. Indian Council of Agricultural Research, New Dehli, 429 pp.

Ossiannilsson F (1951) On the psyllid of the marsh marigold, *Aphalara calthae* (Linn.). Societas Scientiarum Fennica Commentationes Biologicae 12: 3–8.

Ossiannilsson F (1987) Two new Scandinavian species of Aphalarinae (Homoptera: Psylloidea). Entomologica Scandinavica 18: 221–225. https://doi.org/10.1163/187631287X00089

Ossiannilsson F (1992) The Psylloidea (Homoptera) of Fennoscandia and Denmark. Fauna Entomologica Scandinavica 26. E.J. Brill, Leiden–New York–Köln, 346 pp.

Ossiannilsson F, Jansson M (1981) Designation of a lectotype and description of *Aphalara rumicicola avicularis*, n. ssp. (Homoptera: Psylloidea). Entomologica Scandinavica 12: 22–26. https://doi.org/10.1163/187631281X00300

Ouvrard D (2020) Psyl'list – The World Psylloidea Database. https://www.hemiptera-databases.org/psyllist/ [Accessed on 20 July 2020]

Ouvrard D, Chalise P, Percy DM (2015) Host-plant leaps versus host-plant shuffle: a global survey reveals contrasting patterns in an oligophagous insect group (Hemiptera, Psylloidea). Systematics and Biodiversity 13: 434–454. https://doi.org/10.1080/14772000.2015.1046969

Patch EM (1912) Notes on Psyllidae 2. Maine Agricultural Experiment Station 202: 215–234.

Richards WR (1970) *Aphalara steironemicola*, a new psyllid collected on *Steironema ciliatum* in Ontario (Homoptera: Psyllidae). The Canadian Entomologist 102: 1508–1509. https://doi.org/10.4039/Ent1021508-12

WFO (2020) World Flora Online. http://www.worldfloraonline.org [Accessed on 20 July 2020]

ZooKeys 980: 141–154 (2020)
doi: 10.3897/zookeys.980.50934
https://zookeys.pensoft.net

RESEARCH ARTICLE

A peer-reviewed open-access journal
ZooKeys
Launched to accelerate biodiversity research

Plectorhinchus makranensis (Teleostei, Haemulidae), a new species of sweetlips from the Persian Gulf and the Gulf of Oman

Ehsan Damadi[1], Faezeh Yazdani Moghaddam[1,2], Fereshteh Ghassemzadeh[1,2], Mehdi Ghanbarifardi[3]

1 *Department of Biology, Faculty of Sciences, Ferdowsi University of Mashhad, Mashhad, Iran* **2** *Zoological Innovations Research Department, Institute of Applied Zoology, Faculty of Science, Ferdowsi University of Mashhad, Mashhad, Iran* **3** *Department of Biology, Faculty of Science, University of Sistan and Baluchestan, Zahedan, Iran*

Corresponding author: Faezeh Yazdani Moghaddam (yazdani@um.ac.ir)

Academic editor: N. Bogutskaya | Received 8 February 2020 | Accepted 28 August 2020 | Published 28 October 2020

http://zoobank.org/B7357F67-9E93-4161-9FF5-65FAD703D8C9

Citation: Damadi E, Moghaddam FY, Ghassemzadeh F, Ghanbarifardi M (2020) *Plectorhinchus makranensis* (Teleostei, Haemulidae), a new species of sweetlips from the Persian Gulf and the Gulf of Oman. ZooKeys 980: 141–154. https://doi.org/10.3897/zookeys.980.50934

Abstract

Plectorhinchus makranensis **sp. nov**. is described on the basis of 16 specimens from the Persian Gulf and Gulf of Oman, in the Northwest Indian Ocean. The new species can be distinguished from congeners by a combination of dorsal fin rays XII, 18–20, pectoral-fin rays 16–17, tubed lateral-line scales 55–57, gill rakers count (10–12 on the upper limb and 16–17 on the lower limb), 17–18 scales between the lateral line and the first anal-fin spine, 30–31 circumpeduncular scale rows and color pattern. *Plectorhinchus makranensis* **sp. nov.** is distinguished from *P. schotaf* by having the posterior margin of the opercular membrane grey (vs. red in *P. schotaf*), fewer circumpeduncular scale rows, and a shorter base of the soft portion of the dorsal fin, 27.6–29.4% of standard length (SL) (vs. 31–32.3% of SL in *P. schotaf*). The new species resembles *P. sordidus* but is differentiated from it by having more gill rakers, a smaller orbit diameter 27.5–32.1% of head length (HL) (vs. 35.5–37.2% of HL in *P. sordidus*), a longer caudal peduncle 19.2–21.3% of SL (vs. 17.1–17.9% of SL in *P. sordidus*), and the first to third pectoral-fin rays light gray (vs. dark gray in *P. sordidus*). The new species can also be distinguished from the other species, including *P. schotaf* and *P. sordidus*, based on COI and Cyt *b* molecular markers. The phylogenetic position of this new species indicates that it is a sister taxon of *P. schotaf*.

Keywords

Haemulidae, morphology, mtDNA, Northwest Indian Ocean, phylogenetic relationships, *Plectorhinchus*

Introduction

Haemulidae Gill, 1885, is one of the 10 largest families of the order Perciformes, with 19 genera and 136 species. Almost half of the world's haemulid species belong to the genera *Plectorhinchus* and *Pomadasys* (Nelson et al. 2016; Fricke et al. 2019). The genus *Plectorhinchus* Jordan & Thompson, 1912 (Perciformes: Haemulidae) is commonly called sweetlips and includes fish with commercial importance in the Indo-west Pacific Ocean (Liang et al. 2016; Froese and Pauly 2019). Many species of this genus have markedly different color patterns, morphological characteristics, and ecological characteristics (Randall et al. 1997; Johnson et al. 2001; McKay 2001). The genus *Plectorhinchus* is widely distributed in the Indo-Pacific and eastern Atlantic (Tavera et al. 2012; Froese and Pauly 2019) and encompasses 31 valid species worldwide (Fricke et al. 2019). Seven species of *Plectorhinchus* are known to exist in the Gulf of Oman: *Plectorhinchus flavomaculatus* (Cuvier 1830), *P. gaterinus* (Forsskål, 1775), *P. gibbosus* (Lacepède, 1802), *P. pictus* (Tortonese, 1936), *P. playfairi* (Pellegrin, 1914), *P. schotaf* (Forsskål, 1775) and *P. sordidus* (Klunzinger, 1870) (Randall 1995); however, Carpenter et al. (1997) and Bishop (2003) reported only three species in the Persian Gulf (*P. gaterinus*, *P. pictus* and *P. sordidus*). Phylogenetic relationships of the genus *Plectorhinchus* have previously been investigated (Sanciangco et al. 2011; Liang et al. 2016; Tavera et al. 2018). Molecular phylogenetic investigations of ichthyofauna are rare in the studied area (Asgharian et al. 2011; Ghanbarifardi et al. 2016; Polgar et al. 2017; Rabaoui et al. 2019). Asgharian et al. (2011) and Johnson and Wilmer (2015) reported two specimens of *P. schotaf* in the Persian Gulf represented two genetic lineages, based on the COI gene.

The aims of our study are to use two molecular markers (COI, Cyt *b*) and morphological characters to confirm the existence of two lineages proposed by the other authors and to describe a new species of *Plectorhinchus* collected from the Gulf of Oman and the Persian Gulf.

Materials and methods

Sampling and material examined

In the present study 16 specimens of *Plectorhinchus* spp. and 10 specimens of *P. schotaf* were collected from six localities (Gulf of Oman: Beris, Tis, Pozm, Jask; Persian Gulf: Kangan, Hendijan) by gill netting in the time period from August 2017 to June 2018 (Fig. 1). All specimens are deposited in the Zoological Museum, Ferdowsi University of Mashhad (ZM-FUM), Iran. Muscle tissue of the specimens were taken and fixed in absolute ethanol for molecular analysis and the specimens were stored at -20 °C for later morphological study.

DNA extraction, PCR and sequencing

Genomic DNA was extracted from 10 specimens of *Plectorhinchus*, including six *Plectorhinchus makranensis* sp. nov. and four *P. schotaf*, following the GeNet Bio kit pro-

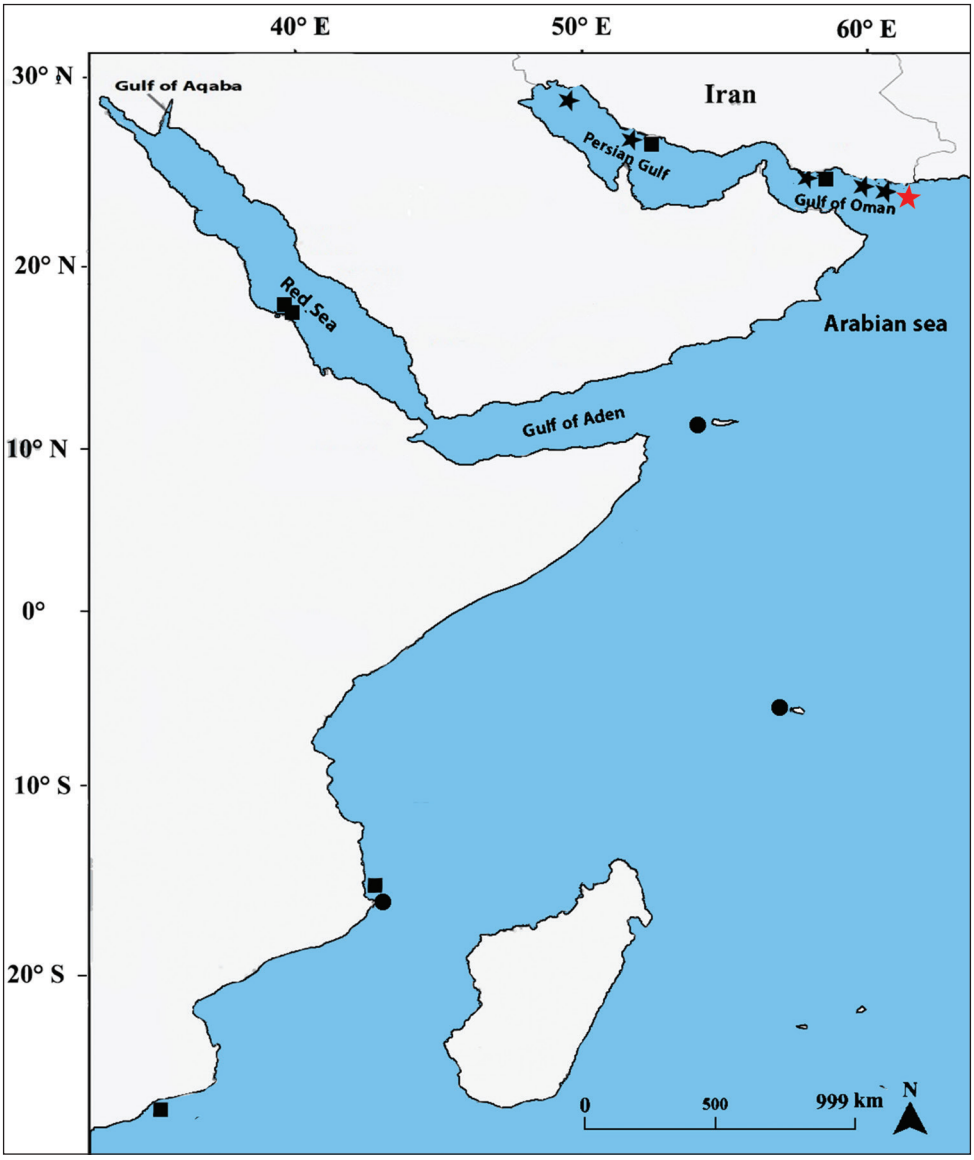

Figure 1. Sampling localities and distribution of *Plectorhinchus makranensis* sp. nov. (stars), *P. schotaf* (squares) and *P. sordidus* (circles) across the Western Indian Ocean. Red star: Beris (type locality).

tocol. Sequences were amplified by PCR using the following primer pairs: cytochrome oxidase subunit 1 (CO1LBC_F: 5' TCAACYAATCAYAAAGATATYGGCAC 3'; CO1HBC_R: 5' ACTTCYGGGTGRCCRAARAATCA 3') and Cytochrome b (GluF: 5'AACCACCGTTGTATTCAACTACAA3; ThrR: 5'ACCTCCGATCTTCGGATT-ACAAGACCG3), following Ward et al. (2005) and Machordom and Doadrio (2001), respectively. PCR conditions for the COI gene included: initial denaturation 94 °C, 1 min then 30 cycles at 95 °C for 30 s, 52 °C for 45 s, and 72 °C for 1 min, followed by

a final extension at 72 °C for 5 min. All amplification conditions were similar the COI gene except for the annealing temperature (54 °C) and the number cycles (35) for the Cyt *b* gene. The quality of PCR products was determined by running them on 1.5% agarose gels in 0.5X TBE buffer. The products were sent to Microsynth Company (Switzerland) for sequencing. We analysed a total of 64 sequences *of Plectorhinchus* species, including 36 for COI and 28 for Cyt *b*. Sequences of *Pomadasys maculatus* (Bloch, 1793) and *Haemulon aurolineatum* Cuvier, 1830 were used as outgroups.

Molecular data analyses

All sequence alignments were performed using the MAFFT algorithm. The pairwise DNA sequence differences within and between species of *Plectorhinchus* were calculated with MEGA 7.0.9 (Kumar et al. 2016) based on the Kimura two-parameter (K2P) model. The best-fit nucleotide substitution models were determined by jModelTest (Posada 2008) for each gene and combination of two genes. Based on Akaike information criterion (AIC), the preferred model for the two molecular markers was TVM + I + G. Analyses of phylogenetic relationships were performed for each gene and combination of two genes (Cyt *b* + COI) using maximum likelihood (ML) and Bayesian inference (BI). ML analysis as implemented in RAxML 7.2.6 (Stamatakis 2014) with 10,000 bootstrap replicates. BI analysis was run for 30,000,000 generations in MrBayes 3·1·2 (Ronquist et al. 2012) with two independent runs of four Markov Chain Monte Carlo (MCMC). The first 25% of the trees were excluded as burn-in and remaining trees sampling were used to compute a 50% majority rule consensus tree. The resulting phylogenetic trees from ML and BI analyses were edited using FigTree v.1.4.4. Additionally, we used from two different approaches for species delimitation including the Automatic Barcode Gap Discovery (ABGD) (Puillandre et al. 2012) and Bayesian Poisson Tree Process (bPTP) (Zhang et al. 2013). The ABGD method based on the COI gene was performed on web http://wwwabi.snv.jussieu.fr/html, under the Kimura (K80) model with the default parameters of Pmin = 0.001 to Pmax = 0.1, steps = 10, X (relative gap width) = 1.5, Nb bins = 20. The bPTP approach used the best ML tree, which was run on the web server (http://species.h-its.org/ptp). This analysis was processed with 500,000 MCMC generations and 25% of burn-in.

Morphological analysis

We used Johnson and Wilmer (2015) for morphometric and meristic characteristics which consisted of 23 morphometric and seven meristic features. The univariate and multivariate analysis were run in SPSS v.16 (SPSS Inc., Chicago IL) and PAST v. 4.03 (Hammer 2020). We assessed the normally distributed parametric data using the Shapiro-Wilk test. The morphometric characters were divided by standard length (SL) and head length (HL) to remove the size effect from the dataset. The univariate Analysis of Variance (ANOVA) was performed for morphometric characters to evaluate the significance of phenotypic differences between species. The principal components analyses (PCA) was used for multivariate analyses to characterize the morphological variation among species.

Results

Molecular analysis

This study used sequence data from 21 species of Haemulidae with two outgroups (38 samples) (Fig. 2). The combined dataset included 1672 bp (Cyt *b*: 1055, COI: 617), of which 629 bp (Cyt *b*: 450, COI: 179) were variable and 413 bp (Cyt *b*: 244, COI: 169) were parsimony-informative. Both ML and BI analyses yielded highly congruent trees with difference only in levels of support. *Plectorhinchus* species formed two clades with high bootstrap and posterior probabilities, including: clade A (*P. cinctus*, *P. gibbosus*, *P. plagiodesmus*, *P. macrolepis*, *P. sordidus*, *P. playfairi*, *P. chubbi*, *P. unicolor*, *P. flavomaculatus P. schotaf* and *P. makranensis* sp. nov.), and clade B (*P. albovittatus*, *P. caeruleonothus*, *P. centurio*, *P. picus*, *P. chaetodonoides*, *P. diagrammus*, *P. polytaenia*, *P. lineatus*, *P. vittatus* and *P. gaterinus*) (Fig. 2). *Plectorhinchus makranensis* sp. nov. was found to be closely related (see below) with *P. schotaf* which together comprised the sister group of *P. flavomaculatus*. The new species formed a highly supported monophyletic clade with low intraspecific genetic diversity for both two mtDNA markers (COI and Cyt *b*) (Fig. 2, Suppl. material 1: Table S1). *Plectorhinchus makranensis* sp. nov. demonstrated minimum interspecific genetic divergence with *P. schotaf* (4.78% for Cyt *b*, and 5.11% for COI) (Suppl. material 1: Table S1). *Plectorhinchus makranensis* sp. nov. exhibited maximum interspecific

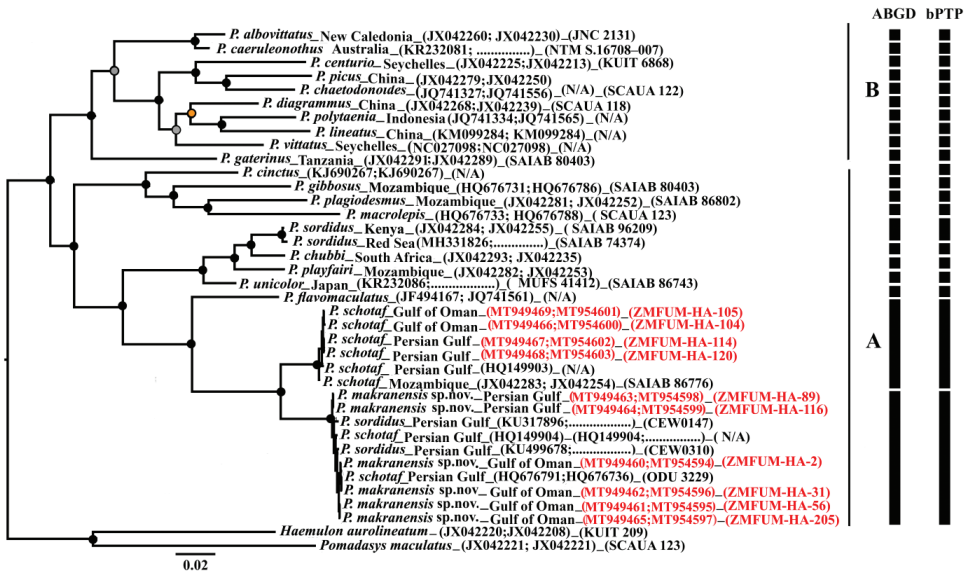

Figure 2. Molecular phylogenetic tree showing *P. makranensis* sp. nov. and other congeners based on two mitochondrial genes Cyt *b* and COI (total length 1672 bp). Supporting values of nodes: black circles (ML bootstrap BP ≥ 70% and BI probability PP ≥ 0.95), orange circles on nodes support by ML (BP ≥ 70%) but not by BI (PP ≥ 0.95), gray circles on nodes support by BI (PP ≥ 0.95) but not by ML (BP ≥ 70%). Bar at the side of the tree represents the results of the analyses of species delimitation. Red font: sequences of this study, COI (first), Cyt *b* (second).

genetic divergence with *P. lineatus* (18.65% for Cyt *b*) and with *P. gaterinus* (20.32% for COI). The ABGD analysis based on the COI gene defined 21 MOTUs a wide range of P values (0.0028–0.0077). The bPTP analysis estimated number of MOTUs identical to ABGD MOTUs using COI and Cyt *b* markers with the support value ranging from 0.86 (*P. caeruleonothus* cluster) to 0.99 (the most cluster). These analyses also recognized the new species and its closest congener as distinct species (Fig. 2).

Morphological analysis

***Plectorhinchus makranensis* sp. nov.**
http://zoobank.org/EAF907D6-B2FB-4BA3-8162-59148206D62F
Figs 1–6; Suppl. material 1: Table S1, Suppl. material 2: Table S2

Holotype. (Fig. 3). ZMFUM-HA-56, 246.5 mm SL Type locality. Iran Gulf of Oman, Sistan and Baluchestan prov, Beris coast, 24°36'14"N, 61°45'77"E, depth 15 m, collected by Ehsan Damadi, 5 Aug 2017.

Paratypes (*N* = 15). ZMFUM-HA-31, 141.2 mm SL, ZMFUM-HA-75, 226.6 mm SL, ZMFUM-HA-205, 345.6 mm SL, ZMFUM-HA-147, 295.3 mm SL and ZMFUM-HA-148 203.1 mm SL, all from the Gulf of Oman, Sistan and Baluchestan prov, Tis coast, 25°7'60"N, 61°6'28"E, depth 5 to 7 m, collected by E. Damadi, 10 Sep 2017; ZMFUM-HA-4, 246.5 mm SL and ZMFUM-HA-2, 228.5 mm SL, Gulf of Oman, Hormozgan prov, Pozm coast, 25°17'48"N, 59°59'12"E, depth 6 m, collected by M. Kahouri, 12 Oct 2017; ZMFUM-HA-44, 268.3 mm SL and ZMFUM-HA-45, 274.5 mm SL, Gulf of Oman, Hormozgan prov, Jask coast, 25°36'63"N, 57°45'37"E, depth 6 m, collected by H. Rahmani, 5 Nov 2017; ZMFUM-HA-74, 248.6 mm SL, and ZMFUM-HA-76, 301.1 mm SL, Gulf of Oman, Hormozgan prov, Jask

Figure 3. Holotype of *Plectorhinchus makranensis* sp. nov. ZMFUM-HA-56, 246.5 mm SL, Gulf of Oman: Beris coast (Photo by E. Damadi).

coast, 25°28'43"N, 57°49'36"E, depth 6 to 9 m, collected by A. Amiri, 7 Dec 2017; ZMFUM-HA-78, 277.5 mm SL, ZMFUM-HA-87, 263.3 mm SL and ZMFUM-HA-116, 287.3 mm SL, Persian Gulf, Bushehr prov, Kangan Bandar, 27°33'20"N, 52° 7'09"E, depth 10 m, collected by H. Tangestani, 13 Apr 2018; ZMFUM-HA-89, 146.5 mm SL, Persian Gulf, Khuzestan prov, Henijan coast, 29°37'35"N, 49°59'79"E, depth 7 m, collected by H. Tangestani, 5 Jun 2018.

Comparative material. ***Plectorhinchus schotaf*** (*N* = 18): **Gulf of Oman:** ZMFUM-HA-103 to 106, four specimens, 268.9–290.9 mm, Jask, 5 Nov 2017, H. Rahmani; **Persian Gulf:** ZMFUM-HA-114 to 120, six specimens, 254.5–313 mm, Bushehr, 13 Apr 2018, H. Tangestani; **Red Sea:** BPBM 20355, 245 mm, Port Sudan, 9 Oct 1974, J.E. Randall; BPBM 20766, two specimens, 234–243 mm, Port Sudan, 14 Oct 1975, J.E. Randall; **Mozambique:** SAIAB 41668, four specimens, 100–121 mm, Inhaca, Sep 1948, J.L.B. & M.M. Smith; SAIAB 19796, 183 mm, Ibo, 8 Aug 1957, J.L.B. Smith.

Plectorhinchus sordidus (*N* = 2): **Seychelles:** BPBM 21661, 230 mm, Caiman Rocks, 7 Jun. 1977, J.E. Randall; **Mozambique:** SAIAB 41668, 81 mm, 1 Sep 1948, J.L.B. and M.M. Smith.

Diagnosis. *Plectorhinchus makranensis* sp. nov. can be distinguished from other congeners by the following combination of features: (1) meristic characters: dorsal fin rays XII, 18–20; gill rakers 10–12 + 16–17 (26–29); tubed lateral-line scales 55–57; transverse scale rows above lateral line 10–11; transverse scale rows below lateral line 17–18; circumpeduncular scales 30–31; (2) morphometric characters: base of soft portion of dorsal fin 27.6–29.4% of SL; orbit diameter 25.5–30.1% of HL; caudal peduncle length 19.2–21.3% of SL; (3) Color pattern: head and body unicolor without markings, the posterior part of the opercular membrane grey; uppermost first to third pectoral-fin rays light grey.

Description. Meristic data and morphometric data are given in Suppl. material 2: Table S2. Dorsal-fin rays XII, 18–20 (modally 19), all soft rays branched except the first; anal-fin rays III, 7–8 (rarely 8), all soft rays branched; pectoral-fin rays 16–17 (modally 16), first and second rays unbranched; pelvic rays fin I, 5, all branched; caudal fin with 9 dorsal and 7 ventral rays (total = 16), uppermost and lowermost unbranched; tubed lateral-line scales 55–57 (modally 56); scales above lateral line to the base of the first dorsal-fin spine 10–11 (modally 10); scales below lateral line to first anal-fin spine 17–18 (modally 17); circumpeduncular scales 30–31 (modally 30); gill rakers on first arch small, 10–12 on upper limb (modally 12) and 16–17 on lower limb (modally 17); branchiostegal rays 7; preopercle with 31–36 serrae.

Body elongate, moderate deep, its depth 2.8–3.4 in SL, compressed laterally and covered with ctenoid scales; scales on the middle of the body largest; lateral line extends slightly as smaller scales onto the caudal-fin base; scales present on suborbital; snout and chin without scales; predorsal scales extending through interorbital. Head moderately large, head length 3.4–3.7 in SL, upper profile convex; mouth moderately small and terminal, lips fleshy, upper jaw protruding slightly beyond the lower jaw; nostrils small, posterior nostril half diameter of anterior nostril, anterior nostril on horizontal line through the lower margin of eye; orbit diameter 3.3–3.9 in HL; three pores on each side of the chin, but no

pit; teeth cardiform, approximately 2 rows laterally and 5 rows anteriorly in the upper jaw, approximately 2 rows laterally and 6 rows anteriorly in lower jaw, approximately 20–24 teeth in the upper jaw on each side and approximately 16–18 in the lower jaw on each side, palatine and vomer without teeth. Opercle with a single, exposed, short and weak spine; preopercle slightly concave and serrate, including few serrae on the posteroventral margin.

Origin of dorsal fin above the pectoral-fin base, first spine shortest, fifth spine longest, first dorsal-fin spine about 1.2 length of fifth, first spine 6.4 (6.1–6.5) in HL, fifth spine 2.6 (2.2–2.7) in HL, 6th and 7th soft dorsal-fin ray longest, 6th and 7th 3.6 in HL, 18th to 20th soft dorsal-fin ray shortest, its length 9.6–9.8 in HL, base of soft portion of dorsal fin 1.1 in base of the spinous portion; anal fin short, with somewhat rounded posterior margin, origin below base of 7th soft dorsal-fin ray, second spine longest, first ray is the longest, anal-fin length 2.5 (2.3–2.6) in HL; posterior margin of caudal fin slightly emarginate, caudal-fin length 1.7–1.8 in HL; pectoral fin reaching vertical between bases of seventh and eighth dorsal-fin spines, pectoral-fin length 1.4–1.5 in HL. Origin of pelvic fins behind pectoral-fin base, its tip reaching vertical at ninth dorsal-fin spine, second ray longest, pelvic-fin length 1.4–1.5 in HL.

Color pattern in preservative. (***Holotype***: Fig. 3). Head and body steel grey; head and edge of fins slightly darker than the rest of the body; posterior part of opercular membrane dark grey; lips grey; ventral part of body including underside of head and belly to lower part of caudal peduncle white; iris yellow.

Color in fresh. (paratypes: Fig. 4). Body silver-grey; all fins dark grey; pectoral-fin base light grey; uppermost first to third pectoral-fin rays light gray; orbital margin orange; iris grey; ventral part of body including subopercle, chest and pectoral-fin margin opaque white; lips and chin pink-grey; posterior part of opercular membrane grey.

Distribution and habitat. The new species has been observed at six localities along the coast of the Gulf of Oman and the Persian Gulf in the Northwest Indian Ocean. Abundance was greater in the Gulf of Oman compared to the Persian Gulf. All specimens have been collected from shallow rocky and coral areas. Other species of this family which occur sympatrically at the type locality (Beris coast) with *Plectorhinchus makranensis* sp. nov. include: *Diagramma pictum*, *Plectorhinchus pictus*, *Pomadasys kaakan*, *P. maculatus* and *P. stridens*.

Etymology. The species name is derived from the Makran coast and refers to the coastal land in southeastern Iran and southwestern Pakistan, north of the Gulf of Oman.

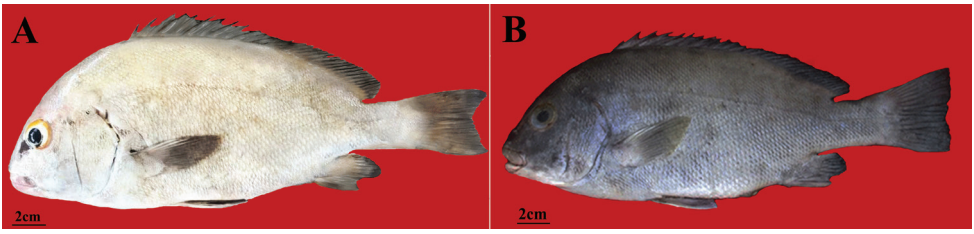

Figure 4. *Plectorhinchus makranensis* sp. nov. **a** ZMFUM-HA-205, paratype, 345.6 mm SL, Gulf of Oman: Tis coast, (Photo by E. Damadi) **b** ZMFUM-HA-75, paratype, 226.6 mm SL, Gulf of Oman: Tis coast, (Photo by E. Damadi).

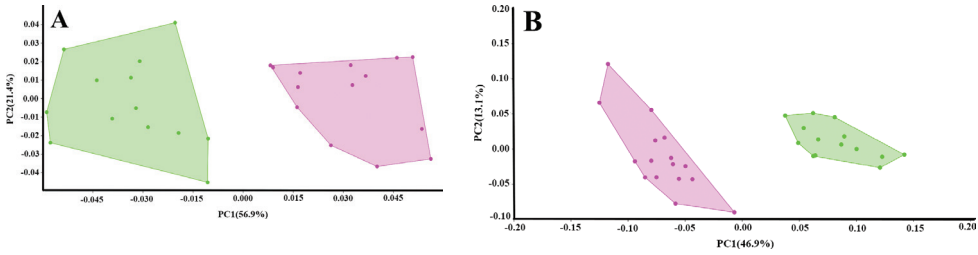

Figure 5. Principal components analysis (PCA) results for **A** meristic and **B** morphometric data of two species of *Plectorhinchus*: *Plectorhinchus makranensis* sp. nov. (pink); *P. schotaf* (green).

Multivariate analysis. The first two Principal Components (PCs) of the meristic and morphological characters accounted for 78.3% and 60% of the variation, respectively (Fig. 5A, B). In the meristic PCA, the number of total gill rakers, circumpeduncular scales and transverse scale rows below the lateral line loaded heavily on the first PC. Both species were completely distinguished along the first axis (Fig 5A). In the morphometric PCA, measurements including the length of the soft dorsal-fin base, body depth and depth of the caudal peduncle separated *Plectorhinchus makranensis* sp. nov. from *P. schotaf* along the first PC1 (Fig. 5B).

Discussion

The present study adds four species (*P. flavomaculatus*, *P. makranensis*, *P. caeruleonothus* and *P. unicolor*) to the previous molecular reconstructions (Sanciangco et al. 2011; Liang et al. 2014; Tavera et al. 2018). Our phylogenetic analysis is consistent with previous morphological and molecular studies. Based on ecological, morphological, color characteristics and biogeography, *Plectorhinchus* is divided into two clades: clade A includes species with deeper body and uniformly dull color compared to clade B (Johnson et al. 2001; McKay 2001; Tavera et al. 2018) (Fig. 2). The species of clade A are usually distributed in the Western Indian Ocean, with two exceptions: *P. macrolepis* and *P. unicolor* are scattered in the Eastern Atlantic and the West Pacific, respectively (Wirtz et al. 2007; Johnson and Wilmer 2015). Species of clade B are usually distributed from the East Indian to the West Pacific Ocean with the exceptions of *P. centurio* and *P. gaterinus*, which are only found in the Western Indian Ocean (Fricke et al. 2018).

A combined morphological and molecular approach should be used to distinguish closely related species (Baldwin et al. 2011; Lavoué and Sullivan 2014; Bogorodsky et al. 2017).

Based on molecular and morphological data (Fig. 2, Suppl. material 2: Table S2), *P. schotaf* is the sister taxon of *P. makranensis* sp. nov. Genetic distance between the new species and *P. schotaf* based on COI and Cyt *b* markers is consistent with species-level divergences in other fish taxa (Johns and Avise 1998; Ward et al. 2005; Hsu et al. 2007; Ward 2009). Also, these two sympatric species in the Persian Gulf and the Gulf of Oman show higher genetic distance than other congeneric species pairs from the East

Africa coast to the Red Sea based on both mtDNA markers 3.42% between *P. chubbi* and *P. sordidus* for the COI gene, and 3.50% between *P. chubbi* and *P. sordidus* for the Cyt *b* gene (Suppl. material 1: Table S1).

Because genetic distances between *P. makranensis* sp. nov. and deposited sequences in GenBank for *P. schotaf* and *P. sordidus* (HQ676736, HQ676791, HQ149904, KU499678, KU317896) are low, these deposited specimens could also represent sequences of *P. makranensis* (Fig. 2).

The new species is morphologically most similar to *P. schotaf* and *P. sordidus*. The coloration of the new species differs from *P. schotaf* by having the posterior margin part of the opercular membrane grey (Fig. 4) (vs. red in *P. schotaf* (Fig. 6A, B). The two species also differ in the number circumpeduncular scales 30–31 (vs. 32–34 in *P. schotaf*). Additionally, there are modal differences in counts, transverse scale rows below the lateral line (17–18, modally 17, vs. 18–20, modally 19 in *P. schotaf*), and morphometric differences, with *P. schotaf* having a shorter base of the soft portion of the dorsal fin (Suppl. material 2: Table S2). *Plectorhinchus makranensis* sp. nov. can be distinguished from *P. sordidus* by the number of gill rakers (10–12, modally 12 upper rakers, 16–17, modally 17 lower rakers, 26–29, modally 28, rarely 26 total rakers, vs. 9–11 upper rakers, 15–16 lower rakers, 24–26 total rakers in *P. sordidus*), a longer caudal peduncle and smaller orbit diameter (Suppl. material 2: Table S2) and the first to the third pectoral-fin rays light grey (Fig. 4) (vs. dark grey in *P. sordidus* (Fig. 6C, D)). Additionally, these two species can be different from each other in the number of tubed lateral-line scales (55–57, modally 56, vs. 48–55, modally 54 in *P. sordidus*).

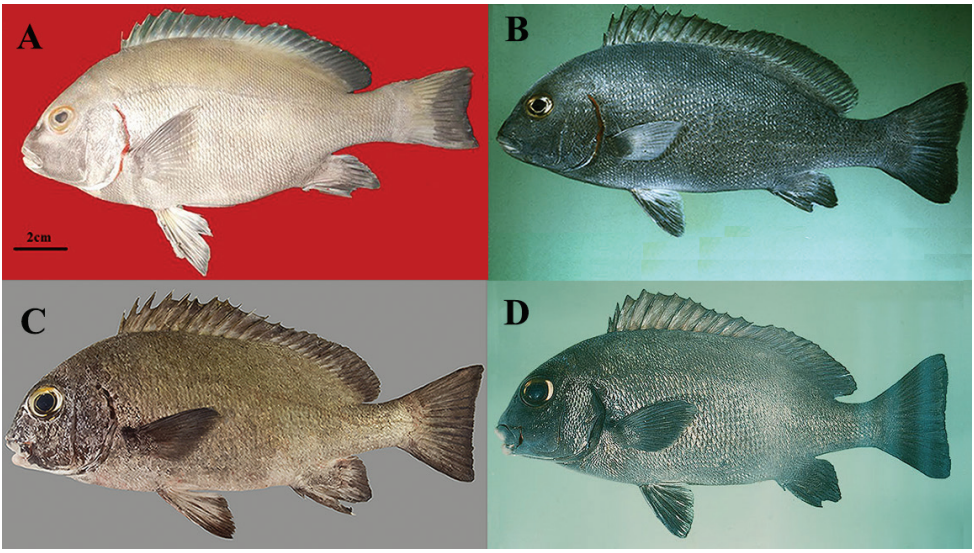

Figure 6. A *Plectorhinchus schotaf* ZMFUM-HA-104, 268.9 mm SL, Gulf of Oman: Jask, (Photo by E. Damadi) **B** *P. schotaf* BPBM 20766, 243 mm SL, Red Sea: Port Sudan, (Photo by J.E. Randall) **C** *P. sordidus* SMF uncatalogued, 220 mm SL, Arabian Sea: Socotra, (Photo by S.V. Bogorodsky) **D** *P. sordidus* BPBM 21379, 228 mm SL, Gulf of Oman. (Photo: J.E. Randall).

Plectorhinchus makranensis sp. nov. is distinguished from other similar congeners as follows: from *P. caeruleonothus* by having 10–12 gill rakers on the upper limb (vs. 7–9 in *P. caeruleonothus*) and 10–11 scales above the lateral line to the base of the first dorsal-fin spine (vs. 15), from *P. unicolor* by having 17–18 transverse scale rows below lateral line (vs. 19–21), from *P. griseus* by having 18–20 dorsal-fin rays (vs. 21–23); from *P. playfairi* in having 55–57 lateral-line tubed scales (vs. 58–60) and 16–17 gill rakers on lower limb (vs. 21–23), from *P. chubbi* by XII dorsal-fin spines and 16–17 gill rakers on the lower limb (vs. XI spines and 21–23 rakers respectively). The number of dorsal-fin spines is XII in new species vs. XIII in *P. chrysotaenia* and XIV in *P. flavomaculatus*, *P. ceylonensis*, *P. gibbosus*, *P. macrolepis* and *P. plagiodesmus*. Furthermore, the ANOVA analysis reveals that the numbers of dorsal-fin spines and soft rays and scales below the lateral line to the first anal-fin spine, as well as the numbers of circumpeduncular scales and total gill rakers, significantly differ from the other examined species. The molecular and morphological differences mentioned above indicate that the new species is separated from other congeners.

Acknowledgements

We would like to express our sincere thanks to Dr Sergey V. Bogorodsky for his photograph of *Plectorhinchus sordidus* and Arnold Y. Suzumoto for their help with providing us with specimens. We would also like to thank the University of Ferdowsi Mashhad in Iran for their invaluable support. We are indebted to local fishermen for their help in collecting specimens. We also thank to Ann Paterson from the University of Arkansas for editing on an early draft of the manuscript.

Funding support for this research was provided by the Iran National Science Foundation (Grant 97009791).

References

Asgharian H, Sahafi HH, Ardalan AA, Shekarriz S, Elahi E (2011) Cytochrome c oxidase subunit 1 barcode data of fish of the Nayband National Park in the Persian Gulf and analysis using meta-data flag several cryptic species. Molecular Ecology Resources 11: 461–472. https://doi.org/10.1111/j.1755-0998.2011.02989.x

Baldwin CC, Castillo CI, Weigt LA (2011) Seven new species within western Atlantic *Starksia atlantica*, *S. lepicoelia*, and *S. sluiteri* (Teleostei, Labrisomidae), with comments on congruence of DNA barcodes and species. ZooKeys 79: 21–72. https://doi.org/10.3897/zookeys.79.1045

Bishop JM (2003) History and current checklist of Kuwait's ichthyofaunal. Journal of Arid Environments 54: 237–256. https://doi.org/10.1006/jare.2001.0874

Bogorodsky SV, Iwatsuki Y, Amir SA, Mal AO, Alpermann TJ (2017) Morphological and molecular divergence between *Crenidens crenidens* (Forsskål, 1775) and *C. indicus* Day, 1873 (Perciformes: Sparidae) and notes on a Red Sea endemic lineage of *C. crenidens*. Marine Biodiversity 47: 1273–1285. https://doi.org/10.1007/s12526-017-0764-6

Carpenter KE, Krupp FD, Jones J, Zajonz A (1997) FAO species identification field guide for fishery purposes: living marine resources of Kuwait Eastern Saudi Arabia Bahrain Qatar and the United Arab Emirates Food and Agriculture Organization of the United Nations. Rome, 324 pp.

Fricke R, Eschmeyer WN, van der Laan R (2019) Catalog of fishes: genera, species, references. http://researcharchive.calacademy.org/research/Ichthyology/catalog/fishcatmain.asp [Version 10/2019]

Fricke R, Mahafina J, Behivoke F, Jaonalison H, Léopold M, Ponton D (2018) Annotated checklist of the fishes of Madagascar southwestern Indian Ocean with 158 new records. FishTaxa 3: 1–432.

Froese R, Pauly D (2019) Fishbase: World Wide Web electronic publication. http://fishbase.org [Version 08/2019]

Ghanbarifardi M, Esmaeili HR, Gholami Z, Aliabadian M, Reichenbacher B (2016) Molecular phylogeny of three mudskippers (Gobiidae) from the Persian Gulf and Gulf of Oman (Makran). Journal of Applied Ichthyology 32: 416–420. https://doi.org/10.1111/jai.12999

Hammer O (2020) PAST Paleontological Statistics v.4.03. Reference Manual. Oslo: University of Oslo.

Hsu KC, Chen JP, Shao KT (2007) Molecular phylogeny of *Chaetodon* (Teleostei: Chaetodontidae) in the Indo-West Pacific: evolution in geminate species pairs and species groups. Raffles Bulletin of Zoology 14: 77–86.

Johns GC, Avise JC (1998) A comparative summary of genetic distances in the vertebrates from the mitochondrial cytochrome *b* gene. Molecular Biology and Evolution 15: 1481–1490. https://doi.org/10.1093/oxfordjournals.molbev.a025875

Johnson JW, Randall JE, Chenoweth SF (2001) *Diagramma melanacrum* new species of haemulid fish from Indonesia Borneo and the Philippines with a generic review. Memoirs of the Queensland Museum 46: 657–676.

Johnson JW, Wilmer JW (2015) *Plectorhinchus caeruleonothus* a new species of sweetlips (Perciformes: Haemulidae) from northern Australia and the resurrection of *P. unicolor* (Macleay 1883) species previously confused with *P. schotaf* (Forsskål 1775). Zootaxa 3985: 491–522. https://doi.org/10.11646/zootaxa.3985.4.2

Kumar S, Stecher G, Tamura K (2016) MEGA7: molecular evolutionary genetics analysis version 7.0 for bigger datasets. Molecular Biology and Evolution 33: 1870–1874. https://doi.org/10.1093/molbev/msw054

Lavoué S, Sullivan JP (2014) *Petrocephalus boboto* and *Petrocephalus arnegardi*, two new species of African electric fish (Osteoglossomorpha, Mormyridae) from the Congo River basin. ZooKeys 48: 43–65. https://doi.org/10.3897/zookeys.400.6743

Liang R, Wang C, Zou Q, Zhou A, Zhou M (2014) Molecular phylogenetic relationships of some common sweetlips (Haemulidae: Plectorhynchinae) and the synonyms controversy of two *Plectorhinchus* species. Mitochondrial DNA Part A 27(3): 2209–2214. https://doi.org/10.3109/19401736.2014.982628

Machordom A, Doadrio I (2001) Evidence of a cenozoic betic-kabilian connection based on freshwater fish phylogeography (Luciobarbus Cyprinidae). Molecular Phylogenetics and Evolution 18: 252–263. https://doi.org/10.1006/mpev.2000.0876

McKay RJ (2001) Haemulidae (= Pomadasyidae). Grunts (also sweetlips rubberlips hotlips and velvetchins). In: Carpenter KE, Niem VH (Eds) FAO Species Identification Guide for Fishery Purposes. The Living Marine Resources of the Western Central Pacific. Volume 5. Bony Fishes Part 3 (Menidae to Pomacentridae). FAO Rome 2961–2989.

Nelson JS, Grande TC, Wilson MV (2016) Fishes of the world. John Wiley & Sons Hoboken, 651 pp. https://doi.org/10.1002/9781119174844

Polgar G, Ghanbarifardi M, Milli S, Agorreta A, Aliabadian M, Esmaeili HR, Khang TF (2017) Ecomorphological adaptation in three mudskippers (Teleostei: Gobioidei: Gobiidae) from the Persian Gulf and the Gulf of Oman. Hydrobiologia 795: 91–111. https://doi.org/10.1007/s10750-017-3120-8

Posada D (2008) Jmodeltest: Phylogenetic model averaging. Molecular Biology and Evolution 25: 1253–1256. https://doi.org/10.1093/molbev/msn083

Puillandre N, Lambert A, Brouillet S, Achaz G (2012) ABGD, Automatic Barcode Gap Discovery for primary species delimitation. Molecular Ecology 21, 1864–1877. https://doi.org/10.1111/j.1365-294X.2011.05239.x

Rabaoui L, Yacoubi L, Sanna D, Casu M, Scarpa F, Lin YJ, Shen KN, Clardy TR, Arculeo M, Qurban MA (2019) DNA barcoding of marine fishes from the coastal water of eastern Saudi Arabia. Journal of fish biology 95: 1286–1297. https://doi.org/10.1111/jfb.14130

Randall JE (1995) Coastal fishes of Oman. Crawford House Publishing Pty Ltd Bathurst, 439 pp.

Randall JE, Allen GR, Steene RC (1997) Fishes of the Great Barrier Reef and Coral Sea. University of Hawaii Press, 541 pp.

Ronquist F, Teslenko M, Van Der Mark P, Ayres DL, Darling A, Hohna S, Larget BL, Liu L, Suchard MA, Huelsenbeck JP (2012) MRBAYES 3.2: Efficient Bayesian phylogenetic inference and model selection across a large model space. Systematic Biology 61: 539–542. https://doi.org/10.1093/sysbio/sys029

Sanciangco MD, Rocha LA, Carpenter KE (2011) A molecular phylogeny of the Grunts (Perciformes: Haemulidae) inferred using mitochondrial and nuclear genes. Zootaxa 2966: 37–50. https://doi.org/10.11646/zootaxa.2966.1.4

Smith JLB (1962) Fishes of the family Gaterinidae of the western Indian Ocean and the Red Sea with a résumé of all known Indo-Pacific species. Ichthyological Bulletin Department of Ichthyology Rhodes University 25: 469–502.

Stamatakis A (2014) RAxML Version 8: A tool for Phylogenetic Analysis and Post-Analysis of Large Phylogenies. Bioinformatics 30(9): 1312–1313. https://doi.org/10.1093/bioinformatics/btu033

Tavera JJ, Acero PA, Balart EF, Bernardi G (2012) Molecular phylogeny of grunts (Teleostei Haemulidae) with an emphasis on the ecology evolution and speciation history of new world species. BMC Evolutionary Biology 12, 57. https://doi.org/10.1186/1471-2148-12-57

Tavera JJ, Acero PA, Wainwright PC (2018) Multilocus phylogeny divergence times and a major role for the benthic-to-pelagic axis in the diversification of grunts (Haemulidae). Molecular Phylogenetics and Evolution 121: 212–223. https://doi.org/10.1016/j.ympev.2017.12.032

Ward RD (2009) DNA barcode divergence among species and genera of birds and fishes. Molecular ecology resources, 9: 1077–1085. https://doi.org/10.1111/j.1755-0998.2009.02541.x

Ward RD, Zemlak TS, Innes HB, Last RP, Hebert PDN (2005) DNA barcoding Australia's fish species. Philosophical Transactions of the Royal Society of London. Series B Biological Sciences 360: 1847–1857. https://doi.org/10.1098/rstb.2005.1716

Wirtz P, Ferreira CE, L Floeter SR, Fricke R, Gasparini JL, Iwamoto T, Schliewen UK (2007) Coastal fishes of São Tomé and Príncipe islands Gulf of Guinea (eastern Atlantic Ocean): an update. Zootaxa 1523: 1–48. https://doi.org/10.11646/zootaxa.1523.1.1

Zhang J, Kapli P, Pavlidis P, Stamatakis A (2013) A general species delimitation method with applications to phylogenetic placements. Bioinformatics 29(22): 2869–2876. https://doi.org/10.1093/bioinformatics/btt499

Supplementary material 1

Table S1

Authors: Ehsan Damadi, Faezeh Yazdani Moghaddam, Fereshteh Ghassemzadeh, Mehdi Ghanbarifardi

Data type: Molecular

Explanation note: Net Sequence divergence obtained for CO1 (below diagonal) and for Cyt b (above diagonal).

Link: https://doi.org/10.3897/zookeys.980.50934.suppl1

Supplementary material 2

Table S2

Authors: Ehsan Damadi, Faezeh Yazdani Moghaddam, Fereshteh Ghassemzadeh, Mehdi Ghanbarifardi

Data type: Morphological

Explanation note: Meristic and morphometric data for all material examined of *Plectorhinchus makranensis* sp. nov. (N = 16), *P. schotaf* (N = 18) and *P. sordidus* (N = 2) (holotype data for *P. schotaf* and from Smith (1962)). All proportional measurements are given in % of SL and HL. Characters in bold show differences between *P. makranensis* sp. nov. and two other species ($p < 0.05$).

Link: https://doi.org/10.3897/zookeys.980.50934.suppl2